EVALUATION OF SURFACE MODIFICATION METHODS TO MITIGATE RUSTING AND PITTING IN WEATHERING STEEL BRIDGES

FINAL REPORT

by

A. RAMAN
PROFESSOR OF MECHANICAL ENGINEERING
LOUISIANA STATE UNIVERSITY
BATON ROUGE, LA 70803

RESEARCH REPORT NO. 197
STATE PROJECT NO. 736-09-06
RESEARCH PROJECT NO. 84-1ST

CONDUCTED FOR

LOUISIANA DEPARTMENT OF TRANSPORTATION AND DEVELOPMENT
LOUISIANA TRANSPORTATION RESEARCH CENTER
in Cooperation with
U. S. Department of Transportation
FEDERAL HIGHWAY ADMINISTRATION

SEPTEMBER, 1986

TABLE OF CONTENTS

LIST OF TABLES

LIST OF FIGURES

ABSTRACT

ASTM A-588 Weathering Steel, used in over 2000 bridge structures in the U.S.A., has been found to be experiencing corrosion problems due to salts used for deicing purposes. Corrosion problems encountered in about 25 bridges located in the states of Louisiana and Texas were studied and analyzed. Bridges chosen for study are located very near the Gulf Coast (near-marine), in the industrial belt of coastal area (industrial, near-marine) and in the central and northern parts of Louisiana. Formation of coarse flakes and measured section losses of 3 to 5 mils per year (mpy) have been found in coastal area bridges in sheltered locations, whereas the metal loss is about 1 mpy in sheltered locations in rural area bridges in the northern parts of Louisiana. Roughly half as much thickness loss as in sheltered locations was registered for exterior, bold-exposed surfaces. The weight losses determined by analyzing field coupons located at several bridge sites yielded average losses of about 1.6 mpy in near-Gulf bridge sites; 1.35 mpy in the Coastal area bridges located in the industrial belt; and about 0.5 mpy in the rural areas in the northern parts of Louisiana for interior, sheltered location exposure, and roughly half as much for exterior, open exposure. These losses observed are compared with the results obtained by other investigators worldwide.

Pitting is another problem encountered in bridges. The exterior faces, as well as bridges in the rural areas, do not show any evidence of pitting. Interior, vertical faces show the least severe pits. Fairly wide and deep pits were observed in partially boxed areas above the gusset plates at the entrance to piers. Pits as deep as 50-60 mils were located in these areas. Such wide and deep pits are attributed to debris

collecting at these spots and retaining water or experiencing wet conditions for fairly long periods, contributing to maximum rusting. Sheet-type of rust forms in these areas.

Accelerated laboratory atmospheric exposure simulation tests with an acceleration factor of 50 and extending for a maximum of 2200 wet-dry cycles (6-year exposure equivalent) gave corrosion loss data that agreed fairly well with the field data derived from field coupons. The tests corresponding to sheltered location exposure showed that the rusting process does not slow down and stabilize with time in humid, tropics - equivalent conditions. Average metal losses were: 0.1 - 0.33 mpy in tests simulating exterior, open exposure, about 1 mpy in tests simulating sheltered location exposure, about 2.5 mpy in total immersion testing, about 40 to 64 mpy in salt fog tests and about 60 to 100 mpy corrosion rate in electrochemical tests for initial corrosion processes.

Structural analysis revealed that the initial rust to form in atmospheric exposure is the so-designated "Amorphous Mix (AM)" phase, which is judged to be a mixture of highly amorphous δ-, γ-FeOOH and ferrihydrite. These and other rust phases, including α-FeOOH and γ-$Fe_2O_3 \cdot H_2O$, form and grow on top of the sedimented AM layer. The amorphous phases are compact and dense and provide for corrosion and rusting resistance, whereas crystalline phases are porous, erode off easily and contribute to corrosion losses. The morphology and growth characteristics of the rust phases are defined.

Surface modifications with rust modifier-type inhibitors are generally found to be beneficial to slow down the corrosion process and stabilize the protective AM layer or the amorphous rust phases. Phosphoric acid application is found to be very effective in this respect and fine rusting

prevails on top of such phosphoric acid-treated surfaces. Based on the results obtained, several recommendations are made for treating the weathering steel in several Louisiana bridge sections with inhibitor-type chemicals.

INTRODUCTION

Weathering Steel, ASTM A588 - grades A and B, used extensively in bridge structures, buildings and other high-rise structures such as sports stadia, has been observed to be plagued with corrosion problems, especially more than allowable metal loss and pitting [1,2]. The metal has been found to be doing well in outdoor, open-bold-exposures, but does not fare well in sheltered areas in chloride-laden environments or where salt has been used for deicing purposes during winter months. Airborne salt and other pollutants reach the steel beams in sheltered locations and contribute to the corrosion problems encountered. Salt concentrations as high as 8% have been found in places where the leaking expansion joints allowed the salt water to seep through and stagnate on beams. In areas touched by the salt spray as much as 3% salt has been found. These data are from Michigan [3]. On account of widespread corrosion problems encountered in Michigan, the weathering steel A588 has been barred from usage in bridges and roadway sections that would be subjected to high salt pick-up. The state of Michigan has subsequently instituted a total ban of its usage in all structures built by the state. Many other states have followed suit and there is now a ban on the use of weathering steels in many places.

The moratorium instituted by the State of Michigan and others applies to new structures. According to a recent poll [4], eighteen states in the U.S.A. do not design bridges with weathering steel, thirteen have no restrictions, and nineteen states design with some restrictions. But there are already upwards of 2000 weathering steel highway bridges in use throughout the U.S.A. and two Canadian provinces [4].

About 80 bridges built with the A588 steel are in the Gulf states of the U.S.A., of which about 25 are in the state of Louisiana. Coarse flaking and pitting have already been encountered in some of the coastal area bridges, the finding of which necessitated a thorough investigation of the magnitude of the corrosion problems and evaluation of corrosion mitigative measures other than regular painting. So much was the indication of the problem that immediate attention was warranted. Accordingly, a research project was initiated at Louisiana State University in full collaboration with the Research and Development Section and the Maintenance Division of the Louisiana Department of Transportation and Development in September 1983.

It was of primary interest to assess the extent of damage by corrosion and section thickness losses by direct measurements in representative weathering steel structures in the states of Louisiana and Texas and seek suitable remedial procedures to mitigate the corrosion processes. Instead of painting, it was felt it would be wiser to let the steel rust but provide it suitable treatment so that a compact and adherent protective rust layer would be formed and maintained on the steel sections already in place on the bridges. An optimum, economical method of surface treatment that would counter the corrosion problems encountered was sought. Three, known, inhibiter-type acids, those that would form chemical conversion coatings on the steel, were planned to be applied alone or in suitable combinations on surfaces of the steel, after cleaning by sand blasting, acid pickling or wire brushing.

Such treatments or any other mitigative measure thought of would be of less value if one would only evaluate the weight or section losses by corrosion on these treated or surface modified steels. A clear knowledge

of the nature and causes for excessive rusting and the characteristics of the rust layer formed under the prevailing conditions on the steels exposed as such, as well as on steel surfaces suitably surface modified or treated with chemicals, is necessary in order to gain a clear understanding of the phenomena and the effects of any mitigative measure suggested. Accordingly, the study also was oriented toward understanding the corrosion processes of weathering steels in the atmosphere and elucidating the characteristics of the rust layers formed.

The project was started with the following specific aims:

(1) Undertake a program of field monitoring of A588 steels in selected, representative bridge sections and document the corrosion data.

(2) Analyze the field rust samples and determine the causes for excessive flaking and corrosion.

(3) Determine the section thickness losses due to continued rusting and removal of rust by natural processes.

(4) Undertake a program of field monitoring and rust analysis from A588 steels in chosen bridge sections after suitably modifying their surfaces by different chemical treatments.

(5) Install suitably surface-modified A588 steel coupons in the field at the bridge locations (in both open and sheltered locations) and evaluate their corrosion behavior and the rust layers formed on them through subsequent periodic analysis.

(6) Undertake a modest program of accelerated corrosion testing in the laboratory with similarly surface-modified A588 steel coupons under conditions that would closely simulate the field conditions and conform to ASTM test specifications.

(7) Evaluate the specific effects of chloride in the rusting and corrosion processes in the A588 steel under the prevailing weather conditions.

(8) Critically analyze the atmospheric corrosion data in the literature on the low alloy and weathering steels in various conditions and correlate the data from this project to the general findings. Discuss similarities and differences.

(9) Determine the optimum surface modification technique that can be applied to offset the problems, and

(10) Develop and specify suitable maintenance procedure for surface-modified A588 steel spans.

The long-term goal of the project was to understand the prevailing and potential corrosion problems, such as pitting, crevice attack, stress corrosion cracking, etc., especially at critical locations and highly stressed areas, and seek suitable remedies.

Between 1983 and 1986 considerable work was undertaken on all aspects of the project and a great deal of data collected from eight representative bridges located strategically in different parts of the states of Louisiana and Texas, as well as from accelerated laboratory tests and field exposures with A588 steel coupons. The results obtained in this research program are being presented in a series of reports and papers intended for publication. This final report encompasses salient data and results from those reports and papers. For detailed information, readers are referred to the respective reports or papers as indicated at appropriate places.

LITERATURE INFORMATION

Corrosion Kinetics.

McKenzie [2] reported increased corrosivity of steel under sheltering in marine environments owing to the air-borne sea salt. Under sheltered conditions in exposure to the atmosphere both the sulphur compounds and chlorides present had significant effects, whereas in open, exterior, bold exposure, chlorides were not found to be as influential due to the frequent washing action by rain. McKenzie also observed the formation of rougher rust in sheltered, marine locations. His study also showed that pitting occurred extensively in sheltered specimens in marine environments and pit depths as high as 25 mils were found.

In semi-tropical Gulf Coast states, where excessive snowing does not occur and the use of deicing salt is minimal, the corrosion problems encountered are from the air-borne sea salt deposited on the structure by wind. Thus, McKenzie's data and results would be directly applicable to conditions in Louisiana.

McKenzie's data from England also showed a lower corrosion rate under bridge sheltering than in open bold exposure in areas where high chloride levels were absent. Corrosion thickness losses of about 150-225 μm (6 to 9 mils) over a five-year period were found for Cor-Ten B (A588 - grade A) in highly industrialized areas of the U.K. On the contrary, a loss of about 75 to 100 μm (3 to 4 mils) for a five-year period was obtained in rural and urban areas. (See Table 8)

Much higher thickness losses than reported by McKenzie have been recorded in Brazil [5]. Annual losses averaged from about 25 μm (1 mil) in moderately high chloride levels (350 m away from the sea) to about

300-375μm (12 to 15 mils) in high chloride levels in marine atmospheres (100 m from the sea line) for the Cor-Ten B (A588 - grade A) steel. The corrosion rate was only about 15 μm (0.6 mil) per year at 600 and 1100 m from the sea line. In industrial areas the corresponding annual losses were about 60 to 75 μm (2.4 to 3 mils). These are for outdoor, open exposures in tropical marine and subtropical industrial climates.

Results obtained in exterior, bold-exposure tests with weathering steels in various other countries can be summarized as follows:

(1) Austen-50 steel, equivalent to A588 - grade B, had about 90 μm (4 mils) thickness loss in 10 years whereas Austen 60 steel, equivalent to A588 - grade A had slightly higher losses, about 120 μm (5 mils) in 10 years in heavily industrialized coastal environments in Australia. Plain carbon steel without copper lost nearly twice as much as these steels. On the contrary, the thickness losses were only about 50 μm (2 mils) in 10 years for the weathering steels and about 60-90 μm (3-4 mils) for plain carbon steel in rural areas [6].

(2) Duncan and Ballance [7] found appreciable chloride in the atmosphere derived from sea salt, far away from the coastline in New Zealand. The chloride content of the atmosphere played a significant role in corrosion, causing more metal loss in sheltered locations than in open exposures.

(3) Perez [8] showed that changes in the atmospheric corrosion in Cuba are primarily due to salinity. More weight loss was obtained with a decrease in temperature in the humid, tropical climate. A higher salinity and lower solar radiation were

ascribed to be the reasons for increased weight loss in the winter months.

(4) The maximum thickness of the patina layer is about 200 μm (8 mils) [9,17]. Corrosion losses of Atmofix 52A (equivalent to A588 - grade B) steel were about 50 μm (2 mils) in outdoor rural, urban and weakly polluted industrial atmospheres but were about 100 to 150 μm (4 to 6 mils) in outdoor heavily polluted industrial areas in 5 years in Czechoslovakia. These values are about similar to the values reported by Townsend and Zoccola in the U.S.A. [10]. Further information and data on corrosion in Czechoslovakia can be obtained from the works of Barton, et al [11].

(5) Atmospheric corrosion testing in Norway and Sweden using electrolytic cells in the atmosphere has indicated that for steel cells the time of wetness is close to the exposure time at RH > 90% at least in the initial stages [12]. The average thickness losses for a weathering steel with low Mn were about 40-50 μm (about 2 mils) in 5 years in rural and urban areas of Norway [13]. Analogous thickness losses for Cor-Ten steel (A588) over a five-year period was about 60 μm (about 2.4 mils) in Finland [14].

(6) An extensive atmospheric corrosion testing program exists in Japan [15]. The Japanese scientists have carried out elaborate work to characterize the structure and properties of the rust layers formed on the weathering steels. The pioneering works of Misawa outlined in Ref. (15) and surveyed briefly later are already well known. These scientists have shown that a good

washing of the surface by rain is most important for the early development of a protective rust film and that it is particularly so in industrial atmospheres. Aging processes activated in colloidal aggregates formed determine the corrosion rates. Copper in the structural steel inhibits the growth of colloidal particles and increases the flocculent forces of the aggregate, thereby leading to better compactness of the rust film and corrosion resistance.

The rust layers formed on iron and steel have the specific ability to absorb and transport selective ion species, which property has been studied in detail by Sato, et al. [16]. These scientists observed that hydrous ferric oxides are anion-selective in neutral chloride solution and are cation-selective in alkaline solution, with a point of iso-selectivity being pH = 10.3. Anion selective ferric hydroxide films would accelerate the anion enrichment and decrease the pH at the rust-metal interface such that the corrosion rate would increase. Such conditions would apply to exposure at interior, sheltered locations.

(7) Studies in Canada by Manning [17] showed that corrosion of weathering steel in open exposure decreased with time and attained "steady state" conditions in about 3 years. In industrial sites the corrosion rate was the highest, but it diminished rapidly.

The industrial effluents could also cause beneficial, inhibitive actions and in one study lower corrosion rates have been recorded in industrial environments than in marine or even

rural environments [17]. Generally, however, maximum corrosion losses have been registered in marine or coastal-industrial environments, the least in rural areas, and intermediate, but fairly high, losses in industrial environments. The corrosion losses in heavily polluted areas are the composite of many factors and are, hence, site sensitive; however, a heavy dependence on atmospheric pollutants has been found. Thus, for example, the works of Atteraas and Haagenrud [13] as well as Knotkova-Cermakova, et al. [9] have established increased corrosion losses with increased SO_2 contents in the atmosphere.

(8) Townsend and Zoccola's data in the U.S.A. [10] showed a maximum thickness loss of about 55 to 70 μm (2 to 3 mils) in industrial areas, about 60 μm (2.4 mils) in rural areas and around 75 μm (3 mils) in marine environments over a period of 5 years. These are similar to the values obtained in Australia.

Data of Reed and Kendrick [18] from California indicated a corrosion thickness loss for weathering steel in open exposure of about 0.1 mil/year in the low rainfall urban environment, about 0.15 mil/year in the low rainfall industrial environment, and about 0.33 mil/year in the marine environment. These values are all on the low side, as compared to other values reported around the world.

One of the most extensive works in the U.S.A. on the effects of chlorides in the atmosphere is that by Ambler and Bain [19]. Their results also showed a direct relationship between corrosion and atmospheric salinity. The early work of Copson [20] showed that the different corrosion rates are basically due to the quantity and quality of water reaching the steel surface.

The corrosion rate of weathering steel is dependent on the time of wetness [21-24], i.e., time for which the surface stays wet in wet-dry cyclic situations, in addition to chloride and sulfate contamination. The wetting of steel is controlled by many factors, particularly temperature and RH, and pollution as well as the heat transfer rates also play dominant roles. It may be controlled by many other factors, such as wind conditions, structure and porosity of the rust layer itself, direct hit from the rain and solar radiation, etc.

Corrosion of weathering steel is not homogeneous and uniform - it varies with the seasons, and certainly it is controlled by the severity of the atmosphere, which is a site variable. Dutra and Vianna [5] have beautifully demonstrated the decreasing effects of chlorides in the atmosphere as a function of distance from the waterline in coastal areas. Their data showed drastic reduction in the corrosion rate of a carbon steel, from about 600 μm (24 mils) to about 20 μm (1 mil) per year, as the test site was moved by about 0.5 km from the waterline at the coast. The effects of increased SO_2 contents in air on corrosion rates have already been alluded to. The composition of the atmosphere at a site can vary periodically and seasonally, thereby altering the corrosion rates. Thus it is well recognized that atmospheric corrosion at a given site is a very dynamic, enigmatic process. Only averages and approximations can be found through periodic tests. It can also be noted here that different parts of a given structure, such as a bridge, get exposed to various types of conditions; for example to highly wet conditions, totally immersed situations in stagnant pools of water, to foggy conditions, wet-dry cycling with and without intermittent rain wash and exposure to solar radiations,

etc. Thus, the corrosion of steel at a bridge is not uniform and should be considered as location sensitive.

In general, the sites are classified into three or four categories rural (very mild) and urban (mild), mild industrial, heavy industrial, marine, marine-industrial, etc. Tests are conducted routinely at various sites representative of the different classes, and data collected and analyzed. A thorough understanding of the various corrosion problems encountered by bridge structures at different locations and sites would require the study of the rusting process and kinetics under diversified conditions of exposure, both in the field as well as in the laboratory.

Mechanism of Rusting and Corrosion of Weathering Steels.

Okada et al. [25] have proposed and shown that during atmospheric rusting there are two layers of rust formed, which, possibly develop through the growth of the outer zone during the wet periods and the inner zone during the dry periods. During the wetting part of the cycle, the high RH is the only source of the electrolyte and the corrosion (anodic) process is accelerated. During drying, circular pits resembling blisters with collapsed roofs develop [26] due to evaporation of moisture and pressure build-up. It was shown that one mode of corrosion extension involves the rupture of such bubbles leading to open pits [27]. The probable mechanism would be similar to the one suggested by Barton, et al. [28]. In this mechanism the concentration of dissolved materials such as sulphates would induce the diffusion of water into the postule and subsequent evaporation would cause swelling of the membrane and eventual rupture.

Inside these blisters, fine nodules of green rust have been observed [29]. This intermediate rust is the basis for further oxidation, and around neutral values of pH it is essential for the progress of the rusting process [30]. Further rusting proceeds by the formation of γ-FeOOH, which has been found to be the dominant structure in atmospheric rusting. The formation of γ-FeOOH is best explained by Misawa, et al. [30,31] in the following manner:

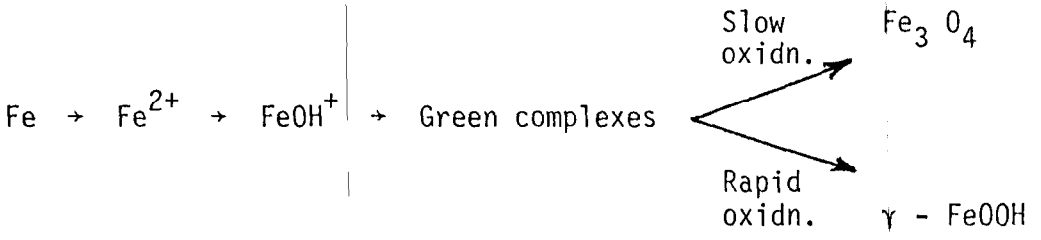

Green complexes formed at the initial stages of rusting by aerial oxidation of $FeOH^+$ result in the precipitation of Fe_3O_4 by slow aerial oxidation and γ-FeOOH by rapid aerial oxidation at pH in the range 6-7. The further advanced state of rusting after formation of γ-FeOOH was shown to consist of a densely-packed inner layer of Fe_3O_4 and green rust in varying proportions. Depending on the environmental factors, other intermediate forms such as β-, δ-, α-FeOOH and amorphous oxyhydroxides have been observed, which, depending on their ability to get reduced to Fe_3O_4, control the cathodic processes, hence affecting the corrosion rate [32]. It has been shown that α-FeOOH does not get reduced to Fe_3O_4, while the others do [33,34].

According to exposure corrosion tests [27,35-37] a large quantity of α-FeOOH (goethite) is believed to be formed by non-dissociated substances such as gypsum and ash particles containing sulphates. On the other hand,

the rusts formed on steels that have been used in marine atmospheres at a pH above 8 were found to contain a large amount of β-FeOOH in addition to α-FeOOH and Fe_3O_4. β-FeOOH can be obtained only when Cl^- or other anions such as F^- are present [31,38-40]. Formation of goethite is directly related to the concentration of lepidocrocite (γ-FeOOH) and its solubility rate [41-44]. The main steps governing the rate of this transformation are [41]: (1) the dissolution of lepidocrocite, and (2) the formation of goethite nuclei and their subsequent growth, each step consisting of further steps. Villiers and Van Rooyen [43] showed the intermediate substeps as the dissolution of γ-FeOOH and formation of γ-Fe_2O_3 which proceeds to change to α-Fe_2O_3 through the following chemical reactions:

$$2\ \gamma\text{-FeOOH} \rightarrow \gamma\text{-}Fe_2O_3 + H_2O$$
$$\gamma\text{-}Fe_2O_3 \rightarrow \alpha\ Fe_2O_3$$

This reaction, though favored by thermodynamics, does not occur due to kinetic reasons and goethite is the most commonly found oxyhydroxide of rust at the final stages. Therefore, this transformation occurs most likely according to the following mechanism proposed by Misawa, et al. [30]:

$$\gamma\text{-FeOOH} \rightarrow\rightarrow \text{Fe III - ions} \rightarrow \text{amorph. ferric oxyhydroxides}$$
$$Fe\ O_x\ (OH)_{3-2x} \rightarrow \alpha\text{-FeOOH}.$$

It is worth noting that γ-FeOOH has about $10^{4.5}$ times larger solubility in water than α-FeOOH [31]. The rate of this crystallization from amorphous Fe III oxyhydroxide depends directly on the pH of the solution [45]. In acid solutions the crystalline product is α-Fe_2O_3. In basic solutions it is a mixture of α-FeOOH and α-Fe_2O_3, and in some cases

pure α-FeOOH. At a pH = 10, the formation of mostly α-FeOOH is favored [45].

Although not identified to be one of the dominant forms in atmospheric rusts, δ-FeOOH is another one of the possible phases involved. Its formation has been well elucidated by Misawa. δ-FeOOH is synthetically produced by rapid oxidation of ferrous hydroxide in sodium hydroxide solution. This oxidation process results in the formation of strongly ferrimagnetic, deep-brown precipitate of δ-FeOOH [30,46-48]. The classic work of Bernal, et al. [49] as well as the works of others [50,51] have explained the violent fast reaction occurring as "topotactic", involving no long-range diffusion in the two structures, with hexagonal, closely packed layers of oxygen and hydroxyl ions. The reaction was stated to occur as follows:

$$Fe(OH)_2 + \tfrac{1}{4}\, O_2 \xrightarrow[\text{oxidn.}]{\text{violent}} \delta\text{-FeOOH} + \tfrac{1}{2}\, H_2O.$$

Violent oxidation of green complexes and green rusts also gives rise to δ-FeOOH, as indicated by Misawa, et al. [30].

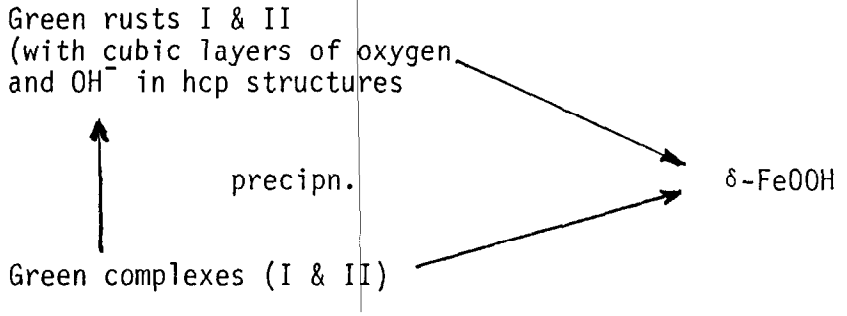

All the reactions discussed above are topotactic in character except

$$\beta\text{-FeOOH} \rightarrow \alpha\text{-}Fe_2O_3$$
$$Fe(OH)_2 \rightarrow \alpha\text{-FeOOH}$$
$$Fe(OH)_2 \rightarrow Fe_3O_4.$$

β-FeOOH and α-Fe_2O_3 have dissimilar structures and renucleation was felt to be necessary for the transformation process. However, Mackay [52] suggested that the hollandite structure of β-FeOOH could be transformed to a spinel by the migration of some of the Fe-ions in the lattice to the tetrahedral sites and adjustment of some bond distances subsequently. If this is feasible, then it would make the β-FeOOH → α-Fe_2O_3 transformation a series of topotactic transitions.

Johnson, et al. [27], who characterized the rust layer formed on mild steel panels after exposing them for short periods in dry, sunny locations, found γ-$Fe_2O_3.H_2O$ and α-FeOOH on the sun-exposed top side but only the γ-$Fe_2O_3.H_2O$ on the underside. They indicated the detection of γ-Fe_2O_3 also. Keiser, et al. [53] studied the rusting process using Raman spectroscopy and identified the various rust phases present using also infrared spectroscopic analysis. Leidheiser, et al. [54,55] stated that the initial corrosion product γ-FeOOH changes to α-FeOOH and γ-Fe_2O_3 during outdoor bold-exposure. Steels exposed for about 25 years contained only γ-Fe_2O_3. These results were deduced based on Mössbauer spectroscopic data.

Singh et al. [56] identified the rust phases formed on steels in open, exterior exposure through Mössbauer spectroscopy and found γ-FeOOH and α-FeOOH, with some β-FeOOH and $Fe_{3-x}O_4$ (x between 0 and 1/3) being present

in the marine environments. Leidheiser, et al. as well as Singh, et al. did not detect any δ-FeOOH in the samples.

During the development of the protective films the rusts present a continuous, double-layered structure, with the inner one being more corrosion resistant [57]. Morphological studies indicated that the inner layer was dense and uniform and offered a greater barrier effect to water and oxygen than the outer layer. Misawa [58] has shown that the inner layer is composed mostly of the amorphous ferric oxyhydroxide. Analysis of Keiser et al. [59] has shown δ-FeOOH as the major component of the inner layer with some 10-20% γ-FeOOH and possibly some α-FeOOH. Okada, et al. [25] found the two layers in the rust deposit to be optically active and isotropic, respectively. Using a polarized light microscope, the main constituent of the rust layer on weathering steels was found to be the optically isotropic layer, which in turn was composed of the amorphous spinel-type iron oxide. This layer, shown to be beneficial in preventing the penetration of water and oxygen to the steel surface, was found to be damaged under very damp conditions. On the contrary, the rust layer on mild steels consisted of both the isotropic and active layers.

Morphology of Rust Phases.

Feigenbaum, et al. [60] refer to the more porous structure of α-FeOOH (goethite), owing to its tendency to grow in needles or oblong platelets, whereas magnetite grows in layer form due to its tendency to aggregate in granules consisting of a large number of crystals grouped around a nucleus. The nest-like honeycomb structure of α-FeOOH is illustrated in rusts and colloids by Johnson, et al. [27] as well as by Matijevic [61], respectively.

Micrographs of β-FeOOH given by Murad [40] show the crystals of this phase to possess star shape and x-shaped twins. The crystals of β appear as somatoids or cigars also. Smith and McEnaney [29] characterized Fe_3O_4 as polyhedral crystals and green rust as hexagonal crystals. Colloidal α-Fe_2O_3 particles appeared as fine spheres, aging of which at 250°C with suitable reducing agents produced magnetite that appeared as polyhedral crystals. Fe_3O_4 particles produced from a ferrous hydroxide gel appeared as uniform spheres [28]. The morphologies of the other phases δ- and γ-FeOOH as well as ferrihydrite and the amorphous rusts are not documented.

Effects of Alloying Elements in Weathering Steels.

It is generally believed that the better corrosion resistance of weathering steels is due to the compact and adherent inner rust layer composed of amorphous phases. The essential reasons for its protective nature are not well understood. It could be due to the barrier effect [25,57] or due to ion-selectivity effects, preventing penetration of harmful anions, as pointed out by Sato, et al. [15,16]. The effects of alloying elements in the weathering steel on the formation and stabilization of this inner layer leading to protection have been investigated.

Alloying elements responsible for the beneficial weathering properties of low alloy steels are Cu, Cr, Si, P, Ni and Mo. Copson [62], Horton [63,] and Bruno, et al. [64] demonstrated the effects of these alloying elements by tracing their migration from the substrate to the outer regions of the rust. Horton et al. [63] showed that the protective effect of alloying elements in weathering steels does not result from any barrier effect and that the beneficial elements function in the electrolyte at the

steel rust interface or elsewhere within the rust layer. Suzuki [65] illustrated the effects of the alloying elements during corrosion exposure and related the effect of copper to the inhibition of growth of iron oxide in the form of various oxyhydroxides and magnetite. Cu, Cr, and P were found to facilitate the formation of the amorphous ferric oxyhydroxide. This is due to the transformation of γ-FeOOH from Fe(II) complexes to amorphous δ-FeOOH by the catalytic action of Cu and P concentrated on the metal surface [58]. Phosphorus alone is well known to form ferric phosphate, which tends to favor the formation of the amorphous form of rust and hinder its transformation to other forms [66]. Phosphorus gives optimum protection at 0.005% and was found to be detrimental to corrosion resistance if present in large amounts [67]. However, a technical report from Nippon Steel Corporation by Zaizen, et al. [68] indicates the effects to be otherwise. Increasing P-contents up to 0.1% were found to be beneficial to corrosion resistance. In spite of their relatively high P-content, these steels could be easily rolled into plates, including heavy plates, and retain weldability even better than the conventional structural steels. Some of these steels with high P-content up to 0.1% are said to be applicable in seawater also.

P, Cu, Ni and Mo are beneficial while C and Cr are harmful in steel for service in highly saline, highly humid environments [68]. For seawater service, Cr, Si, Al and Mo are beneficial, while C and S are damaging.

Fyfe et al. [69] related that the beneficial effect of Cu was present only when 'S' in the steel was tied up with Mn as MnS rather than being present in FeS. FeS is a good electronic conductor with low hydrogen overvoltage and therefore forms local corrosion cells in steel, whereas MnS of low Fe content is a poor conductor and does not form such cells [70].

It was also suggested that the deleterious effect of 'S' is nullified by precipitation of S^{2-} ions from the rust cell electrolyte as CuS, which, being highly insoluble, will be incorporated harmlessly in the rust. The addition of small amounts of 'S' to pure Fe increases its dissolution rate (up to 100 times) in acids for two reasons: (a) couple action of Fe-FeS, resulting in pitting and (b) absorption on the Fe surface of sulphide ions, which catalyze both the anodic dissolution reaction and the cathodic hydrogen evolution. Mn addition counteracts effect (a) and reduces the S-content in solid solution in Fe but does not completely prevent effect (b), since MnS is more soluble in acids than FeS. Cu-addition counteracts effect (b) in the dissolution process by combining with S^{2-} ions to form Cu_2S, which is insoluble in acids [70]. The effects of sulphide inclusions on pitting in mild steels are well studied and documented [71-73].

Effects of Atmospheric Inhibitors and Rust Modifiers.

Phosphates, tannates and benzoates have long been studied for their beneficial effects on forming stable forms of rust during atmospheric exposure. Achieving suitable phase transformations is the major goal in employing the inhibitors known as rust transformers.

The effect of phosphates in the form of different salts and acids has been studied by various investigators [74-77]. Phosphoric acid is used to produce phosphate layer that would prevent rerusting after pickling. It has been shown [74] that phosphates tend to form $Fe\ PO_4.4\ H_2O$, $Fe_3\ PO_4.8\ H_2O$ after the reaction with metallic iron, $Fe_3\ O_4$ and Fe O on the steel surface, but acid phosphate $Fe\ H_3\ (PO_4)_2.\ 2.5\ H_2O$ is formed when they react with α-, β-, and γ-FeOOH or with α-, and γ-$Fe_2\ O_3$. The latter product exhibits a relatively high stability and results in slow coverage of the

steel surface with time, resulting in a decrease of the corrosion rate with time [75].

Tannin in pure form, as well as in various proprietary preparations, is recommended as a rust modifier. It is said to convert the prevalent rust to a black form, supposed to be magnetite, that is highly adherent and protective. It is found in general that tannates or tannic acid reacts with the steel surface to form a crazed outer layer of ferric tannates [78]. From studies of surface pretreatments prior to application of tannic acid it has been found that optimum rust stabilization is achieved when it is applied on a rusted surface after the loose rust has been removed by wire brushing [79-81]. The reaction between the tannate layer and the steel substrate is believed to be oxygen dependent [82]. Iron tannate forms at the anodic sites and hydrogen is liberated at the cathodic sites. It is believed that the reaction product based on tannin application has either of the two forms - amorphous tannate or $Fe_3 O_4$. This film has been found to break down when excessive moisture both extracts the unreacted tannin and allows it to react with the existing rust, causing it to grow.

Benzoates on the other hand can inhibit the corrosion reaction in the presence of dissolved oxygen. Their inhibition mechanism is entirely different from those of phosphates and tannates in that they do not react with the steel to form stabilized solid products. It has been demonstrated [83] that benzoates react very slowly with the substrate metal, forming very small iron benzoate particles, which are produced at the sites of breakdown of the rust layer. At these local anodes the pH may be depressed considerably below that of the bulk solution, thus favoring precipitation of the less basic compound, $Fe\ (C_6 H_5 CO_2)_x\ (OH)_{3-2x}$. While this substance may be unable to form a truly passivating layer, relatively gross deposits

of it may nevertheless be capable of sealing pores in the oxide film. Other factors, such as the ability of the absorbed benzoate ions to retard the iron dissolution reaction [84], may also contribute to their inhibitive action.

Cumulative effects of inhibitors have been not so widely studied. Shreir [85] found that the addition of phosphoric acid to a tannin solution produced a coating with far better corrosion resistance than that formed by either of the individual constituents alone.

Detailed studies on long-term effects of these inhibitors applied on steel surfaces have not been undertaken anywhere.

EXPERIMENTAL PROCEDURE

The experiments carried out were of three different kinds - field tests, laboratory tests, and rust analysis. Procedures adopted in these tests are described briefly below:

General.

Five different steels were used in various tests of the program. These were: A588 - grades A and B made by U.S. manufacturers, A588 - grade A and Riverten R made by Kawasaki Steel Co., Japan and the regular A36 steel. The A588 - grade A (U.S.) was obtained from U.S. Steel Co. directly and the grade B made by Bethleham Steel Co. through a bridge contractor. The two Kawasaki Steel Co.'s steels were obtained from Kawasaki Steel Co. in Japan while A36 was bought from local suppliers.

The steels were sliced into 3 in. x 5 in. (grade B) or 4 in. x 6 in. (grade A) coupons and exposed in sets of three for each surface treatment at each site. These were optimum sizes for coupons whose weights could be measured accurately (to 0.01 g. accuracy) using digital electronic balance. Coupons of size 1 in. x 2 in. were also used so that they can be studied as such in the analytical instruments for rust characterization. Two or three coupons of the small size were used for each surface treatment so that weight loss data could also be generated from such small samples.

The coupons were cleaned by either sand blasting (SB) or acid pickling (AP) and degreased using acetone and dried prior to weighing. Such coupons were then surface treated with 25% phosphoric acid (PA), or 25% phosphoric acid-benzoic acid mixture (PA-BA) in equal proportion, or 10% tannic acid

(TA) by spraying and smearing with suitable brushes. The samples were designated suitably by stamping prior to acid treatments as follows:

Four digit designation: P Q R S - for field coupons

where P = Bridge Site: 1. Gibbstown; 2. High Island; 3. Leesville; 4. Boeuf River and 5. Luling;

Q = Rack number 1 through 9 designating various exposure times at sheltered locations, 1 to 6 and 8 for 1, 3, 6, 9, 12, 15 and 18 months exposure, respectively; that is, 1 for 1 month, 2 for 3 months, etc. 7 and 9 were racks in which the specimens were retreated with similar chemicals after 1 year and later withdrawn after 15 and 18 months total exposure, respectively.

R = Surface treatment designation given as follows:

1 - SB only

2 - SB + application of 25% PA

3 - SB + application of 25% PA-BA

4 - AP + 1st application of 10% TA + 2nd application of 25% PA

5 - AP + 1st application of 10% TA + 2nd application of 25% PA-BA

6 - AP + application of 10% TA

7 - AP only

9 - uncleaned specimens with mill scale

S = number of specimen in a set. 1 to 3 for big coupons; 4, 5 for small coupons along with big coupons in a rack; and 6 to 8 for small coupons bold-exposed at the open, exterior location. Exterior racks in the open were similarly designated, except there were only two or three racks at each bridge site.

3 digit designation: XYZ for laboratory coupons

where X = set of specimens corresponding to specific exposure time.

Y = treatment number (similar to field coupons)

Z = specimen number in a set.

Specimens on some of the racks were reused after first-time exposure and analysis after suitable cleaning.

Specimens were suitably mounted and held tightly in wooden racks. They were exposed freely in the open atmosphere either in the sheltered locations (under the bridges) or in exterior, open locations at the edges of the bridges. Since the racks had to be held close to the edge vertical web plate when the specimens were bold-exposed, only one surface was getting exposed to the sun. This duplicated the conditions of the edge web plates of the briges. However, in order to study the effects of total exposure on both sites to the sun and rain, sets of samples in racks (both big and small coupons) were bold-exposed at the roof of the Engineering CEBA building of the Louisiana State University for various periods of time 1, 3, 6, 12 and 24 months. Data for the first four exposures have been collected and the 2-year exposure is continuing.

Only small specimens were used in laboratory tests. Again, at least three specimens were used for each treatment and time of exposure.

The corroded coupons were cleaned by using Clark's reagent (25% HCl solution in water with stannous chloride and antinonous oxide inhibitors) at room temperature after removing bulk of the removable rust by dry and wet wire brushing. Suitable corrections were applied to account for the rust that was still adherent on the steel surface after careful cleaning whenever this was the case. The weight loss per dm^2 was calculated from

the initial and final weights after cleaning. The data from the three specimens usually showed some expected deviations and the average was obtained only from consistent data. The purpose of taking three specimens was mainly to identify such consistent data. Values which were too far deviant from the consistent ones were discarded.

Dividing wt. loss in g/dm^2 by the density of steel in g/dm^3 gives the thickness loss in dm. Thus the weight loss value in g/dm^2 was multiplied by 12.72 to get the thickness loss in μm. Bearing in mind 25 μm = 1 mil (10^{-3} in.), the thickness loss in mils can be obtained.

Field Tests.

Two types of field tests were undertaken in the research program. The first one, by using suitably treated field coupons mounted in wooden racks, has already been described. There were 9 interior (sheltered location) racks under 5 bridges and 2 exterior racks located one on either side of the bridge parallel to the bridge for each site. The five bridge sites where the samples were exposed have also been mentioned. These encompassed near-marine, industrial, and rural areas.

Field tests were also carried out on the bridge structures themselves, on the weathering steel beams, after cleaning and surface treating selected areas at six representative locations on each bridge as for field coupons. Since acid pickling could not be applied on the bridge structures, wire brushing (WB) was the chosen substitute. 1 ft. x 1 ft. or 2 ft. x 2 ft. areas at each of the six locations were used for each treatment 1 through 7. The cleaned areas were surface treated, using similar treatments as for field coupons. Prior to surface treatments the thicknesses of the beams or plates were measured with a digital ultrasonic thickness gauge that read

the thickness accurate to 1 mil (10^{-3} in.). The instrument was calibrated using standard blocks of specified thicknesses.

The six locations at each bridge site were chosen to lie on two opposite sides of the bridges on two adjacent piers close to the waterline. Locations I & III were exterior on the vertical web plates, II & IV were on the vertical web plates opposite to locations I & III, but at the interior sheltered locations of the bridges. These were also on adjacent piers. Location V was on the horizontal beam under the bridge parallel to the pier in sheltered locations, while location VI was on inclined beams directly above location V on the pier.

In addition to these six locations, extensive examinations were made in partially boxed locations above the gusset plates at the entrance to the piers. These were the places where owl and other wildlife take refuge and build their nests. After removing the debris, these places were cleaned by sand blasting in order to study the corrosion problems, particularly pitting at such sites.

Part of the areas of the rusted surfaces at each location in each bridge were retreated with similar chemicals after 6 months and 1 year and parts of the areas retreated after 6 months were also retreated after 1 year. Rusts formed on the originally treated as well as retreated areas were removed after 6 months, 1 year and 2 years from the first dates when the chemicals were applied and subjected to rust analysis in order to study the rusting process and mechanism. Thickness readings have been taken annually at each location on each bridge in the last three years and two sets of data besides the original were available. The section thickness losses have been computed out of these for various locations.

Another important study in the field pertained to pit depth measurements in order to evaluate the pitting characteristics. This was accomplished using a digital linear depth gauge that reads translations accurate to 1/10th of a mil. (10^{-4} in.). Taking readings on the top and at the bottom parts of the pits, the pit depths could be found. The small sized gauge could be mounted on a magnetic chuck and a linear translator to hold it on the steel beam in any location, even upside down for taking readings on the lower faces of the beams facing the ground, and moved suitably so that readings could be taken accurately. The data is, hence, felt to be very accurate.

Since pits of varying depths occur at a given location, extremely accurate readings are not essential, nor of any use unless one could study the pit depth variations in a given pit as a function of time. It is extremely difficult to isolate one pit among many and errors are likely. Hence the growth characteristics of the pits were not studied in this project. Where pit depths varied a great deal, at least twenty readings were taken in order to determine the pitting profile, that is to determine the average number of pits vs. pit depths in small intervals of depth ranges and draw the relevant plots. Some of these plots are given in this report.

Observations were made during periodic visits and inspections on the nature of the rust layer formed on the various treated areas at different locations of the bridges. From these observations, deductions were made on the particle size and rusting rate at various locations on the differently treated surfaces.

Finally, the locations of the bridges under study (the field exposure sites) are given in Fig. 1. There were seven bridges in the state of

Louisiana in this study and one in the state of Texas at High Island (HI) near Beaumont, Texas, located within 2 km from the Gulf Coast. The bridges in Louisiana are as follows:

1. Forked Island (FI) in Vermillion Parish, Str. No. 207-01-14.12-1.
2. Gibbstown (GT) in Cameron Parish, Str. No. 193-02-08.53-1.
3. Leesville (LV) in Vernon Parish, Str. No. 025-01-00.34-2.
4. Boeuf River Bridge (BR) in W. Carroll Parish, Str. No. 037-02-00.00-1.
5. Luling (LU) on the Mississippi River in St. Charles Parish, Str. No. 450-37-00.00-1.
6. Doullut Canal (DC) in Orleans Parish, Str. No. 062-05-08.96-1.

and 7. Larose (LR) in LaFourche Parish, Str. No. 407-02-03.50-1.

Of these the Leesville bridge is a small railroad bridge (on account of which only 4 locations were chosen instead of normal six, one exterior Loc. I, one interior on the vertical web plate Loc. II, and two interior locations III & IV), and Luling is the longest, made of two sections - the main span using the Kawasaki A588 - grade A steel from Japan and the approach span using the U.S.A588 - grade A. The Luling bridge is also the youngest, about 3 years old, while the rest of the bridges are about 12 years old. The bridges at HI, LV and BR have the A588 - grade B variety while the rest have the A588 - grade A variety. These two differ essentially in their Ni-content, the former grade B having about 0.4 - 0.5% Ni while the grade A variety usually has no Ni or a very small amount, although the ASTM specification allows some Ni content in grade A. Thus the Kawasaki A588 - grade A in use at Luling has about 0.1% Ni. This steel also has very low S, 0.005%, much lower than in other steels. The compositions of the steels in the various bridges are given in Table 1.

Laboratory Tests.

Five different laboratory corrosion tests were undertaken. These were:

(1) Accelerated Atmospheric Exposure Simulation Test-Sheltered Location Equivalent.

(2) Accelerated Atmospheric Exposure Simulation Test - Open, Bold Exposure Equivalent.

(3) Salt Fog Test

(4) Continuous Immersion Test, and

(5) Electrochemical Tests

Accelerated Atmospheric Exposure Simulation Test - Sheltered Location Equivalent. Hot and humid environmental conditions as in Louisiana were duplicated in a closed chamber. Specimens were tested in wet-dry cyclic conditions as in nature. One wet-dry cycle would correspond to one day of actual exposure. Each wet-dry cycle was of one half hour duration with 20 minutes of wetting time and 10 minutes of drying time simulating approximately the natural conditions of exposure. To bring about wet-dry cycling at slightly elevated temperatures, steam generated in a water boiler was let into the closed chamber at one far end. Specimens were set vertically standing on the other side of the chamber, so that the steam condensed on them and caused wetting. Warm air blowers were turned on automatically in the drying part of the cycle and the steam entry stopped so that drying conditions were simulated. To study the effects of two of the most important air pollutants, SO_2 and Cl^-, 0.1% H_2SO_4 and 3.5% NaCl solutions were sprayed on the surfaces of the specimens once a day. Five coupons were used for each surface treatment and one of them was not

sprayed on in order to determine the differences the polluting agents caused. Specimens were removed periodically after 200, 500, 750, 1200 and 2200 cycles and analyzed for weight loss and corrosion mechanisms. The weight loss data were plotted against time and the resultant plots were analyzed to determine the rate constants.

Accelerated Atmospheric Exposure Simulation Test - Open, Bold - Exposure Equivalent. This test was similar to the previous one except rain simulation was activated in this case. Another chamber in which water could be sprayed on the surfaces of specimens simulating the rain was used. Such spraying was used for 1 or 2 minutes once in every twenty cycles during the day time, i.e. the rain simulation was carried out twice a day - once in the morning and once at night, approximately 12 hours apart. This was equivalent to one rain in approximately 20-25 days. However, in a different run of the test, specimens were soaked wet in each cycle during the wetting part using the atomized water spray, which approximated to the wet conditions in rain. This corresponded to one rain every day throughout the period of exposure. Specimens were sprinkled with 0.1% H_2 SO_4 and 3.5% NaCl solutions twice a day in order to introduce the sulfate and chloride ions into the corrosive medium. Specimens in batches were removed after similar number of cycles as in the previous test and analyzed.

Salt Fog Test. This test was performed according to the ASTM Standard B117-73. A 3.5% salt solution was used as the electrolyte in the initial study. However, the tests were repeated with tap water without any additive in subsequent tests. The data pertaining to the kinetics of rusting are from the use of 3.5% salt solution. The temperature inside the

chamber was 110°F and the RH was 100%. Samples in sets of five for each treatment were removed after 1, 2, 4, 7, 15, 45 and 90 days, cleaned and weighed to determine the weight loss. One representative specimen from each batch corresponding to a given surface treatment was subjected to various analytical procedures for rust characterization.

Continuous Immersion Test. Two different electrolytes, 3.5% salt water and plain tap water, were used in this test. They were taken in separate fish tanks and specimens were hung and kept immersed in them using nylon threads and plastic clamps. Specimens were kept at least one inch below the water line. The solution was kept stagnant throughout this test, but it was changed once every fifteen days during long time exposures. Specimens with different surface treatments were kept in separate tanks. Specimens in batches of five for each treatment were removed after 7, 15, 30, 100 and 180 days and studied. The loose rust formed on the samples was collected by tapping the specimens before they were removed from the tanks, filtered and dried. The wet specimens with the adherent rust were dried in the laboratory atmosphere before collecting the rust for analysis. Specimens were cleaned by using wire brushes and Clark's solution.

Electrochemical Tests. These were both potentiostatic and potentiodynamic runs. The latter was used to determine the open circuit corrosion potential, corrosion current from Tafel slopes as well as from linear polarization plots and generally to determine the pitting tendencies, if any. Specimens were held at constant potentials around the open circuit potential and the current variations with time were determined. Pulse polarographic tests were also undertaken to determine

the Fe II/Fe III ratios during the potentiostatic tests. Tests were conducted not only with steels acquired from the steel companies but also with the core steel samples obtained from the various bridges as well.

Rust Analysis.

Natural rusts formed on steel sections (both interior and exterior), obtained from the various bridges, as well as those received from the states of California and West Virginia, were initially studied. Subsequent studies dealt with the rusts formed on the steel coupons subjected to various laboratory tests as well as to natural exposures in the field and also those that were formed in differently treated and retreated surfaces in bridge sections at different locations.

The rusts were studied generally for structure, size and morphology and phase growth features. Structural studies were accomplished using X-ray diffraction (XRD) and Infrared Absorption Spectroscopy (IRAS), sizes determined by using an optical microscope and the morphological and growth features studied using a scanning electron microscope (SEM) fitted with an energy dispersive X-ray analyzer (EDAX). Mössbauer spectroscopy (MS) was used to further characterize representative rust samples already analyzed by the other techniques mentioned.

Extensive chemical analysis was undertaken only in the first part of this study when natural rusts from bridge sections were analyzed. Wet chemical analysis techniques as well as atomic absorption spectroscopy (AAS) were used. Leachates (100 ml) extracted using deionized water from fixed amounts of powdered rusts (100 mg) were analyzed for chloride content as well as for pH of the extract. The relative values recorded were used to interpret some of the features of rusting or rust phase transformations.

Multiple data were derived wherever possible to eliminate errors and assure the correctness of the data. Innumerable samples were tested in each test such that consistent and reliable results could be obtained. The results reported are still to be construed as the best of the average data derived in both field and laboratory tests.

RESULTS AND DISCUSSION

The results obtained in this project are so numerous that they cannot be put in one report. Several technical papers have been written and submitted for publication. Some references to these papers and other specialized reports have to be made in this report such that all the data need not be duplicated here. The data and results contained therein are condensed and presented here. The readers are referred to the following other reports for details:

(1) Corrosion problems in unpainted highway weathering steel structures in Louisiana and Texas;

(2) Rusting characteristics of weathering steels studied in field tests;

(3) Rusting characteristics of weathering steels studied in laboratory corrosion tests;

(4) Study of rusts from weathering steels in Louisiana bridges;

(5) Characterization of rusts formed on weathering steels using infrared absorption spectroscopy, and

(6) Characterization of rusts formed on weathering steels using Mossbauer Spectroscopy.

All these reports have been generated under the aegis of this project and submitted to the LA-DOTD.

Corrosion Problems Encountered in the Bridges.

Two major problems seen on weathering steels in bridges are: (1) Formation of coarse, non-adherent flake-type rust leading to more than

anticipated metal loss, and (2) pitting underneath the rust. Another potential problem identified is crevice attack in loose joints.

The rust on weathering steels occurs generally as flakes or particles. The exterior sun exposed surfaces have fine powdery rust particles of average diameter about 0.5 mm. This is due to repeated washing of the rust by rain which not only removes some rust but prevents the particles from growing to big sizes. The rain wash may also have a stabilizing effect on an amorphous rust layer, designated as "amorphous mix" (AM) layer, which usually forms as a dense layer and does not allow growth of flakes to big sizes.

The exterior surfaces are devoid of any damaging corrosion problems. They show no pitting or any excessive metal loss by rusting. In dusty areas the rust on exterior surfaces can be slightly coarser, but they are still relatively small in size, < 1 mm.

In contrast, the rusts formed in the interior, sheltered locations of some of the coastal area bridges are flaky or sheet-typed. The latter forms in boxed locations where water stays stagnant, i.e., the steel stays wet for longer periods of time. Stratification can be observed in sheet-type of rusts as well as in flakes, indicating different growth kinetics based on seasonal variations. The reasons for the demarkation of various layers could be related to phase transformations that take place in rust layers, but this has not been well researched. The amorphous rust "AM" gets converted to crystalline forms of rust, which grow on the surface of the amorphous layer. The amorphous rust is adherent to the surface of the steel, but is postulated to lose the adherence when it crystallizes. The crystalline rust phases formed on the top surface can also be washed away by rain or removed by wind.

Sheet-type rust with 2 or 3 layers has been formed on the Kawasaki steel used in the main span of the Luling bridge. This rust sheet peeled off easily also. The sheet-type rust itself is theorized to have been formed by the steel staying wet for a long period of time during storage and transit to the U.S.A. from Japan on a ship. Considerable dusting could have helped in the development of this sheet-type of rust. However, once this sheet-type of rust, which feels like a dried up soil layer, peeled off, further rusting that is taking place on the steel in this bridge at Luling is of the flake-type. Further sheet-type rusting has been observed on this bridge only in horizontal locations where water from rain was allowed to remain stagnant for considerably long periods of time.

Rusting rate is dictated principally by the moisture condensed and the time of wetness. However, presence of salt or other conductive ions dissolved in the condensed water accelerates the corrosion process and more rust, usually in the form of coarser flakes, forms.

In totally wet situations the rust forms as a sheet-type or sedimentary layer which gets thicker with time, but at a much slower rate than in air due to condensed moisture or in the presence of wet film. This would be due to the slower oxygen supply and hindrance to mass and ion transport in the amorphous sedimentary layer in the former.

Generally the rust formation in sheets occurs in partially boxed locations at the entrance to the piers where wildlife takes refuge and builds nests. Rust debris collects in such areas and prevents the free drainage of water. The debris itself holds much of the water and keeps this area wet for most of the time. Several bolts in such boxes form also sheet-type rusts. This could cause severe problems to some of the bolts and, hence, to the joint. Stratified sheet-type rusting also was observed

on the edges of some of the beams in areas where water retention is high and chloride content of the atmosphere is appreciable, as at the Doullut Canal bridge.

Flakes formed on the steel in the interior sheltered locations showed a good correlation to the chloride content in the rust. The sizes of the flakes from several bridges are given in Table 2, where the chloride contents of the rust samples, as well as the pH of the extracted solutions, are also indicated. The flakes are very coarse, sharp-edged and loosely attached to the metal in bridges such as the ones at Doullut Canal (DC) and High Island (HI), which are in close proximity to the ocean (latter) or salt water lakes (former). The atmosphere at these locations is not only highly humid, but carries larger amounts of salt coming from the salt water.

The flakes are about 3 to 5 mm in mean dia. when the chloride-content of the rust is high, 2.5 to 6.5 ppm. As the chloride-content decreases, so does the flake size (see Fig. 2). When the chloride-content drops to below 1 ppm, the flakes are very fine, with an average dia. of about 0.5 mm. There is thus a direct correlation of the flake size and the chloride content.

Section Thickness Losses in Weathering Steel Bridge Sections.

The averages of at least ten readings at a given testing place on the steel beams at different locations in various bridges (taken in 1984, 1985 and 1986), were used to derive the section thickness losses. Averages of reasonable and consistent data were used in such determinations. As these section thickness losses were small (a few mils in magnitude) and the values derived for different areas with surface treatments could not be

differentiated from the others in such a short span of time (2 years), averages of section thickness losses were calculated using the data from all surface treatments at a given location.

The following general comments on the data are pertinent at this time.

(1) Much of the data collected was found to be inconsistent, and in several instances readings of thicknesses taken in later years came out larger than the previous readings. Each time the reading was taken after scraping the rust off from the surface of the steel at the place where the ultrasonic transducer made contact with the steel. The discrepancies encountered are felt to be due to (a) different gauges being used at three different times, and (b) perhaps due to inconsistent calibration.

(2) Thickness readings have not been taken very near the same spot every time. Though this may not cause large deviations, small differences in readings could be due to this factor.

Even in spite of these deficiencies, the averages of reasonable section thickness loss values derived from a large number of readings taken on a given bridge (at least 70 readings on each location on a particular single beam in a bridge and six different locations on each bridge) were analyzed carefully and they yielded the general results of section thickness losses for weathering steel sections in various bridges given in Table 3.

The results can be summarized as follows:

(1) In rural, mild environments the weathering steel experiences minimum corrosion losses. Results of section losses at Leesville (LV) and Boeuf River (BR) bridges, as well as the phase analysis of rusts formed on the steel in these bridges, indicate a loss of

about 0.5-1 mil/year on the exterior sections and about 1 mil/year at the sheltered interior locations. Data from field coupons as well as laboratory tests indicate still lower thickness losses, even half as much, for steel in these bridges.

(2) In bridges located in moderately harsh industrial environments, within about 20-30 km from Gulf Coast, the section losses are about 2 to 3 mils/year for exterior surfaces and 2 to 4 mils/year in sheltered areas. Luling approach span, Gibbstown, Larose, etc. are in this category.

(3) Bridges that are located in close proximity to salt water, such as the DC and HI bridges, seem to lose about 2 to 3 mils/year at the exterior surfaces and about 3 to 5 mils/year in the sheltered areas. Thus the steel in these bridges is subjected to more serious corrosion. Appreciable pitting is also encountered in steels in these bridges.

(4) The data reveals the general trend that exterior surfaces erode much less (only about half as much) than the interior surfaces in sheltered regions of bridges.

(5) Regarding the various surface chemical treatments, it could be noticed that treatments 2 and 3 lead to formulation of fine rusts and somewhat lower section losses than the rest of the treatments. However, the period of data collection is not long enough and the data not consistent enough to make a precise estimate of the magnitude of thickness losses in such treated sections.

Loss of about 1 mil/year or a fraction thereof cannot be determined accurately by taking measurements over a two-year period. Long-term

monitoring is needed. The readings should continue to be taken once every year for about 10-12 years with the same instrument after duly calibrating it every time at the bridge site just prior to taking the readings. Also, the thicknesses should be measured at locations very close to the previously measured places in order to guarantee consistency. They should not be taken on the exactly same spots, since the grease used to create good contact between the transducer and the steel would alter the rusting kinetic.

Corrosion weight losses or thickness losses could not be measured by removing the rust formed on the steel from a fixed area, say 1 sq. ft., as was planned earlier. This is due to various reasons. It is very windy at the location, and thus much of the fine, powdery rust gets lost. Also, the locations where the rust is to be removed are not simple, easily accessible sites. Hence, it poses great difficulty to collect precisely all the rust formed at such precarious locations. Furthermore, suitable equipment to collect the rust could not be assembled. A few attempts made were futile. Hence, that technique was not perfected in this project.

Pitting.

Pitting was found to be significant in coastal area bridges. Steel on bridges located far away from the coastal area, such as at Leesville (LV) and Boeuf River (BR), did not show any pits.

The maximum and average depths of pits from several readings taken at various locations on four of the six coastal area bridges on which measurements were made are given in Table 4. The averages of all the maximum readings and the average readings at similar locations on various

bridges are given in the last two columns of this Table, from which some general conclusions are drawn and interpreted as follows:

(1) Sun and rain exposed exterior surfaces generally are devoid of pitting or show very fine and shallow pits so closely located that it can be construed as a general form of uneven attack.

(2) Maximum pit depths are seen in partially enclosed, boxed locations (#5 in Table 4) above the gusset plates at the entrance to a pier, where owls and other wildlife take shelter and build their nests. Rust debris usually collects here and holds moisture for longer duration. Formation of sheet-type rust in such locations has already been explained. Fairly wide and deep pits have been seen underneath such sheet-type rust. Maximum readings of about 52 mils (1.3 mm) have been recorded at this location in the Doullut Canal bridge. The average of all the maximum values from the four bridges in the Table is 28 mils (0.7 mm) and the average of all the readings in the boxed locations is about 17 mils (0.42 mm).

Such pits have also been found on horizontal surfaces at the edge locations of a pier in the Luling bridge. Rainwater has access to this place and it has been held stagnant here. The highest reading of 41 mils (1.03 mm), recorded on the horizontal skyward face of the steel plate here, is similar to readings obtained in partially enclosed, boxed locations.

The pits at these locations, formed under sheet-type rust, are also considerably wider, compared to pits formed at other locations. They are generally round, about ¼-½ in. (6 to 12 mm.) in diameter.

Such wider and deeper pitting is due to excessive rusting on account of the steel remaining wet in this area for longer periods of time. Electron microscopic observations of the rusting process point frequently to the water aggregating in circular pools and causing hemispherical bubbles and blisters. The metal at the central regions of such water circles would be anodic and corrode in the pitting mode. The "differential aeration cell mechanism" developed by Evans [71,86] would adequately explain the mechanism of pitting. According to this mechanism, the central regions of such droplets lack oxygen supply whereas the peripheral zones get continuous, more supply of oxygen. The oxygen starved regions act as anodes and corrosion by dredging progresses. The circular nature of pits observed supports the view that water aggregates as circular droplets on the rust and contributes to the differential aeration cells.

Another possibility is that the sedimentary rust layer itself may not be uniformly dense all over, in some places possibly more so than in others. Also, it could be somewhat more adherent to the metal surface in some places than at others due to differential wetting and drying. These could also lead to the establishment of differental aeration cells.

Periodic cleaning and removal of the debris at this location, thus assuring drainage of water, is essential to prevent continued excessive pitting at such locations.

The Luling bridge on the Mississippi River near New Orleans, LA. This bridge, built with the A588 - grade A steel from the Kawasaki Steel Co., Japan (in the main span) and U.S. Steel Co. (in the approach span on both sides of the bridge), is the youngest of all the bridges in LA, opened to traffic in 1983. The bridge is located close to Lake Pontchartrain in New Orleans and petroleum refineries and petrochemical companies nearby and finds itself vulnerable to severe corrosion problems. The rust formed on the steel is already starting to coarsen. Cleaning and maintenance methods for this bridge are proposed later in this report to mitigate the severity of the attack and metal loss.

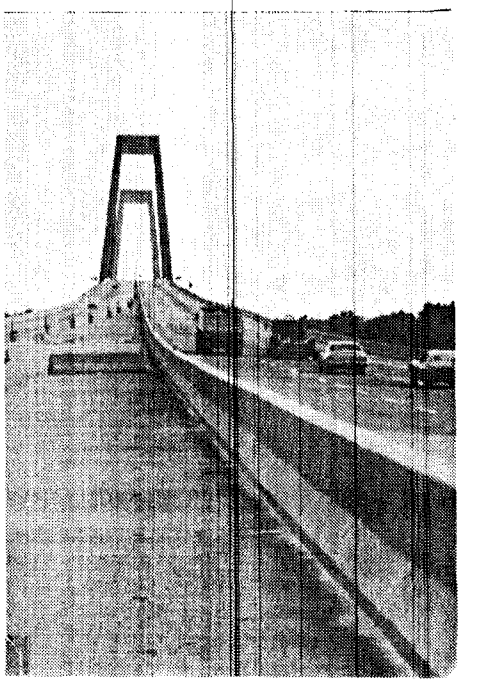

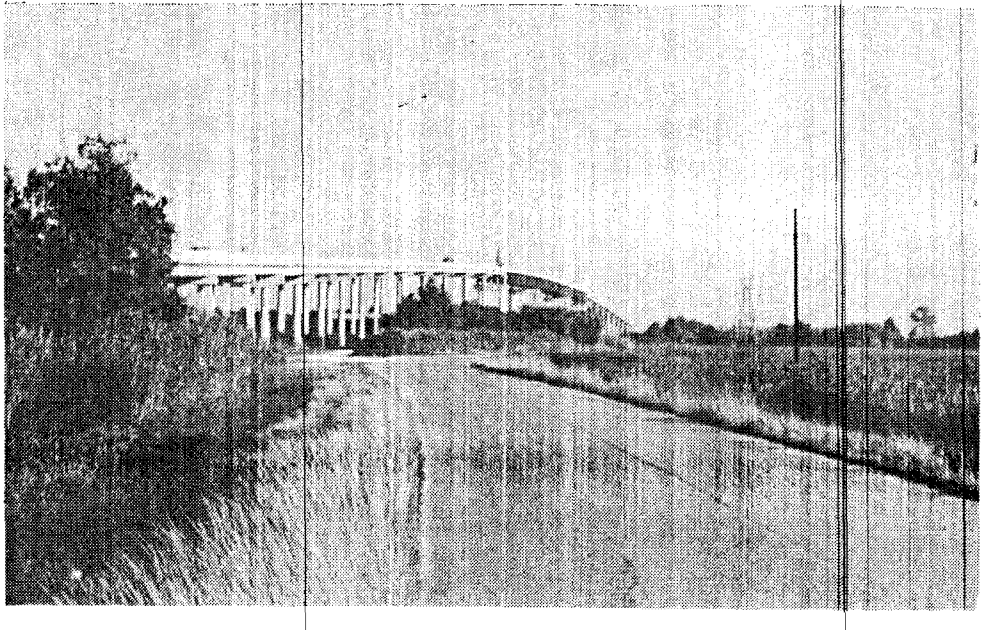

View of the Doullut Canal (DC) bridge with the middle span made out of A588 - grade A weathering steel. This bridge parallels the Mississippi River, flowing very close to it on one side, and a salt water lake on the other side. It spans over the lake at its periphery. The steel picks up salt from the air and experiences coarse rusting and pitting. The problem is not severe on the exterior faces, and it is judged that maintenance treatments proposed in this report would adequately take care of the problems.

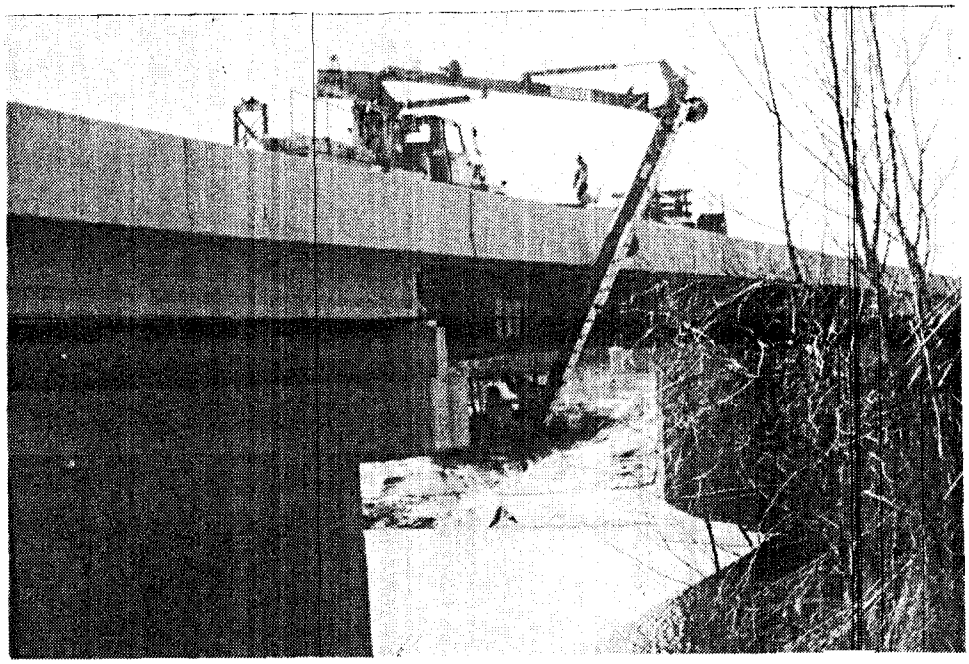

View of the Boeuf River (BR) bridge with the snooper in place during the study. This bridge is built with the A588 - grade B steel. Being in the rural area, far away from the Gulf coastline, it is free from any serious corrosion problem.

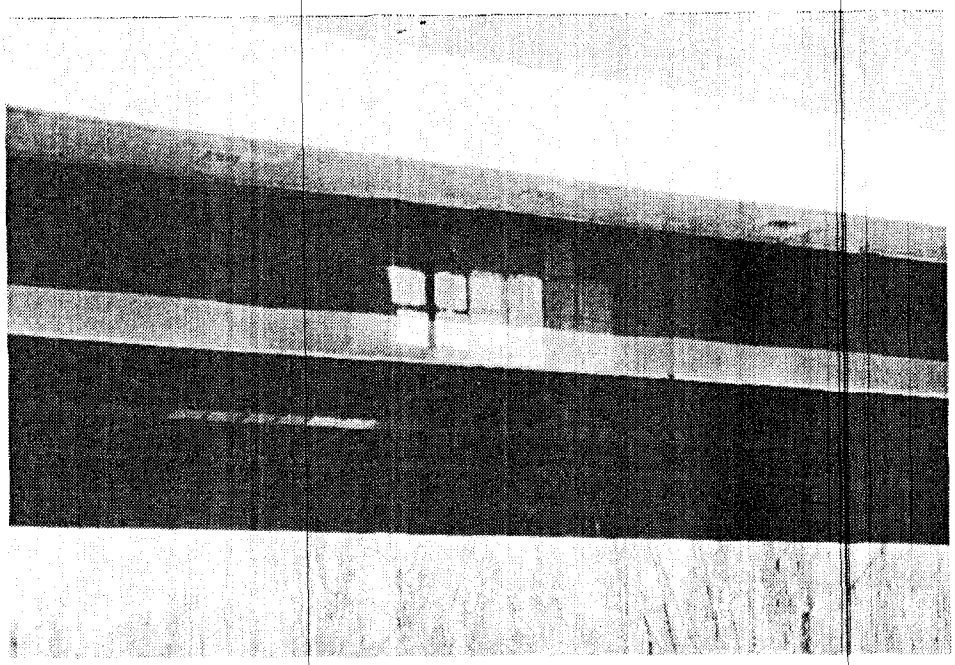

Exterior surface, as shown here on the BR bridge, gets exposed to sunlight and rain wash and hence experiences in general the least damage, whereas the interior areas that are sheltered encounter more corrosion loss. Even so, this is not serious at BR. This can be taken as a model bridge devoid of problems.

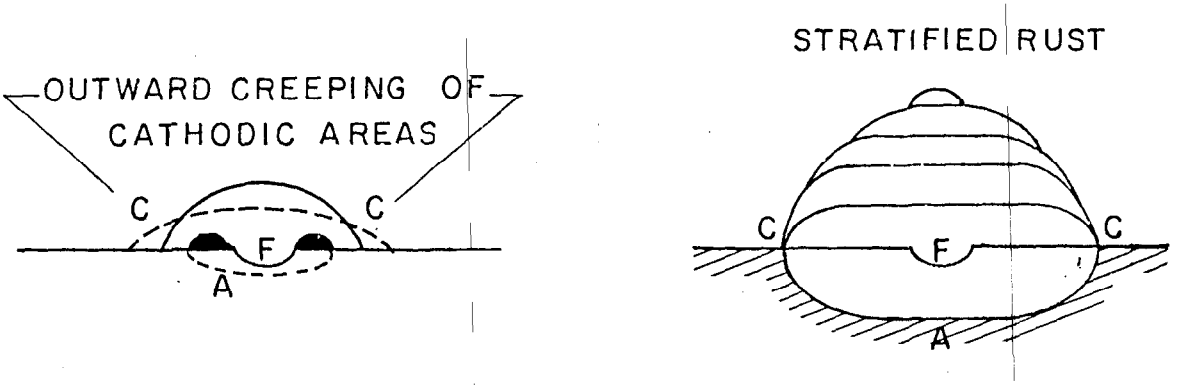

DIFFERENTIAL AERATION CELLS

(A) EVANS SALT SOLUTION DROPLET MODEL

(B) PROPOSED MODEL FOR PITTING UNDER A RUST MOUND OR FLAKE

(C = Cathodic, A = Anodic, F = Site of First Attack)

MECHANISM FOR PITTING IN STEELS

(3) Pits somewhat less severe, but about half the size of the pits seen in boxed locations, are seen on the bottom faces of horizontal and inclined beams (#4, 7, 10 in Table 4). The average of the maximum readings on such surfaces from various bridges is about 13 mils (0.32 mm) and the average pit depth from all the readings is about 9 mils (0.23 mm) on the surfaces facing downward. In contrast, the pits on similar beams on surfaces facing upward (#3, 9 in Table 4) are slightly less deep. The average value of the maximum readings is about 10 mils (0.25 mm) and the average pit depth from all readings is about 7.6 mils (0.19 mm). The readings on the top surfaces were consistently smaller than the readings on the bottom surfaces.

It appears that at least in some bridges the pits on the surfaces of beams facing downward are slightly deeper than the pits on opposite faces, on the surfaces facing upward. The gravitational forces do not apparently play a dominant role in determining the pitting mechanism in weathering steel. Instead, the surface tension forces which would make the water form droplets or collect into circular pools seem to be exerting a dominant influence. In other words, the wetting characteristics of the rust by water seems to be an important issue. Water may evaporate more from such pools formed on skyward surfaces than from analogous pools on lower surfaces facing downward. At any rate, this should be studied further more thoroughly.

(4) The bottom faces of the edge girder beams on both sides of the bridges (#8 in Table 4) seem to experience less severe pitting than the bottom faces of the inner beams. This could be due to

somewhat better drying due to more aeration and heating of the exterior web plates by solar radiations.

(5) The vertical faces of the beams and side plates (#1, 2 in Table 4) experience perhaps the least amount of pitting. The average of maximum pit depths is about 9 mils (0.22 mm) and the average of all readings is about 6 mils (0.15 mm). These low values can be explained as due to the fact that the vertical faces hold less water as it collects and drains down continuously.

The above discussions pertained to maximum as well as average pit depth values at different locations. It should be realized that pitting is a statistical phenomenon, that is, that pits of different depths would be seen at all locations; however, pits around the average size would prevail widely. This implies that shallower as well as deeper pits, though small in number, would be found at each location. This necessitates pit depth profile studies wherever pit depths vary widely.

Representative pit depth profiles for four different locations on the Luling bridge are shown in Fig. 3. All of them show bell-shaped plots. Fig. 3 (A) shows pit depth variations at a spot corresponding to the partially boxed locations, where water pooling was high. There are more pits in the 15 to 20 mil depth range than in other size ranges, giving a peak at around 18 mils in the bell-shaped profile.

Fig. 3 (B) corresponds to the nearly vertical face of a trapezoidal box corresponding to location #1 in Table 4. This figure shows that there are more pits in the 4 to 8 mils depth range than in others. Fig. 3 (C) and (D) represent, likewise, depth profiles corresponding to location 2 (vertical face) and location 4 (horizontal surface, facing down) in Table 4, respectively.

The number of pits ranged from 10 to 20 per $in.^2$ in most locations but was much less, about 6 per $in.^2$, in the partially boxed areas. The pit density was much larger wherever finer pits were seen.

It was found also that sulfides or other inclusions are not needed to nucleate the pits in weathering steels. Uneven wetting and retention of water on the surface in some areas more than in others would cause more rust to form in such regions, which would activate the formation of differential aeration cell. More rusting occurring underneath such regions and seasonal variations of the rusting kinetic lead to stratification of the rust mound and to lateral spreading or widening of the pitted areas. As such, sharp and deep pits do not form, but wider and less deep pits abound.

Increased salt content of the atmosphere would not only increase the corrosion rate and, hence, the pitting rate, but would also affect the surface tension and wetting characteristics of the water. It can be noted that wider and deeper pits were seen in chloride-laden environments.

The bulk of the data indicate that partially boxed edge locations in sheltered zones are worthy of considerable attention. They should not only be periodically cleaned but treated, if necessary painted, to prevent the pitting and excessive corrosion (section loss) problems.

Results from Field Tests

Sheltered Location Exposures. The plots of weight losses in g/dm^2 vs. exposure time in days are given in Fig. 4 (a to d). These contain the data from the II set of exposure, that is from the samples that have been exposed once, brought to the laboratory, analyzed, reprocessed for second time exposure in the field and exposed again at respective bridge sites for

periods up to 20 months. The plots from data of specimens brought to the laboratory after the first exposure were similar in the cases of Gibbstown and High Island exposures, but yielded linearly or exponentially increasing weight losses with time for some treatments, which could be due to experimental errors.

As is commonly found, the regression analysis of data with the power fit relation $y = K.t^N$, where Y = wt.loss in g/dm^2, t = exposure time in days and K & N are rate constants gave the best results, R values being > 0.97. During analysis of data one or two deviating data points were discarded, but usually five or more out of seven data points were good and used.

In the power fit relation given above the value of K provides a measure of the inherent reactivity of the metal surface, whereas the value of N relates the resistance to transport processes within the corrosion product [8]. A value of N close to 0.5 indicates good parabolic oxidation, congenial for stabilization of the rusting process. On the other hand a value close to 1 indicates the dominance of the linear corrosion process, while the value close to zero indicates great stabilization tendency.

Table 5 summarizes the values of K & N obtained for various treatments for atmospheric exposure at various bridge sites. Data from Gibbstown exposure show the lowest values for all treatments, values of N for surface treatments being around 0.25. These and the corresponding plots indicate good stabilization tendencies. Specimens located at High Island likewise show a good bit of tendency for the corrosion process to become stabilized and this is certainly a welcome result.

Data from specimens located at Leesville and Luling, in contrast, do not show good tendency toward stabilization. This could be due to the fact

that not enough rust is formed at the Leesville site, but the observation that the rusting process does not slow down at Luling as easily as at Gibbstown or High Island might be significant, for it could be due to pollution effects. Luling bridge, being in the vicinity of petroleum refineries and chemical plants, does get exposed to considerable industrial effluents, along with dust from grain elevators nearby on the banks of the river.

It is noteworthy from the figures that the chemical conversion type treatments are generally good to minimize the thickness losses and to stabilize the rusting process. Treatment 3 seems to be ideally suited for Luling and High Island, whereas Treatment 2 is found to be good for Leesville and Gibbstown. The IRAS data has shown also that Treatment 3 is good for Gibbstown insofar as it enabled the retention of the protective amorphous rust phase for over 2 years.

The results obtained over 18 months exposure give rise to the approximate thickness loss values given in Table 6. (Note that thickness loss in μm is obtained by multiplying the weight losses suitably, in our case by multiplying the wt. loss in g/dm^2 by 12.72. Also 1 mil = 10^{-3} in. = 25 μm). There is a large weight loss in about the first three months, beyond which there is a drop in the rate of weight loss; that is, there is a change in the slope of the curve after the first 3 months. This would mean that initially the corrosion process starts off at a rapid pace, but after the initial corrosion product layer has formed, it continues at a reduced pace. This could be due to a changeover in the mechanism of the rusting process.

The losses at High Island site are about 25-40% more than the losses at Gibbstown, which are about similar to the values obtained at Luling.

Leesville location shows very low thickness losses, about 1/6 - 1/3 of the values at locations close to the Gulf Coast. These losses in sheltered locations are about 50-200% more than for exterior exposure results from CEBA exposures, see Table 6. The values from Leesville are about 50-60% smaller than the CEBA exterior exposure losses.

Open, Exterior Location Exposures. The solar radiations hitting the exterior surfaces of the bridges were found to raise the temperature of the side web plates well over the ambient levels. The rust layers formed on the steel surface must be good absorbers for solar radiations. The plates, usually about 3/8" - 1/2" thick and vast in area, had their temperatures raised to 120-140°F (50-60°C) as the radiations fell directly on them. This was the case for nearly six hours in a day for each surface, as most of the bridges are nearly parallel to north-south. Obviously this caused good drying and baking of the rust, and the surfaces facing east can be expected to be wet for less time than the surfaces facing west.

It is very windy at the Gibbstown bridge location, and it appeared also that the wind swirls and blows much stronger underneath the bridge in sheltered locations than on the exterior side faces. Visits to the bridge during different seasons to retrieve the racks indicated that this was the general case most of the time.

Plots of weight loss data from specimens of A588 - grade A steel exposed at the Engineering CEBA building at LSU, Baton Rouge, as a function of exposure time up to 1 year are given in Fig. 5 (a,b). The plots for both the grade A varieties made by the U.S. Steel Co. as well as the Kawasaki Steel Co., Japan, are similar, though the latter has a very small addition of nickel. The similarity of the two sets of data would prove the

validity of results, for these were collected at different time periods for the two varieties.

The K & N values obtained for the plots from the regression analysis are given in Table 7. The plots show highest weight losses for steels with the mill scale left as such, indicating the removal of the mill scale layer in the first three months. Thereafter the plots are nearly parallel to the plots for Treatments 1 to 7. All these plots are essentially linear and the power constant N is close to 1 for Trts. 1 and 7, which do not have any chemical treatment. These two conditions obviously do not lead to stabilization of the rusting process within one year and indicate a nearly linear corrosion process. Trt. 6 with 10% tannic acid solution yields somewhat lower corrosion losses than for Trts. 1 and 7, but the loss is higher than for other treatments. The value of N is high for Trt. 6 also. Trts. 3 and 5 show similar curves, but the weight losses are somewhat lower than for Trt. 6. In contrast, Trts. 2 and 4 seem to show better characteristics. The weight losses are not only minimum, the curves show better stabilizing tendencies as well. Based on these data, it would seem that Trts. 2 or 4 utilizing phosphoric acid would be good for exterior, bold-exposed surfaces.

The results give rise to the following approximate thickness losses in the first year.

Trts. 1 & 7:	20μm (0.8 mil);	Trt. 6:	15μm (0.6 mil);
Trts. 3 & 5:	10μm (0.4 mil);	Trts. 2 & 4:	9 μm (0.35 mil)

Location of the exposure site at LSU in Baton Rouge can be considered to fall in a mildly industrialized area and the losses determined compare

favorably with the values determined by Townsend and Zoccola [10], for a loss of about 3 mils can be expected over a five-year period. These values are somewhat similar to the values determined in Australia, but are much less than the values obtained by McKenzie in England [2].

The values obtained in exterior bold-exposure in Baton Rouge are about 1/3 to 2/3 of the values obtained for steel coupouns in exposure at sheltered locations under the bridges in the Gulf Coast area, the lower ratios 1/3 to 1/2 being obtained for treated conditions and slightly higher ratios 1/2 to 2/3 for the sandblast-cleaned condition. However, these values are about equal (for Trts. 3 and 5) or nearly 2 (for Trts. 1, 2 & 4) and 3 (for Trt. 6) times the values obtained for sheltered location exposure at Leesville in rural areas. These results indicate the importance of location, and particularly industrial pollution, in altering the corrosion weight losses of weathering steels by rusting, and more losses can be obtained in exterior bold-exposure in an industrial site than for exposure under sheltered conditions in rural areas. However, at a given site in a given type of environment in Louisiana and Texas, it is found that the losses in exterior exposure are about one half of the losses at the sheltered locations.

The thickness losses reported by various investigators around the world are compared with the results obtained with field coupons in this study in Table 8. Our results with field coupons compare favorably with those of Townsend and Zoccola [10] for exterior, bold exposures, and McKenzie [2] seems to have obtained much larger losses for exterior exposure in industrial environments. The industrial atmosphere must have been more severe and harsher than the mild industrial atmosphere in Baton Rouge, LA or in Bethlehem, PA. McKenzie has obtained lower losses in

industrial atmospheres in sheltered locations than in open, exterior exposures. Our results are in reverse and we have obtained about 50 to 100% more losses in sheltered locations in industrial environments than in exterior locations. The losses we found in rural and marine atmospheres would approximate the values of McKenzie for sheltered locations. The losses in sheltered locations averaged to about 1 mil/year in industrial atmosphere and there is a good bit of tendency for the corrosion process to stabilize in Gibbstown, but not at Luling. Thus we can expect a loss of about 4 to 5 mils in 5 years in sheltered locations in industrial atmospheres, compared to about 3 to 4 mils in open, outdoor exposure. These values, however, are of similar magnitude as obtained by others. However, our values are definitely much higher than reported by Reed and Kendrick [18] from California, but compare favorably with those obtained by Townsend and Zoccola in exterior exposure. No data is available for losses in sheltered locations apart from those of McKenzie.

Laboratory Test Results.

Accelerated laboratory tests enable the identification of the behavior of the weathering steels in long-time exposure under field conditions. Though in practice the factors that contribute to corrosion vary periodically and seasonally and abrupt changes could be brought about, the laboratory tests are performed keeping most of the secondary variables constant and varying only one or two of the primary parameters. As wet-dry cycling is an important variable in the actual exposure, accelerated atmospheric exposure simulation included wet-dry cycling. The effects of chloride and sulfate ions introduced by pollution were also analyzed. Two different types of accelerated wet-dry cyclic tests were undertaken - one

to simulate the conditions in sheltered areas, which was done in a closed chamber in darkness, and the other simulating rainfall on the exterior, bold exposed surfaces. In addition to these two tests, tests performed in salt fog chamber with water containing 0.1% salt approximated the exposure to Louisiana's hot and muggy atmospheres, which contain traces of salt in coastal areas. The total immersion test was performed to identify the performance characteristics of the steel and analyze the rust layers formed under these conditions. Such situations prevail in areas where the condensed or rain water accumulates and stagnates due to drainage holes being plugged in. The electrochemical tests were performed to identify, if possible, the corrosion mechanism and to see under what conditions pitting occurs. The results from these tests are described below and correlated to field data.

Fig. 6 (a to d) shows the plots for weight losses vs. exposure time for the four steels studied in the Accelerated Atmospheric Exposure Simulation Test - Sheltered Location Equivalent. The corresponding plots for the four steels in analogous tests simulating exposure at exterior locations are given in Fig. 7 (a to d).

Fig. 8 (a to d) likewise shows the results in plots for the salt fog test and Fig. 9 (a to e) gives those for the continuous immersion test in 3.5% salt water.

The average corrosion losses that occur in the various tests are summarized in Table 9. The plots for 2200 cycles in the atmospheric exposure simulation tests yield thickness losses over a six-year equivalent period. The plots for the sheltered location equivalent exposure do not seem to stabilize, whereas the plots for the open, bold exposure equivalent tests indicate only slight stabilization tendency for the rusting process.

The results of average thickness losses for 2200 cycles (6-year equivalent) are divided by 6 to yield average annual losses, which are also given in the table. The values of N are also close to 1, indicating the nearly linear process of corrosion. Thus the averaging is justified and the values are not far from the true annual losses.

The results show that minimum losses of about 0.2 to 0.5 mpy occur for all steels in the bold exposure equivalent test in the presence of chloride and sulfate ions. However, tests performed without these yield still lower results, about 0.04 to 0.1 mpy. The latter values compare favorably with those of Reed and Kendrick [18] in outdoor exposure tests in California. The rest of the values approximate those of the other scientists. The exterior bold exposure at CEBA has yielded 0.8 mpy for the first year and, given the tendency for slow stabilization, the results in exterior, bold exposure at CEBA would approximate our laboratory test results. The actual losses in exterior, bold exposure appears to be very site dependent and more losses can be expected in the marine and industrial sites than in rural areas. They are also very dependent on rain wash.

There is good correlation between the results obtained in the simulated sheltered location exposure test and the results of exposure tests performed in the field at the bridge sites. The average loss is about 1 mpy for the industrial site and slightly higher about 1.5 mpy for the near-marine site. These values compare favorably with the average loss of about 1 mpy in analogous laboratory test. (See Table 12.)

The immersion test yields slightly higher thickness losses, about 2.5 mpy, than these atmospheric exposure simulation tests.

Of the five steels tested in immersion, Riverten R of the Kawasaki Steel Co. is the one which showed some tendency for stabilization. The

values of K and N in the power fit relation are given in Table 10. These values for various steels were compared by taking the averages of the values for treatments 2 to 6 for all steels. Both Riverten R and A588 - grade A (U.S.) had low values for both K and N, signifying slower rusting process and tendency for stabilization.

Treatment 6, representing 10% tannic acid application prior to immersion and drying, yields best results for all steels in the immersion test. The average thickness losses for 6 months are: 0.46 mils for A588 - grade A (U.S.), 0.87 mils for grade A (Kaw) and grade B, which translate to the losses in the first year of: 0.8 mil for grade A (U.S.) and 1.6 mil for grade A (Kaw) and grade B. The steels still show some stabilizing tendency of the rusting process when their surfaces are chemically treated with the passivating acids used.

For Trt. 6, comparing the results of Riverten R for 100 days exposure with those of others, it can be seen that the average thickness loss is about 0.2 mil, which is about 1/2 and 1/4 as much as that for A588 grade A and grade B, respectively (data compared in figures). In untreated conditions, for Trts. 1 and 7 the corrosion losses increase linearly with immersion time for most steels. Trt. 9 with mill scale seems to show some stabilization tendency compared to Trts. 1 or 7 for both A588 - grade A (Kaw) and A36 steels. Results for Trt. 7 - grade A (U.S.) and Trt. 1 - Riverten R appear to be anomalous and some of the data could be wrong.

Taking Trt. 1, for which data is available for all steels, the average thickness losses in immersion in the first year could be about: 65 μm (2.5 mil) for grade A (U.S.), grade A (Kaw) and grade B varieties, about 60 μm (2.4 mil) for A36 steel and perhaps about 50 μm (2 mil) for the Riverten R.

These are values extrapolated for 1 year and may be slightly inaccurate. However, the trend can be analyzed from these data.

The important findings in immersion tests are that the thickness losses are generally linear for the untreated conditions and they could be as much as 2 - 2.5 mils per year. With chemical treatments or even with a mill scale layer being present to start with there is a tendency for the corrosion process to slow down and stabilize, and Trt. 6 with the tannic acid works best in immersion situation. A slimy layer seems to be formed on the surface in the latter case, which appears to be beneficial. Bacterial action on such layers could be responsible for promoting the formation and retention of the "amorphous bulk (AB)" layer, along with some ferrihydrite. This would be discussed again later under rust analysis and relative merits of different surface chemical treatments.

In comparison to these three tests, the salt fog test as well as the electrochemical test yield much higher weight and thickness losses. The average value of the thickness loss is about 30 to 60 mpy in the salt fog test, whereas in the electrochemical test values of about 60 - 100 mpy have been obtained. The latter test evaluates in a fast manner the corrosion losses during the initial dissolution process and usually the corrosion process starts out very fast initially. These values indicate also the maximum losses possible and such conditions could prevail in certain localized corrosion processes. The presence of deep pits is certainly an indication of high rates of corrosion losses, if not to the large extent as obtained in the electrochemical test.

That the salt fog test yields maximum and linear corrosion rates is not surprising, for the corrosion progresses in a hot and 100% humid atmosphere in this test. Presence of chloride also aids vastly in the

corrosion process. Due to high humidity, a film of water should always be present and in conjunction with chloride ions the dissolution rates are very high, as much as in the electrochemical test under open circuit conditions. Slightly elevated temperature aids also the corrosion process.

Both in the salt fog as well as electrochemical test, the protective amorphous rust apparently does not get stabilized and this enables the corrosion process to continue unmitigated. However, in the total immersion test, a protective amorphous rust layer does form and hence the corrosion rates are low. An average loss of about 2 to 3 mpy is indeed acceptable under total immersion conditions. However, pitting could occur. Also, what the average losses would be under total immersion conditions when the electrotyte (fluid) moves (flows) needs to be ascertained further. This could be high due to erosion losses.

The losses obtained in field tests with coupons, as well as from field thickness measurements at various time periods, are compared with the losses found in the various laboratory tests in Table 12. Several photographs taken in the field at the bridge sites illustrating the rusts and conditions observed, as well as the methodology used, are included in Appendix.

Structure and Morphology of Rust Phases.

There are various forms of rust and counting the amorphous varieties at least a dozen different phases can be recoganized. In atmospheric exposure, under wet conditions, the oxyhydroxides of iron form and are retained. The most stable form of rust is α - Fe_2O_3 (hematite), which results only when these oxyhydroxides are heated at elevated temperatures.

A major contribution of this study is the sound establishment of the usefulness of the infrared spectroscopic (IRS) technique in rust structure and phase analysis. The IRS spectra of several standard forms of rust have been obtained, compared with those known in the literature and used to identify not only the rust phases present in the various field rusts, as well as those that have been obtained in the various tests, but also to follow the rust phase transformation sequences. Fig. 10 indicates the IRS spectra of several standard rust phases that are commonly encountered in various types of rusts. Fig. 11 shows several field rusts obtained from various bridges analyzed by this technique.

Fig. 11 (c) shows γ- and δ-FeOOH in a brown colored rust scraped off from an A36 steel beam bold-exposed to the ambient conditions. Under bold-exposure similar phases form on weathering steels also. Powder rust collected from the Luling bridge shows also δ- and γ-FeOOH (γ*) phases with traces of an unknown phase, Fig. 11 (d). Coarse flakes obtained from the field also have these two phases, Fig. 11 (f).

Unlike these samples, rust samples collected from the air-side or from intermediate layers of some of the sheet specimens show γ - $Fe_2O_3 \cdot H_2O$ designated as γ, Fig. 11 (h). This phase has been found to have different degrees of crystallinity. A pattern from its highly amorphous analogue is shown in Fig. 11 (j).

Upon exposure to the atmosphere, within the first month or so, the first semi-stable rust forms. This rust has been identified using IRS to be either the amorphous γ-FeOOH or the so-called "Amorphous Mix (AM)", which was judged to be a potpourri of γ-, and δ-FeOOH, ferrihydrite and possibly one or two other initial intermediate complexes. FeO and ferrous hydroxide have likewise been observed in some samples. As time of exposure increases, various crystalline rust phases develop from the amorphous mix phase. Initially, these different phases exhibited high degree of non-crystallinity and only after a long duration were fully crystalline phases encountered.

IRS data also showed that in open, bold-exposed specimens the stable phases that were obtained even after a 2-year exposure were γ-FeOOH and δ-FeOOH, both still exhibiting a considerable degree of non-crystallinity. δ-FeOOH remained highly non-crystalline. The X-ray diffraction patterns could not establish the presence of this δ-phase, although its presence was well established through IRS patterns of rusts.

Nearly similar results were obtained in interior, sheltered location exposure also. γ-FeOOH formed initially, along with the amorphous rust fraction. This was identified in the X-ray diffraction patterns from a broad peak at $2\theta \cong 12°$ from the planes that give rise to the strongest peak at this location for Mo - K_α X-rays. The pattern also indicated a large degree of amorphous nature. However, rusts collected after longer exposure time periods showed successively the diminution of amorphous γ-FeOOH and formation of crystalline phases, particularly γ-$Fe_2O_3 \cdot H_2O$, with a strong peak at $2\theta \sim 16.5°$ (for Mo - K_α). Even the latter phase has the strongest peak, according to ASTM-data [88] for diffraction from planes at $2\theta \sim 12°$. However, since several other rust phases (magnetite, β - & δ - FeOOH,

etc.) have their strongest peaks at the location corresponding to 2θ ~ 16°, the appearance of the strongest peak at 2θ ~ 16° was not surprising. It was deduced that the highly amorphous γ-FeOOH and "AM" components formed initially and gave rise to crystalline γ-$Fe_2O_3 \cdot H_2O$ and δ-FeOOH phases. α-FeOOH was likewise found to increase in amount and become somewhat more crystalline. Its strongest peak occurs at 2θ ~ 9.8° (for Mo - K_α).

The variations in the intensities of the X-ray diffraction lines in the low-angle region as a function of exposure time are shown in Fig. 12 for rusts collected from A588 - grade B specimens, exposed in sheltered locations under the bridge at High Island, TX. Unlike in exterior exposure, crystalline phases form much sooner in sheltered location exposure.

XRD and IRS patterns of rusts formed on inhibitor acid treated surfaces were also obtained and analyzed. These showed that Trts. 2 and 3 with phosphoric acid and phosphoric-benzoic acids, respectively, enabled the retention of the amorphous phase "AM" for considerably longer time periods. The results from IRS analysis are discussed later under the sub-heading "Relative Merits of Different Surface Inhibitor Treatments". These results, coupled with the relatively lower weight losses for these surface treatments, indicate that these treatments are good to promote rusting resistance. In contrast, Trt. 6 with 10% tannic acid enabled the crystallization of δ- and α-FeOOH. The weight losses for specimens with this treatment were also much higher. This is interpreted as being due to the crystallization process that leads to more porosity and access of water and oxygen to the substrate, resulting in more corrosion. The morphological studies with SEM substantiated these findings.

Representative microstructures of rust phases developed on the weathering steel surface during various exposures are given here and discussed. Detailed descriptions of morphological features are given in separate papers.

The salient feature of the "amorphous mix, AM" phase appears to be its various growth patterns on top of a flat, dense, sedimentary-type layer. This layer shows several cracks that have been developed during drying, Fig. 13 (a). Odd pillars, mounds, etc. seen (Fig. 13, b to d) with no structural features are deduced to be the AM-phase. Hemispherical and cylindrical swellings are common, Fig. 13 (e). These are probably formed due to gas or vapor evolution and many of them burst out at the initial stages, leading to subsequent development of crystalline phases in a circular area, Fig. 13 (f). These are also shown in the SEM photographs of rusts presented in Fig. 13 (g,h).

Crystalline phases such as γ-, δ-, and α-FeOOH as well as ferrihydrite form directly on top of the amorphous rust layer. All these phases form plate-like grains, but the different phases could be identified through certain unique features which have been identified in single phase rust specimens derived both from the various tests as well as from laboratory chemical synthesis.

The microstructure of γ-FeOOH is seen vividly in Fig. 13 (i). The crystals of this phase grow in thick plates, which bend and wiggle around. The plates are also laid close to each other so that a cross sectional view of an aggregate of γ-plates, i.e., a colony of γ-FeOOH, appears as a collection of worms, Fig. 13 (j). The plates are considerably thicker, indicating the faster growth rate of this phase out of the amorphous mix layer.

Crystals of δ-FeOOH are also plate-formed; they also bend and fold. However, these plates often show flowery patterns. The beautiful rose-type flowery pattern of δ-FeOOH has been observed in both the synthetic rust, as well as in the field rusts from several bridges and rusts formed on field-exposed weathering steel coupons. Representative microstructures are given in Figs. 13 (k,l).

Crystals of α-FeOOH take on different shapes. Besides forming directly from the amorphous layer, they have been found to form on top of the plates of γ-FeOOH also. α-crystals are generally thin, needle-shaped, rod-shaped, petal-like, and thin, flat-plate-shaped with sharp edges. Needle-shaped crystals appear as whiskers on γ-FeOOH plates at the initial stages of growth, Fig. 13 (m). These grow into rods in time. The rods of α-FeOOH have been found to start out of the amorphous layer as well, Fig. 13 (n). The whiskers could grow into plates as well, but these plates probably do not grow to great extent. They probably become small petal-shaped. Several small petals formed on a hemispherical dome of the amorphous layer appear as a carnation flower. Representative flower patterns of α-FeOOH are shown in Fig. 13 (o,p).

Thin, petal-shaped crystals of α formed directly from the AM-layer appear as a collection of rice grains, as seen in Fig. 13 (q). Though the identity of these phases had not been firmly established at the time of photographing the microstructures during SEM analysis, correlation with the structural data from XRD and IRS analysis and inference from several photographs indicate that the designations made are the most likely ones.

α-FeOOH is known to form "nest-like" spongy patterns, as seen in Fig. 13 (r) [61]. Such patterns, as well as whiskers, have been recognized in

field rusts [89]. Another mode for the formation of α-FeOOH shall be discussed a little later.

Morphological studies firmly establish the transformation of γ-FeOOH and possibly also ferrihydrite into α-FeOOH. The transformation occurring on the surfaces of plates of γ-FeOOH is seen in Fig. 13 (s). It appears that possibly both γ-FeOOH and ferrihydrite transform to α-FeOOH, whereas such was not found on the plates of δ-FeOOH.

δ-FeOOH itself is very closely related to α-FeOOH and the transformation from δ to α could occur very easily through topotactic processes.

In the long run, γ-FeOOH and ferridydrite would be converted to α-FeOOH and a mixture of α- and δ-FeOOH phases should exist. Eventually, after the topotactic transformation of δ-FeOOH, only α-FeOOH should remain. But it is found that the establishment of equilibrium is not achieved that easily in nature. Thus, due to frequent rain wash in exterior, bold-exposure and fresh wetting taking place in sheltered locations due to condensation, rusting progresses and the final equilibrium that would dictate the presence of only α-FeOOH is reached only very rarely. In reality, a mixture of γ- and δ-FeOOH with some α-FeOOH is seen on bold-exposed surfaces, Fig. 13 (t), whereas δ-FeOOH is found to be dominant in the rusts formed on weathering steels in sheltered locations.

Ferrihydrite probably has been observed in many specimens collected from two bridges - Leesville and Luling. In the latter, it is found in the old rust, possibly the powdery rust that was left after the plate-shaped initial rust layers have been removed. The Kawasaki Steel Co.'s A588 - grade A variety in the main span was completely covered with a sheet-type patch rust at the beginning. These layers started peeling and subsequently

they were removed in open areas, as well as in towers, by air blasting. They are still present at the interior of trapezoidal boxes. Ferrihydrite mixed with quartz was seen in the powdery rust (dust) collected after these layers were removed. Based on other IRS data, a structural variant of ferrihydrite is also believed to be present. This was obtained, along with magnetite, on the dark rust-metal contact surface of the rust. These were established from the X-ray patterns of the sheet-type of rust on the rust-metal contact surface, as well as from IRS patterns of rusts scraped off from this face. At Leesville, it has been found not only in the rust removed from some bridge sections, but also on coupons exposed at this location. IRS has been the only source of identification of this phase. Its XRD pattern, however, resembled the pattern of β-FeOOH. There seems to be thus a close correlation between ferrihydrite and β-FeOOH.

The crystals of ferrihydrite appeared mostly as very fine, powdery aggregates or as aggregates of rectangular plates, laid one on top of the other, Fig. 13 (V2). The fine powdery mass can aggregate into porous mounds, tubes and walls that resemble mud walls. It appeared that several odd plates that appeared like mud walls, as seen in Fig. 13 (V1), are also made up of ferrihydrite, but clear proof is lacking. Ferrihydrite grows also in the form of uniform cylindrical tubes (noodle-shaped). These have been observed in some specimens formed in the immersion test, Fig. 13 (v). Our deductions are also in conformity with the observations of Chukrov, et al. [90].

Another phase observed in sheet-type rust samples from Luling and Doullut Canal is γ-$Fe_2O_3 \cdot H_2O$. This phase was recognized first from its XRD pattern, and later clearly differentiated from γ-FeOOH or γ-Fe_2O_3 from its unique IRS pattern. It was found on the air-side of the sheet rust

samples. SEM observations of phases at this location indicated sandy grains, Fig. 13 (w), or aggregates of such sand grains into mounds that appeared like "ant" or "termite" nests [89]. Such microstructures are deduced to be those of γ-$Fe_2O_3 \cdot H_2O$. This phase has also been obtained in salt fog tests carried out with solutions containing salt to different extent (0 to 3.5%). It also formed when pure water was used in this test. Based on these facts, it was deduced that γ-$Fe_2O_3 \cdot H_2O$ forms more easily under highly humid conditions, especially in the presence of salt. But immersion in salt water or continuous wetting of surfaces, as in exterior exposure by rain, stabilizes γ-FeOOH and leads to its transformation to α-FeOOH.

The structure and morphology of rust phases formed in several laboratory tests have also been studied. In the accelerated atmospheric exposure simulation tests, similar results as in field exposure have been obtained. In the test containing rain simulation, γ- and δ-FeOOH were the dominant phases. Rust specimens showed colonies of both these phases adjacent to each other, both formed on the "AM" layer. In contrast, in the sheltered location exposure simulation test, α-FeOOH was the most dominant phase after long time exposure. The α-FeOOH was found to form first in the form of a cloudy layer, which closely resolved at very high magnifications to fine whiskers. This cloudy layer was judged to be amorphous α-FeOOH, from which crystalline α grows. The growth of whisker-type crystals of α-FeOOH could be seen at the periphery of such clouds, as seen in Fig. 13 (x). Thus, this would constitute an alternate mechanism for the formation of FeOOH. It forms directly from the amorphous α-FeOOH layer.

Another important result in this work is the finding that all of the rust phases first occur in the highly non-crystallized form. Amorphous mix

"AM" itself is an agglomeration of highly amorphous rust phases. Out of "AM" developed individual rust phases in a highly non-crystallized form as well. Thus, for instance, ferrihydrite or γ-FeOOH or δ-FeOOH formed first in the amorphous form, either alone or in combinations. These were evident from XRD analysis. Only after long time periods was crystallinity developed to near completion. The IRS patterns of all these phases showed corresponding broadening of the absorption peaks.

The "Amorphous Bulk (AB)", which was detected from its typical IRS pattern, was the important phase to form in the sedimentary rust deposit developed on the surfaces of not only the weathering steels but on regular structural steel A36 as well. This phase, as can be seen in Fig. 10, has a broad transmission peak in the wave number range 1000 to 1400 cm^{-1}, with maximum intensity occurring at around 1200 cm^{-1}. The "amorphous mix, AM" was not obtained in the immersion test. The compositional and other physical differences between "AM" and "AB" are still to be established. It is possible that the "AB" has more ferrous ions incorporated in it and AM perhaps none. Further studies are underway.

The AB converts to crystalline phases steadily and the outer porous, loose layer developed on immersed specimens is composed mostly of crystalline rust phases. In the presence of chloride ions, β-FeOOH and magnetite have been obtained. The occurrence of the former phase is not definitely established through a well-defined IRS pattern. Its presence is inferred from XRD data.

As stated earlier, γ-$Fe_2O_3 \cdot H_2O$ forms easily in the salt fog test under high humidity conditions. It may form from γ-FeOOH that forms first in the first few hours or directly on the metal itself. Another important phase obtained in the salt fog test is magnetite, which was seen to form in

several layers, as in Fig. 13 (y). This magnetite layer showed swelling at its periphery, Fig. 13 (z1), which could be due to phase transformation. At the periphery of the magnetite layers, powdery and sandy γ-$Fe_2O_3 \cdot H_2O$ could be recognized, Fig. 13 (z2). It is likely that the magnetite changes to γ-$Fe_2O_3 \cdot H_2O$. How the magnetite forms and stays stable in such a highly humid and oxygen-enriched atmosphere is not obvious. It may be developed through cathodic reduction processes changing some γ to ferrous ion containing Fe_3O_4 (M). The former has only ferric ions. Through slow oxidation, M transforms perhaps back to γ or to α-FeOOH. These are being studied further.

That magnetite forms through cathodic reduction processes when rust forms through fast kinetic in large amounts is indicated by the result obtained in the sheet-type rust sample. As indicated earlier, magnetite was observed in the rust sheet at the rust-metal contact surface. This magnetite could have been formed through cathodic reduction of γ-FeOOH or AM formed first. It is unlikely that magnetite formed os at,ps½jeroc ristomg directly on the metal surface is stable in the presence of large amounts of oxygen.

Phase Formation and Transformation Mechanisms.

The mechanisms and schemes of rust phase formations and transformations given by Misawa, et al. [30,91] can be used in conjunction with the general schemes given by Bernal, et al. [49]. These are the only complete and cogent schemes found in the literature encompassing all the rust phases. Our results are compared with the schemes given by these scientists and modifications and/or amplifications are proposed.

The transformation characteristics of γ-FeOOH in air were studied using synthesized rusts. Though β-FeOOH was not obtained in any of the field samples, its transformation characteristics were also studied in air and in vacuum with a view to identifying the topotactic transformation processes.

In air γ-FeOOH transformed first to γ-$Fe_2O_3 \cdot H_2O$ upon heating at around 190°C. The latter formed in highly amorphous form first and seemed to gradually crystallize. It subsequently became amorphous again and transformed to α- Fe_2O_3. The latter was obtained in a highly non-crystalline form at first and changed to completely crystalline form slowly.

The β-FeOOH changed in air, likewise, to γ-$Fe_2O_3 \cdot H_2O$ in a highly amorphous form, which subsequently became crystalline and non-crystalline before converting to α-Fe_2O_3. α-FeOOH was not obtained in either case. γ-$Fe_2O_3 \cdot H_2O$ seemed to change straightaway to α-Fe_2O_3.

In vacuum, however, β-FeOOH first changed deminantly to β-Fe_2O_3, which has been identified easily from the water peak slowly disappearing [92]. β-FeOOH obvisouly did not lose all the water or β-$Fe_2O_3 \cdot H_2O$ must have been formed, for upon further heating γ-$Fe_2O_3 \cdot H_2O$ formed. Further transformation sequence was as in γ-FeOOH.

The following transformation sequences are proposed:

In air and in vacuum:

$$\gamma - FeOOH \rightarrow \gamma\text{-}Fe_2O_3 \cdot H_2O(\gamma)(am) \rightarrow \gamma \rightarrow \gamma(am) \rightarrow \alpha(am) \rightarrow \alpha - Fe_2O_3(\alpha).$$

In air and in vacuum:

$$\beta - FeOOH \rightarrow \beta - Fe_2O_3 \cdot H_2O \rightarrow \beta.Fe_2O_3 \cdot H_2O(am) \rightarrow \gamma(am) \rightarrow \gamma \rightarrow \gamma(am) \rightarrow \alpha(am) \rightarrow \alpha \ .$$

[(am) = not well crystallized].

$\alpha - Fe_2O_3$ forms only when heating is applied. Otherwise, as explained earlier, α - FeOOH would formafter a very long period of time. These transformations are all judged to be topotactic in nature.

The results given above for the transformation of γ-FeOOH to α-FeOOH through γ-$Fe_2O_3 \cdot H_2O$ is one of the paths and this perhaps does not require nucleation and growth. However, as seen from SEM micrographs, γ-FeOOH can change directly to α-FeOOH through nucleation and growth. This scheme is advocated by Misawa [30]. However, we see that these are not the only paths. α-FeOOH can form directly from an amorphous analogue, which itself forms directly under certain circumstances on steel in the form of a cloud-layer. It is deduced that fast reactions at high pH levels might induce the formation of such amorphous α-FeOOH clouds.

In outdoor, exterior exposures either γ-FeOOH (am) or amorphous mix forms at a pH around the neutral level. These slowly change to δ-FeOOH and α-FeOOH, as already explained. Ferrihydrite apparently forms only under specific conditions. Its formation might require dusting (silicon and/or calcium) and sulfur. Sulphate-reducing bacterias might be responsible for its formation and growth. No information is available on the conditions of formation of ferrihydrite in the atmosphere-exposed specimens. Since it is formed in Leesville extensively, these inferences appear to apply. It may form in the presence of chloride ions under bacterial activity instead of β-FeOOH. More work is needed on ferrihydrite.

Due to frequent rain wash, the amorphous rust layer is stabilized and this provides for improved corrosion resistance. The Japanese scientists are of similar view. But why this occurs needs to be studied further. The effects of solar irradiations could play a dominant role. These effects are not known.

The results indicate that in the absence of rain wash and solar irradiations in the sheltered locations, the rusting continues unabated in the marine and marine-industrial areas. Crystallization is readily obvious and the porous crystalline phases formed are not curtailing the corrosion processes. In the presence of chloride and alternate wetting and drying, the rusting continues at about twice the pace as compared to the exterior, open-exposed surfaces.

The initial scale layer found on the as-received (rolled) steel is composed of magnetite. This layer wears off in about 3 months in exterior exposure, but lingers longer in sheltered locations. In regions where the magnetite layer has defects, attack by water vapor is made. Such regions probably act anodic to the rest of the areas and anodic oxidation processes occur, converting the Fe^{2+} ions in magnetite to Fe^{3+} ions. Fe_3O_4 converts to γ-Fe_2O_3 with compositional defects, that is having oxide-ion vacancies. This is turn becomes hydrated γ-$Fe_2O_3 \cdot H_2O$. This transformation then progresses, converting magnetite to γ-$Fe_2O_3 \cdot H_2O$, which in turn transforms to δ- or α-FeOOH. Evidence for this has been obtained in the field. The transformation causes loss of adhesion and peeling. It is possible that some ferrihydrite forms at the magnetite scale-metal interface, which leads to slight passivation of the metal. The magnetite-peeled metal seems to passivate more easily in the absence of chloride,

probably because of the presence of ferrihydrite. This needs to be verified.

Based on the results obtained in this study, the following structural transformations can be proposed:

Initial Fast Process:

$$Fe \rightarrow Fe^{2+} \rightarrow Fe(OH)^{+} \rightarrow Fe(OH)_2 \rightarrow \begin{matrix}\text{Green rust} \\ \text{complexes}\end{matrix} \rightarrow \begin{matrix}\text{AM (or)} \\ \gamma\text{-FeOOH(am)}\end{matrix}$$

Slow Further Transformations:

$$Am \rightarrow (am) \begin{cases} \gamma\text{-FeOOH} \\ \delta\text{-FeOOH} \\ \text{Ferrihydrite} \end{cases} \rightarrow \text{am.}\delta\text{-FeOOH} + \gamma\text{-FeOOH(cryst.)}$$

$$\begin{matrix}\text{under alk. or} \\ \rightarrow\ \rightarrow\ \rightarrow\ \rightarrow \\ \text{acidic conditions}\end{matrix} \quad \delta\text{-FeOOH} \pm \alpha\text{-FeOOH} \quad \begin{matrix}\text{topotactic} \\ \rightarrow\end{matrix} \quad \alpha\text{-FeOOH.}$$

Alternate routes in chloride-laden environments:

(i) $AM \rightarrow \gamma\text{-FeOOH} \rightarrow \gamma\text{-}Fe_2O_3 \cdot H_2O \rightarrow \delta\text{-FeOOH} + \alpha\text{-FeOOH} \rightarrow \alpha\ FeOOH$

(ii) $AM \rightarrow \beta\text{-FeOOH} \rightarrow \beta\ Fe_2O_3 \cdot H_2O \rightarrow \gamma\text{-}Fe_2O_3 \cdot H_2O \rightarrow \delta\text{-FeOOH} +$ $\alpha\text{-FeOOH} \rightarrow \alpha\ FeOOH$

(iii) $AM \xrightarrow[\text{redn.}]{\text{cath.}} Fe_3O_4 \xrightarrow[\text{oxidation}]{\text{anodic}} \gamma\text{-}Fe_2O_3 \cdot H_2O \rightarrow \delta\text{- or } \alpha\text{-FeOOH.}$

Final Transformation:

$$\alpha\text{ - FeOOH} \rightarrow \alpha\text{ - }Fe_2O_3.$$

The results of immersion tests indicate:

$$Fe \rightarrow Fe^{2+} \rightarrow Fe\ OH^{+} \rightarrow Fe(OH)_2 \rightarrow \text{Amorphous Bulk (AB)}$$

Fe O

AB → cryst. (in loose rust) (adherent rust)

- γ-$Fe_2\ O_3 \cdot H_2O$
- δ-FeOOH
- α-FeOOH
- β-FeOOH
- ferrihydrite
- $Fe_3\ O_4$

The transformation processes prior to the initial stages are not well established in this study. However, the results obtained have indicated fairly fast formation of γ-FeOOH (am) or AM in open atmospheric exposure. The rust deposit formed on weathering steels after electrochemical tests also indicates the formations of these two phases. FeO and perhaps $Fe(OH)_2$ have been obtained in a few cases, mostly in the laboratory tests or in inhibitor-treated specimens in exterior, open-exposure at the initial stages, in the first month. These phases, as well as the green rust complexes, form only under such suppressed kinetic conditions. They readily change over to γ-FeOOH, as Misawa pointed out, and hence their influence on corrosion processes would be minimum. Hence it appears that the amorphous phases, particularly AM and amorphous δ-FeOOH, determine the rusting and corrosion resistance of steels. The longer they are retained, the greater the resistance seems to be to continued rusting.

These amorphous films form macropassive layers and, unless some specific components are included, their continued retention without

crystallization would be difficult. It appears that incorporation of Si and Cu might be beneficial, for the ferrihydrite formation might be induced, which could be held stable due to the presence of these impurities. It is also found that incorporation and retention of phosphate ions in these layers is very helpful to increase the rusting resistance. This is discussed in the next section.

Relative Merits of Different Surface Inhibitor Treatments.

The merits of different surface chemical treatments could be assessed by two different methods - a) by direct weight loss determinations and study of passivation (rust stabilization) characteristics, and b) by structure and phase analysis, especially by infrared spectroscopic analysis of rust. Electrochemical studies yielded some additional supportive data.

The results of weight loss analyses have already been discussed. It was shown that treatments with 25% phosphoric acid (Trt. 2) and 25% phosphoric-benzoic acid mixture (Trt. 3) were beneficial in reducing the corrosion losses. The losses were not only minimized but the steels also showed better rust stabilization tendencies, i.e., the slowing down of the rusting process occurred much faster with these treatments. Treatment 6 with 10% tannic acid was not found to be beneficial except for total immersion or bold-exposure situations. The tannic acid treated specimens rusted nearly as fast as the sand-blasted (Trt. 1) or acid pickled (Trt. 7) specimens in sheltered location exposure tests. There was no indication of the stabilization process as well. However, in the continuous immersion test and in the bold-exposure simulation test, treatment 6 showed better characteristics than the other treatments and also showed stabilization tendencies. Treatments 2 and 3 generally led to fine powdery rust, whereas

treatment 6 formed coarse flakes in sheltered location exposure. In the immersion and in highly wet, bold-exposure simulation tests, a jelly-like complex was found to develop on surfaces treated with tannic acid, which led to better protection.

The general results discussed earlier also indicate that there is not much of a difference in the composition and structure of rust layers formed on various grades of steel, between the rusts formed at the sheltered locations or at the open, exterior (bold) locations. Some of the phases, such as ferrihydrite or hydrated maghemite, γ-$Fe_2O_3 \cdot H_2O$, form only under certain specific conditions and only in certain places. Other than that, the mechanism of formation of rust phases, as well as their subsequent transformations, seem to be nearly similar at all sites on the differently treated surfaces. Only the kinetics of transformations seems to be controlled by the environmental factors, as well as the specific surface treatment involved.

As stated and proved elsewhere, the initial phase to form in the rust on weathering steel exposed to the atmospheric conditions is the amorphous mix (AM), which is a mixture of γ-FeOOH, δ-FeOOH and ferrihydrite in the highly amorphous form. The crystalline phases corresponding to these forms, as well as α-FeOOH, emerge out of this initial rust. The amorphous mix forms as a sedimentary deposit on top of the steel, completely covering it. It is found to be dense, but cracks develop at later stages due to drying.

Under immersion condition, the other amorphous phase, Amorphous Bulk (AB), develops and grows steadily. Linear growth kinetic is found in the immersion situation on non-treated surfaces, whereas surfaces treated with

inhibitor chemicals, particularly with 10% tannic acid or 25% phosphoric acid, show rust stabilization and growth-arresting tendencies.

Misawa has explained that the corrosion resistance is due to the formation of this amorphous oxy-hydroxide rust layer on the surface of the metal, owing to its being compact and adherent to the metal. The results obtained by other Japanese scientists, as well as those obtained in our laboratory, strongly support this contention.

For continued protection, two requirements must be satisfied. First, the amorphous rust layer should remain stable and not grow further; that is, the growth process should have slowed down and no more growth should occur, at least to large extent. This is favored by the growth-inhibiting stabilization tendencies. Second, the amorphous rust should not get converted to crystalline fractions, for these are generally porous and would allow the penetration of water and oxygen to the metal surface, activating the corrosion process again. The cracks forming on the rust layer are unavoidable, but some sealing agent should be provided to plug these cracks as they develop or the corrosion process itself should be self-plugging. Provision of these measures would assure corrosion resistance.

Our results confirm that the formation and preservation of AM or any of the rust phases, such as δ-FeOOH or ferrihydrite in the amorphous form, would enable the attainment and preservation of rusting resistance. The rust layer formed would act as a patina and stop the further corrosion process.

With the basic background arguments given above, the relative merits of the various surface treatments can be analyzed in terms of mitigating the corrosion process. Discussions are based on IRS results from rusts

collected from various bridges that have been grouped to fall in three exposure-type categories - mild, medium-severe, and severe. Figure 14, A to L, and Table 11 are referred to in this context.

Treatment 1, the plain, sand-blasted conditions, as well as Treatment 7, acid-pickled or wire brush-cleaned situation, are not able to hold down the fast rusting process. Rusting takes place fastest on these surfaces and, depending on the severity of the atmosphere, the AM phase quickly passes on to δ- + γ-FeOOH (γ^*). This takes place slowly under mild environmental conditions, such as at Leesville (LV) or Boeuf River (BR) locations, Fig. 14, A and B, where the formation of ferrihydrite is also favored, or fast as at Luling (LU), Fig. 14 E, experiencing medium-severe environmental conditions. It can be mentioned that the formation of ferrihydrite would be indicative of the slow rust phase transformation and prevalence of dusting that would be helpful to plug the pores or the cracks developed. The rust layer is made up of δ + γ^* after two years of exposure at BR, but only 6 months is needed to form these phases at LU. The rust formed at the latter site may include also considerable amounts of α-FeOOH and γ-$Fe_2O_3 \cdot H_2O$.

Treatment 6 with 10% tannic acid also yields the AM phase and enables it to be retained over a period of 2 years in mild environments, though some amorphous δ and γ^* have been formed, Fig. 14 B (e,f,g) and Fig. 14 C (d,e). Formation of considerably more amorphous δ is indicated. These two phases δ and γ^* have been formed within 1 year under bold-exposure conditions in medium-severe industrial environments, Fig. 14 I(e). The sequence of transition from the first-formed am γ^* to δ + γ^* can be followed in Fig. 14 I (a to e). Under severe environmental conditions

relating to presence of large amounts of chloride, as at High Island (HI), TX or at Doullut Canal, DC, the stable phases δ and γ^* are formed within the first six months, but seem to retain the amorphous nature for longer periods of time, up to 2 years, Fig. 14 L (a to c). Under bold-exposure situations tannic acid treatment would yield more of the amorphous phases δ and γ^* and still hold AM. There is also the indication that γ^* goes through γ-$Fe_2O_3 \cdot H_2O$ to δ-FeOOH in such highly humid marine atmospheres. The γ-$Fe_2O_3 \cdot H_2O$ is also highly non-crystalline under various circumstances. Thus treatment 6 is judged to be generally helpful even in severe environmental conditions for exterior, bold-exposure situations when applied repeatedly, as in our retreatment experiments, in as much as such treatments stabilize the re-formation of the AM phase and its retention for longer periods of time, Fig. 14 L (e,f).

Treatments 2 and 3 with 25% phosphoric acid and 25% phosphoric-benzoic acid mixture, respectively, can be considered together, for they yield similar results. The results obtained with these treatments are generally very satisfactory. They not only yield the AM phase easily but also enable its retention for long periods of time. Trt. 3 may be slightly better in this respect than Trt. 2, for the benzoic acid may be acting slowly in the cracks formed and lead to plugging, with similar AM rust at these cracks as well.

At the HI bridge site, located within a couple of km from the Gulf Coast, these treatments enabled the stabilization of mostly AM in sheltered locations, with the concurrent formation of small amounts of amorphous δ-FeOOH and only traces of γ-FeOOH, Fig. 14 J. Retreatment after 6 months results in the AM phase being retained for 2 years, with only slight amounts of amorphous δ and γ^* getting formed, under exterior bold-exposure

conditions, Fig. 14 K (c,d). Fig. 14 G shows the results obtained with treatment 3 at the Gibbstown (GT) bridge location for treated panels exposed under the bridge deck. AM phase is very stable even after 18 months and only a very small amount of amorphous δ-FeOOH is indicated to be present along with it. Similar results are seen for Trt. 2, Fig. 14 F (a to c), for exterior surfaces of the web plate at the GT site treated with the phosphoric acid. However, at Luling (LU) trt. 3 does not seem to hold AM for long, showing the formation of δ and γ^*, though still much of the AM component is retained after 2 years at the exterior location, Fig. 14 H (a to g). Retreatment at about 6 months from the original date of treatment seems to be helpful to retain the AM component for longer periods. Trt. 2 yields similar results. Both these treatments yield very fine powdery rusts on exterior surfaces and only small amounts of rust were formed on treated surfaces.

Treatment 2 stabilizes the ferrihydrite phase along with AM at Leesville (LV) and retreatment is generally helpful to re-form the AM phase and hold it for longer periods of time. Trt. 3 is likewise very beneficial for retaining the AM component formed.

Treatments 4 and 5 can be discussed together since again their performances are similar at a given bridge location. As discussed earlier, treatment 6 alone is not as beneficial as the treatments 2 or 3. However, when applied one after the other, as in treatments 4 and 5, their characteristics are improved. Though the steels with these treatments also form the AM phase, it is not held stable but changes over to $\delta + \gamma^*$. The PA or PA-BA second surface treatment does not seem to help and the initial tannic acid treatment plays the dominant role. Trt. 5 seems to work better than Trt. 4, for at BR, Fig. 14 D (a to c), the AM phase is retained for 2

years with only slight formation of ferrihydrite in areas retreated after 1 year.

Trt. 4 is showing good results at GT, Fig. 14 F (d to f), but Trt. 5 is not yielding good results at Luling (LU), Fig. 14 E (d to G). In panels exposed under this bridge in sheltered locations, the progressive change of AM to $\delta + \gamma^*$ can be clearly seen. Slight segregation of amorphous ferrihydrite and δ is indicated even after 1 month exposure at this site, Fig. 14 E (d). Specimen after 3 months exposure shows considerable δ, Fig. 14 E (e), and the one after 15 months shows the complete transformation to δ, γ^* and possibly some α, Fig. 14 E (h). Trt. 5 gives rise to am. γ^* after 1 month exterior exposure, Fig. 14 I (a), as Trt. 7, Fig. 14 I (f), under similar conditions. A very heavy rain could remove the chemical conversion layer and make the surface behave similar to non-treated condition.

Likewise, Trt. 4 shows the transformation of AM to $\delta + \gamma^*$ in severe, near-marine environments, Fig. 14 K (h). Similar results have been obtained for trt. 5 also in such locations. Still it is interesting to note that these treatments enable the retention of the AM phase in the exterior, bold-exposed surfaces, even under near-marine conditions.

The results obtained and discussed above clearly demonstrate the benefits derived from the chemical treatments of bare weathering steel surfaces with phosphoric acid and phosphoric-benzoic acid mixtures. Whereas Trt. 3 is ideal for the GT bridge, Trt. 2 can be recommended for the Luling bridge and for other bridges located in the medium-severe, sub-tropic, humid environmental zone. For bridges at the near-marine locations also, treatment 2 can be recommended, but careful retreatments would be needed. The bridges close to the coast line or in a severe

industrial belt (equivalent to HI and DC of our study) can get retreatment every six months in the first year and one after the first 2 years. The bridge at Luling and others in a medium severe environment could use one retreatment after the first year. These are for interior surfaces in sheltered locations. The boxed locations over the gusset plate could get a treatment with tannic acid. Those in the near-marine area should get retreatments once every year for the first two years. As already pointed out, cleaning of debris and rust collected at such places should be undertaken once every year.

The exterior surfaces could use Trt. 6 in these two types of atmospheres. They would require no retreatment.

The bridges located in rural areas which experience mild environmental conditions, such as the LV and BR bridges, do not require any treatment, especially in the exterior areas. If warranted, the interior surfaces can be washed with a weak PA or PA-BA solution after cleaning. Periodic water jet cleaning itself should be adequate for the weathering steel at these locations. In areas where saline water flows, stagnates and gives rise to sheet-type of rusting, treatment with tannic acid can be used if the wetting is continuous. Otherwise treatment with PA could be beneficial. Perhaps for such areas, mixtures of TA with PA or TA with PA-BA could be useful. The characteristics of such mixtures have not been studied in this project. For Louisiana situations, such mixtures are still applicable to exterior, bold-exposed surfaces and also in boxed locations above gusset plates. The characteristics of weathering steel treated with TA-PA and TA-PA-BA mixtures should be studied further.

Specific Recommendations.

As stated in the previous section, bridges located in the northern and central parts of the state of Louisiana do not experience any serious corrosion problems. As such, they do not require chemical treatment. However, washing of the bridges to remove rust debris and bird excretions would be highly desirable once in a while. The bridges at Leesville (LV) and Boeuf River (BR) can be cleaned with water jet once every ten years or so.

The bridges in the medium-severe industrial environment require chemical treatment. The bridges at Luling, Larose, Gibbstown and Forked Island fall in this category. They are not very close to the Gulf Coast, yet they do experience some air-borne chloride contamination. The high humidity prevalent in this region would not allow the rusting process to stabilize in sheltered areas, as shown in the laboratory test. It is expected that the rusting process would continue unmitigated, though at a slow pace, at a steady rate consuming about 2 to 3 mils of section thickness per year. Localized pitting has been proven to exist and, if left unattended, would cause considerable erosion in some places in a short time. Losses as much as 5-6 mils per year could occur in such places as the partially boxed areas above the gusset plate.

The rusts in the sheltered areas are flaky and rough, indicative of crystallization processes and continued growth of rust. The powdery rust seen after the initial removal of the sheet-type of rust on the Kawasaki A588 - Grade A steel in the main span of the Luling Bridge is already starting to grow into flakes and in a few years the situation of rusting at Luling would be equivalent to the rusting at Larose or Gibbstown, etc.

bridges. Also, pits as deep as 40-50 mils have been observed in areas where water collects and stays in pools forming sheet-type rust.

The bridges at Empire, LA (Doullut Canal, DC) and High Island, TX (HI) are in the severe environment category. They experience considerable humidity and appreciable salt from the sea and the conditions at these bridge sites could at times become similar to those in the salt-fog test. Coarsest flakes averaging about 2 to 5 mm (1/8 to 1/4 inch) in diameter and about 1/32 inch in thickness are common in sheltered areas. Deep pits, about 50-60 mils in depth and about 1/4 to 1/2 inch in width, have been seen in these bridges. At DC, even the bolt heads at the semi-boxed areas, where water and debris collect, form sheet-type rust layers. Severe *weakening of the bolts in a short span of time is possible.*

Because of these facts, the interior, sheltered locations at these coastal area bridges need to be cleaned and treated with chemicals as indicated below:

Medium-Severe Atmospheric Conditions:

Luling, Larose, Gibbstown, Forked Island Bridges:

Interior Areas: Clean the surface with water jet containing sand. This process should remove all of the rust. Cleaning to white metal is not needed. Thereafter, surface treat (by spraying or brushing) with 25% phosphoric acid. Soak thoroughly the areas of the bolt-head, nuts, etc. with the acid. Proper collection of the acid and prevention of spilling should be instituted. After drying, apply the acid solution a second time.

Retreatment with this acid would be needed after 1 year. The acid should be applied on previsouly treated areas without removing the rust or cleaning the surface. One time application is adequate.

Boxed Locations: Clean the surface with air jet and water jet containing sand. Clean the bolt heads, nuts, etc. thoroughly also. Thereafter, apply 10% tannic acid solution and let it dry. The horizontal and vertical surfaces (about 2 feet high) close to the bottom horizontal surfaces should get this treatment. The rest of the areas should get the phosphoric acid treatment.

Remove the debris, bird excretions, etc. and reapply these chemicals after one year. Air blasting is adequate to remove the debris. Clean and reapply the chemical one more time after two years at these locations. This should prevent excessive rusting and pitting.

Exterior Surfaces: Clean with water jet containing sand. Apply 25% phosphoric acid solution. (These surfaces alternatively could use a mixture of phosphoric and tannic acids, 10% each.) No retreatment is necessary.

Repeat all the above mentioned treatments at the beginning of every ten-year cycle.

Severe (Near-Marine) Atmospheric Conditions:

Doullut Canal (DC) and High Island (HI) Bridges:

Interior Areas: Clean the surfaces with water jet incorporating sand. Cleaning to near white metal is necessary. Thereafter apply the 25% phosphoric acid solution (by spraying or brushing). Reapply one more time after drying. Soak the areas at the bolts, nuts, etc. thoroughly.

Retreat the treated areas first after six months and then again after six more months and after two years from the first treatment. The rust

formed on the surfaces need not be removed. The retreatment is better handled by spraying thoroughly on the rusted steel.

Boxed Areas: These require treatment with 10% tannic acid + 25% phosphoric acid mixture. Recleaning and reapplication would be necessary after six months, 1 year and 2 years from the first-time treatment. Thereafter, these areas should be cleaned thoroughly once every year and the chemical should be sprayed thereafter. If debris is not excessive, retreatment with the acid can be stopped after the second year. However, if there is any indication of water collection, it is prudent to apply at least the 10% tannic acid solution after cleaning.

Exterior Surfaces: Clean with water jet containing sand and apply a 10% tannic acid + 10% phosphoric acid solution. Retreatment after 1 year would be necessary. This can be done by spraying.

Repeat the treatments given above at the beginning of every ten-year cycle.

Marine locations very close to the coastal areas could use similar treatments as for the near-marine locations. Treatment of the entire bridge with 25% phosphoric acid can be recommended for vertical areas, both interior and exterior. Retreatments after 6 months, 1 year and two years from the first treatments can be recommended. For exterior areas two more annual treatments could be adequate. Where water would stagnate and cause sheet-type rust, apply the 10% tannic acid solution annually three times. If water does not stagnate, apply the 25% PA solution at these areas also. Areas where the wind brings in and deposits large amounts of salt would

require painting at the horizontal and near vertical (up to 3 foot high) surfaces.

Fortunately, such marine locations are not encountered in any Louisiana bridge built with the weathering steel.

Finally, bridges can be continued to be built with the weathering steel in the central and northern parts of the state and these can be handled as the Leesville and Boeuf River bridges, by periodic cleaning with water jet. In industrial areas away from the coastline, they can still be used with institution of adequate maintenance procedures. In near-marine locations their use should be checked thoroughly. They could still be used in places similar to Doullut Canal, High Island, etc. with adequate caution and institution of maintenance procedures. In marine locations very close to the coastline, painting might be warranted. Each location should be judged individually and the optimum choice made. By the same token, painting might not be needed for the entire bridge. Only certain areas likely to experience severe corrosion problems might require painting. Careful analysis is essential.

Conclusions:

Based on the results of this study, the following conclusions are reached:

(1) Excessive rusting leading to formation of coarse flakes that adhere loosely to the steel and pitting are two of the common problems encountered in weathering steel bridge spans in Louisiana and Texas. Sheet-type rust develops in areas where water stays stagnant for long periods of time. Such rusting occurs also on bolt heads and nuts in partially enclosed boxed areas above the gusset plates at the entrance to

the piers. These problems are more severe in bridges located close to the coastline.

(2) The rust flake size is proportional to the chloride-content in the atmosphere and deposited in the rust. The higher the chloride-content, the coarser, thicker and sharper are the flakes that develop. Thus the coastal area bridges are found to develop coarse flakes that peel off easily.

(3) Section thickness losses are maximum, as much as 3 to 5 mils per year, in horizontal areas at sheltered locations in some of these bridge spans, and are caused mainly by chloride accumulation. The chloride penetrates to the rust-metal interface and is not removed by subsequent peeling of the rust.

(4) The bridges far away from the coastal region, as well as the exterior surfaces of coastal area bridges, develop fine, powdery rust and do not show any serious corrosion problem.

(5) Pits are generally found in the coastal area bridges in sheltered locations. The pitting is correlatable to flake size, though pits of maximum depth are found in areas where sheet-type rusting occurs, and to chloride content of the atmosphere.

(6) Most of the pits are about 10 mils (0.25 mm) deep in the interior locations of coastal area bridges. Vertical surfaces experience the least severe pitting. Horizontal and inclined surfaces have much deeper pits.

(7) Partially boxed locations above the gusset plates at the entrance to the piers where birds take refuge and build nests collect debris and allow water to stagnate, leading to more rusting, sheet-type rust formation and wider and deeper pits. Pit depths as great as 52 mils (1.3 mm) have been recorded at Doullut Canal. Salt and chloride accumulation lead to

considerable metal loss. Deepest and widest pits are directly correlated to enhanced chloride-content and water retention, leading to more rusting and sheet-type rust formation. Our pitting data agree well with those given by McKenzie [2].

(8) Measured average section losses are about 1 mpy in rural area bridges (LV and BR), 2 to 4 mpy in bridges located in the medium-severe industrial environment (LU, GT, FI and LR) and 3 to 5 mpy in severe near-marine coastal atmospheres (HI, DC) in the interior, sheltered locations. Roughly half as much thickness loss is registered in exterior locations. These losses, obtained by use of an ultrasonic thickness gauge, are generally two to three times as much as those obtained from tests with field coupons exposed at these bridge sites. (See Table 12.)

(9) The thickness losses obtained by exposing field coupons in sheltered locations are about 0.5 mpy at Leesville (rural area), 1.35 mpy at Luling and Gibbstown and about 1.6 mpy at High Island for the sand-blasted condition. Nearly similar but slightly lower values are obtained for specimens treated with 10% tannic acid (Trt. 6). However, the rest of the chemical treatments with rust modifiers give rise to a third or two-thirds lower losses. (See Table 12.)

(10) Treatments with 25% phosphoric acid or 25% phosphoric-benzoic acid mixture are very effective in reducing the rusting rate. Some indication of the slowing down of the rusting process with time, i.e. rust stabilization, was obtained.

(11) Initial rusting is found to be fast, but after about 3 months of exposure there is a definite drop in the rusting rate.

(12) Data for losses in exterior exposure indicate that losses in exterior, bold-exposures are about 33 to 50% less than in analogous

exposures in sheltered locations. However the losses in exterior exposures in the medium-severe industrial areas are about twice as great as at the sheltered locations in mild, rural area bridges. Correspondingly larger losses can be expected in the near-marine coastal bridges also. Average losses are about 0.2 to 1 mpy in exterior locations, depending on the bridge site.

(13) At a given site in Louisiana, nearly twice as much loss occurs in the sheltered locations as compared to exterior areas. In coastal area bridges, much higher losses occur in the sheltered locations, particularly in partially boxed areas, as mentioned already.

(14) The thickness losses experienced in Louisiana are quite different from those reported by other scientists. Only the data from the rural area bridges approximate the results reported by others. Our results agree somewhat with those reported by McKenzie in England [2]. However, we did not see any loss at an exterior location larger than the loss at the analogous interior sheltered locations at any site. The losses in sheltered locations were always larger and nearly twice as great as at the corresponding exterior location.

(15) In laboratory accelerated atmospheric exposure simulation tests similar to sheltered location exposures, an average thickness loss of about 1 mpy was obtained. This compares favorably with the losses obtained in field exposures with field coupons. As a result, it is judged that an acceleration factor of 50 used in these tests did not distort the results. The corrosion losses over 2200 wet/dry cycles, corresponding to 6 years of field exposure, were linear and showed only slight tendency for slowing down. Such behavior corresponds to somewhat warm and humid tropical conditions.

(16) In laboratory simulation tests corresponding to exterior, bold-exposure, average thickness losses of about 0.1 (rural area equivalent) to 0.33 (industrial area equivalent) mpy were obtained. The latter values are about half as great as found in actual exterior exposure carried out at CEBA, LSU.

(17) Average thickness losses under total immersion and stagnant conditions were about 2.5 mpy, and large losses of about 40 to 65 mpy were obtained in the salt-fog test. These tests showed also linear kinetic of the rusting process.

(18) Weathering steels with chemical treatments generally underwent about 50 to 80% of the losses experienced by analogous specimens with no surface treatments.

(19) No pitting was observed in electrochemical tests. Initial corrosion processes resulting in thickness losses of 60 to 100 mpy were obtained for all steels. The surface treatment with phosphoric acid reduced this initial loss by an order of magnitude which would indicate its protective nature. The phosphoric acid-treated surface did not degrade and corrode as easily as the bare weathering steel surface.

(20) The initial rust to form in atmospheric exposure is proved to be the "Amorphous Mix (AM)" phase, which is judged to be a mixture of highly amorphous γ- and δ-FeOOH and ferrihydrite from its infrared absorption pattern. It gives way to individual amorphous phases γ- or δ-FeOOH or ferrihydrite. Gradually, crystalline phases belonging to these forms, as well as γ-$Fe_2O_3 \cdot H_2O$ and α-FeOOH, form directly on its surface and grow.

(21) γ-FeOOH grows more in the form of thick plates that fold and bend. An aggregate of these plates in their cross-sectional view would appear as a bunch of worms.

(22) δ-FeOOH forms thin plates that bend and fold too. They form flowery patterns.

(23) Ferrihydrite is fine powdery or cylindrical or square tube-shaped. It also grows as mud walls, and all of these are formed and grown probably by bacterial activity.

(24) γ-$Fe_2O_3 \cdot H_2O$ has sandy grain structure, and both γ and ferrihydrite could form mounds.

(25) α-FeOOH develops directly from the AM layer and grows in the form of rods or short petals of flowers. Beautiful patterns resembling carnation and cactus flowers are judged to be of this phase. α forms as whiskers on top of the plates of γ-FeOOH and ferrihydrite. This is judged to be due to phase transformation processes. All of the phases ultimately convert to α-FeOOH under atmospheric conditions. α-FeOOH also forms nest-like, foamy patterns with sharp plates. The plates of α do not bend and fold, unlike the plates of δ- and γ-FeOOH. They are also very thin.

(26) Magnetite and γ-$Fe_2O_3 \cdot H_2O$ form in the salt fog test. It is found that magnetite transforms to γ and ultimately to α-FeOOH in wet environments. It is highly adherent to steel in the wet condition, forms in layers and converts to γ or α through anodic oxidation processes converting Fe^{2+} ions to Fe^{3+} ions. The reverse transformation of magnetite to γ or α is probably the cause for loss of adherence and peeling.

(27) The stable phases in exterior bold-exposure are δ- and γ-FeOOH. Some α-FeOOH might also be formed. The AM phase is more stable under exterior exposure situations than in sheltered locations.

(28) In continuous immersion situation, another amorphous phase designated as "amorphous bulk (AB)" forms. Unlike "AM", this phase may have more Fe^{2+} ions in it. It transforms to all crystalline rust forms

including magnetite. Magnetite and α-FeOOH have been obtained more commonly in the loose rust fraction formed. FeO was also obtained in the immersion test.

(29) The amorphous rust layer is stabilized on exterior surfaces due to frequent rain wash. This contributes to improved rusting resistance.

(30) Based on the results obtained, the following structural transformations are proposed:

Initial Fast Process:

$$Fe \rightarrow Fe^{2+} \rightarrow Fe(OH)^{+} \rightarrow Fe(OH)_2 \rightarrow \underset{\text{complexes}}{\text{Green rust}} \rightarrow \underset{\text{am.}\gamma\text{-FeOOH}}{\text{AM (or)}}$$

Slow Further Transformations:

$$AM \rightarrow (am) \begin{cases} \gamma\text{-FeOOH} \\ \delta\text{-FeOOH} \rightarrow \text{am.}\delta\text{-FeOOH} + \gamma\text{-FeOOH (cryst)} \rightarrow \rightarrow \rightarrow \\ \text{ferrihydrite} \end{cases}$$

$$\underset{\text{acidic conditions}}{\overset{\text{alkaline or}}{\rightarrow \rightarrow}} \quad \delta\text{-FeOOH} + \alpha\text{-FeOOH} \quad \overset{\text{topotactic}}{\rightarrow \rightarrow} \quad \alpha\text{-FeOOH}$$

Alternate routes in chloride-rich environments:

(i) $AM \rightarrow \gamma\text{-FeOOH} \rightarrow \gamma\text{-}Fe_2O_3 \cdot H_2O \rightarrow \delta\text{-FeOOH} + \alpha\text{-FeOOH} \rightarrow \alpha\text{-FeOOH}$

(ii) $AM \rightarrow \beta\text{-FeOOH} \rightarrow \beta\text{-}Fe_2O_3 \cdot H_2O \rightarrow \gamma\text{-}Fe_2O_3 \cdot H_2O \rightarrow \delta\ FeOOH + \alpha\text{-FeOOH} \rightarrow \alpha\text{-FeOOH}$

(iii) $AM \xrightarrow{\text{Cathodic redn.}} Fe_3O_4 \xrightarrow[\text{oxidn.}]{\text{Anodic}} \gamma\text{-}Fe_2O_3 \cdot H_2O \xrightarrow{\text{topotactic (?)}} \alpha\text{-FeOOH}$

Final transformation:

$$\alpha\text{-FeOOH} \xrightarrow[\text{dehydration}]{\text{slow}} \alpha\text{-}Fe_2O_3$$

Under immersion conditions:

Fast Process:

$$Fe \rightarrow Fe^{2+} \rightarrow Fe(OH)^{+} \rightarrow Fe(OH)_2 \rightarrow \text{Amorphous Bulk (AB)}$$

FeO

Slow Process:

AB → cryst.

(adherent rust) → (in loose outer rust)

- $\gamma\text{-}Fe_2O_3 \cdot H_2O$
- δ-, γ-, α-, β-FeOOH
- ferrihydrite
- FeO, Fe_3O_4

(31) Different surface chemical treatments are generally beneficial. Various test results indicate that applications of 25% phosphoric acid or 25% phosphoric-benzoic acid mixture are highly beneficial for reducing the corrosion losses in the sheltered locations. The "AM" rust formed on these treated surfaces degrades slowly and is retained for fairly long periods of time, even over 2 years.

(32) Tannic acid treatment is beneficial for highly wet situations. It is recommended for application in partially boxed locations, on exterior bold-exposed surfaces in industrial areas and on surfaces where water collects and stays stagnant for considerable time. Alternatively, a mixture of tannic acid and phosphoric acid can be used. A jelly-like

complex forms on such treated surfaces and contributes to rusting resistance.

(33) Treatment with phosphoric acid stabilizes ferrihydrite in areas where dusting is prevalent. Incorporation of Si and Ca are congenial for stabilizing the ferrihydrite, which could be more protective.

(34) Incorporation of phosphate ions in the amorphous rust layer is very helpful to increase the rusting resistance.

(35) Painting is not needed for any weathering steel bridge located in Louisiana or Texas. Surface chemical treatments would be capable of handling the corrosion problems encountered in some of these bridges.

(36) Specific recommendations for surface inhibitor treatments would include initial cleaning with water jet containing sand and application and reapplication after 1 year of 25% phosphoric acid in sheltered locations, in bridges located in the medium-severe industrial and near-coastal area environment at Luling, Larose, Gibbstown and Forked Island. The boxed locations are recommended to be treated with 10% tannic acid solution annually for the first two years. Proper cleaning and removal of debris collected at this location are essential. Exterior surfaces can be treated once with the 25% phosphoric acid solution. These treatments are recommended to be repeated once in every ten-year cycle.

(37) For near coastal area bridges at High Island, TX and Doullut Canal the suggested treatments are as above but the frequency of reapplication is greater. Thus the 25% phosphoric acid treatment is recommended for interior, sheltered areas initially and 6 months, 1 year and 2 years after the first applications. The boxed areas are recommended to be treated with 10% tannic acid + 25% phosphoric acid mixture up to a height of about 3 feet from the bottom level. The exterior areas are to be

treated with 10% tannic acid + 10% phosphoric acid solution and a retreatment after one year is recommended. Again, the treatments should be repeated once in every 10 year cycle.

(38) Bridges can continue to be built with weathering steel A588 and adequate maintenance procedures can be instituted. There is no need to remove the surface scale at the beginning. As in current practice, it can be allowed to degrade and wear out. After about one or two years, the entire cleaning and coating procedure can be instituted and cycled as necessary.

Acknowledgement:

This work was made possible by a contract from the Louisiana Department of Transportation and Development and the Federal Highway Administration, Washington, D.C. - LA State Project No. 736-09-06; LA HPR. 0010 (007); 84-IST. Messrs. Verdi Adam and Al Dunn were very eager to have the project undertaken and LA-DOTD's Kirt A. Clement, Richard William, Ronny Alan, William E. Graves, and Mike Bailey provided valuable assistance and support throughout the project. Mr. Sashikant Shah of the LA-DOTD provided valuable advice throughout the tenure of the project. Several students, both at the undergraduate and graduate level, participated in this project and bulk of the data were derived and analyzed by the graduate assistants Ahmad Razvan (M.S.), Laxminarayan Sharma (M.S.), Saifullah Nasrazadani (M.S., currently enrolled in the Ph.D. program), Baha Kuban (Ph.D.) and Viswajeet Deshmukh (currently enrolled in the M.S. program). Vasudevan Raman (undergraduate), Sudharsan Iyengar (graduate student - computer science), Orlando Herrera (B.S. Mechanical Engineering), John Epperson (B.S. Mechanical Engineering) are some of the valient ones who performed great deal of experimental work. My heartfelt thanks to all concerned for making this project a great success and enjoyable one.

REFERENCES

(1) Atmospheric Corrosion, W. H. Ailor, ed., John Wiley & Sons, NY, 1982.

(2) M. McKenzie, "The Corrosion Performance of Weathering Steel in Highway Bridges", in Ref. (1), pp. 717-741.

(3) J. D. Culp and G. L. Tinklenberg, "Interim Report on Effects of Corrosion on Bridges of Unpainted A588 Steel and Painted Steel Types", Res. Rept. No. R-1142, Michigan Transportation Commission, Michigan Dept. of State Highways and Transportation, Lansing, Michigan, 1980.

(4) Results from "Weathering Steel Questionnaire", Rept. to State Highway Departments by "Bridge Maintenance Task Force", AASHTO Subcommittee on Maintenance, U.S.A., 1983.

(5) A. C. Dutra and R. de O. Vianna, "Atmospheric Corrosion Testing in Brazil", in Ref. (1), pp. 755-774.

(6) N. E. Wallace and G. T. Badger, "Atm. Corr. Testing of Plain Carbon and Austen Steels - 10 Year Results", Rept. PK/TSR/80/027, Corr. Res. Dept., Australian Iron & Steel Pty. Ltd. - Port Kembla, Australia, 1980.

(7) J. R. Duncan and J. A. Ballance, "Marine Salts Contribution to Atmospheric Corrosion", paper presented at the ASTM Symposium on "Degradation of Metals in the Atmosphere", Philadelphia, PA, May 1986.

(8) F. C. Perez, Corr. - NACE, Vol. 40, pp. 170-175 (1984).

(9) D. Knotkova - Cermakova, J. Vlckova and J. Honzak, "Atm. Corr. of Weathering Steels", in ASTM-STP 767, 1982, pp. 7-44.

(10) H. E. Townsend and J. C. Zoccola, "Eight Year Atmospheric Corrosion Performance of Weathering Steel in Industrial, Rural and Marine Environments", ASTM STP-767, 1982, pp. 45-59.

(11) D. Knotkova, K. Barton and M. Cerny, "Atm. Corr. Testing in Czechoslovakia", in Ref. (1), pp. 991-1014.

(12) S. Haagenrud, V. Kucera and J. Gullman, in Ref. (1), p. 691.

(13) L. Atteras and S. Haagenrud, in Ref. (1), p. 877.

(14) T. Hakkarainen and S. Ylasaari, in Ref. (1), p. 790.

(15) T. Fukushima, N. Sato, Y. Hisamatsu, T. Matsushima and Y. Aoyama, in Ref. (1), pp. 841-872.

(16) M. Sakashita and N. Sato, Corr. Sci., Vol. 17, p. 473 (1977); Corr. - NACE, Vol. 35, p. 351 (1979); other references given in Ref. (15).

(17) D. G. Manning, "Accelerated Corrosion in Weathering Steel Bridges", paper presented at the Canadian Structural Engineering Conference, 1984.

(18) F. O. Reed and C. B. Kendrick, "Evaluation of Weathering Effects on Structural Steel", Rept. FHWA/CA/TL-82/04, California Dept. of Transportation, Sacramento, CA, 1982.

(19) H. R. Ambler and A. A. J. Bain, J. Appl. Chem., Vol. 5, pp. 437-467 (1955).

(20) H. R. Copson, Proc. Amer. Soc. Testing Metals, Vol. 45, p. 584 (1945).

(21) F. H. Haynie, J. W. Spence and J. B. Upham, "Effects of Air Pollutants on Weathering Steel and Galvanized Steel: A Chamber Study", in ASTM STP-646, ASTM, Philadelphia, PA, 1978, pp. 30-47.

(22) H. Schwitter and H. Boeni, J. El. Chem. Soc., Vol. 127, pp. 15-20 (1980).

(23) J. Dearden, J. Iron and St. Inst., Vol. 159-II, p. 261 (1948).

(24) O. B. Ellis, Proc. Amer. Soc. Testing Matls. Vol. 47, pp. 152-170 (1947).

(25) H. Okada, Y. Hosoi, K. Yukawa and H. Naito, Proc. 4th Internat. Congr. Met. Corr., 1969, pp. 392-398; Trans. ASM, Vol. 63, pp. 278-281 (1969); Corr., Vol 26, p. 429 (1970).

(26) B. R. de Maybaum and E. S. Ayllon, in Ref. (1), pp. 423-430.

(27) J. B. Johnson, P. Elliott, M. A. Winterbottom and G. C. Wood, Corr. Sci., Vol. 17, pp. 691-700 (1977).

(28) K. Barton, D. Kuchynka, Z. Bartonova and E. Beranek, ibid., Vol. 11, pp. 937-942, (1971).

(29) D. C. Smith and B. McEnaney, Corr. Sci., Vol. 19, pp. 379-394 (1979); Vol. 20, pp. 873-886 (1980).

(30) T. Misawa, K. Hashimoto and S. Shimodaira, Corr. Sci., Vol. 14, pp. 131-149 (1974).

(31) T. Misawa, ibid, Vol. 13, pp. 659-676 (1973).

(32) J. T. Keiser, C. W. Brown and R. H. Heidersbach, Corr.-NACE, Vol. 38, pp. 357-360 (1982).

(33) I. Suzuki, Y. Hisamatsu and N. Masuko, J. El. Chem. Soc., Vol. 127, p. 2210 (1980).

(34) J. T. Keiser, C. W. Brown and R. H. Heidersbach, ibid, Vol. 129, pp. 2686-2689 (1982).

(35) U. Schwertman and H. Thalmann, Clay Minerals, Vol. 11, pp. 189-200 (1976).

(36) H. Sugawara and S. Shimodaira, J. Jap. Inst. Met., Vol. --- , p. 1210 (1965).

(37) W. H. J. Vernon, Trans. Faraday Soc., Vol. 31 - Part 2, pp. 1668-1700 (1935).

(38) St. Karaivanov and G. Gawrilov, Werkst. u. Korr., Vol. 24, pp. 30-31 (1973).

(39) A. L. Mackay and M. A. Miner, Phil. Mag., Vol. 32, pp. 545-557 (1960).

(40) E. Murad, Clay Minerals, Vol. 14, pp. 273-283 (1979).

(41) P. Keller, Werkst. u. Korr., Vol. 20, pp. 102-108 (1969).

(42) U. Schwertman and R. M. Taylor, Proc. Internat. Clay Conf., Madrid, 1972, pp. 343-350.

(43) J. M. De Villiers and T. H. Van Rooyen, Clay Minerals, Vol. 7, pp. 229-235 (1967).

(44) K. Hashimoto and T. Misawa, Corr. Sci., Vol. 13, pp. 279-281 (1973).

(45) A. N. Christensen, P. Convert and M. S. Lehmann, Acta Chem. Scand. Vol. A34, pp. 771-776 (1980).

(46) S. Okamoto, J. Amer. Cer. Soc., Vol. 51, pp. 596-599 (1968).

(47) P. Chevallier, Compt. Rend., Vol. 184, pp. 674-676 (1927).

(48) O. Glemser and E. Gwinner, Z. Anog. Allgem. Chem., Vol. 240, pp. 161-166 (1939).

(49) J. D. Bernal, D. R. Dasgupta and A. L. Mackay, Clay Miner Bull., Vol. 4, pp. 15-30 (1959).

(50) M. H. Fracombe and H. P. Rooksby, ibid, Vol. 4, pp. 1-14 (1959).

(51) A. W. Simpson, J. Appl. Phys., Vol. 33, pp. 1203-1205 (1962).

(52) A. L. Mackay, Miner. Mag., Vol. 32, p. 209 (1960).

(53) J. T. Keiser, C. W. Brown and R. H. Heidersbach, Amer. Lab., Vol. 14, p. 17 (1982).

(54) H. Leidheiser, Jr. and S. Music, Corr. Sci., Vol. 22, p. 1089 (1982).

(55) H. Leidheiser, Jr. and I. Czako-Nagy, ibid, Vol. 24, p. 569 (1984).

(56) A. K. Singh, T. Ericsson, L. Hagstrom and J. Gulman, ibid, Vol. 25, p. 931 (1985).

(57) B. R. de Maybaum and E. S. Ayllon, Corr. - NACE, Vol. 36, p. 345 (1980).

(58) T. Misawa, K. Asami, K. Hashimoto and S. Shimodaira, Corr. Sci., Vol. 14, pp. 279-289 (1974).

(59) J. T. Keiser, C. W. Brown and R. H. Heidersbach, Corr. Sci., Vol. 23, pp. 251-259 (1983).

(60) C. Feigenbaum, L. Galor and J. Yahalom, Corr.-NACE, Vol. 34, pp. 65-70 (1978).

(61) E. Matijevic, in Ref. (1), pp. 123-137.

(62) H. R. Copson, Proc. ASTM, Vol. 60, pp. 650-666 (1960).

(63) J. B. Horton, M. M. Goldberg and K. F. Watterson, Proc. 4th Internat. Congr. Met. Corr., 1969, pp. 385-391.

(64) R. Bruno, A. Tamba and G. Bombare, Corr.-NACE, Vol. 29, pp. 95-99 (1973).

(65) I. Suzuki, Y. Hisamatsu and N. Masuko, "Nature of Atmospheric Rust on Iron", J. El. Chem Soc., Vol. 127, pp. 2210-2215 (1098); Corr. Sci., Vol. 19, pp. 521-535 (1979)/

(66) E. P. Egan, Jr., Z. T. Wakefield and B. B. Luff, J. Phys. Chem., Vol. 65, p. 1265 (1961).

(67) J. J. Cleary and N. D. Greene, Corr. Sci., Vol. 7, pp. 821-831 (1967).

(68) T. Zaizen, T. Watanabe, K. Okamoto, K. Kanaya, M. Sato, T. Haze and Y. Ohno, "Low C-Cu-P Type Superior Atm. Corr. Resistant Steel for Welded Structures", Nippon Steel Tech. Rept. No. 22, Dec. 1983.

(69) D. Fyfe, C. E. A. Shanahan and L. L. Shreir, Proc. 4th Internat. Congr. Met. Corr., 1969, pp. 399-407.

(70) G. Wranglen, Corr. Sci., Vol. 9, pp. 585-602 (1969); Vol. 14, pp. 331-349 (1974).

(71) U. R. Evans, "Metallic Corrosion, Passivity and Protection", Longmans Green Co., NY 1948, pp. 269-273.

(72) Z. Szklarska-Smialowska, Intl. Conf. on Localized Corr., Williamsburg, VA, NACE, 1971; Corr.-NACE, Vol. 28, pp. 388-396 (1972).

(73) L. J. Gainer and G. R. Wallwork, ibid, Vol. 35, pp. 435-443 (1979).

(74) W. Meisel, H. J. Guttmann and P. Gutlich, Corr. Sci., Vol. 23, pp. 1373-1379 (1983).

(75) V. S. Muralidharan and K. S. Rajagopalan, ibid, Vol. 19, pp. 199-207 (1979).

(76) O. Lahodny-Sarc and L. Kastelan, ibid, Vol. 16, pp. 25-34 (1976).

(77) G. H. Awad and T. P. Hoar, ibid, Vol. 15, pp. 581-588 (1975).

(78) T. K. Ross and R. A. Francis, ibid, Vol. 18, pp. 351-361 (1978).

(79) S. N. Emery, Australas Corr. Engng., Vol. 7, p. 39 (1963).

(80) P. Bauer, Met.-Reinig., Vorbehandl, Vol. 13, p. 41 (1964).

(81) J. B. Pelikan, Stud. Conserv., Vol. 11, p. 109 (1966).

(82) E. Knowles and T. White, J. Oil Colour Chem. Asso., Vol. 41, p. 10 (1958).

(83) C. L. Page and J. E. O. Mayne, Corr. Sci., Vol. 12, pp. 679-681 (1972).

(84) E. J. Kelley, J. El. Chem. Soc., Vol. 115, p. 1111 (1968).

(85) L. L. Shreir, New Scient., Vol. 23, p. 332 (1964); Br. Pat. 802276 (1958).

(86) U. R. Evans, J. Soc. Chem. Ind., Vol. 43, p. 315T (1924).

(87) U. R. Evans, Corr. Sci., Vol. 9, p. 813 (1969).
U. R. Evans and C. A. J. Taylor, ibid. Vol. 12, p. 227 (1972).

(88) ASTM Powder Diffraction File, ASTM STP 48-M2, 1963, Am. Soc. Testing Matls., Philadelphia, PA.

(89) A. Razvan and A. Raman, "Morphology of Rust Phases Formed on Naturally Weathered Weathering Steels in Bridge Spans", Pract. Met., Vol. 23, pp. 223-236 (1986).

(90) F. V. Chukrov, B. B. Zfyagin, L. P. Ermilova and A. I. Gorshkov, Proc. Intl. Clay Cong., Madrid, 1972, J. M. Serratosa, ed., Div. Ciencias C.S.I.C., Madrid, pp. 322-341.

(91) T. Misawa, T. Kyuno, W. Suetaka and S. Shimodaira, Corr. Sci., Vol. 11, pp. 35-48 (1971).

(92) K. J. Gallagher, Nature-Phys. Sci., Vol. 240, p. 11 (1972).

TABLES

TABLE 1 : Chemical Compositions of Representative Weathering Steels

Type of Steel	Chemical Composition, wt.%										Mechanical Properties			
	C	Si	Mn	P	S	Cu	Ni	Cr	Mo	V	Y.St. (ksi)	UTS (ksi)	%Eln.	Imp. Str. (ft.-lb.)
Kawasaki Steel A588-Grade A	0.14	0.25	1.23	0.018	0.005	0.28	0.11	0.47	---	0.043	50.5	76.9	34	198
Kawasaki Steel	0.08	0.34	0.39	0.082	0.008	0.27	0.20	0.47	---	---	51	60	22	---
Riverten-R	0.10	0.40	0.47	0.082	0.013	0.26	0.31	0.51	---	---	38	53	35	---
Kawasaki Steel A325-Type 3-(c)	0.17	0.25	0.89	0.027	0.017	0.28	0.33	0.41	---	0.03	---	---	---	---
U.S. Steel A588-Grade A	0.19	0.23	1.05	0.018	0.03	0.28	---	0.40	---	0.055	55	78	25	22
Bethlehem Steel A588-Grade B	0.09	0.30	1.15	0.01	0.02	0.22	0.32	0.59	---	0.068	65	95	22.5	60
Mild Steel, A36	0.093	0.025	0.47	0.007	0.008	0.02	0.03	0.02	---	---	---	---	---	---

Table 2. Rust Flake Sizes and Chloride Contents in Representative Rusts from Various Bridges.

Bridge Designation	Rust Particle Size, mm Max.	Ave.	pH of extract with distilled water	Cl^-, ppm	Distance from Ocean or salt water lake, km.
DC (eastern part)	5.0	3.0	7.5-8.5	2.5-6.5	0 (in (lies at the edge of a salt water lake; Cl^- content: 3400 ppm)
HI (in western part)	4.5	2.0	5.0-6.5 (in flakes) 7.5-8.5 (in a sheet of rust)	4.7 (in flakes) 1.5-5 (in sheet)	~1.5
LR (in eastern part)	3.5	1.0	-	1-2	~10
GT (in western part)	2.5	1.0	~8	<1-1.5	~15
LU (in eastern part)	1.5 Sheets: up to 2.5 mm thickness in 3-layered samples	1.0	- 8-8.5	<1 0.8-1.6 (in sheets)	~10
LV (in central part)	0.75	0.5	5.7-7.3	0.6-1.2	~150
BR (in northern part)	0.75	0.5	5.8-7.9	0.5-1.5	~300

TABLE 3: . Average section thickness losses obtained from direct measurements at various locations in bridge spans in Louisiana and Texas

Bridge Locations	Average Section Thickness Losses, mils/year	
	Exterior vertical surfaces	Interior walls, horizontal and inclined faces
ZONE 1: Mild, rural atmosphere		
Boeuf river (BR)	about 1	inconclusive
Leesville (LV)	inconclusive	inconclusive
Average:	about 1	----
Estimate from field coupon data	about 0.2	about 0.5
ZONE 2: Medium severe, industrial, near coastal atmosphere		
Forked Island (FI)	2-2.5	inconclusive
Gibbstown (GT)	2-3	2-4
Luling (LU)- (approach span)	2-3	2-3
Larose (LR)	inconclusive	2-3
Average:	2-3	2-4
Estimate from field coupon data	about 1	1-1.5
From pitting data	----	2-4*
ZONE 3: Severe, near marine atmosphere, close to Gulf coast		
High Island (HI)	3	4-5
Doullut Canal (DC)	3	3-4
Luling (LU)- Main Span	1.5-2	4-5
Average:	3	3-5
Estimate from field coupon data	1-2	1.5-2
From pitting data	----	2-5*

* Conservative estimates from average and maximum pit depths measured. The losses should be higher than these values since some of the metal in the pitted area is also being uniformly corroded off. Thus the maximum values could be higher by one or two mils in selected localized areas of attack.

Table 4: Maximum and Average Pit Depths at Selected Locations in Representative Bridges. (Data in parenthesis refer to analogous locations on another pier, on the opposite side of the bridge)

Location in Bridge	Pit depth, 10^{-3} in. (mil)†									
	Eastern Sector				Western Sector				Averages	
Bridge:	Luling (LU)		Doullut Canal (DC)		High Island (HI)		Gibbstown (GT)		All Bridges	
	Max.	Ave.	Max.	Ave.	Max.	Ave.	Max.	Ave.	Max.	Ave.
(1) Vertical face on the side wall (inner, sheltered side)	9.7 (nearly equivalent surface)	5.8	12.0 (9.0)	7.7 (6.1)	7.4 (7.3)	4.5 (4.3)	9.0 (7.3)	5.6 (5.4)	8.8	5.6
(2) Vertical face on inner web plate,	24*	9.1*	8.	6.2	7.0 (6.7)	6.2 (5.1)	8.7 (13.5)	5.7 (7.7)	8.8	6.2
(3) Horizontal beam on pier, facing up	-	-	10.5 (12.9)	7.2 (10.4)	13.3 (6.8)	10.5 (4.7)	10.5 (7)	7.3 (5.1)	10.2	7.5
(4) Horizonal beam on pier, facing down	19.5 (14.8)	8.8 (9.5)	10.4 (14.0)	10.1 (10.3)	18.3 (9.6)	16.3 (6.2)	8.0 (11.0)	5.9 (7.3)	13.2	9.3
(5) Boxed location over gusset plate, facing up	41.2 (equivalent location)	21.8	52.4** 20.2 (20.0)	11.6 (10.6)	-	-	32 (30)	22.2 (17.8)	28.7	16.8

Table 4: Maximum and Average Pit Depths at Selected Locations in Representative Bridges. (Data in parenthesis refer to analogous locations on another pier, on the opposite side of the bridge)

Location in Bridge	Pit depth, 10^{-3} in. (mil)+									
	Eastern Sector				Western Sector				Averages	
Bridge:	Luling (LU)		Doullut Canal (DC)		High Island (HI)		Gibbstown (GT)		All Bridges	
	Max.	Ave.	Max.	Ave.	Max.	Ave.	Max.	Ave.	Max.	Ave.
(6) Horizonal surface, facing up, on gusset plate, outside of box	-	-	23.5 (12)	16.4 (10.3)	18.3 (17.3)	13 (8.7)	11.2 (6.5)	8.8 (5.1)	14.8	10.4
(7) Horizontal surface, facing down, on gusset plate, outside of box	-	-	13	10.3	-	-	15.7 (7.5)	12.4 (5.9)	12.1	9.5
(8) Edge flange at the entrance to the pier, facing down	-	-	12(16) (16)	10.3 (11)	9.3	4.5	5.5 (6)	4.3 (4.9)	9.8	7.0
(9) Inclined beam, top surface	7(7.9)	6(5.2)	7(7)	5.5(5.8)	15.7	11.6	16.5(11)	10.3(9.6)	10.3	7.7
(10) Inclined beam, bottom surface	-	-	20(12)	9(8.7)	12.9	10.2	18(6)	11.6(4.6)	13.8	8.8
(3) & (9)									10.3	7.6
(4), (7) & (10)									13	9.2
(1) & (2)									8.8	5.9

* Pits formed under sheet-type rust; values are anomalously high.

** Few such high readings were obtained; they do not include also perhaps some general thickness loss.

+ multiply mil by 25 to get values in μm.

Table 5: Constants K and N for power fit relation $Y = K t^N$ for data from steels exposed at various bridge sites.

Constants	Surface treatment no.					
	1	2	3	4	5	6
GIBBSTOWN BRIDGE						
K	.464	.6ØØ	.34Ø	.396	.4Ø7	.3Ø8
N	.297	.168	.277	.234	.236	.331
HIGH ISLAND BRIDGE						
K	.267	.195	.176	.251	.148	.Ø58
N	.427	.411	.412	.371	.446	.649
LEESVILLE BRIDGE						
K	.Ø21	.Ø43	.369	.Ø14	.ØØ9	.Ø14
N	.641	.352	.466	.526	.73Ø	.585
LULING BRIDGE						
K	.09113	.032	.032	.022	.025	.041
N	.562	.679	.649	.769	.733	.696

TABLE 6 . Average thickness losses obtained for weathering steel specimens exposed at sheltered locations under the bridges at various bridge sites and in bold-exposure mode at CEBA building, LSU, Baton Rouge.

Treatment Number	Average Thickness Losses, μm(mil)								
	Bridges								
	Gibbstown (GT)		High Island (HI) (Sheltered)		Luling (LU)		Leesville (LV)		CEBA, LSU (open)
	1 yr.	18 months	1 yr.	18 months	1 yr.	18 months	1 yr.	18 months	1 yr.
1	33 (1.3)	38 (1.5)	41 (1.6)	51 (2.0)	31 (1.25)	40 (1.6)	12 (0.5)	16 (0.6)	20 (0.8)
2					22 (0.9)	29 (1.2)	4(0.16)	5 (0.2)	9 (0.35)
3	21 (0.8)	23 (1.0)	27 (1.1)	32 (1.3)	19 (0.75)	24 (1.0)	7.5(0.3)	9 (0.4)	10 (0.4)
4					27 (1.1)	35 (1.4)	4(0.16)	5 (0.2)	9 (0.35)
5					24 (0.95)	31 (1.25)	9 (0.4)	12 (0.5)	10 (0.4)
6	27 (1.1)	32 (1.3)	34 (1.4)	46 (1.8)	31 (1.25)	40 (1.6)	5 (0.2)	7 (0.3)	15 (0.6)

Type of Site: GT, Lu - Industrial, coastal, semi-rural; HI - Coastal, near-marine, semi-industrial; LV - rural; CEBA, LSU - semi- industrial.

Table 7 : Constants K and N for power fit relation $Y=Kt^N$ for Exterior Exposure at CEBA, LSU.

Constants	Surface treatment no.							
	1	2	3	4	5	6	7	9
A-588 Grade A (Kaw)								
K	.016	.028	.016	.016	.022	.019	.013	.212
N	.778	.552	.685	.453	.621	.690	.815	.396
A-588 Grade A (US)								
K	.023	.042	.030	.02	.017	.010	.016	.424
N	.700	.471	.551	.601	.655	.789	.767	.258

TABLE 8 Average thickness losses for weathering steels reported by various investigators around the world. Exposure time in years is given in parenthesis.

Exposure condition	Average Thickness Losses, μm (mil)									
	Country	U.K.	Brazil	Australia.	Czech.	Norway	U.S.A.	U.S.A.	U.S.A.	
	Ref.	Mckenzie (2) (5 yrs)	Dutra & deO Vianna (5)(per yr)	Wallace & Badger (6)(10yr)	Knotkova et al(9)	Atteras et al(13) Finland Hakkarainen (14)(5yr)	Townsend Zoccola (10) (5 yrs)	Reed & Kendrick (CA-HD,18) (per yr.)	Raman, et al present work (1 yr) Trt.1	Passivn. Trts.
Exterior Bold	Rural	75-100 (3-4)	15 (0.6)	50 (2)	50 (2)	40-60 (2)	60(2.4)	2-3(0.1)	----	----
	Industrial	150-225 (6-9)	60-75 (2.4-3)	100-125 (4-5)	100-150 (4-6)	----	55-70 (2-3)	4 (0.15)	20(0.8)	9-15 (0.4-0.6)
	Marine	75(3)	300(12)-25(1)	----	----	----	75 (3)	8(0.33)	----	----
Interior Sheltered	Rural	75(3)	----	----	----	----	----	----	12(0.5)	4-10 (0.2-0.4)
	Industrial	75(3)	----	----	----	----	----	----	30(1.2)	20-30 (0.8-1.2)
	Marine	150(6)	----	----	----	----	----	----	----	----
	Near-Marine	----	----	----	----	----	----	----	40(1.6)	25-35 (1-1.4)

TABLE 9 . Summary of Laboratory Test Results- Average thickness losses in μm (mil) obtained for different steels in various tests in the untreated and chemical-treated conditions.

Type of Test	Average Thickness Losses, μm (mil)							
	Type of Steels							
	A588-Grade.A (US Steel)		A588-Grade.A(Kaw.steel)		A588-Grade.B(Beth.Steel)		A36 steel	
	Untrtd.	Treated	Untrtd.	Treated	Untrtd.	Treated	Untrtd.	Treated
AAEST-EBL								
-2200 cycles	50 (2)	30 (1.2)	15*(0.6)*	6*(0.25)*	40 (1.6)	30 (1.2)	75(3)	40 (1.6)
-1 yr.aver.	8 (0.33)	5 (0.2)	2.5*(0.1)*	1*(0.04)*	7 (0.27)	5 (0.2)	12.5 (0.5)	7 (0.27)
AAEST-ISL								
-2200 cycles	145 (5.8)	115 (4.6)	160 (6.4)	150 (6)	140 (5.6)	125 (5)	200(8)	190 (7.6)
-1 yr.aver.	25 (1)	20 (0.8)	27 (1.1)	25 (1)	23 (0.9)	21 (0.8)	33(1.33)	31(1.25)
Salt Water Immersion								
-1 yr. aver.	65 (2.5)	40 (1.6)	65 (2.5)	50 (2)	65 (2.5)	45 (1.8)	60 (2.4)	----
Salt Fog								
-100 days	280 (11)	235 (9.5)	190 (7.5)	150 (6)	445 (17.5)	318 (13)	300 (12)	215(8.5)
-1 yr.aver.	1025(41)	850 (34)	700 (28)	550 (22)	1625(65)	1150(46)	1100(44)	800(32)
Electrochem. -initial rate (mpy)	1500-2500 (60-100)	---- **	----	----	1500-2500 (60-100)	---- **	1500-2500 (60-100)	---- **

* Results obtained without periodic application of 3.5%NaCl solution or a 0.1% soln. of H_2SO_4.

** In potentiostatic tests performed with coupons treated with 25% phosphoric acid the magnitude of the anodic current after stabilization was about an order of magnitude smaller than for untreated surfaces. Accordingly, an order of magnitude lower corrosion losses can be assumed for phosphoric acid treated surfaces.

Table 10A: Constants K & N calculated for power fit relation relating weight loss vs exposure time in the Continuous Immersion Test.

Constant	Surface treatment 1	2	3	4	5	6	7	9
A 588 Grade A (Kaw)								
K	.029	.062	.025	.111	.076	.090	.039	.319
N	.865	.654	.824	.570	.650	.560	.800	.406
A 588 Grade A (US)								
K	.032	.056	.024	.022	.028	.036	.053	.253
N	.855	.609	.808	.885	.801	.633	.677	.481
A 588 Grade B (US)								
K	.036	.155	.049	.022	.062	.008		
N	.843	.506	.699	.849	.648	1.03		
Riverten R								
K	.052	.098	.052	.042	.019	.0634	.033	.085
N	.703	.485	.612	.704	.911	.415	.900	.723
A-36 Mild Steel								
K	.040						.034	.167
N	.877						.922	.592

Table 10B- Constants K and N calculated for power fit relation, relating weight loss vs exposure time for A588-grades A,B, and A36 mild steels.

1- AAEST-EBL (A588-A Kaw.)	Treatment Numbers 1	2	3	4	5	6	7	9
K+	0.038	0.132	0.023	0.039	0.019	0.006	0.004	---
N	0.359	0.132	0.367	0.291	0.452	0.611	0.751	---
AAEST-EBL (A588-A USS)								
K	0.003	0.003	0.004	0.011	0.009	0.021	---	---
N	0.943	0.918	0.859	0.703	0.746	0.596	---	---
AAEST-EBL (A588-B BS)								
K	0.007	0.005	0.001	0.014	0.007	0.038	---	---
N	0.786	0.836	1.04	0.678	0.778	0.524	---	---
AAEST-EBL (A36-MILD)								
K-	0.003	0.015	0.005	0.010	0.040	0.008	---	---
N	0.984	0.684	0.847	0.736	0.530	0.777	---	---
2- AAEST-ESL (A588-A Kaw.)								
K	0.015	0.004	0.006	0.004	0.010	0.007	0.013	0.008
N	0.874	1.040	0.987	1.050	0.914	0.938	0.887	0.948
AAEST-ESL (A588-A USS)								
K	0.024	0.007	0.003	0.004	0.004	0.020	0.004	---
N	0.764	0.936	1.030	1.040	1.020	0.785	1.050	---
AAEST-ESL (A588-B BS)								
K	0.086	0.050	0.012	0.034	0.005	0.010	---	---
N	0.624	0.687	0.894	0.726	1.010	0.909	---	---
AAEST-ESL (A36-MILD)								
K	0.005	0.031	0.004	0.001	0.0004	0.004	---	---
N	1.030	0.781	1.070	1.230	1.380	1.110	---	---

Table 10B - Continued

		1	2	3	4	5	6	7	9
3- Salt fog test (A588-A Kaw.)									
	K	0.218	0.120	0.092	0.097	0.088	0.098	0.167	0.228
	N	0.914	1.030	1.080	1.010	1.050	1.070	0.995	0.986
Salt fog test (A588-A USS)									
	K	0.464	0.065	0.094	0.019	0.055	0.073	0.253	---
	N	0.817	1.230	1.150	1.450	1.310	1.310	0.992	---
Salt fog test (A588-B BS)									
	K	0.294	0.116	0.113	0.120	0.124	0.255	0.356	---
	N	1.050	1.210	1.150	1.140	1.160	1.070	1.010	---
Salt fog test (A36-Mild)									
	K	0.696	0.196	0.284	0.104	0.173	0.796	0.825	---
	N	0.762	0.973	0.925	1.110	1.000	0.729	0.709	---

Abbreviations:
Kaw = Kawasaki Steel Co., Japan; USS = U.S. Steel Co.;
BS = Bethleham Steel Co.; Mild = mild steel

TABLE 11

ANALYSIS OF IR ABSORPTION PATTERNS FOR RUSTS FORMED ON WEATHERING STEEL SURFACES WITH VARIOUS TREATMENTS

Trt. No.	Trt. (No., appln.)	Phases present (dominant phase given first)	Figure 14-
		Mild Environmental Conditions (Rural)	
		a) Lv at Interior Locations	
1	3 MAT	AM + tr. γ(am)	A(a)
1	6 MAT	F + γ^* + AM + δ(am)	A(b)
1	15 MAT	F + γ^* + δ	A(c)
1	18 MAT	F + γ^* + δ	A(d)
2	1 MAT	AM	A(e)
2	3 MAt	F + AM	A(f)
2	1 YAT	F + γ^* (am) + AM	A(g)
		b) BR at Exterior Locations	
Rust as is		δ(am) + γ^* (tr.)	B(a)
2	2 YAT	AM + tr. δ	B(b)
2	2 YAT + 1 YRT	AM	B(c)
12	2 YAT	AM + δ(am) + γ^* (tr.) + γ (tr.)	B(d)
6	1 YAT	δ(am) + γ^* (am) + AM	B(e)
6	2 YAT	δ(am) + γ^* (am. tr.) + AM	B(f)
16	2 YAT	AM	B(g)
7	1 YAT	δ(am) + γ^* (am. tr.)	B(h)
7	2 YAT	δ + γ^* + tr. γ	B(i)

c) LV at Interior Locations

Rust as is		δ(am) + γ^* (am. tr.)	C(a)
4	2 YAT	AM + δ(am) + tr.γ^*	C(b)
4	2 YAT + 1 YRT	δ(am) + tr.γ^* + AM	C(c)
6	2 YAT	AM + γ^* (am. tr.) + δ(am. tr.) + F(am. tr.)	C(d)
6	2 YAT + 1 YRT	AM + δ(am. tr.) + γ^* (am. tr.)	C(e)
6	2 YAT + 1 YRT (another location - violet brown rust)	δ + γ^* (tr.) + AM	C(f)
16	1 YAT	δ(am) + γ^* (am) + AM + + I_1	C(g)
16	2 YAT	AM + δ(am)	C(h)

d) BR at Interior Locations

5	1 YAT	AM	D(a)
5	2 YAT	δ(am) + γ^* (am. tr.) + AM	D(b)
5	2 YAT + 1 YRT	AM + δ(am) + F(am)	D(c)
3	1 YAT	AM	D(d)
3	2 YAT	AM + δ(am. tr.) + γ^* (am. tr.)	D(e)

Environment of Medium Severity (Mild Industrial)

a) LU at Interior Locations

1	6 MAT	δ + γ^* + α(am) + AM	E(a)
1	9 MAT	δ + γ^* + AM	E(b)
1	1 YAT	δ + γ^* (tr) + α(am)	E(c)
5	1 MAT	AM + δ(am. tr.) + F(am. tr.) + γ(am. tr.)	E(d)
5	3 MAT	AM + δ + γ^* (am. tr.)	E(e)
5	9 MAT	AM + δ + γ^* (am. tr.)	E(f)
5	1 YAT	AM + δ(am) + α(am) + γ^* (am.tr.)	E(g)

5	15 MAT	$\delta + \gamma^{*} + \alpha$	E(h)

b) GT at Exterior Locations

2	6 MAT	AM	F(a)
2	1 YAT	AM	F(b)
2	2 YAT + 1 YRT	AM	F(c)
4	6 MAT	$\delta + \gamma^{*}_{*} + \alpha$ + AM	F(d)
4	1 YAT	$\delta + \gamma^{*}$ (tr.) + AM(tr.)	F(e)
4	2 YAt + 1 YRT	$\delta + \gamma^{*}$ (am. tr.) + AM	F(f)

c) GT at Interior Locations

3	6 MAT	AM	G(a)
3	9 MAT	AM	G(b)
3	1 YAT	AM	G(c)
3	18 MAT	AM + δ(am. tr.)	G(d)

d) LU at Exterior Locations

3	6 MAT	AM + δ(am) + F(am) + γ^{*} (a.m tr.)	H(a)
3	1 YAT	AM + δ(am) + γ^{*} (am.)	H(b)
3	2 YAT	AM + δ + γ^{*} (tr)	H(c)
3	1 YAT + 6 MRT	AM + δ + γ^{*} (tr)	H(d)
3	2 YAT + 6 MRT	AM + δ	H(e)
3	2 YAT + 1 YRT	$\delta + \gamma^{*}$ (tr) + AM	H(f)
3	2 YAT + 6 MAT + 1 YAT	AM + δ + γ^{*} (tr)	H(g)

e) CEBA at Exterior Locations

5	1 MAT	γ^{*} + AB + δ (am. tr.)	I(a)
6	1 MAT	I_1	I(b)
6	1 MAT another specimen	γ^{*} + I_1 + δ (am. tr.)	I(c)
6	3 MAT	γ^{*} + δ (am) + AB	I(d)
6	1 YAT	δ + γ^{*} + AB	I(e)
7	1 MAT	γ^{*} + δ (am. tr.)	I(f)
9	3 MAT	γ^{*} + δ + α	I(g)

Very close to Sea Shore (Marine)

a) HI at Interior Locations

2	6 MAT	AM + γ^{*} (tr) + δ	J(a)
2	2 YAT	AM + δ + γ (tr)	J(b)
2	2 YAT + 1YRT	AM + δ + γ (tr)	J(c)
3	1 YAT	AM + γ^{*} (am. tr.) + δ	J(d)
3	1 YAT + 6 MRT	AM + γ^{*} (am. tr.) + δ	J(e)
3	2 YAT	AM + δ + γ^{*} (tr)	J(f)
3	2 YAT + 1 YRT	AM + γ + γ^{*} (tr)	J(g)

---

b) HI at Exterior Locations

2	1 YAT	AM + δ (tr) + γ^{*} (tr)	K(a)
2	2 YAT	γ + δ (am. tr.) + γ^{*} (am. tr.)	K(b)
2	1 YAT + 6 MRT	AM	K(c)
2	2 YAT + 6 MRT	AM	K(d)
2	2 YAT + 1 YRT	AM + δ (am. tr.) + γ^{*} (am. tr.)	K(e)
12	2 YAT	γ (am) + tr. AM	K(f)
4	6 MAT	AM + δ (am. tr.) + γ^{*} (am. tr.)	K(g)
4	1 YAT	AM + δ + γ^{*} (tr)	K(h)

c) HI at Exterior Locations

6	6 MAT	$\delta + \gamma^{*} + \alpha$	L(a)
6	1 YAT	δ(am) + γ^{*}(am. tr.) + AM	L(b)
6	2 YAT	δ(am) + γ^{*}(am. tr) + γ(am. tr.)	L(c)
6	1 YAT + 6 MRT	δ(am) + γ^{*}(am.) + AM	L(d)
6	2 YAT + 6 MRT	AM + δ(am) + γ^{*}(am. tr.)	L(e)
6	2 YAT + 1 YRT	AM + δ(am) + γ^{*}(am. tr.) + γ(am. tr)	L(f)

TABLE 12. Comparison of Average Thickness Losses of Weathering Steel A588 in Field Exposure, with those obtained in Simulated Laboratory Corrosion Tests and with those determined on the Steel Beams in Bridge Sections.

Exposure Condition	Environment type	First Year Thickness Losses, μm (mil)					
		Field Coupons		Field Readings	Pitting Characteristics & Pit depths, (mils) max./ave.)	Laboratory Tests	
		SB only (Trt.1)	Chemical Trts.2-6	SB and WB (Trts.1&7)	(after about 12 yrs in use)	SB&AP (Trts.1&7)	Chemical Trts.2-6
Exterior, Bold	Rural	----	----	(1-2)	No pitting	2.5(0.1)	1 (0.04)
	Industrial	20 (0.8)	9-15 (0.4-0.6)	(2-3)	Very fine and shallow pits	8 (0.33)	5 (0.2)
	Near-Marine	----	----	(2-3)	Very fine, 5 mils deep	----	----
Interior, Sheltered	Rural (LV)	12 (0.5)	4-10 (0.2-0.4)	(2)	No pitting	----	----
	Industrial (GT,LU)	30 (1.2)	20-30 (0.8-1.2)	(2-4)	(9-41/6-17); low on vertical faces, deepest at boxed locations; max. 41 mil at LU	25 (1.0)	20 (0.8)
	Near-Marine (HI)	40 (1.6)	25-35 (1.0-1.4)	(3-5)	(8-52/6-16) Max. pit depth: 52 mil at DC	----	----
Complete Wetting, hot, muggy	Tropical Marine	----	----	----	Very wide and shallow pits	1000-1625 (40-65)	500-1000 (20-40)
Complete Immersion	Stagnant sea water	----	----	----	No visible pitting	65 (2.5)	40-50 (1.6-2)
Electro-chemical	0.1% chloride soln.	----	----	----	No pitting at low current densities	(60-100)	(5-10)

FIGURES

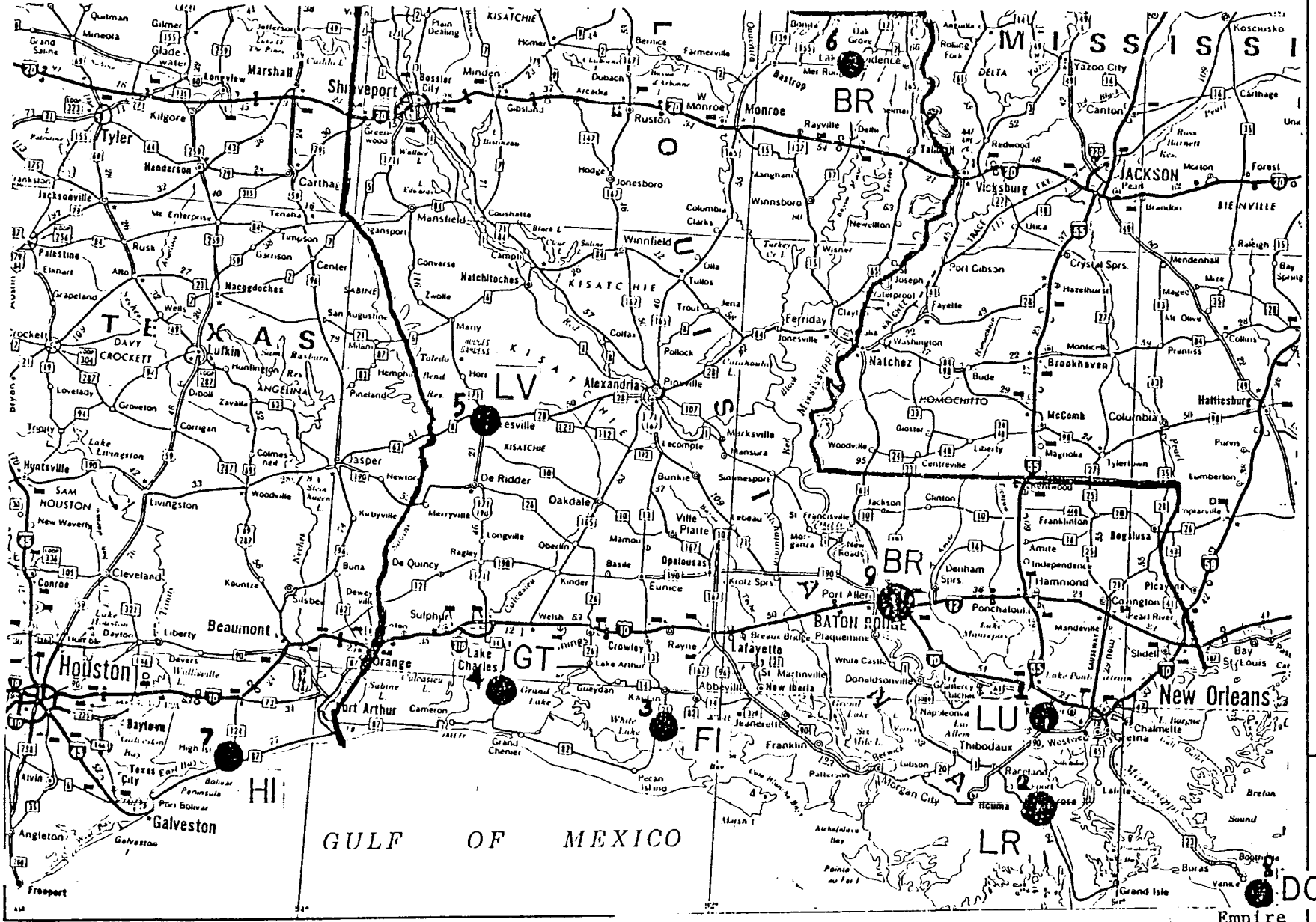

LOCATIONS OF CHOSEN BRIDGE SITES FOR FIELD STUDY

FIG. 1

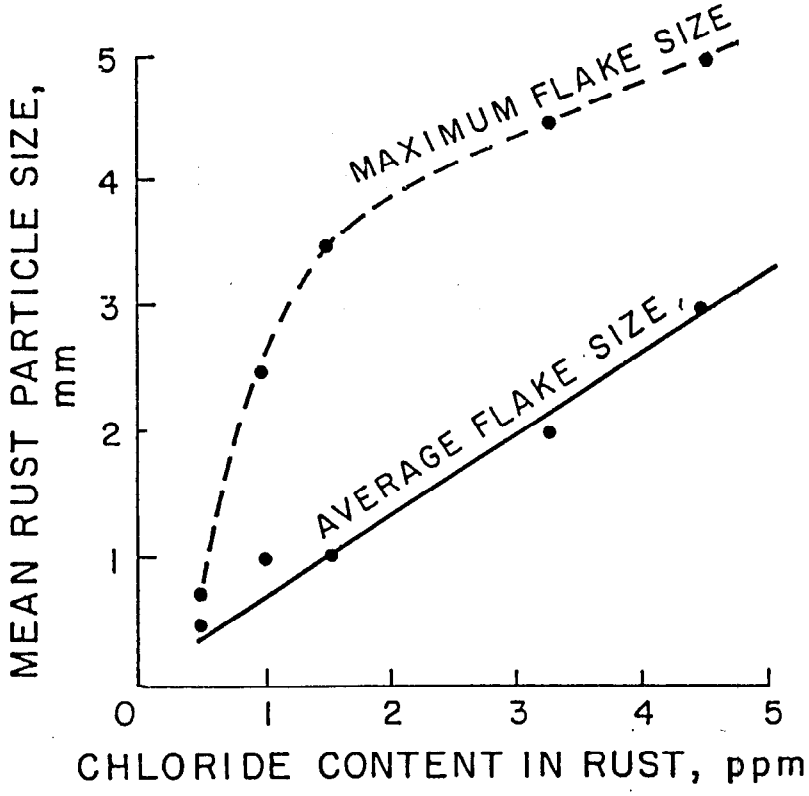

FIG. 2
DEPENDENCE OF RUST PARTICLE SIZE
ON CHLORIDE CONTENT IN RUST

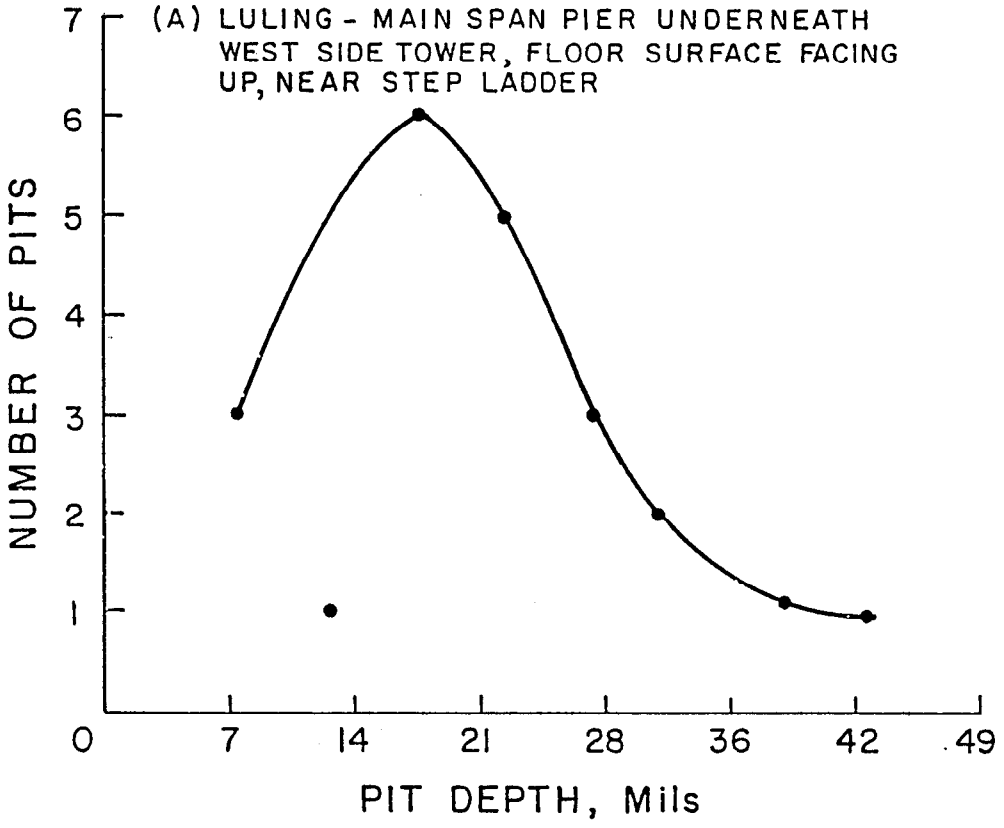

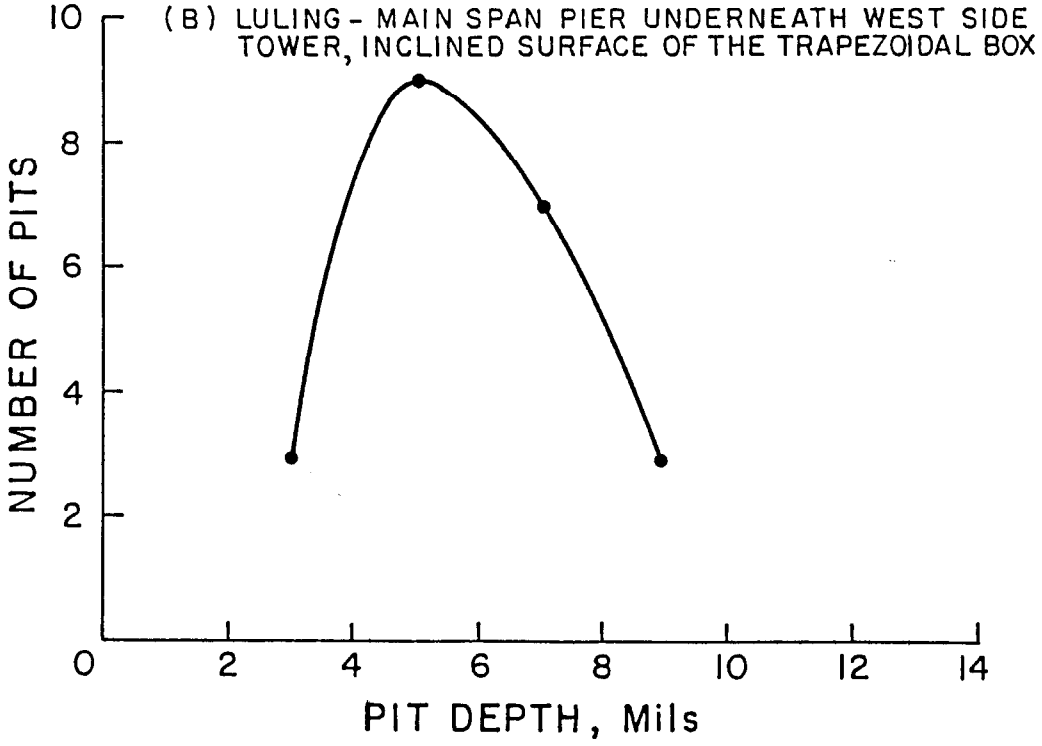

FIG.3

PIT DEPTH PROFILES

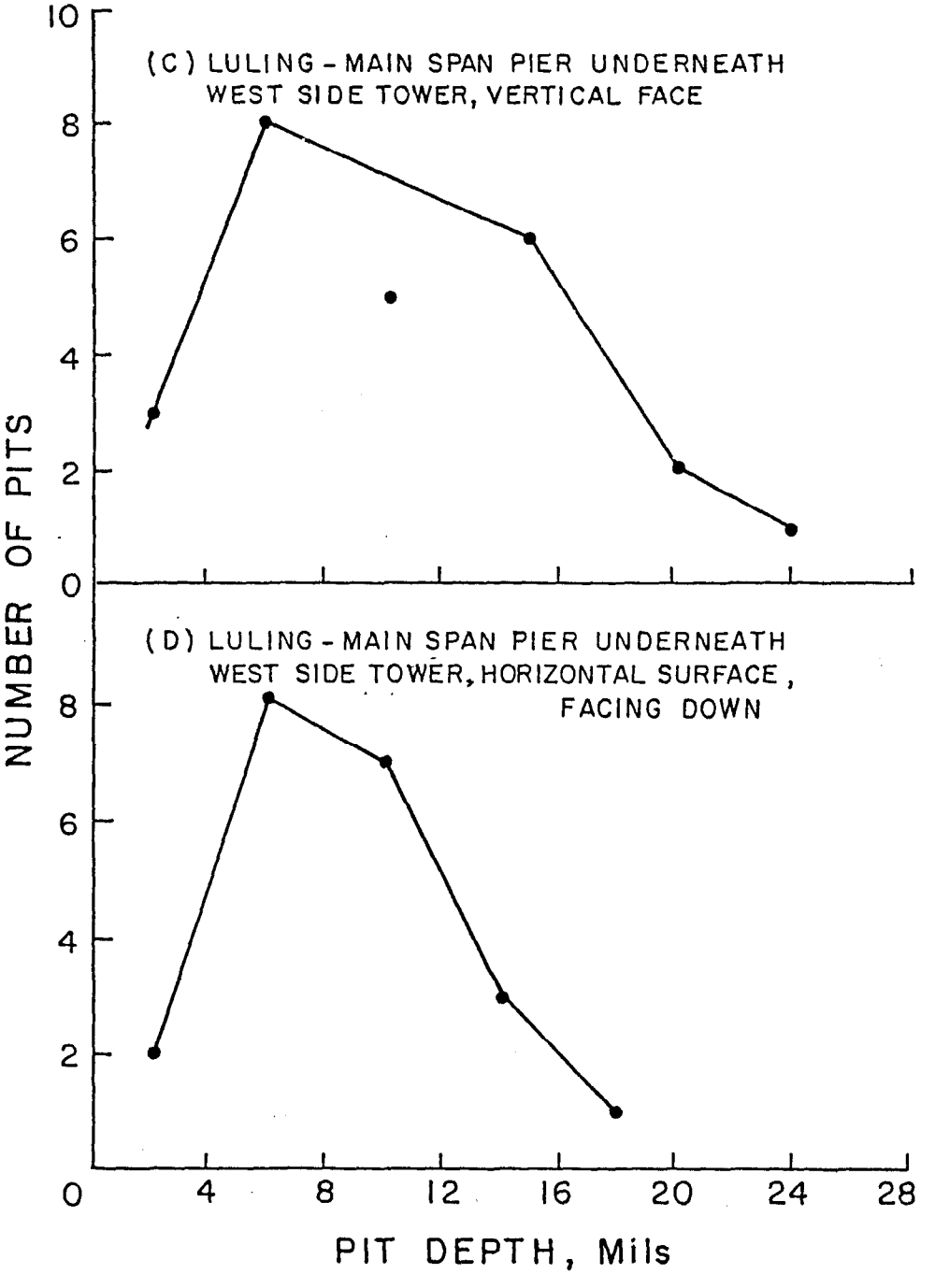

FIG.3

PIT DEPTH PROFILES

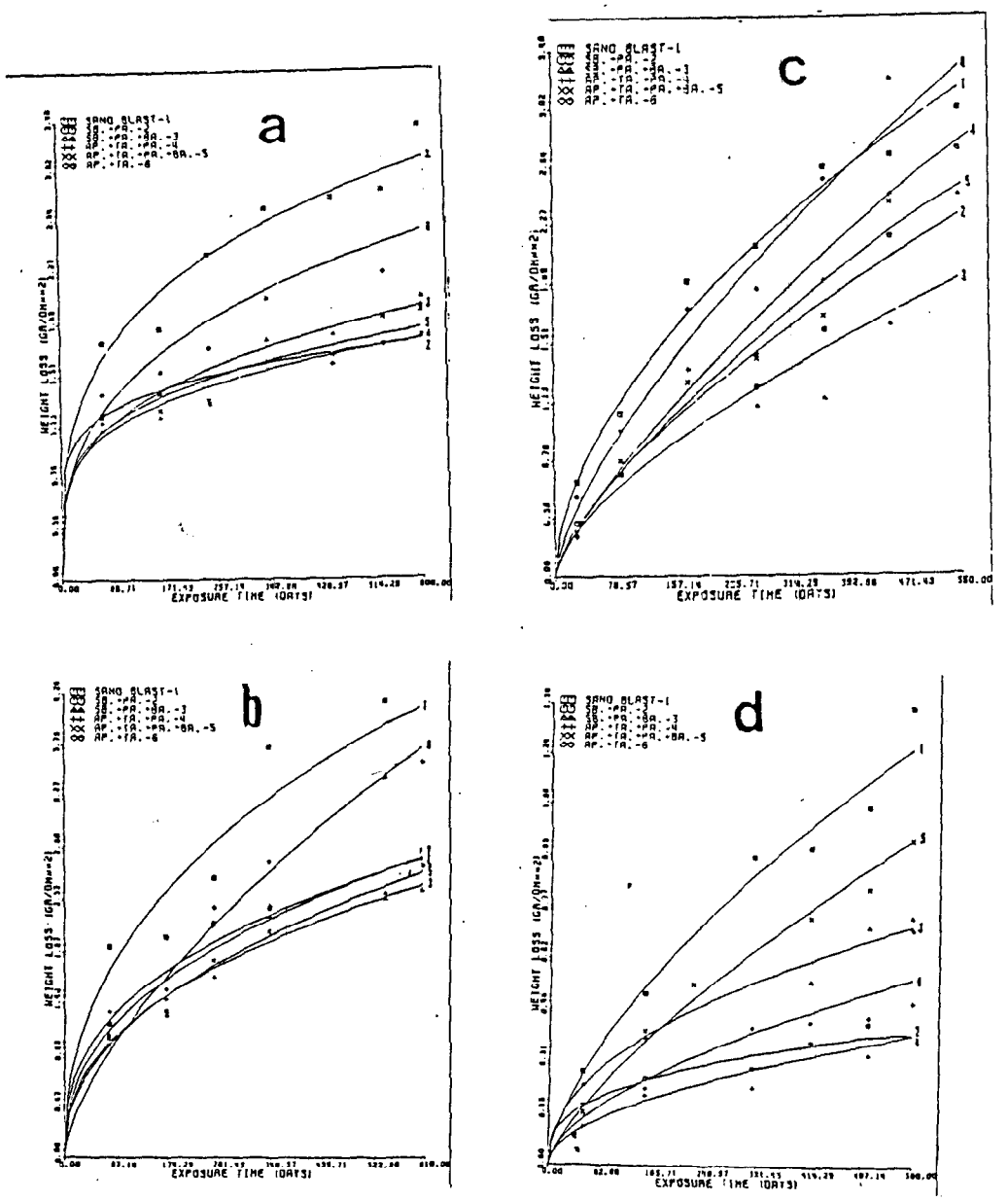

Fig.4

Fig. 4. Wt. Losses vs. Exposure Time for Weathering Steel Field Coupons Exposed in Sheltered Locations at the Four Bridge Sites

(a) GT, (b) HI, (c) LU and (d) LV

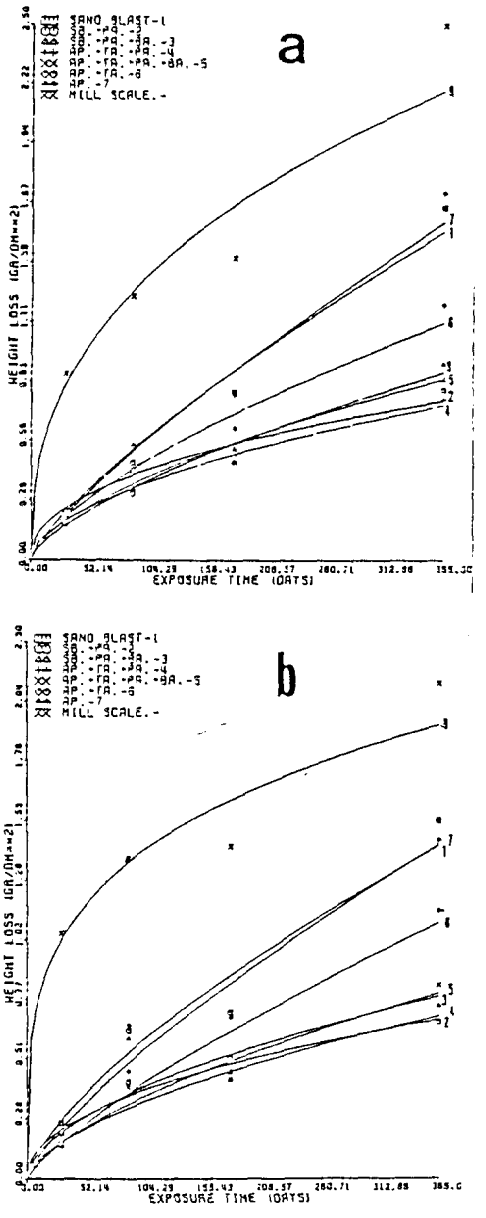

Fig.5

Fig. 5. Wt. Losses vs. Exposure Time for Weathering Steel Coupons Bold - Exposed at CEBA, LSU

(a) U.S. Steel - A588 - Grade A
(b) Kawasaki Steel - A588 - Grade A.

CAPTIONS TO FIGURES

Fig. 6. Wt. Losses vs. No. of Wet-Dry Cycles for Weathering and Mild Steels in the Accelerated Atmospheric Exposure Simulation Test Sheltered Location Exposure Equivalent (AAEST-SLE)

a) A588 - Grade A (U.S. Steel)
b) A588 - Grade A ((Kawasaki Steel)
c) A588 - Grade B
d) A36 Steel

Fig. 7. Wt. Losses vs. NO. of Wet-Dry Cycles for Weathering and Mild Steels in the Accelerated Atmospheric Exposure Simulation Test Bold Location Exposure Equivalent (AAEST-BLE)

a) A588 - Grade A (U.S. Steel)
b) A588 - Grade A (Kawasaki Steel)
c) A588 - Grade B
d) A36 Steel

Fig. 8. Wt. Losses vs. Exposure Time for Weathering Steels in the Salt Fog Test

a) A588 - Grade A (U.S. Steel)
b) A588 - Grade A (Kawasaki Steel)
c) A588 - Grade B
d) A36 Steel

Fig. 9. Wt. Losses as a Function of Exposure Time for Weathering and Mild Steels in the Continuous Immersion Test in Salt Water

a) A588 - Grade A (U.S. Steel)
b) A588 - Grade A (Kawasaki Steel)
c) A588 - Grade B
d) Riverten Steel (Kawasaki Steel)
e) A36 Steel

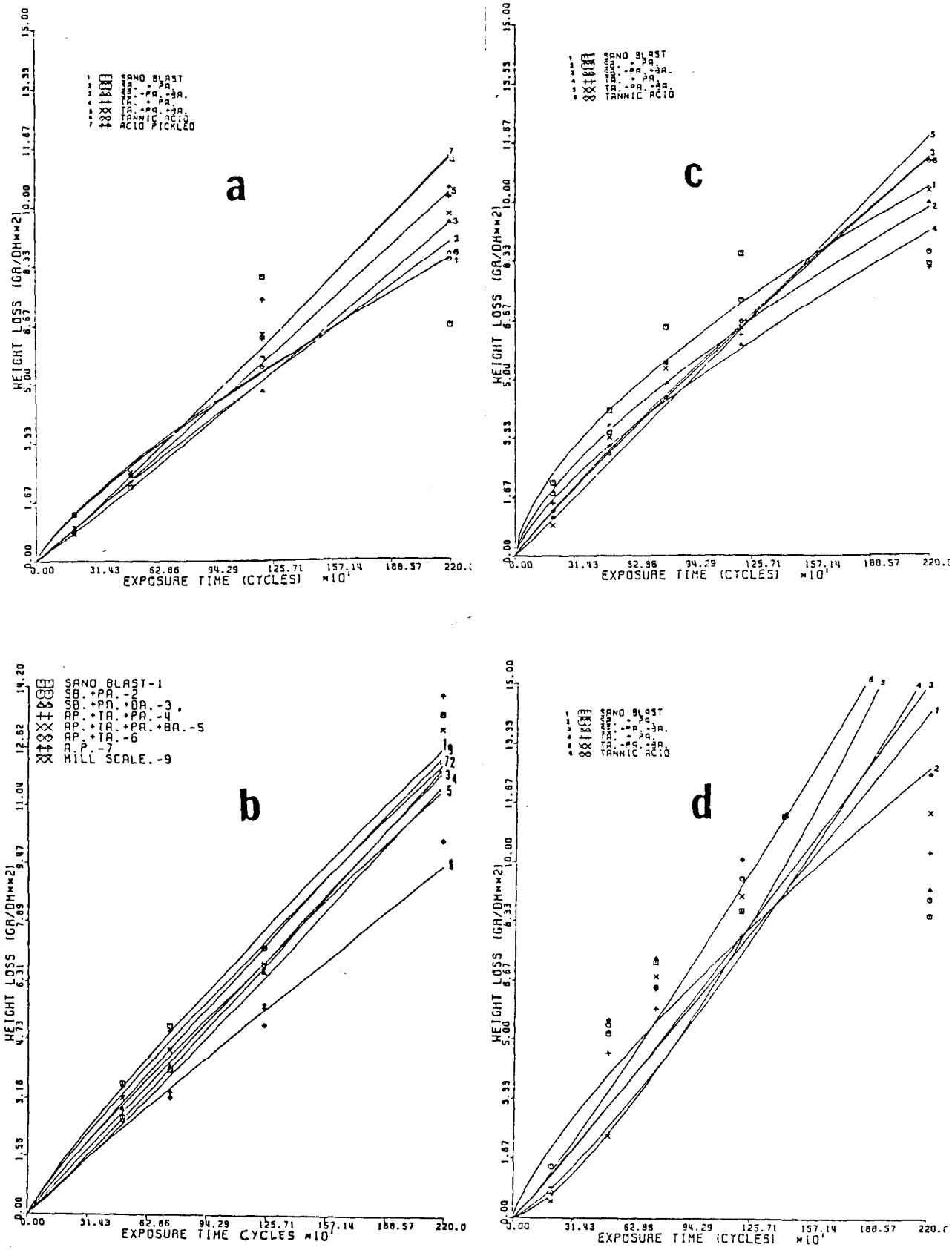
a
b
c
d
HEIGHT LOSS (GR/DM**2)
EXPOSURE TIME (CYCLES) *10'
EXPOSURE TIME CYCLES *10'
SAND BLAST
TANNIC ACID
SAND BLAST-1
SB.+PA.-2
SB.+PA.+BA.-3
AP.+TA.+PA.-4
AP.+TA.+PA.+BA.-5
AP.+TA.-6
A.P.-7
MILL SCALE.-9

Fig. 6

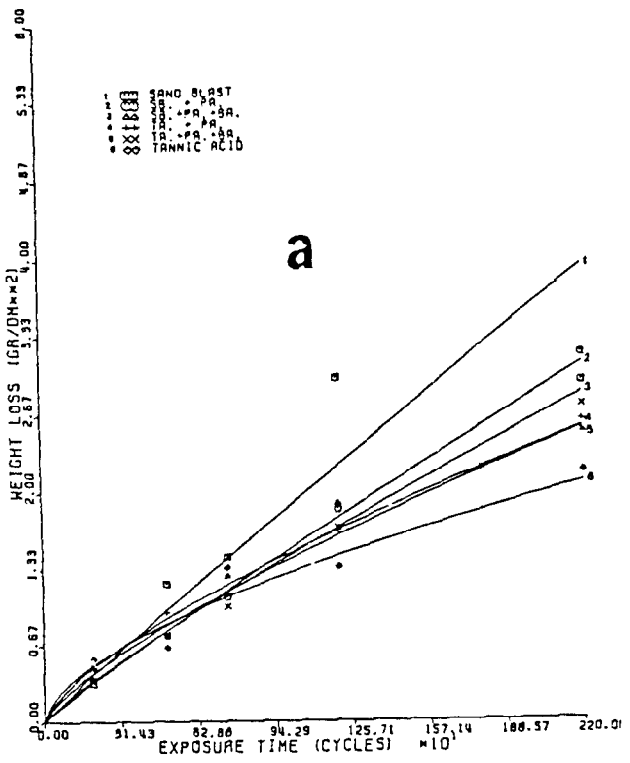
a
SAND BLAST
TANNIC ACID
WEIGHT LOSS (GR/DM*M2)
EXPOSURE TIME (CYCLES) *10

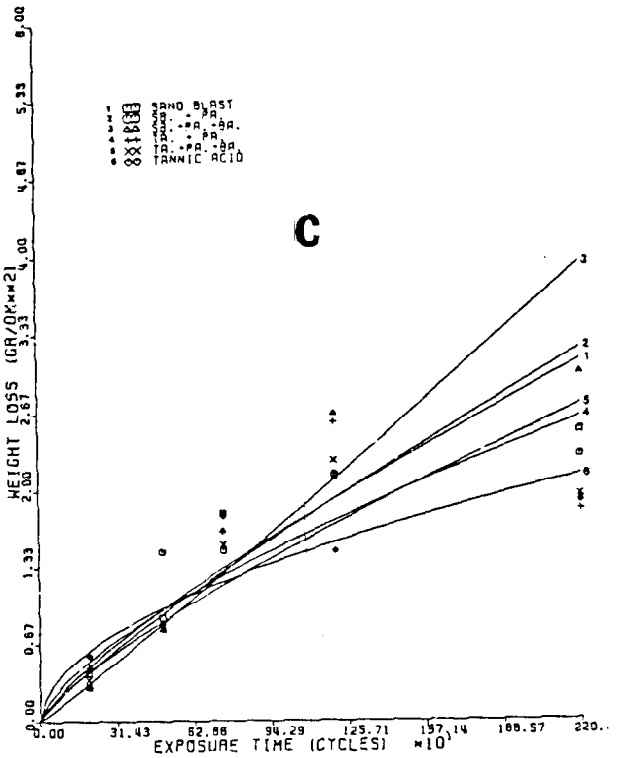
c
SAND BLAST
TANNIC ACID
WEIGHT LOSS (GR/DM*M2)
EXPOSURE TIME (CYCLES) *10

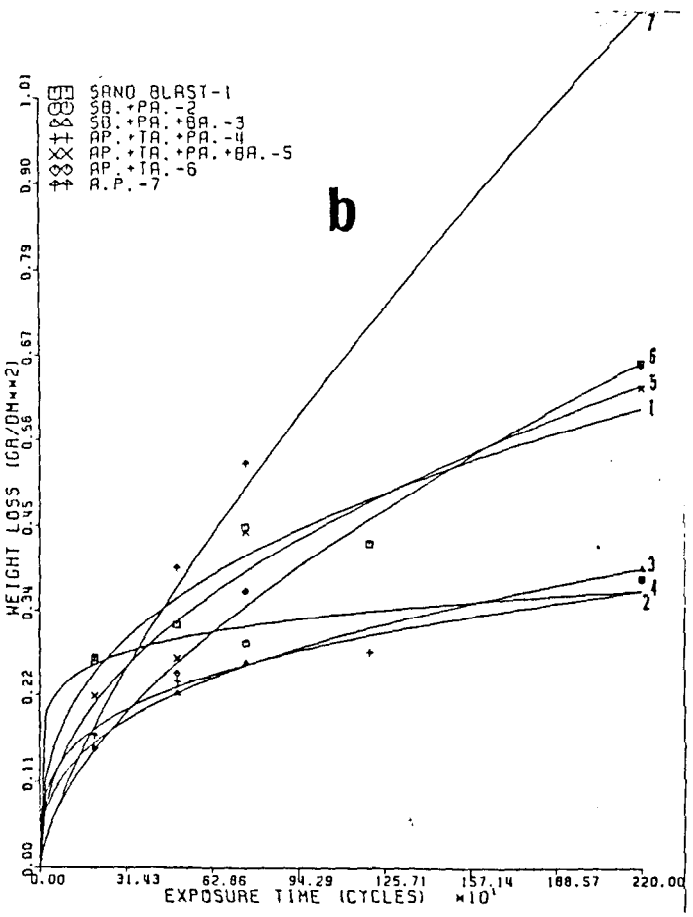
b
SAND BLAST-1
SB.+PA.-2
SB.+PA.+BA.-3
AP.+TA.+PA.-4
AP.+TA.+PA.+BA.-5
AP.+TA.-6
A.P.-7
WEIGHT LOSS (GR/DM*M2)
EXPOSURE TIME (CYCLES) *10

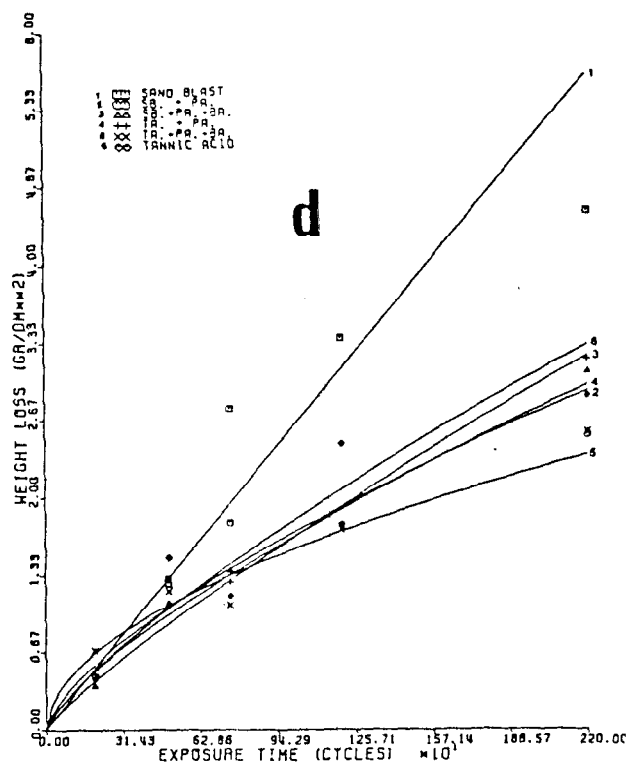
d
SAND BLAST
TANNIC ACID
WEIGHT LOSS (GR/DM*M2)
EXPOSURE TIME (CYCLES) *10

Fig.7

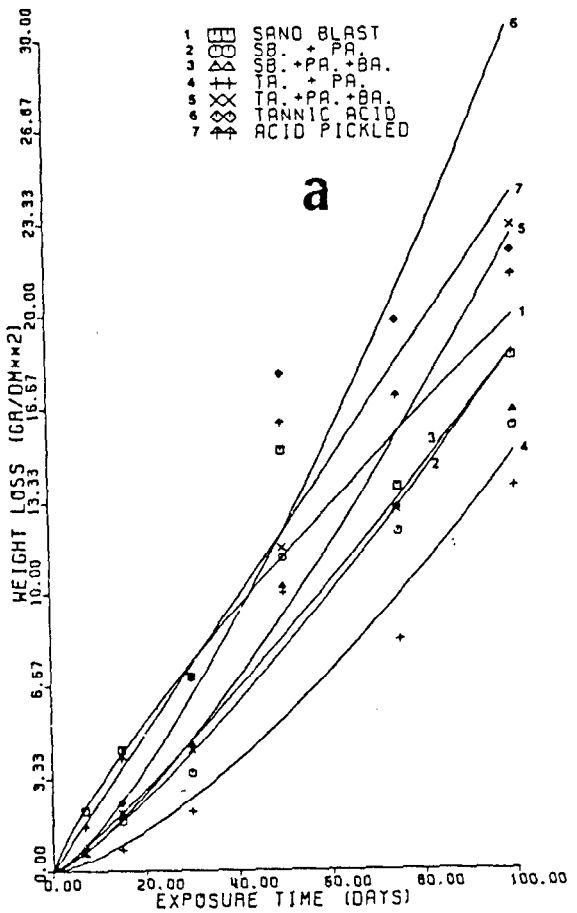
1 SAND BLAST
2 SB. + PA.
3 SB. +PA. +BA.
4 TA. + PA.
5 TA. +PA. +BA.
6 TANNIC ACID
7 ACID PICKLED
a
WEIGHT LOSS (GR/DM**2)
0.00
3.33
6.67
10.00
13.33
16.67
20.00
23.33
26.67
30.00
0.00
20.00
40.00
60.00
80.00
100.00
EXPOSURE TIME (DAYS)

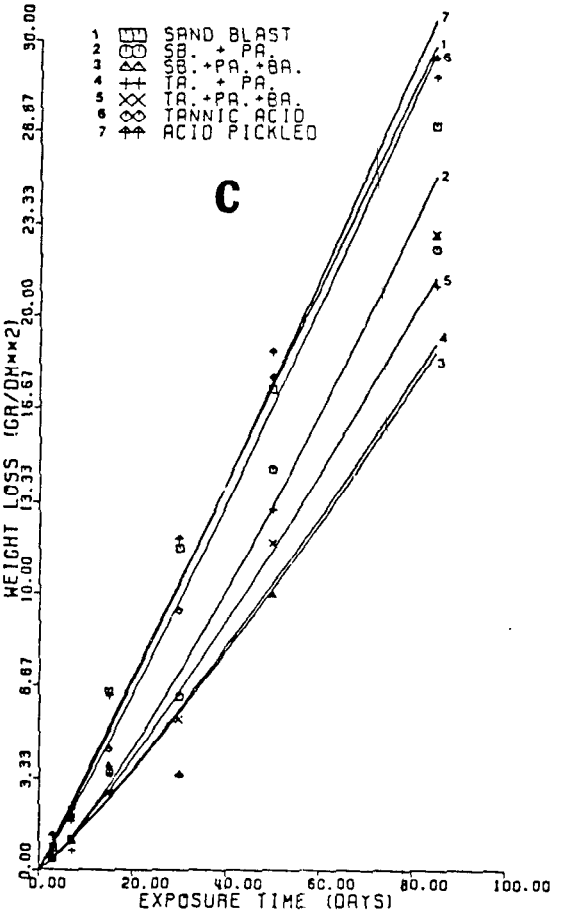
1 SAND BLAST
2 SB. + PA.
3 SB. +PA. +BA.
4 TA. + PA.
5 TA. +PA. +BA.
6 TANNIC ACID
7 ACID PICKLED
c
WEIGHT LOSS (GR/DM**2)
0.00
3.33
6.67
10.00
13.33
16.67
20.00
23.33
26.67
30.00
0.00
20.00
40.00
60.00
80.00
100.00
EXPOSURE TIME (DAYS)

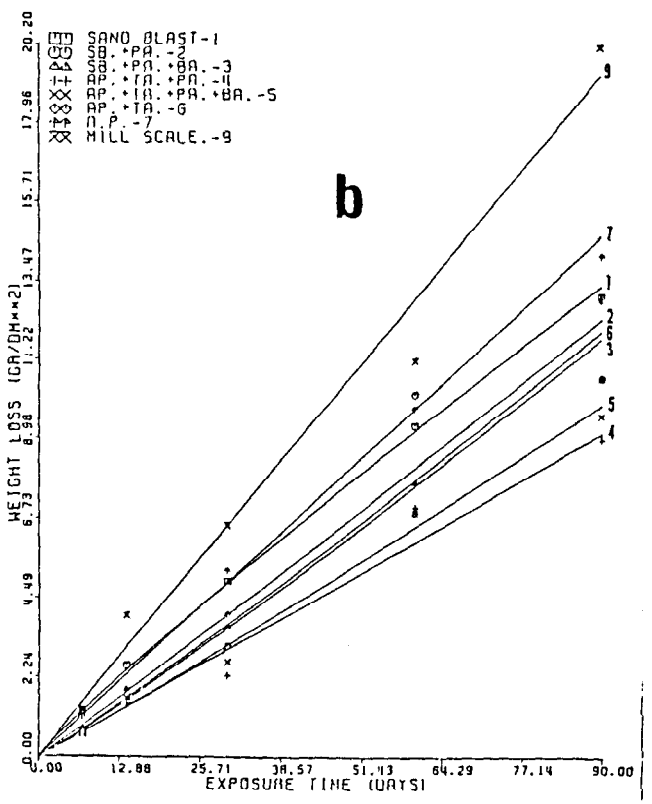
SAND BLAST-1
SB. +PA.-2
SB. +PA. +BA.-3
AP. +TA. +PA.-4
AP. +TA. +PA. +BA.-5
AP. +TA.-6
N.P.-7
MILL SCALE.-8
b
WEIGHT LOSS (GR/DM**2)
0.00
2.24
4.49
6.73
8.98
11.22
13.47
15.71
17.96
20.20
0.00
12.86
25.71
38.57
51.43
64.29
77.14
90.00
EXPOSURE TIME (DAYS)

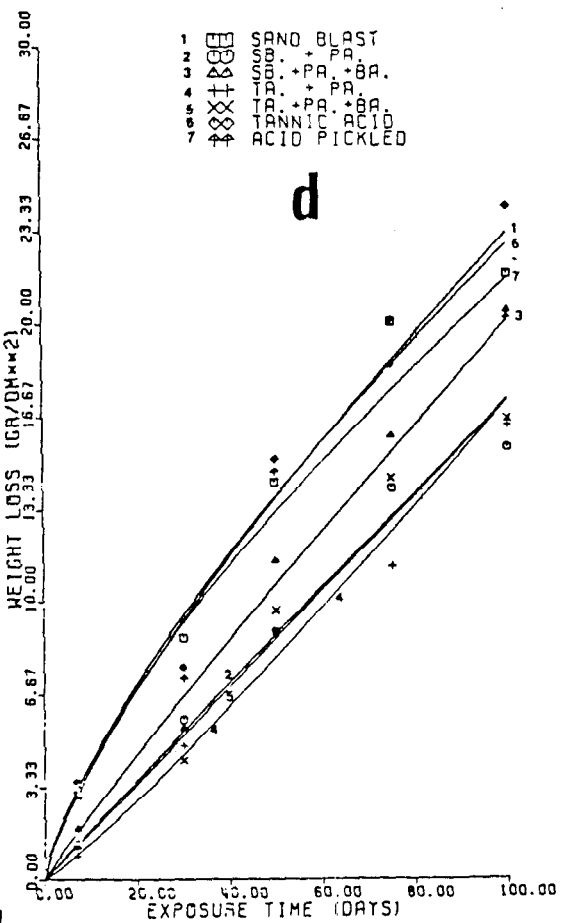
1 SAND BLAST
2 SB. + PA.
3 SB. +PA. +BA.
4 TA. + PA.
5 TA. +PA. +BA.
6 TANNIC ACID
7 ACID PICKLED
d
WEIGHT LOSS (GR/DM**2)
0.00
3.33
6.67
10.00
13.33
16.67
20.00
23.33
26.67
30.00
0.00
20.00
40.00
60.00
80.00
100.00
EXPOSURE TIME (DAYS)

Fig.8

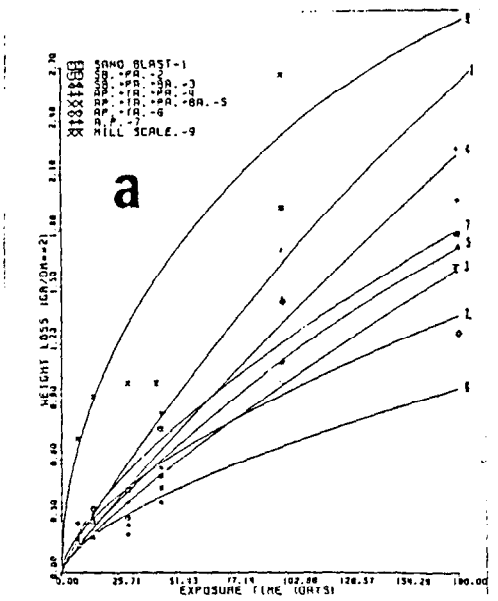
a
SAND BLAST-1
MILL SCALE.-9
HEIGHT LOSS (GR/DM**2)
EXPOSURE TIME (DAYS)

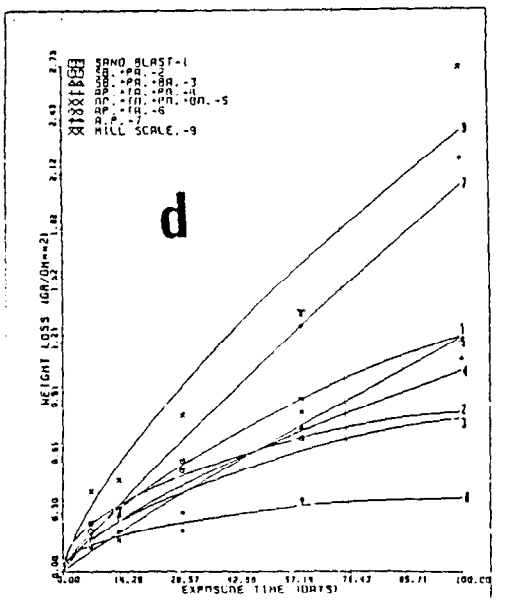
d
SAND BLAST-1
MILL SCALE.-9
HEIGHT LOSS (GR/DM**2)
EXPOSURE TIME (DAYS)

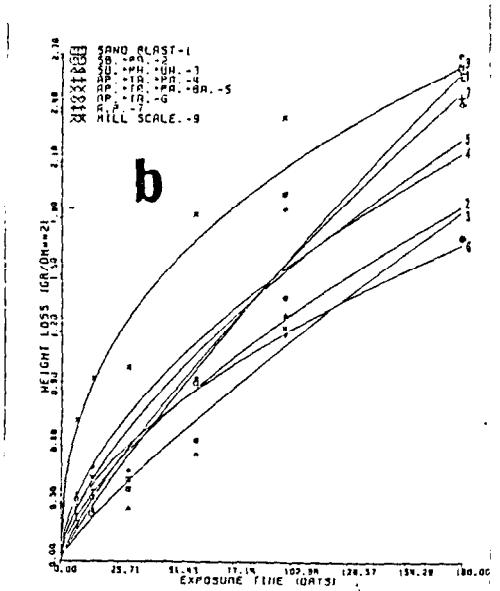
b
SAND BLAST-1
MILL SCALE.-9
HEIGHT LOSS (GR/DM**2)
EXPOSURE TIME (DAYS)

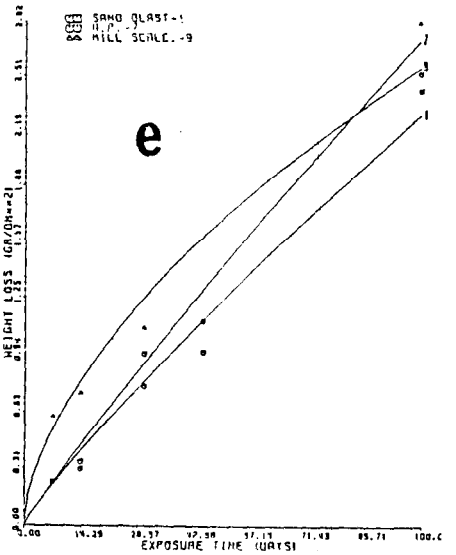
e
MILL SCALE.-9
HEIGHT LOSS (GR/DM**2)
EXPOSURE TIME (DAYS)

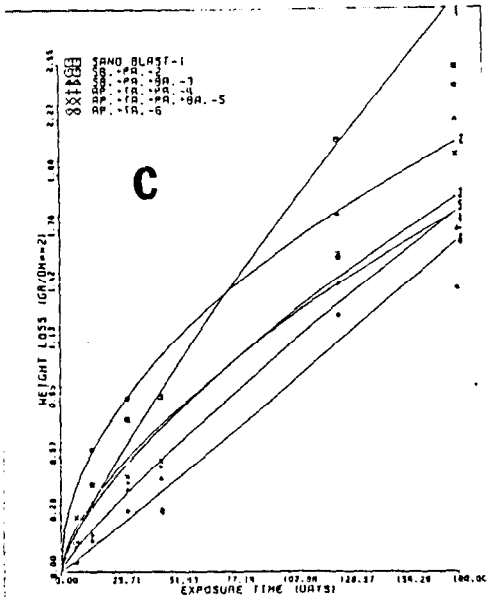
c
SAND BLAST-1
HEIGHT LOSS (GR/DM**2)
EXPOSURE TIME (DAYS)

Fig. 9

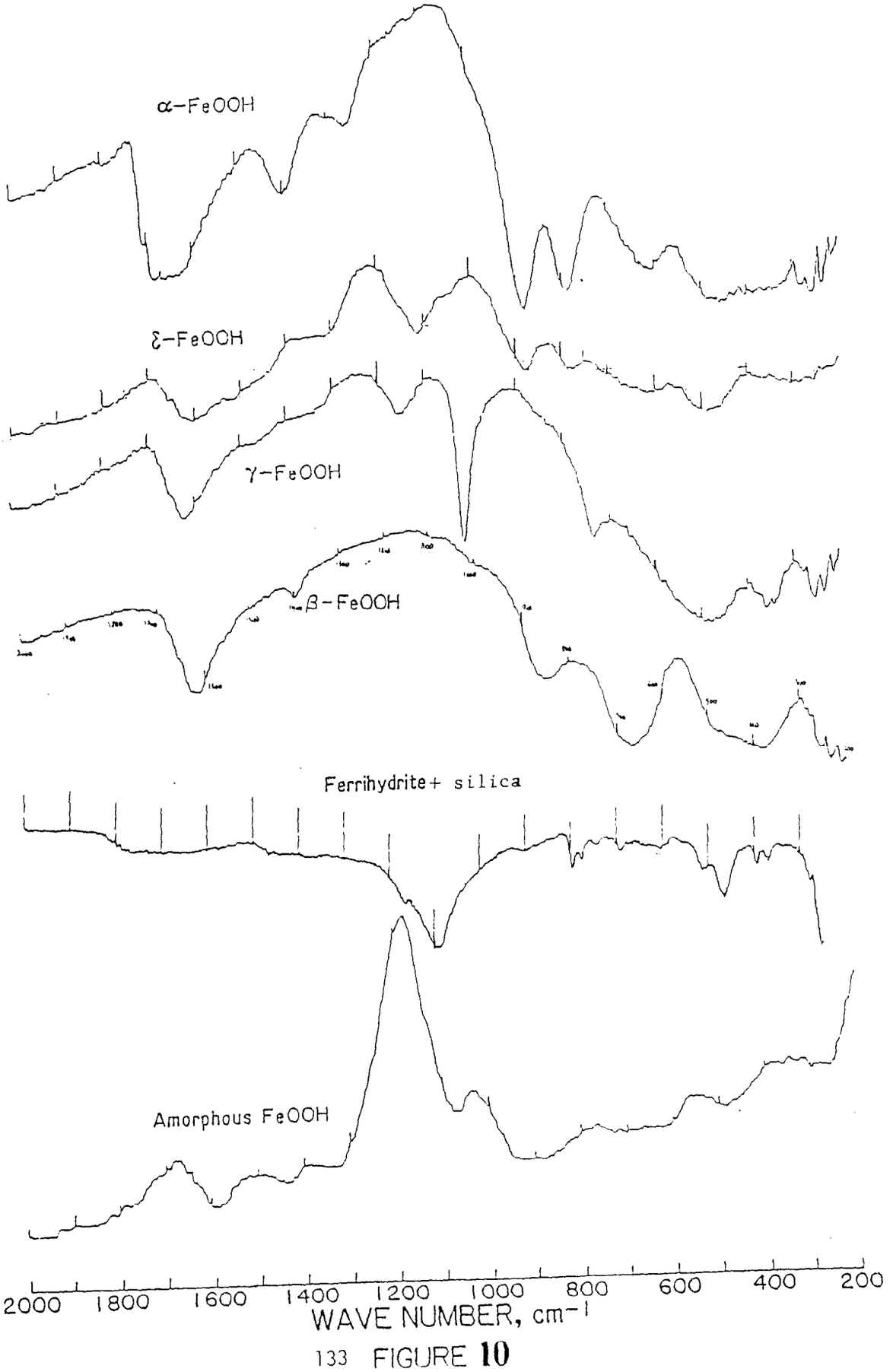

133 FIGURE **10**

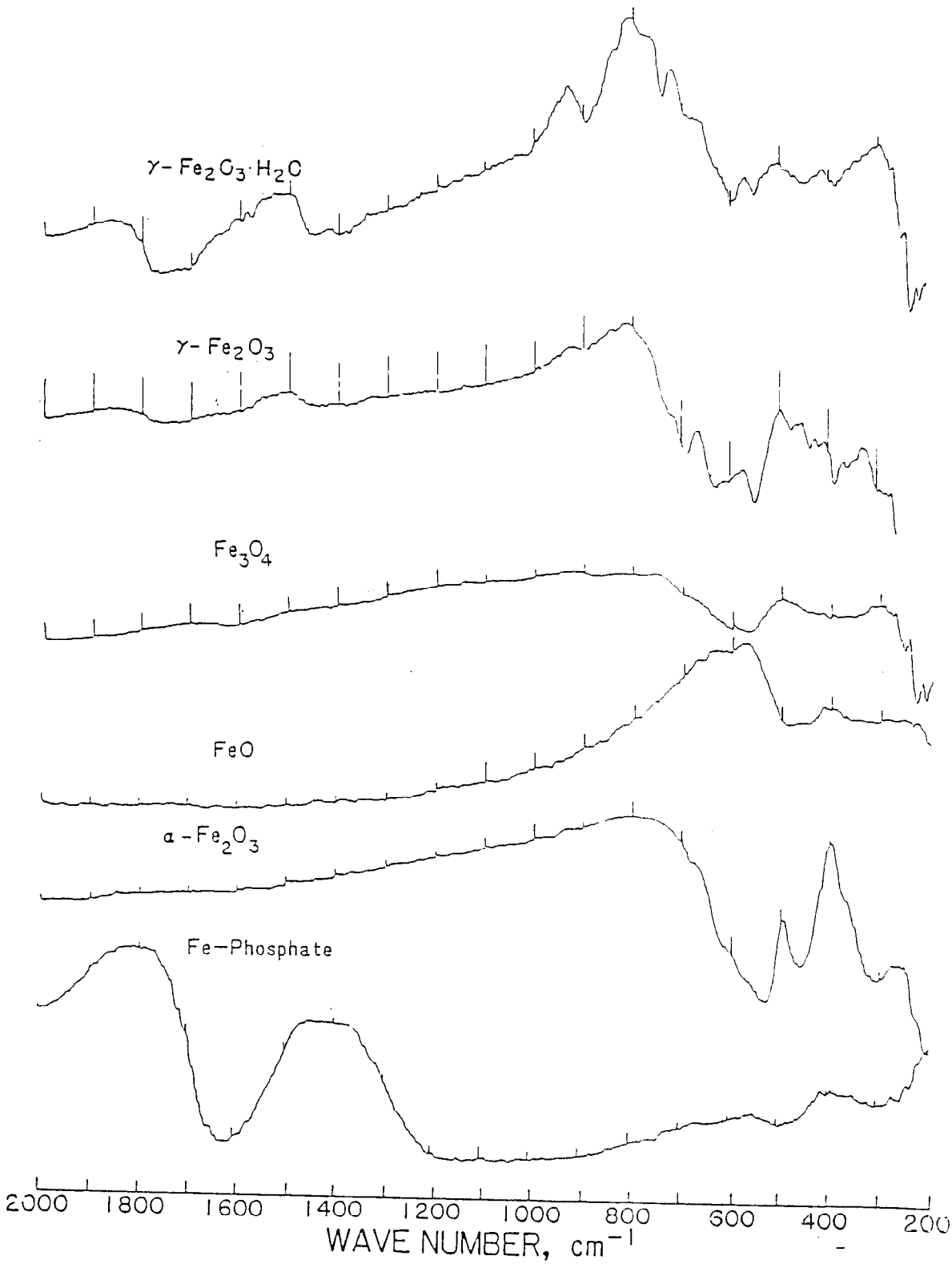

FIGURE **10**

Fig. 10. IR Absorption Spectra of Standard Rust Phases

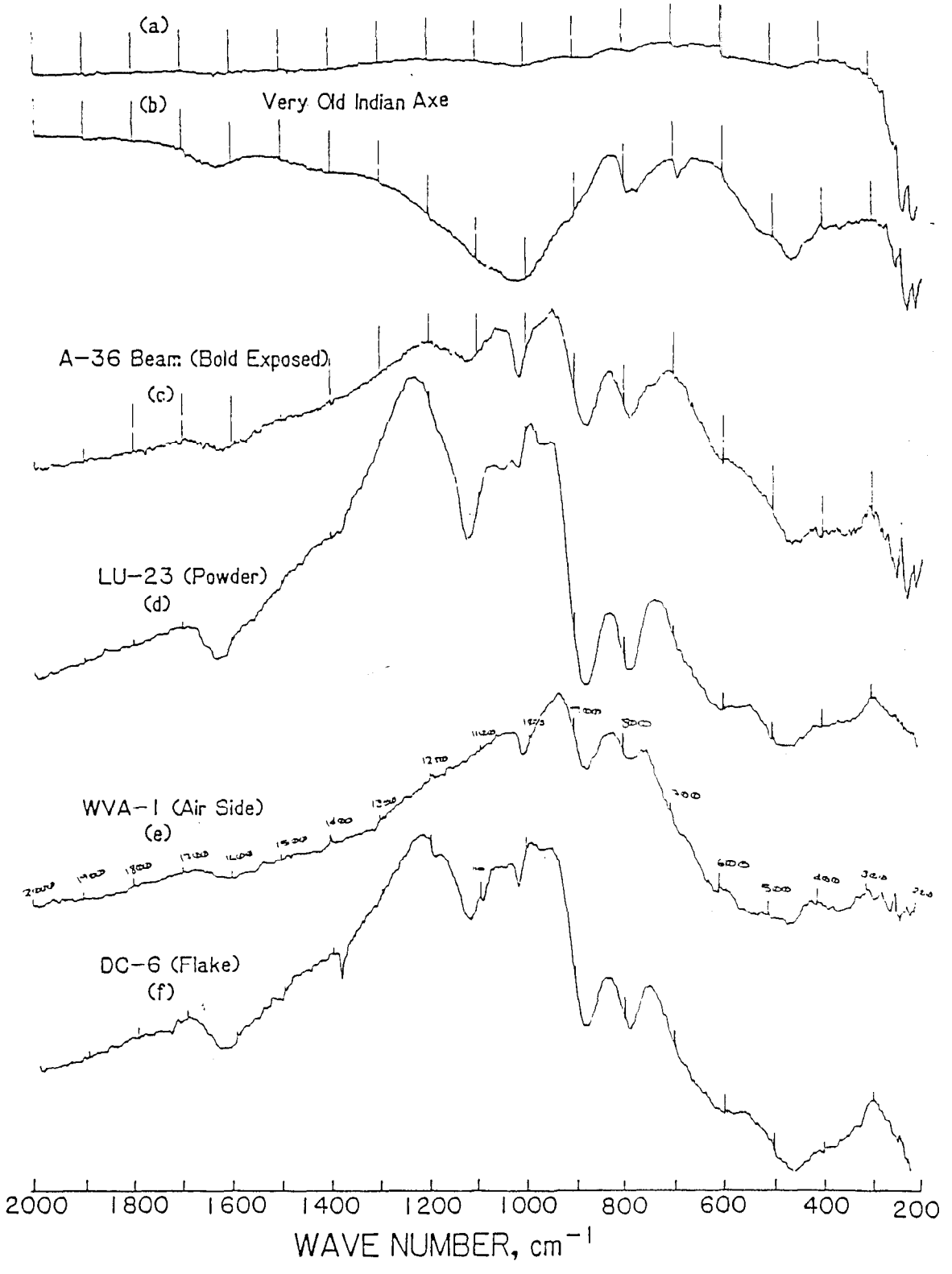
(a)
(b)
Very Old Indian Axe
A-36 Beam (Bold Exposed)
(c)
LU-23 (Powder)
(d)
WVA-1 (Air Side)
(e)
DC-6 (Flake)
(f)
2000
1800
1600
1400
1200
1000
800
600
400
200
WAVE NUMBER, cm⁻¹

FIGURE 11

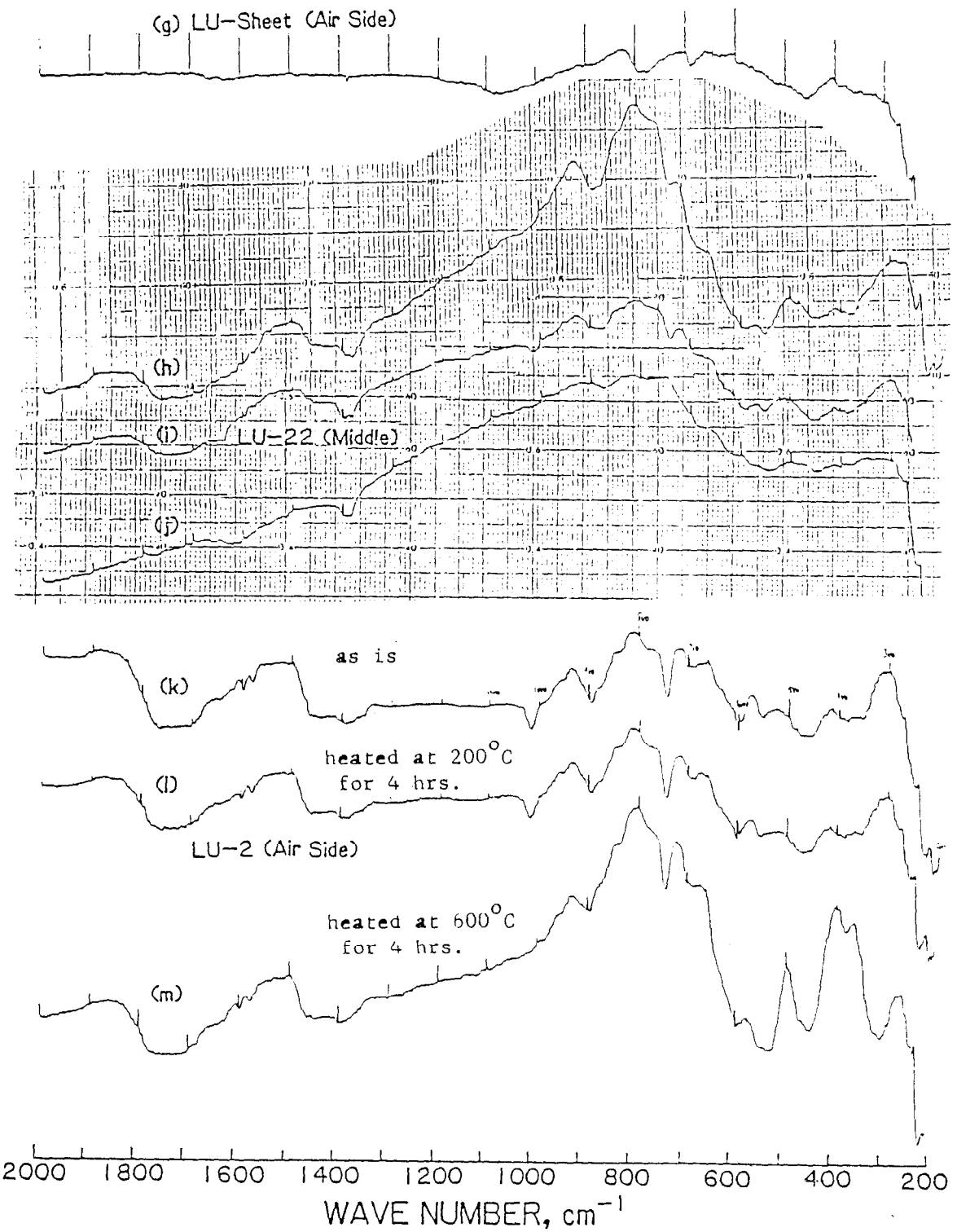

FIGURE 11

Fig. 11. IR Absorption Spectra of Selected Field Rusts

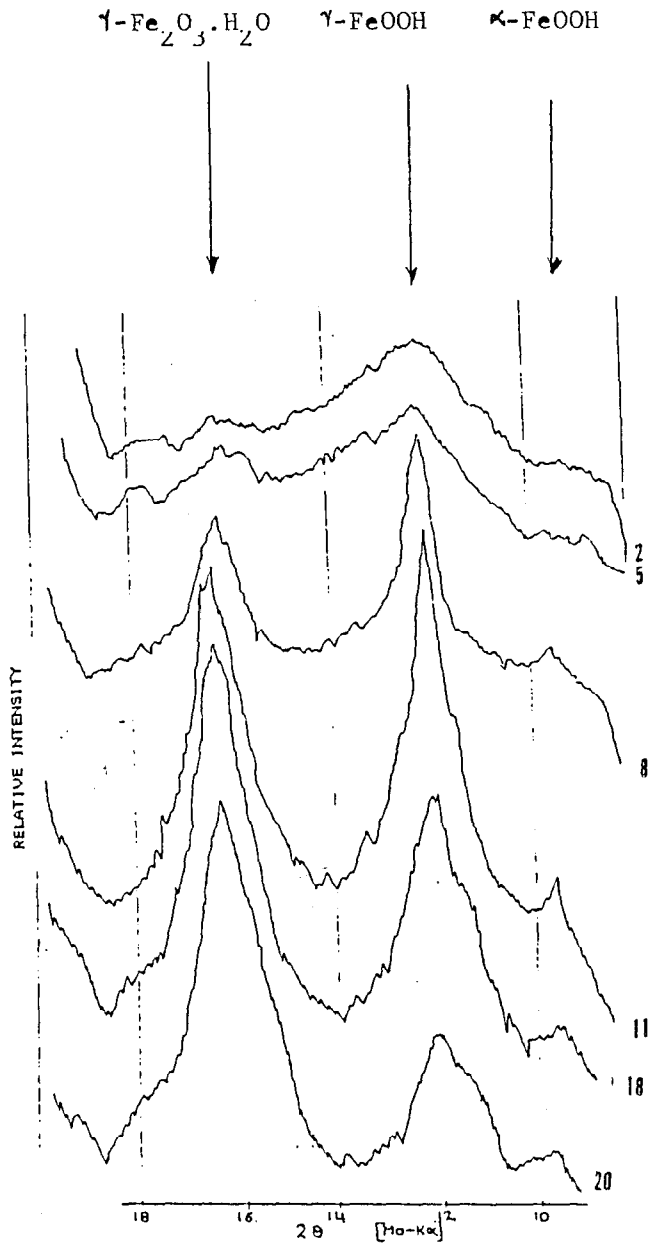

Fig. 12

Fig. 12. Variations in the Relative Intensities of Prominent Diffraction Peaks of γ-FeOOH, γ-$Fe_2O_3 \cdot H_2O$ and α-FeOOH in Field Rusts as a Function of Exposure Time

Fig. 13. Microstructures of Various Rust Phases Formed on Weathering Steels as Observed in a Scanning Electron Microscope (SEM) (A588 - Grade B, except for those exposed at CEBA, LSU, which are A588 - Grade A)

(a) Trt. 4 - 2 yrs. (HI) (E), amorphous layer with cracks, 1420 X

(b) Trt. 1 - 1 yr. (CEBA, LSU) (E), amorphous rust growing in the form of a circular mound, 890 X

(c) Trt. 1 - 8 months (HI) (S), amorphous rust growing as pillar aggretate, 1500 X

(d) Trt. 6 - 1 yr. (LU) (S), the amorphous layer swells sometimes due to gas or water vapor accumulation, bursting out, if the pressure reaches high levels. Several bubbles closely aggregating, some ruptured, are seen in the picture, 3700 X

(e) Trt. 3 - 9 months (LU) (S), the amorphous rust grows sometimes in the form of swollen cylindrical mounds; each mound shows several fine layers, and some cracks can be seen also, 4800 X

(f) Trt. 3 - 3 months (CEBA, LSU) (E), this photograph shows a hemispherical bubble that burst and allowed δ-FeOOH petals to grow at its center. The bright rust on the wall of the burst bubble is probably the amorphous rust, 1000 X

(g) Trt. 4 - 6 months (GT) (S), formation of γ-FeOOH plates within the bulged, bud-shaped postule; the goosebumps in the amorphous layer to the left of the bud are probably amorphous γ-FeOOH; rods of α-FeOOH seem to shoot out of the AM layer on the right, 1000 X

(h) Trt. 1 - 1 month (CEBA, LSU) (E), Growth of δ-FeOOH crystals in the hemispherical area; it appears that the bud has blossomed into a nice flower mass, 1000 X

(i) Trt. 7 - 2200 cycles, AAEST-SLE, bent and wiggled plates of γ-FeOOH; each plate has fine layers laid perpendicular to it, 1000 X

(j) Trt. 7 - 18 months (GT) (S), fully crystallized plates of γ-FeOOH aggregating at a place and appearing as a bunch of worms, 830 X

(k) δ-FeOOH powder prepared in the laboratory shows flowery pattern resembling roses, 5000 X

(l) Trt. 1 - 1 month (LU) (S), plates of δ-FeOOH bending and aggregating to show flowery pattern in a field rust, 600 X

(m) α-FeOOH forming as whiskers on top of plates of γ-FeOOH. This has been found on the top part of an intermediate layer in a sheet-type of rust with multiple layers from the Luling bridge - main span (A588 - Grade A, Kawasaki Steel)

(n) Trt. 2 - 15 months (HI) (S), α-FeOOH crystals shoot out of the AM layer as rods. The whiskers are inferred to grow into such rods, 2000 X

(o) Trt. 1 - 20 months (HI) (S), α-FeOOH crystals in the form of thin plates aggregating to show flowery pattern; the plates of α are straight and not bent, 3800 X

(p) Trt. 2 - 1 month (Salt Fog Test), fully grown whiskers of α-FeOOH aggregate to show flowery pattern, 1400 X

(pp) One side of coarse flake showing carnation flower patterns of α-FeOOH crystal aggregates, 5000 X

(q) Trt. 2 - 2 months (HI) (S), rice grain like tiny crystals of α-FeOOH formed on top of the amorphous layer, 1600 X

(r) Trt. 7 - 3 months (BR) (S), α-FeOOH plates aggregating to show a spongy, nest-like structure, 2000 X

(s) Trt. 5 - 6 months (GT) (E), transformation of γ → α can be seen here; whiskers of α-FeOOH nucleate and grow on top of the γ-FeOOH plates, 4300 X

(t) Trt. 7 - 6 months (GT) (E), formation of γ-FeOOH (top left) and δ-FeOOH (right) colonies separated by what appears as a wall of ferrihydrite; γ- and δ-FeOOH coexist in rusts formed on specimens during bold-exposure, 1500 X

(u) Trt. 3 - 1 yr. (CEBA, LSU) (E), ferrihydrite seems to grow in the form of walls of compartments in this photograph, 1400 X

(v) Trt. 1 - 100 days (immersion in salt water), ferrihydrite in the form of cylindrical tubes aggregating as cooked spaghetti, 1000 X

(vv) Trt. 2 - 3 months (LV) (S), ferrihydrite forms as tiny, tiny plates which aggregate to show a unique pattern as seen here. It is a collection of several ferrihydrite plates growing along different directions, 5200 X

(w) Trt. 3 - 15 days (immersion in salt water), γ-$Fe_2O_3 \cdot H_2O$ grows as sand grains; not so well defined grains may denote the amorphous nature of γ, 1700 X

(x) Trt. 2 - 20 months (HI) (S), formation of α-FeOOH in the form of a white cloud on top of the amorphous layer; the cloudy layer itself indicates amorphous nature of α; tiny whiskers of α can be seen growing at the periphery of the cloud, 1500 X

(y) Trt. 6 - 1 month (Salt Fog Test), magnetite grows in layers as seen here, 100 X

(z1) Trt. 6 - 1 month (Salt Fog Test), swelling occurs at the periphery of the magnetite layer formed; such swellings show interesting swirling structures that resemble a snake in motion and donuts, 50 X

(z2) Trt. 5 - 2 weeks (Salt Fog Test), magnetite transforms either to γ-$Fe_2O_3 \cdot H_2O$ or to α-FeOOH; such a transformation is seen at the periphery of the magnetite layer, 500 X

(z3) Trt. 3 - 1 month (Salt Fog Test), magnetite layer showing bulges at the periphery present along with tiny, tiny grains of α-FeOOH or γ-$Fe_2O_3 \cdot H_2O$. Magnetite itself might grow devouring such grains, 100 X

Captions to Figures

Figure 14 : IR patterns of Rusts Formed on Weathering Steels coupons and surfaces in Bridge Structures with Different Surface Treatments, Exposed at Various Bridge Locations.

A) Field coupons with treatments 1 and 2 Exposed in Sheltered Locations at Leesville, La.

B) Exterior, bold-exposed Surfaces at Boeuf River Bridge with Treatments 2, 6 and 7.

C) Interior, Sheltered Surfaces of Steel in the Leesville Bridge with Treatments 4 and 6.

D) Interior, Sheltered Surfaces of Steel in the Boeuf River Bridge with treatments 3 and 5.

E) Field coupons with treatments 1 and 5 exposed at Sheltered Locations at the Luling Bridge.

F) Exterior Surface of Steel at the Gibbstown Bridge with Treatments 2 and 4.

G) A588 Grade B Field coupons with Treatment 3 Exposed at Sheltered Locations at Gibbstown Bridge.

H) Exterior Surfaces of Steel at the Luling Bridge with Treatment 3.

I) A588 Grade A Coupons with Treatments 5, 6, 7 and 9 Exposed at the Roof of the CEBA Building, LSU, Baton Rouge.

J) Interior Surfaces at the High Island Bridge, Tx. with Treatments 2 and 3.

K) Exterior Surfaces at the High Island Bridge, Tx. with Treatments 2 and 4.

L) Exterior Surfaces at the High Island Bridge, Tx. with Treatment 6.

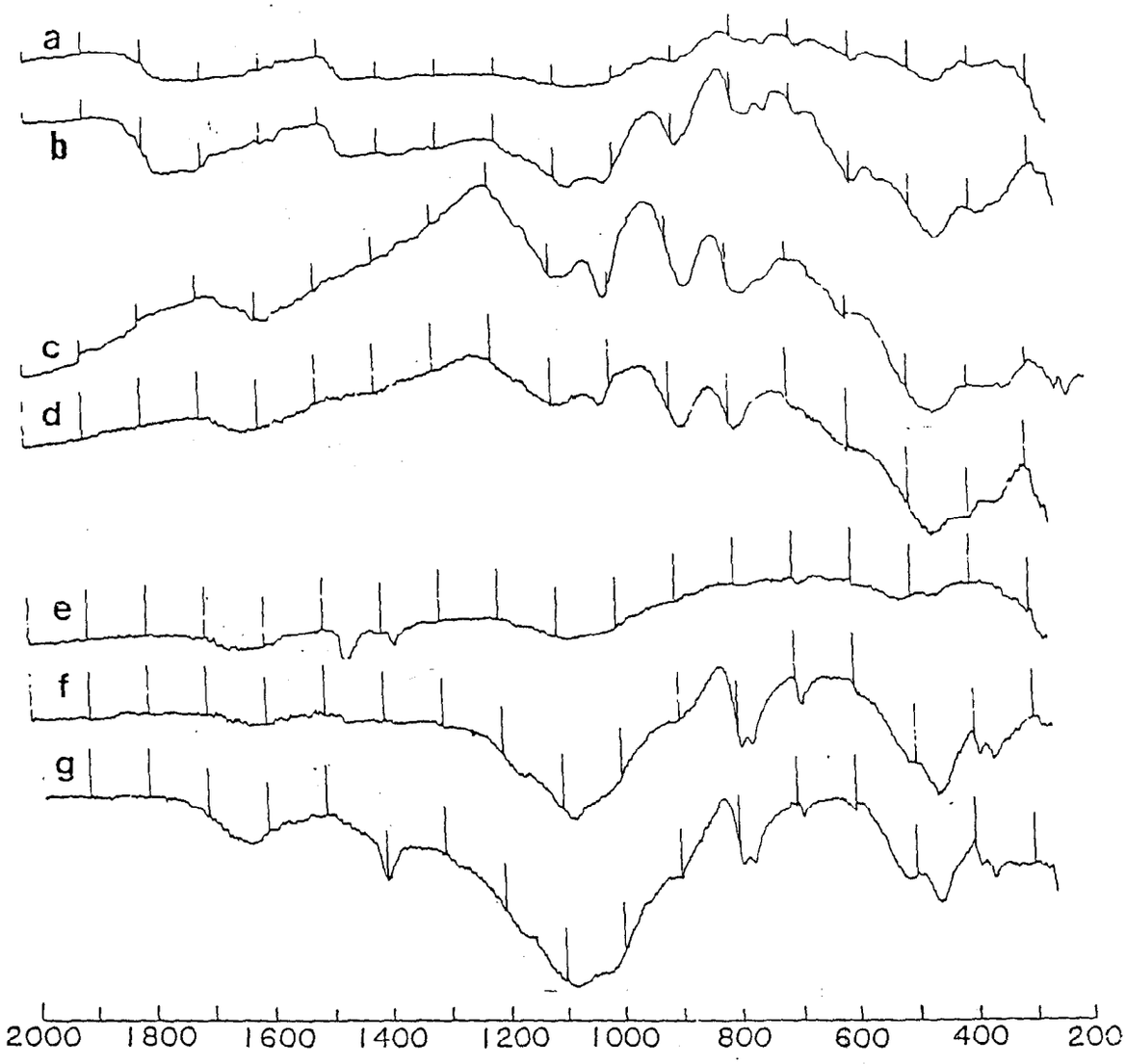
a
b
c
d
e
f
g
2000
1800
1600
1400
1200
1000
800
600
400
200
WAVE NUMBER, cm⁻¹

FIGURE -A

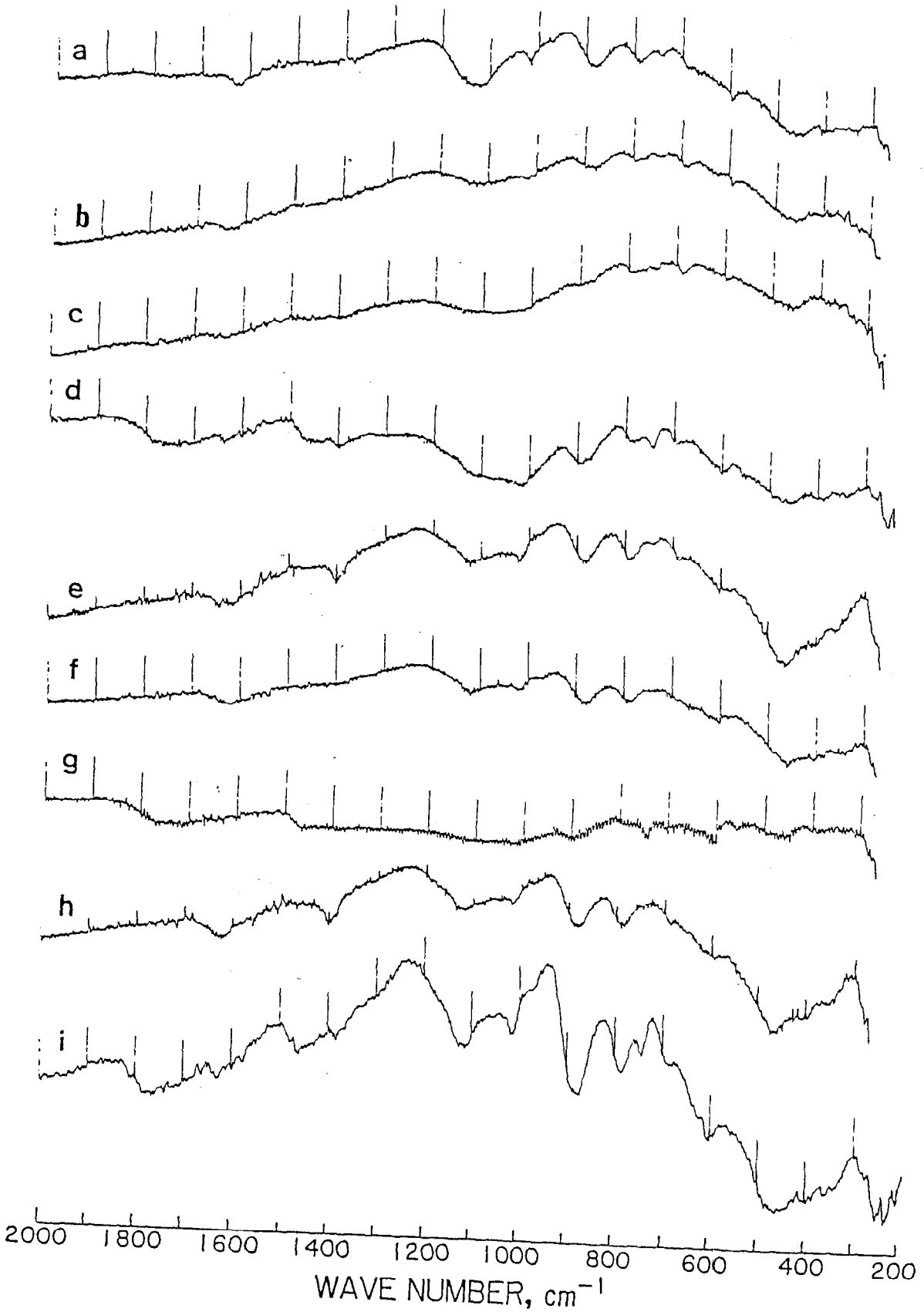
a
b
c
d
e
f
g
h
i
2000
1800
1600
1400
1200
1000
800
600
400
200
WAVE NUMBER, cm⁻¹

FIGURE -B

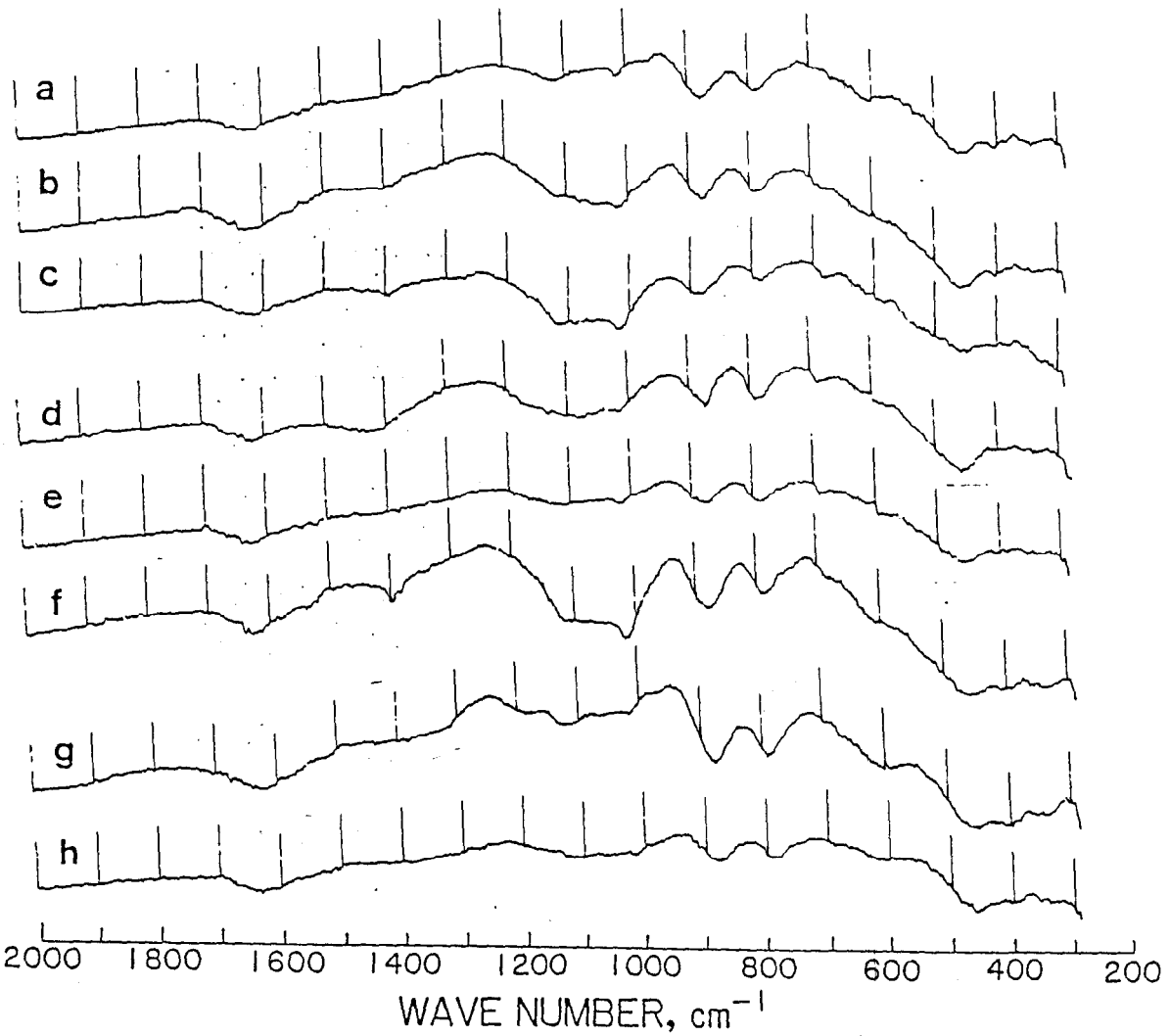
a
b
c
d
e
f
g
h
2000
1800
1600
1400
1200
1000
800
600
400
200
WAVE NUMBER, cm⁻¹

FIGURE -C

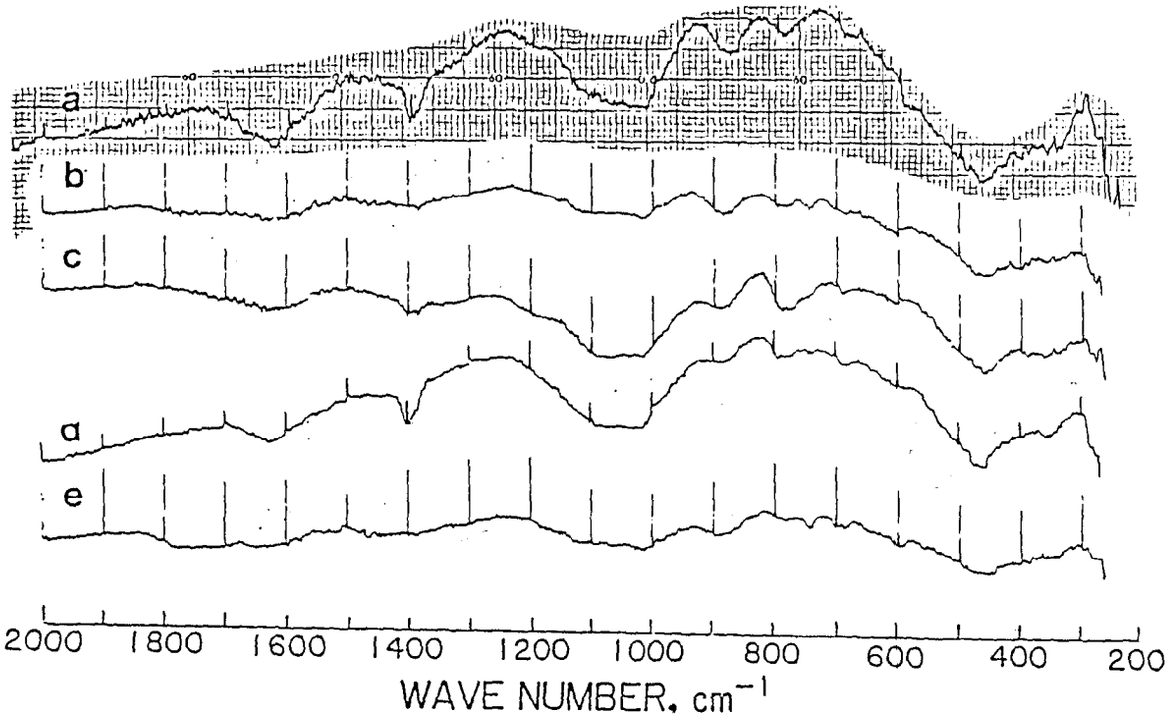
a
b
c
d
e
2000
1800
1600
1400
1200
1000
800
600
400
200
WAVE NUMBER, cm⁻¹

FIGURE -D

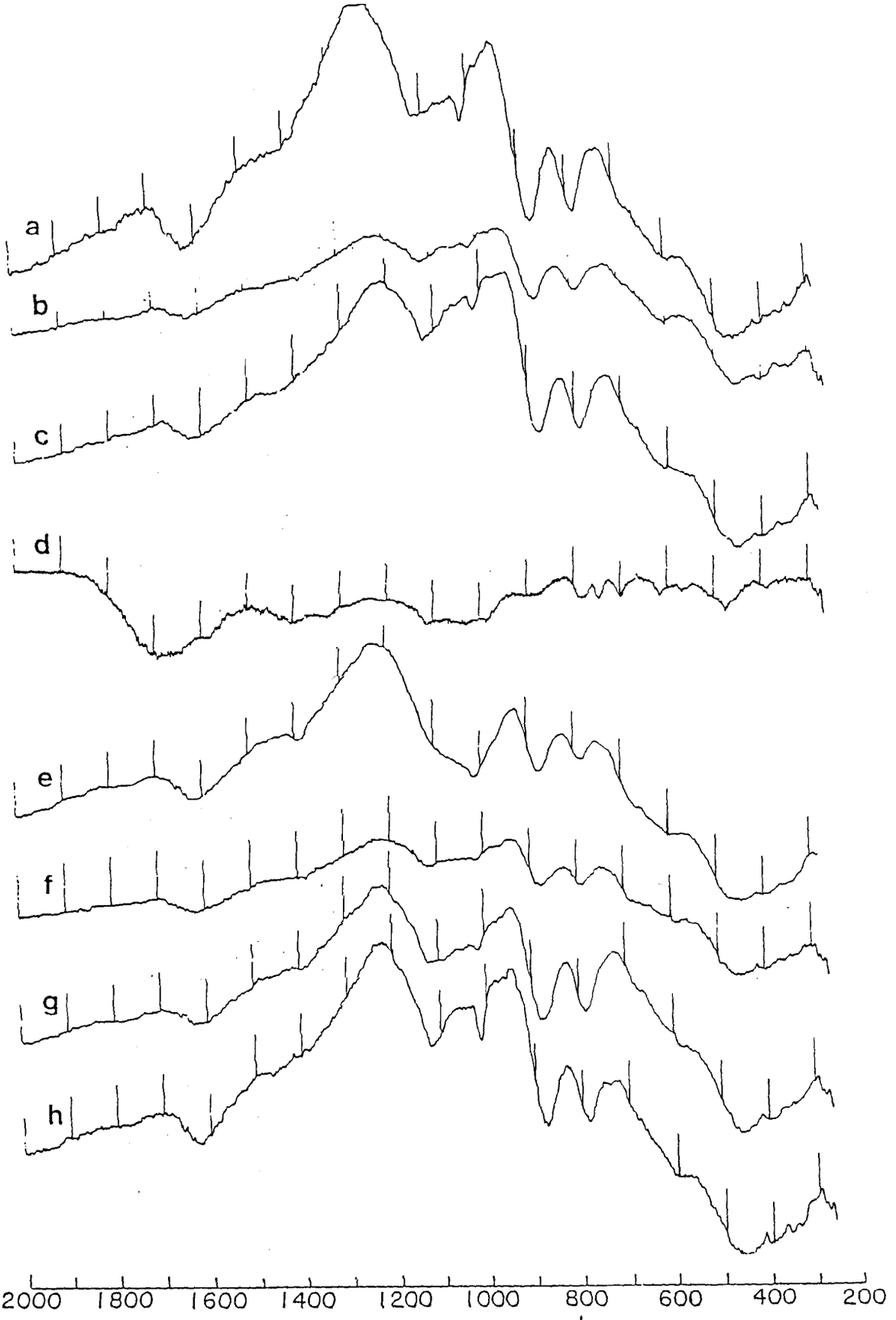
a
b
c
d
e
f
g
h
2000
1800
1600
1400
1200
1000
800
600
400
200
WAVE NUMBER, cm^{-1}

FIGURE -E

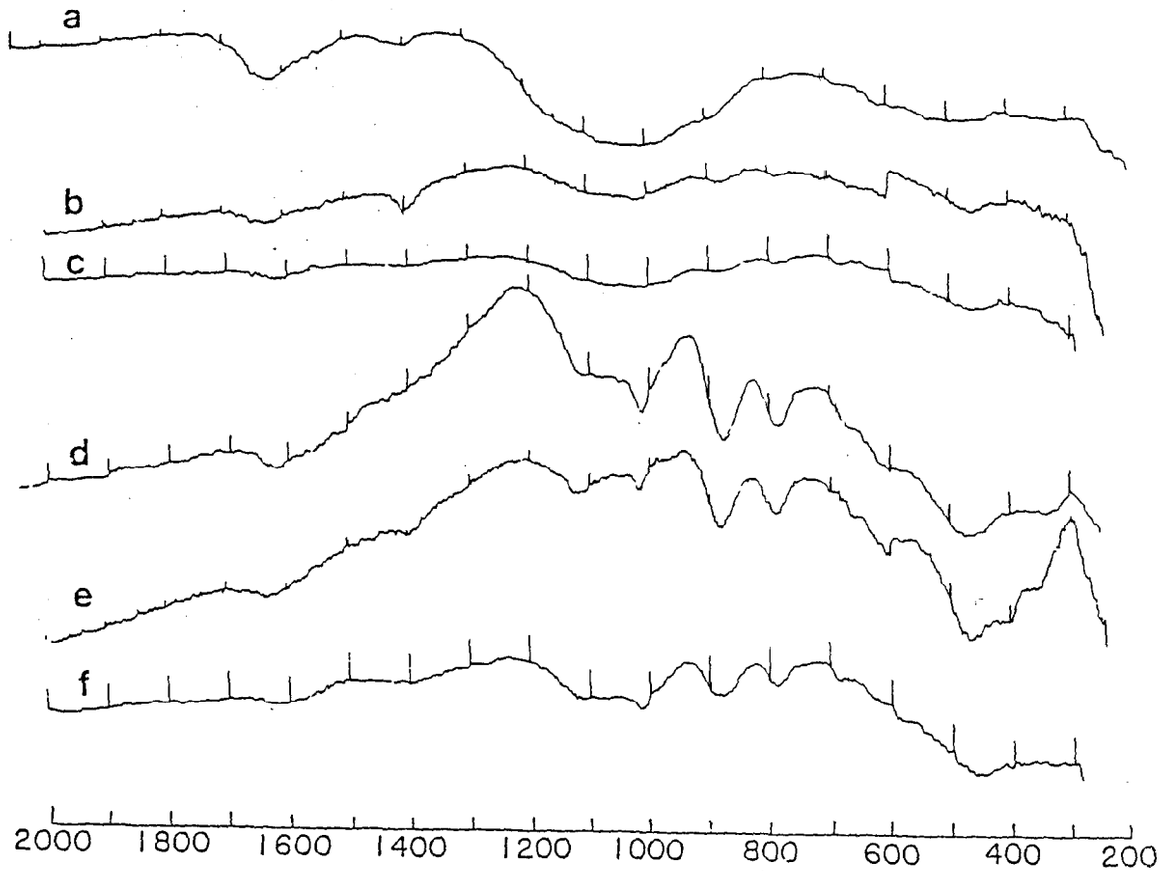
a
b
c
d
e
f
2000
1800
1600
1400
1200
1000
800
600
400
200
WAVE NUMBER, cm⁻¹

FIGURE -F

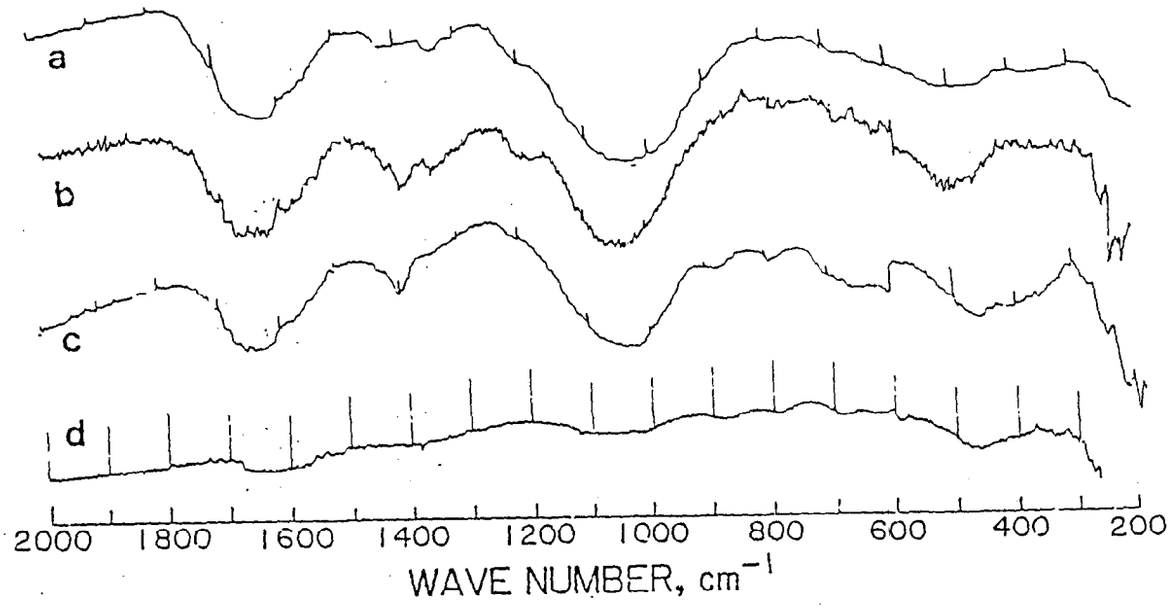
a
b
c
d
2000
1800
1600
1400
1200
1000
800
600
400
200
WAVE NUMBER, cm^{-1}

FIGURE -G

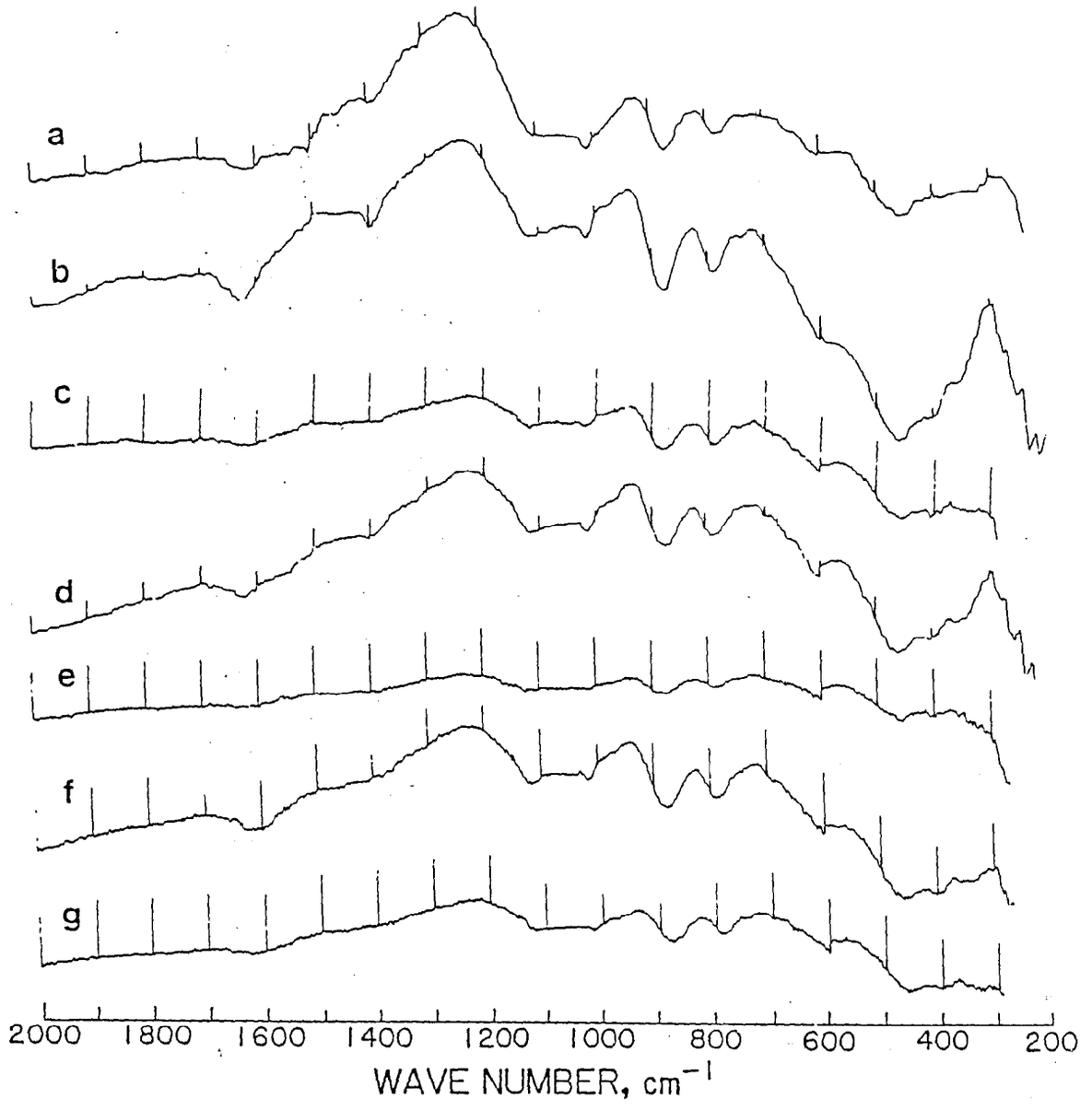
a
b
c
d
e
f
g
2000
1800
1600
1400
1200
1000
800
600
400
200
WAVE NUMBER, cm⁻¹

FIGURE -H

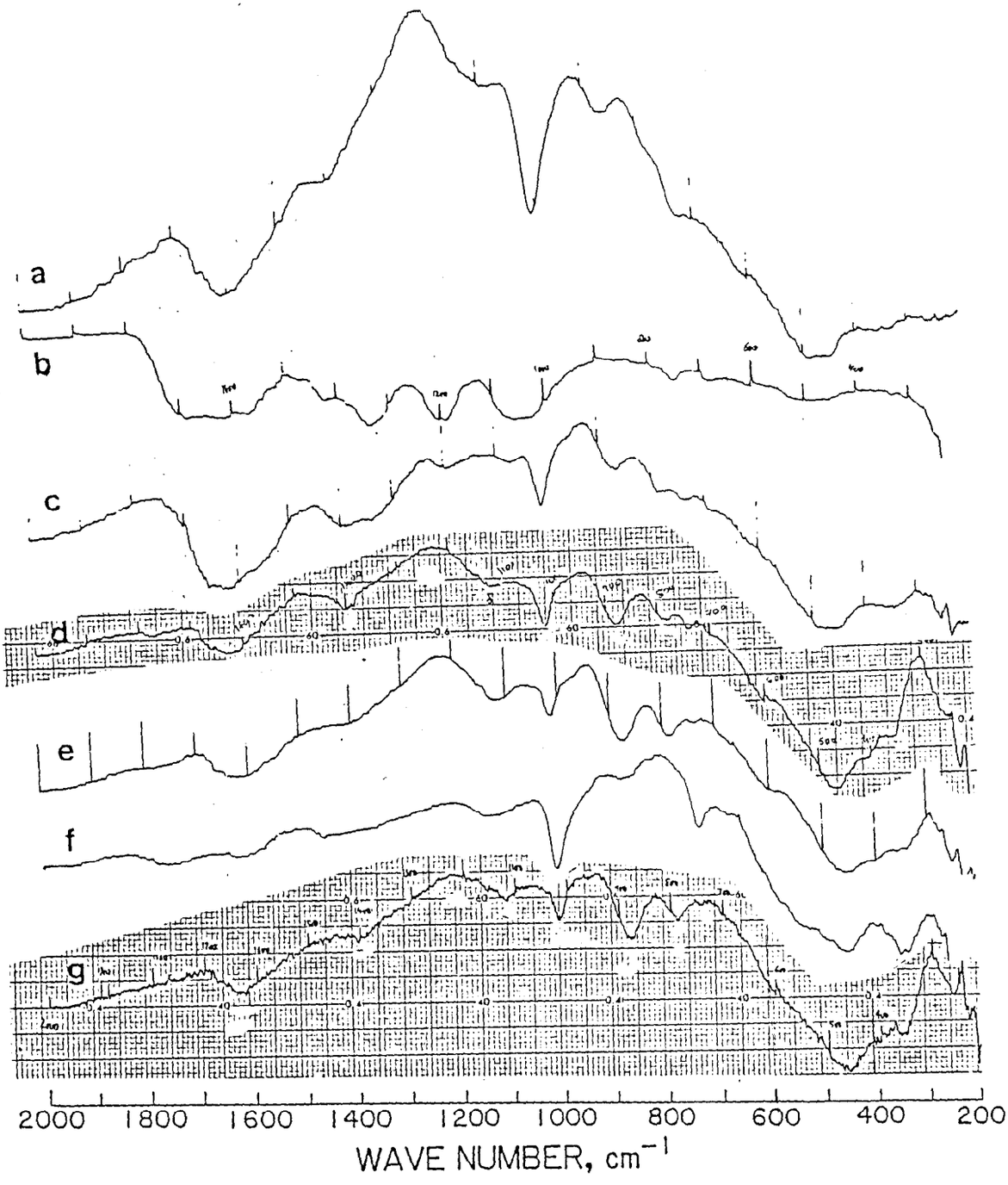
a
b
c
d
e
f
g
2000
1800
1600
1400
1200
1000
800
600
400
200
WAVE NUMBER, cm⁻¹

FIGURE -1

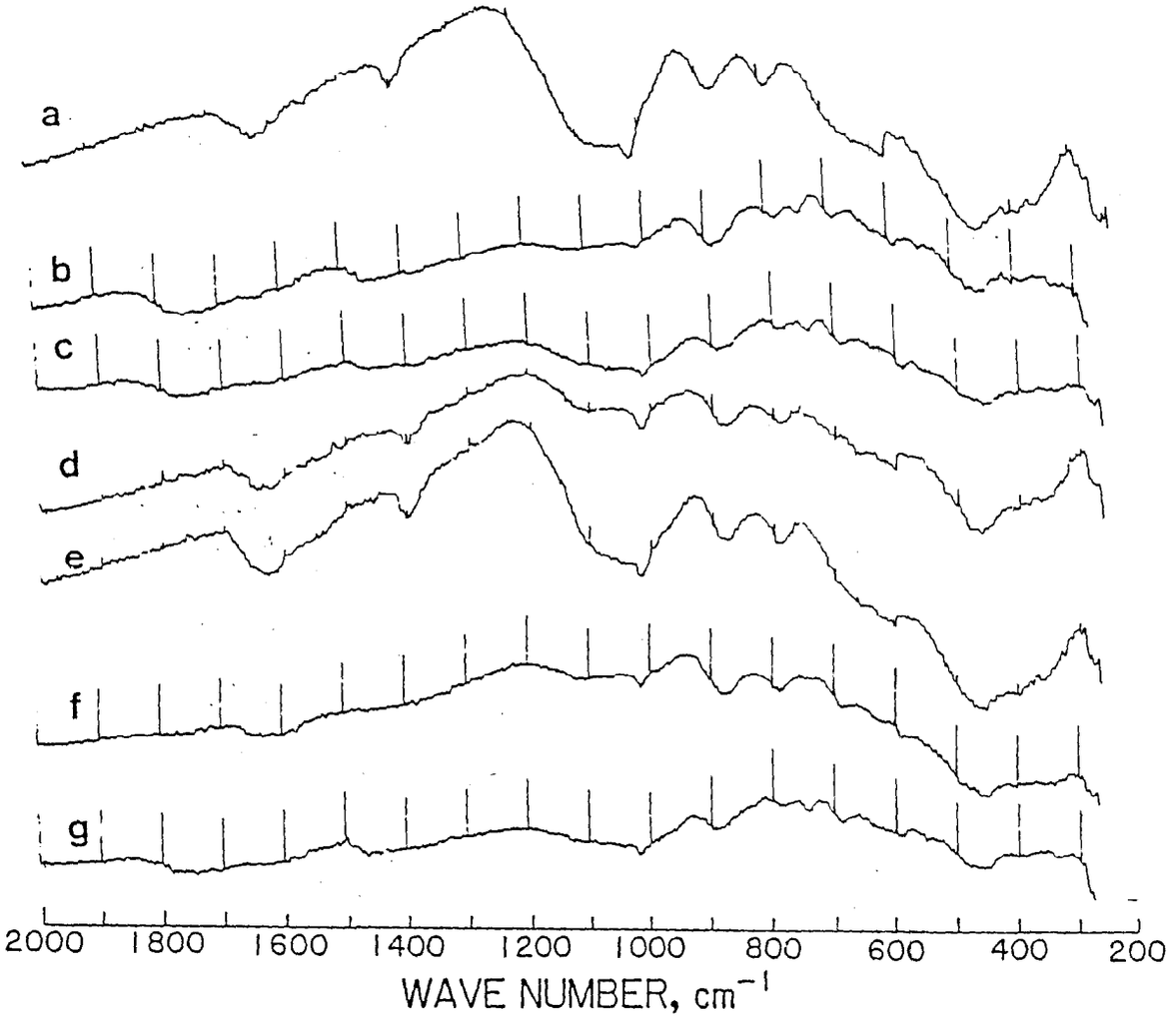
a
b
c
d
e
f
g
2000
1800
1600
1400
1200
1000
800
600
400
200
WAVE NUMBER, cm⁻¹

FIGURE -J.

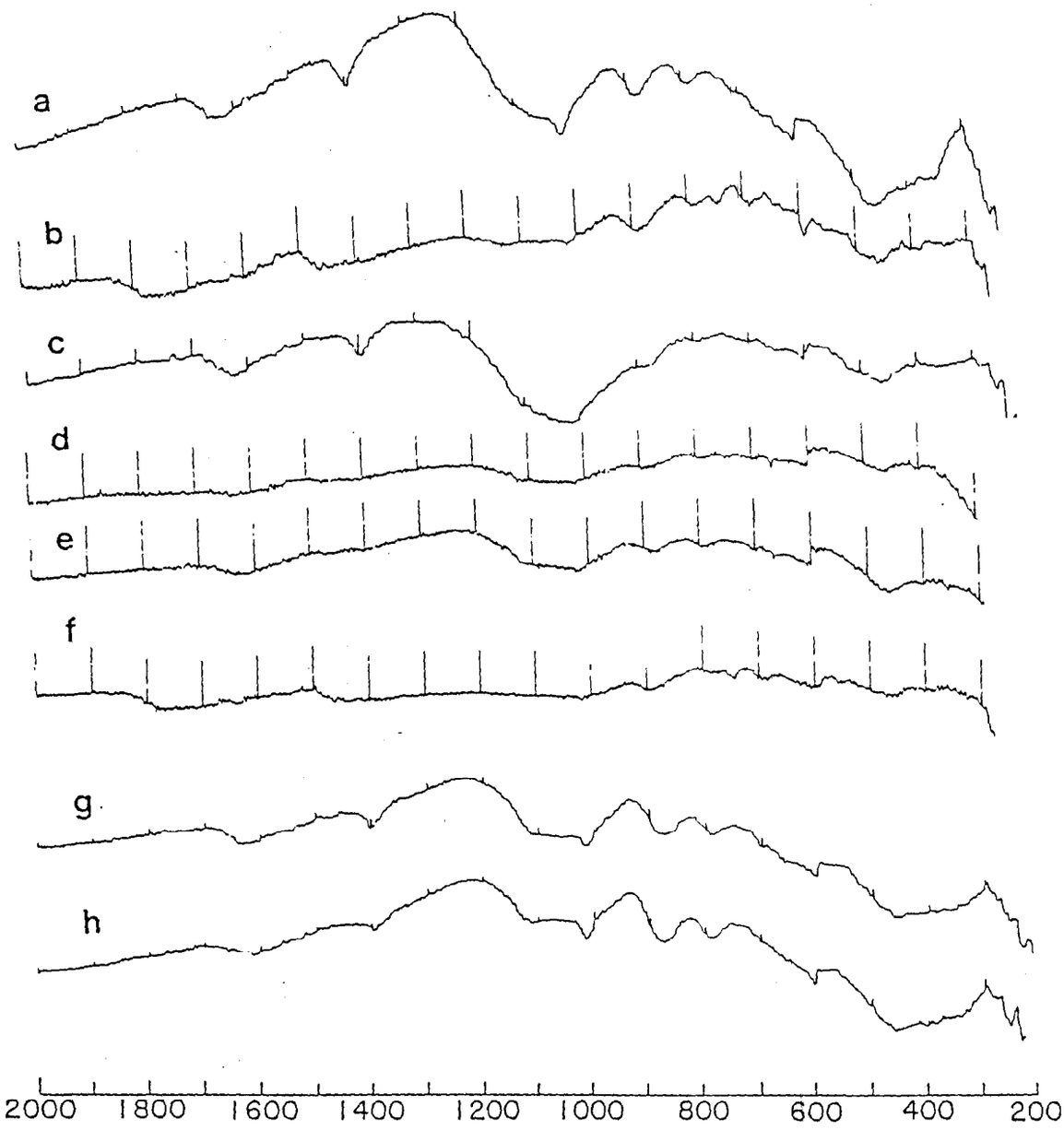
a
b
c
d
e
f
g
h
2000
1800
1600
1400
1200
1000
800
600
400
200
WAVE NUMBER, cm⁻¹

FIGURE -K

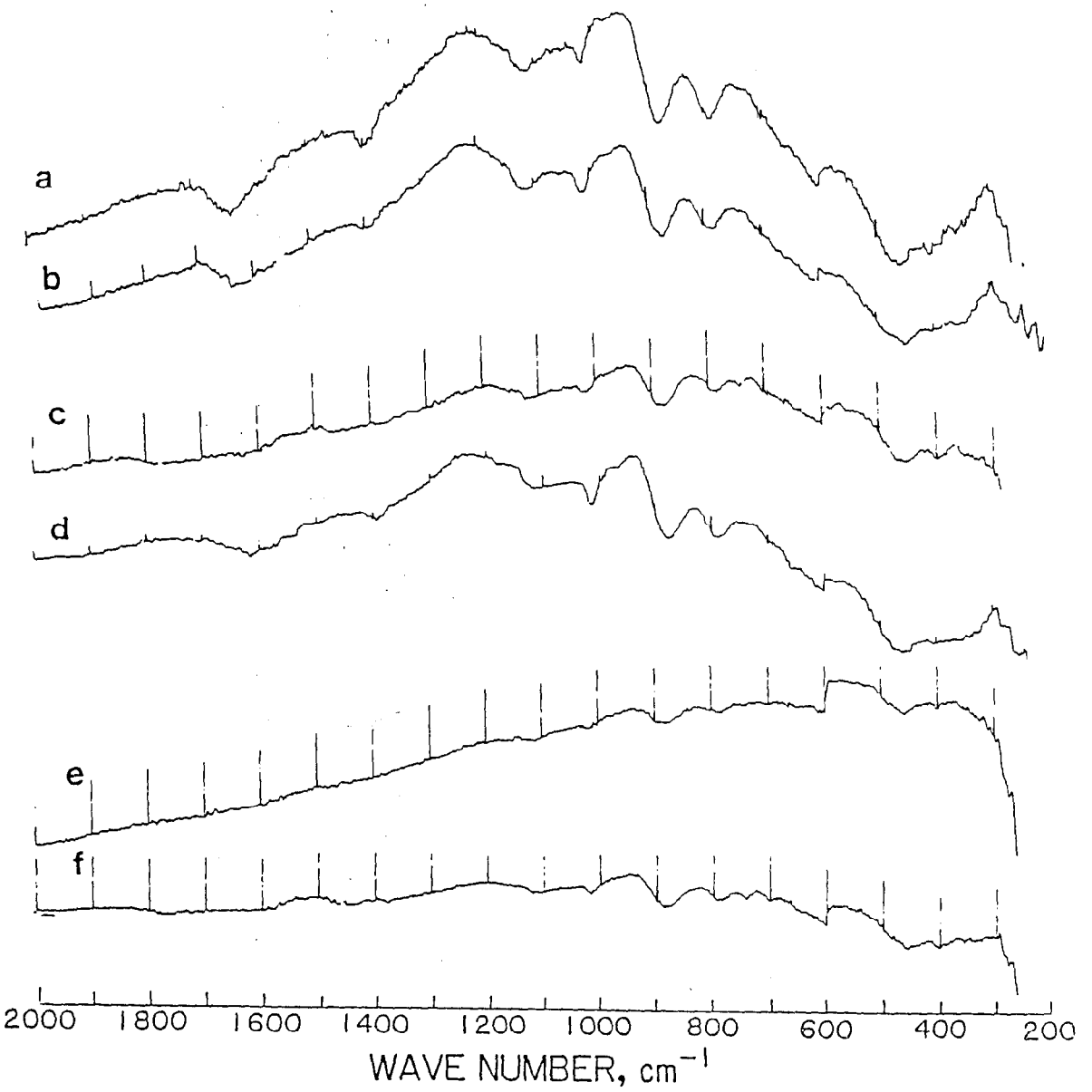
a
b
c
d
e
f
2000
1800
1600
1400
1200
1000
800
600
400
200
WAVE NUMBER, cm⁻¹

FIGURE -L

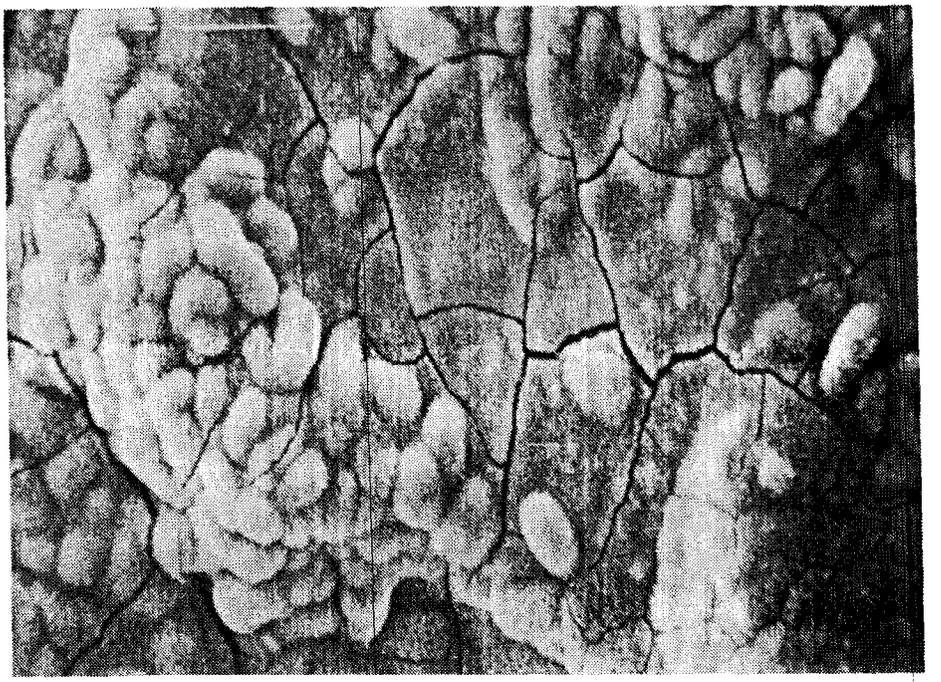

a

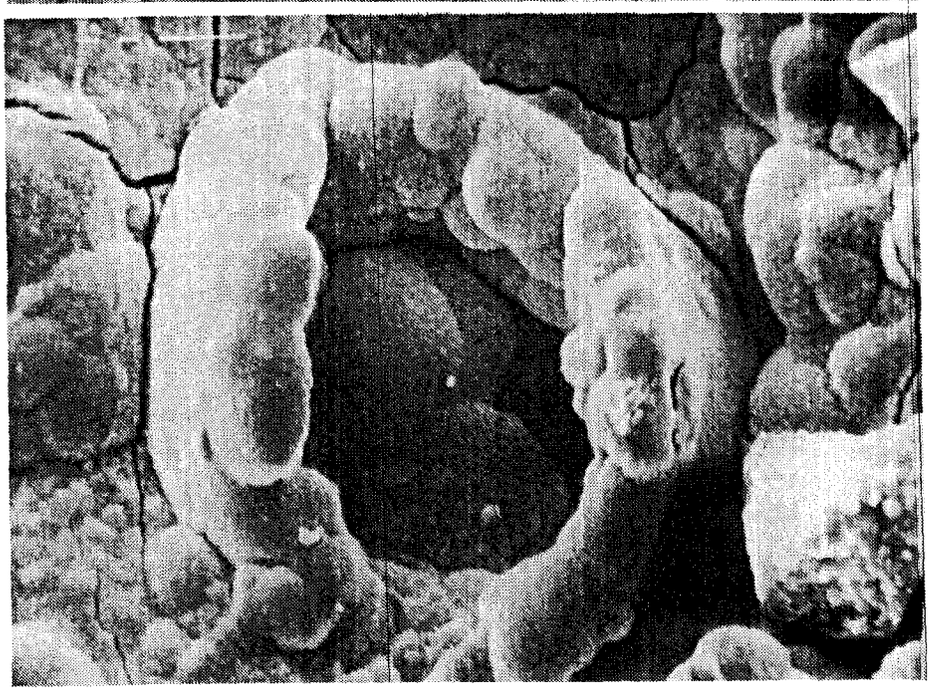

b

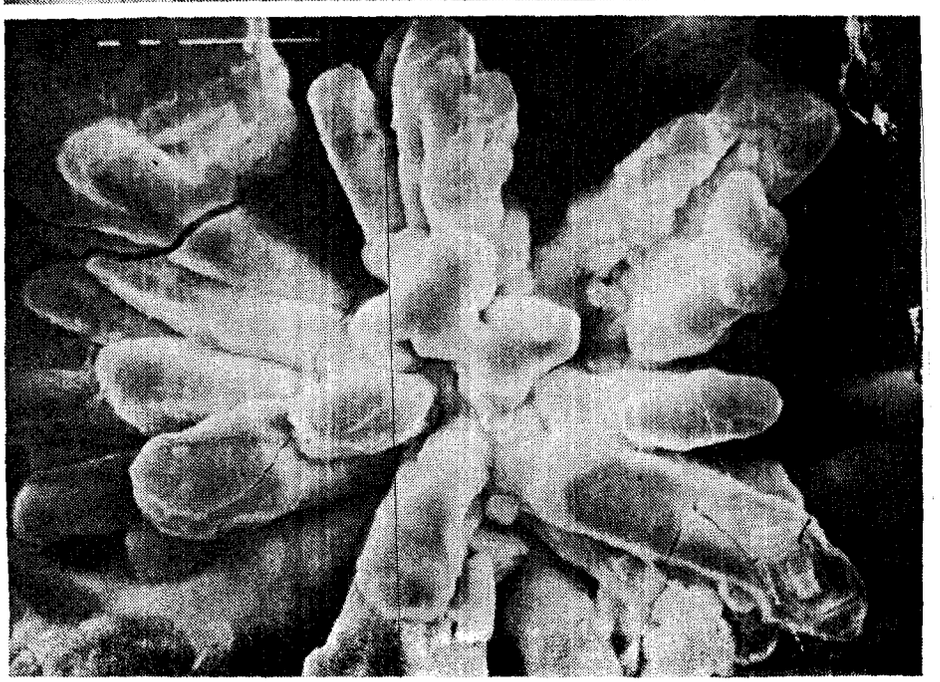

c

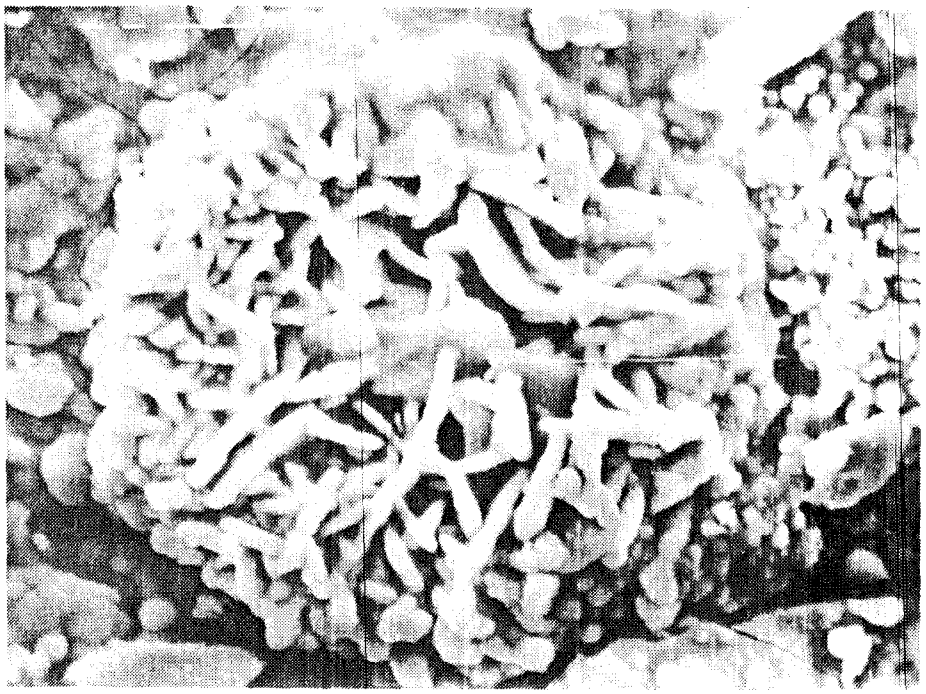

g

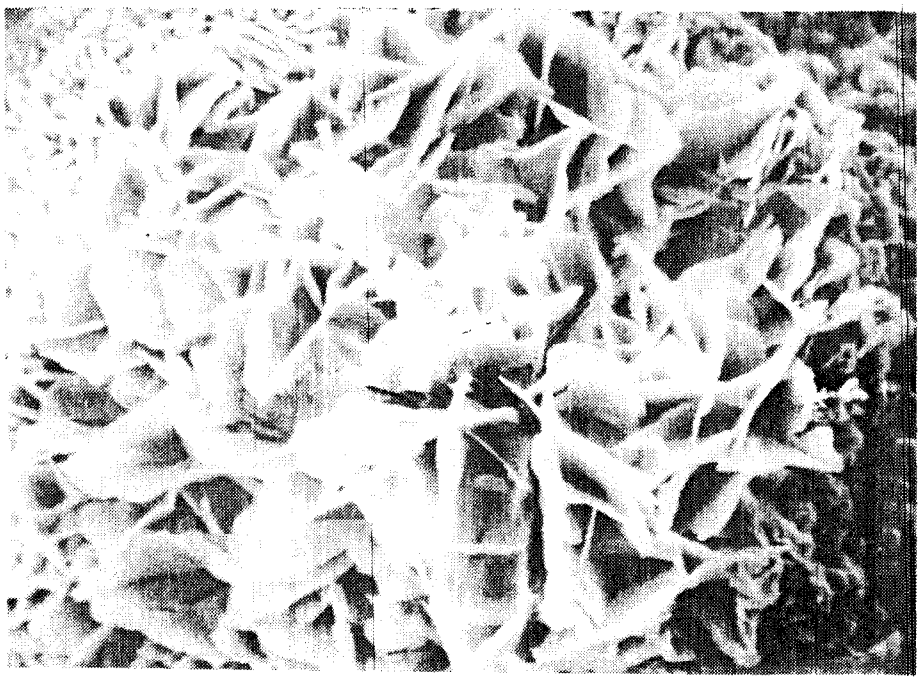

h

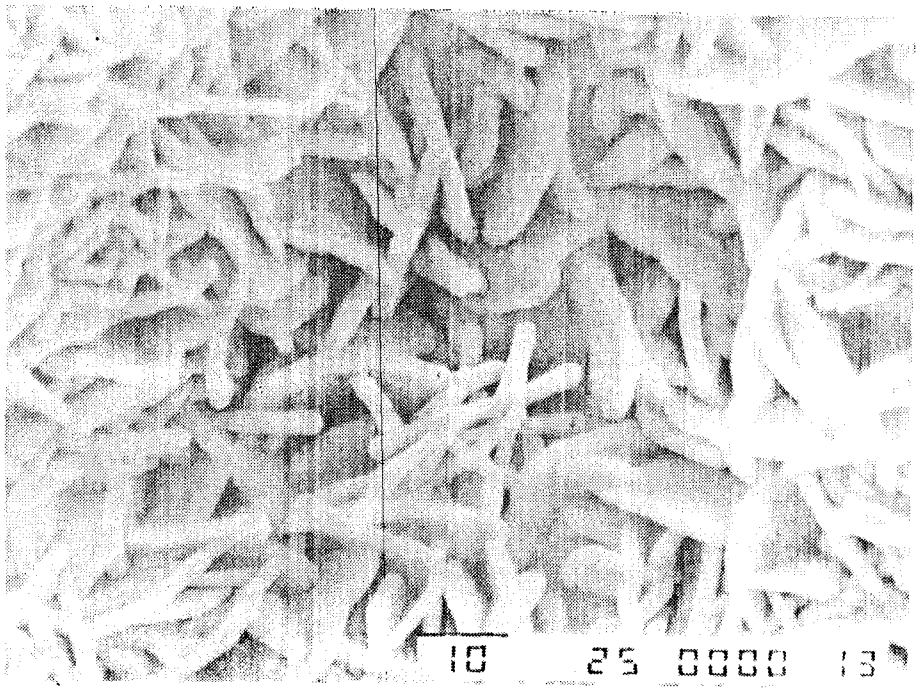

i

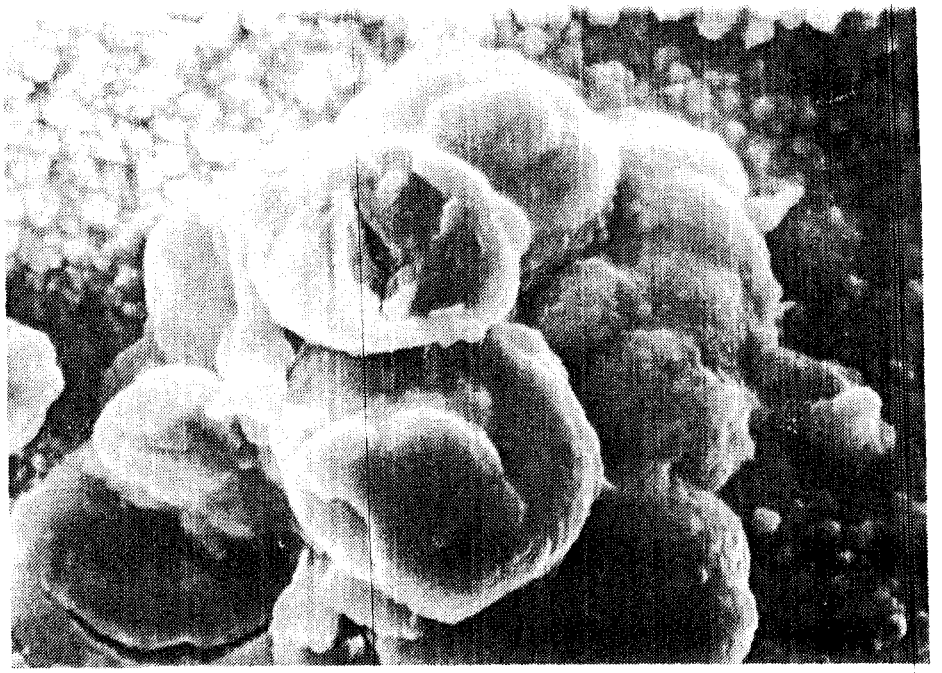

d

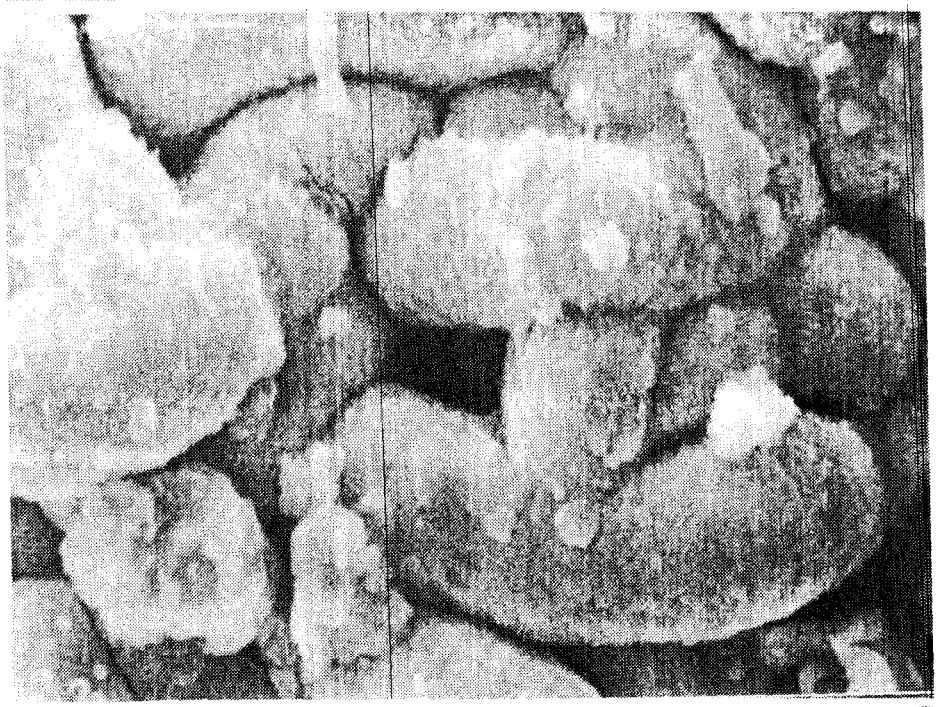

e

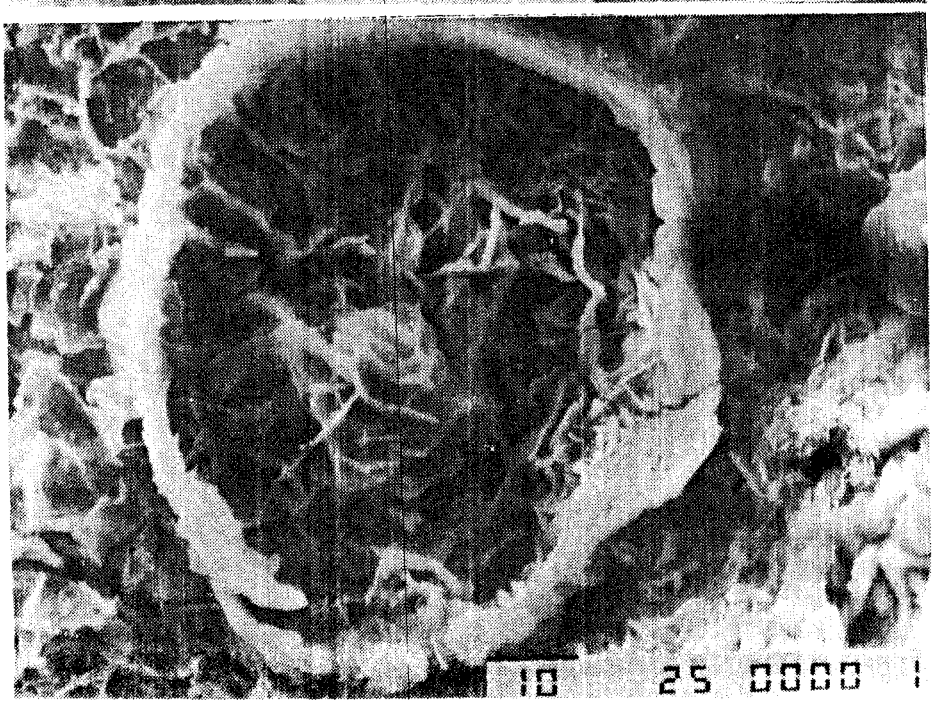

f

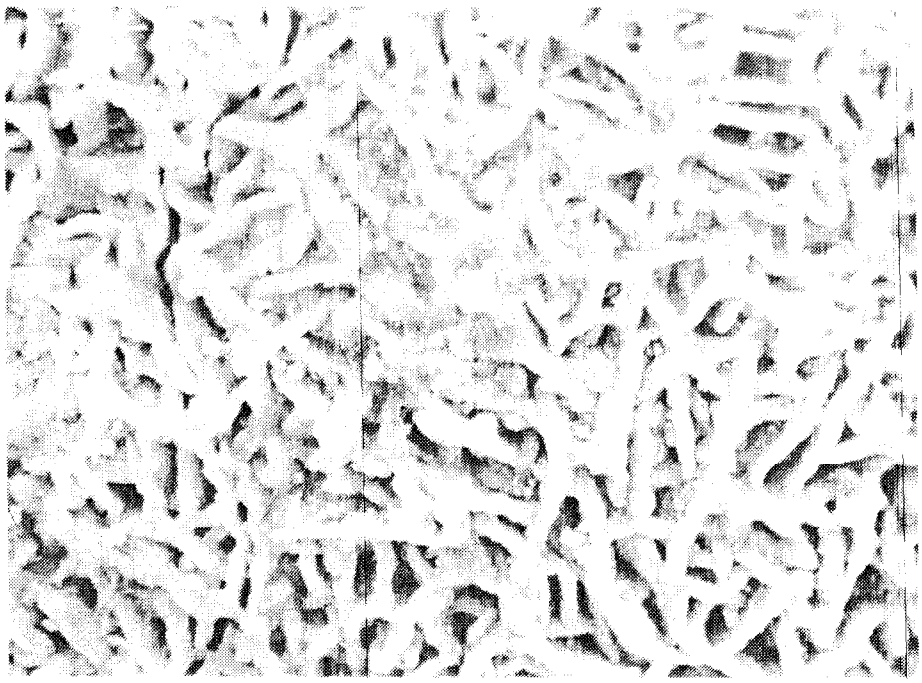

j

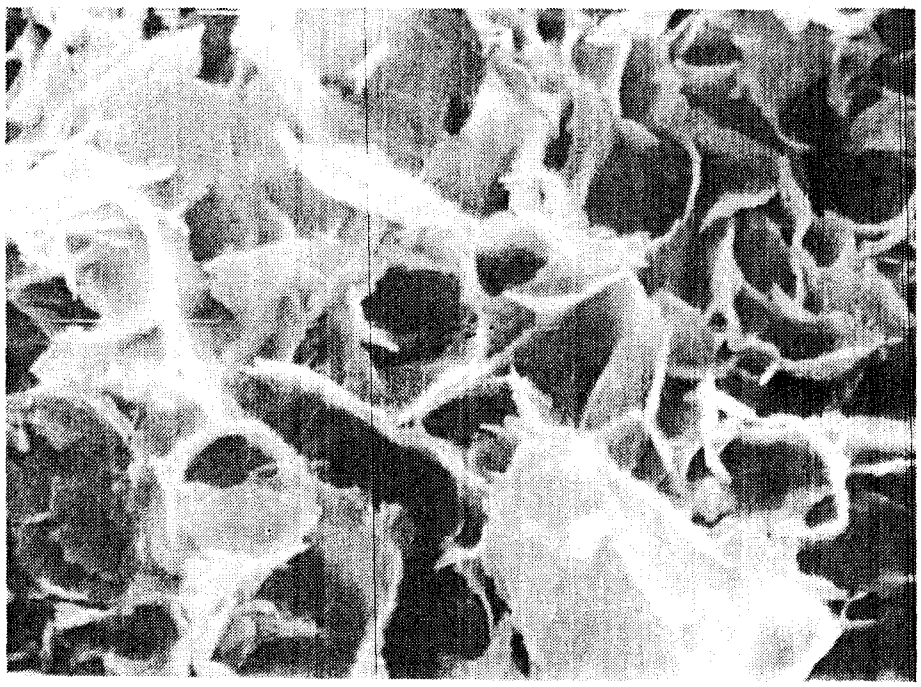

k

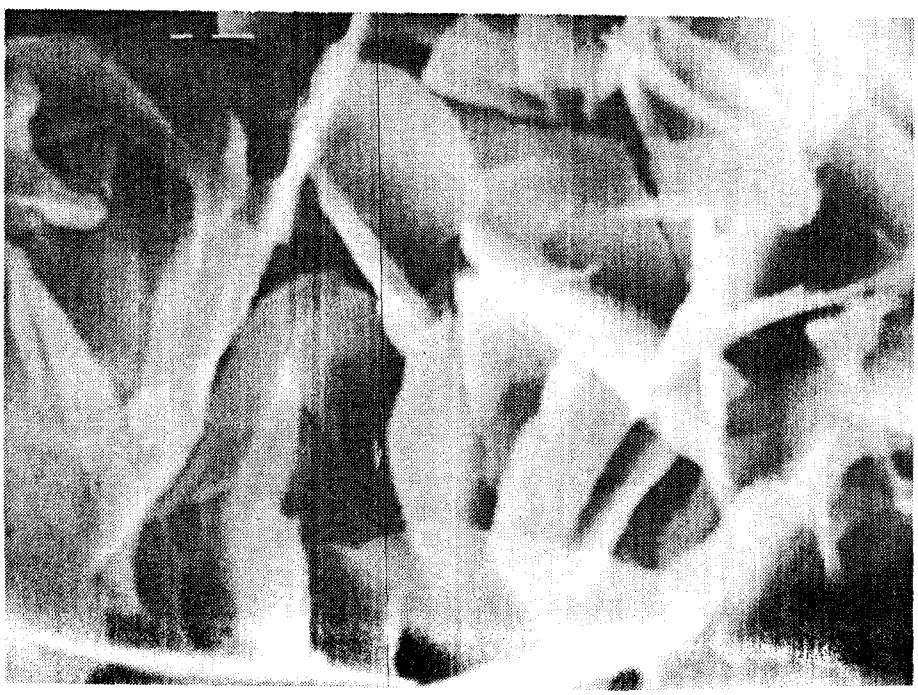

l

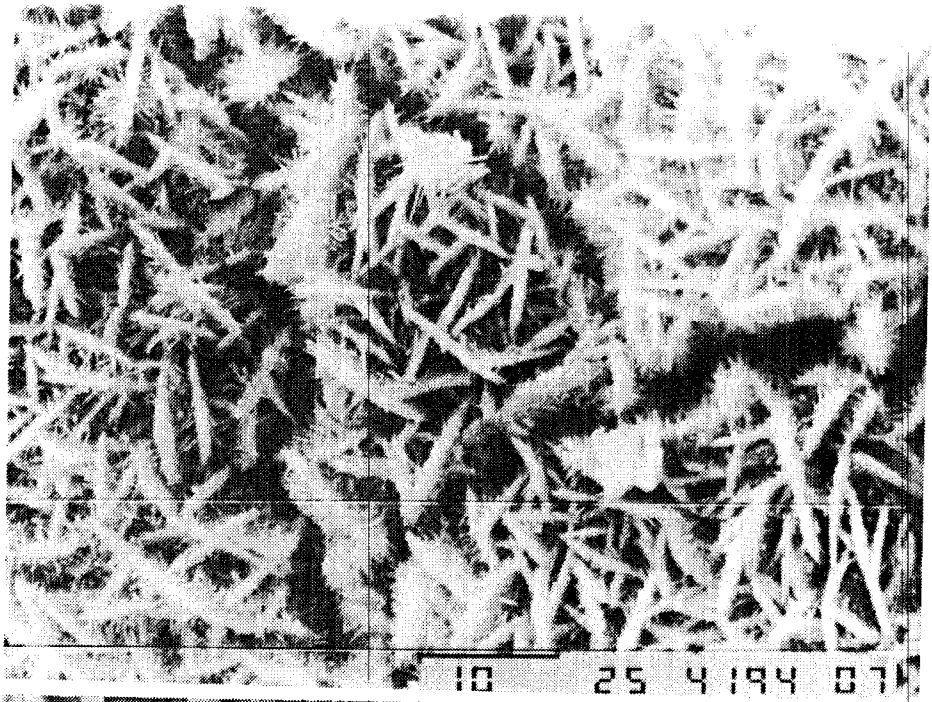

m

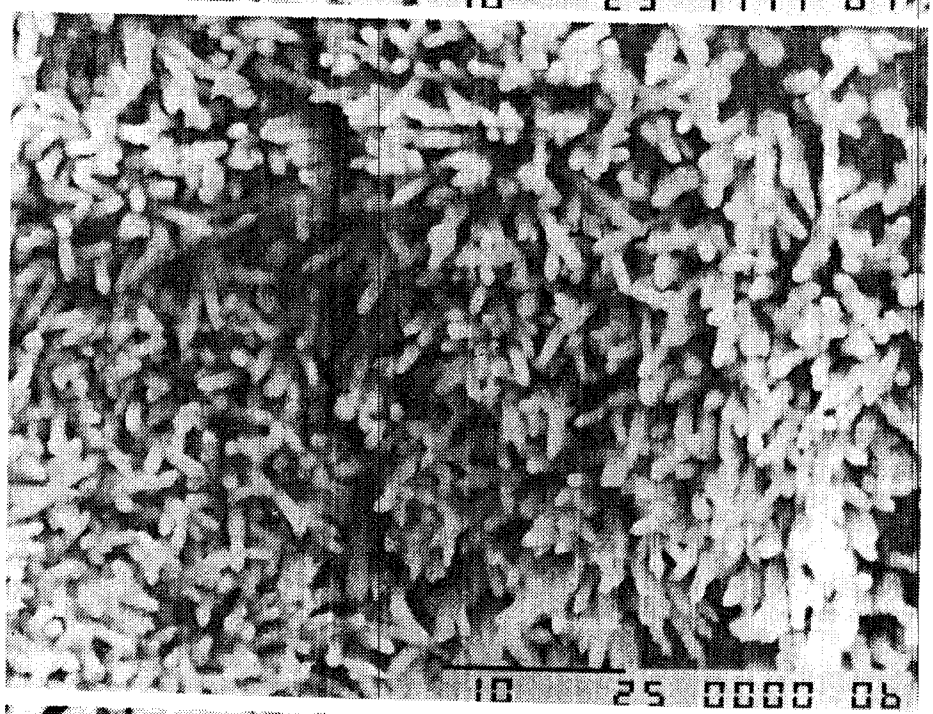

n

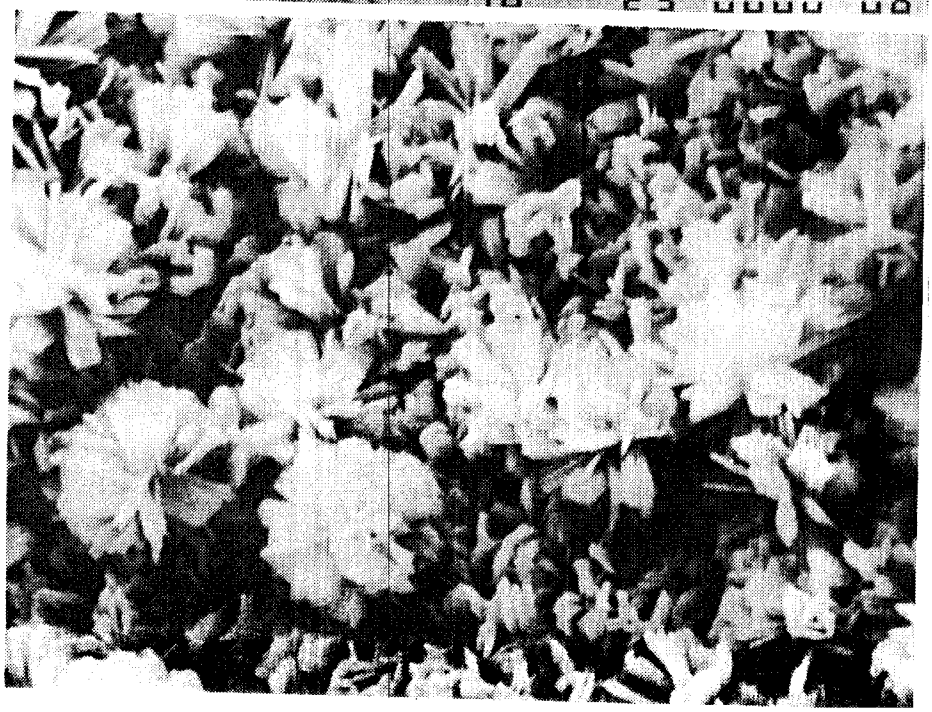

o

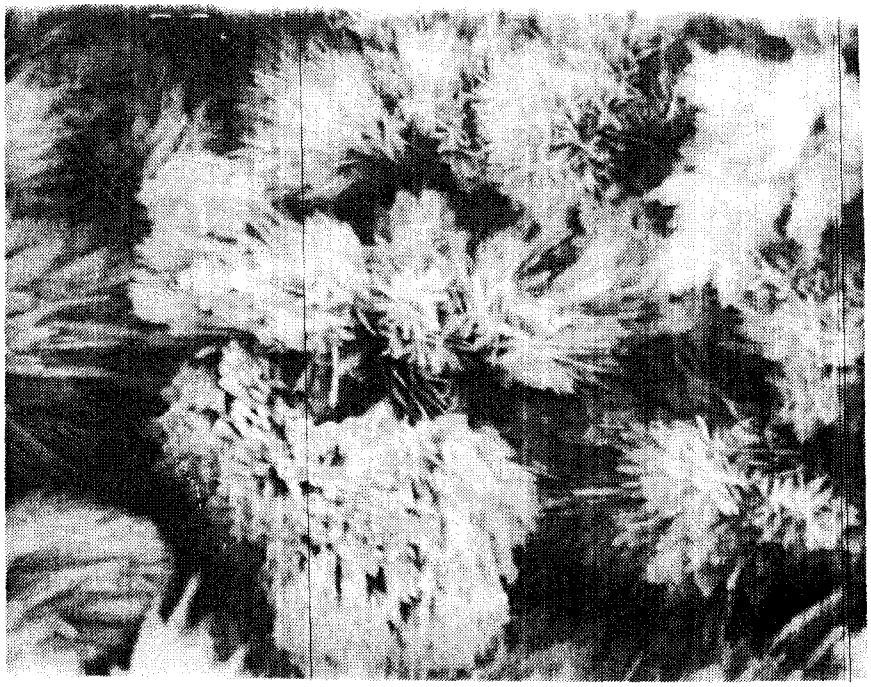

p

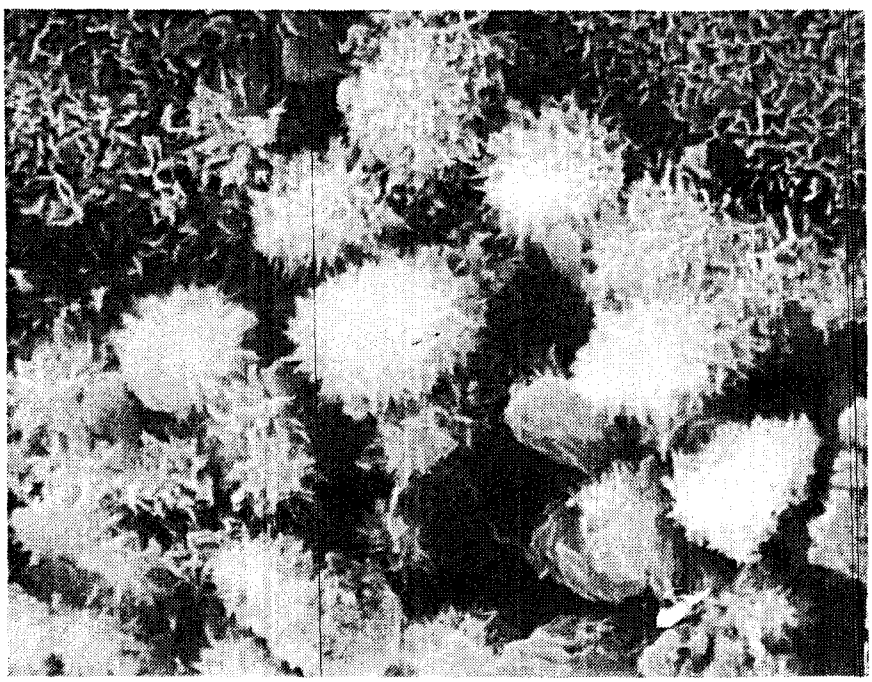

p p

q

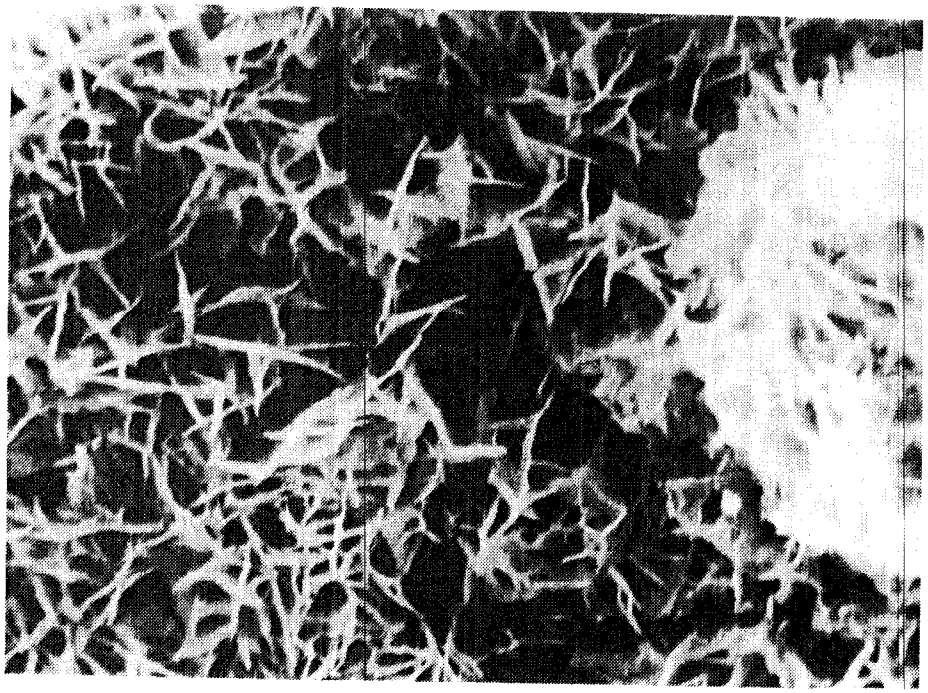

r

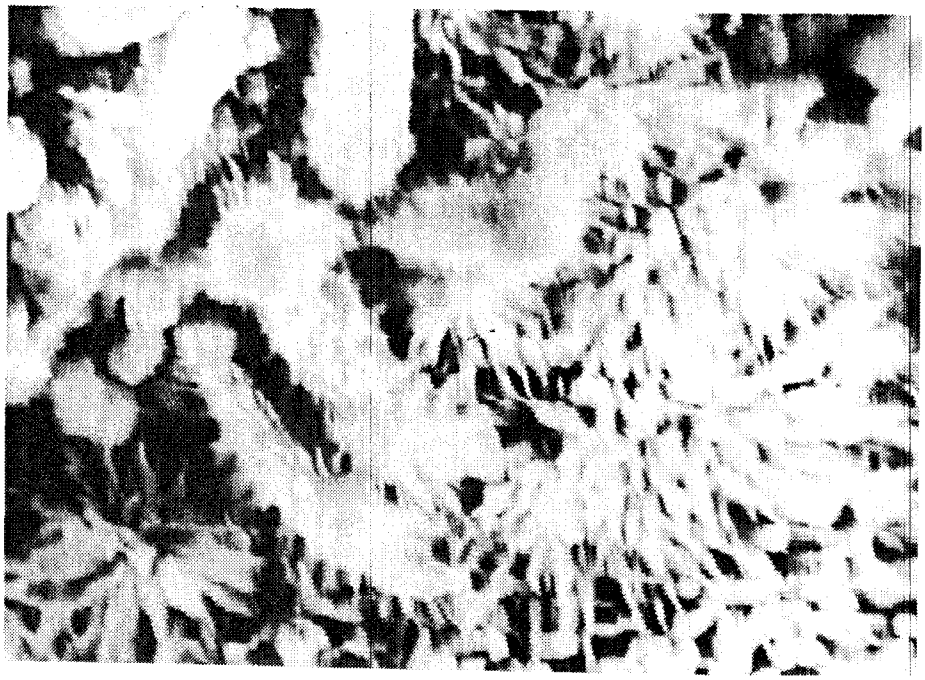

s

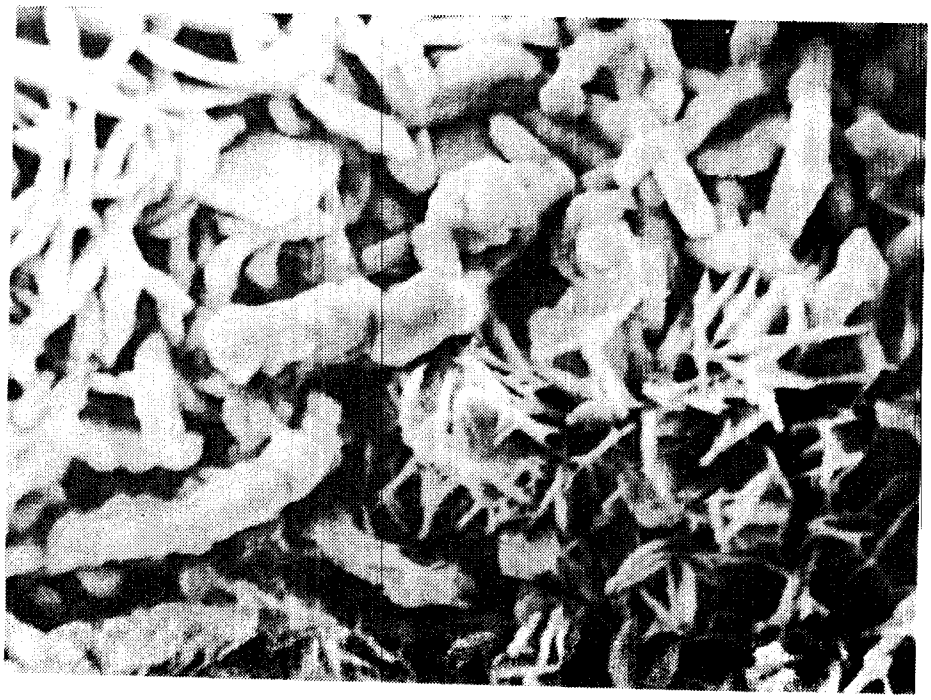

t

u

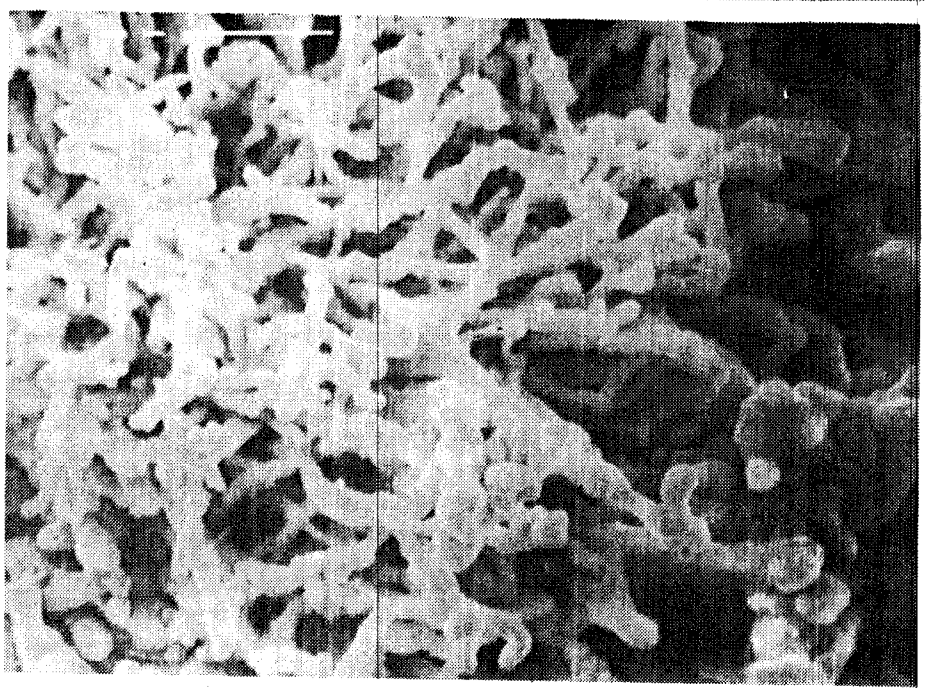

v1

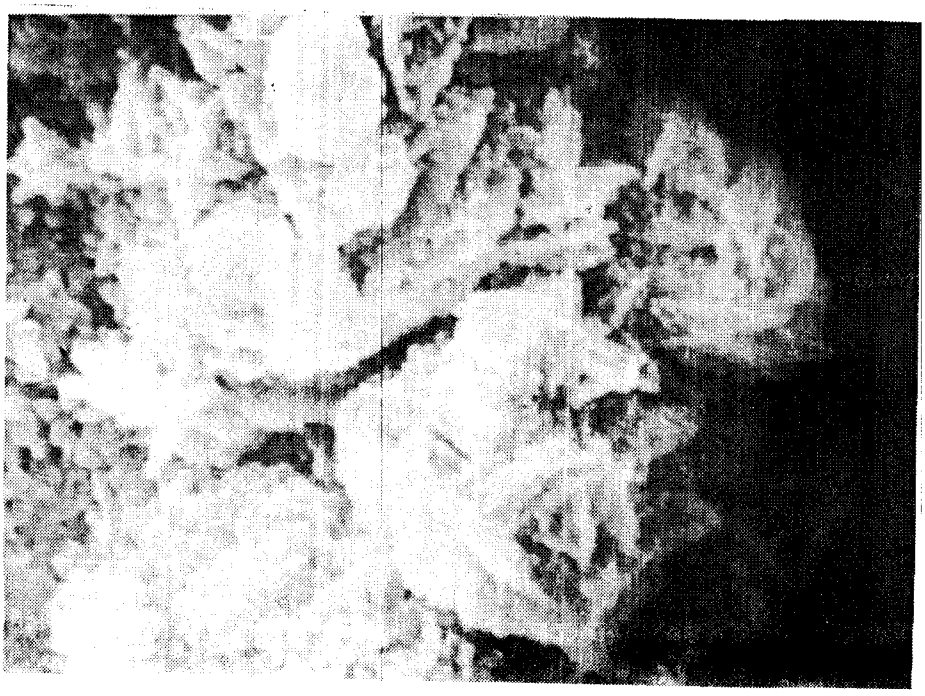

v2

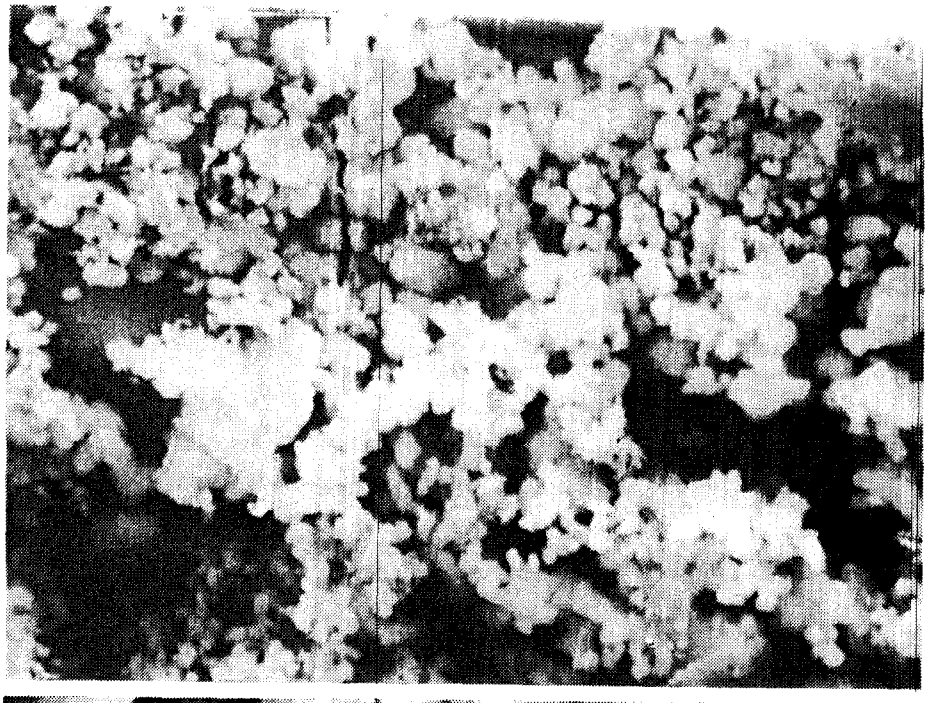

w

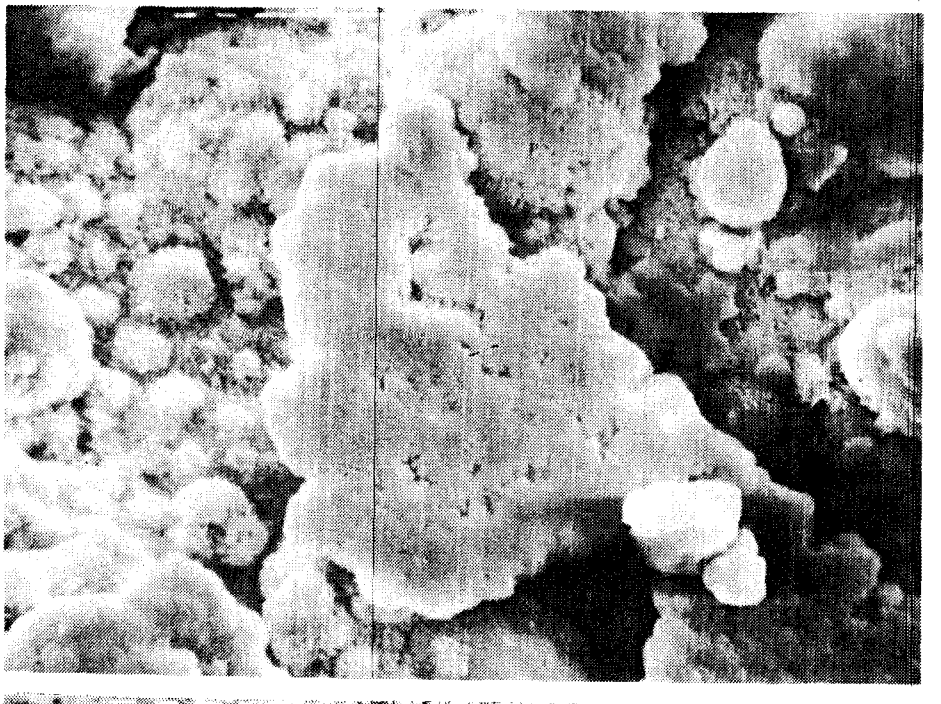

x

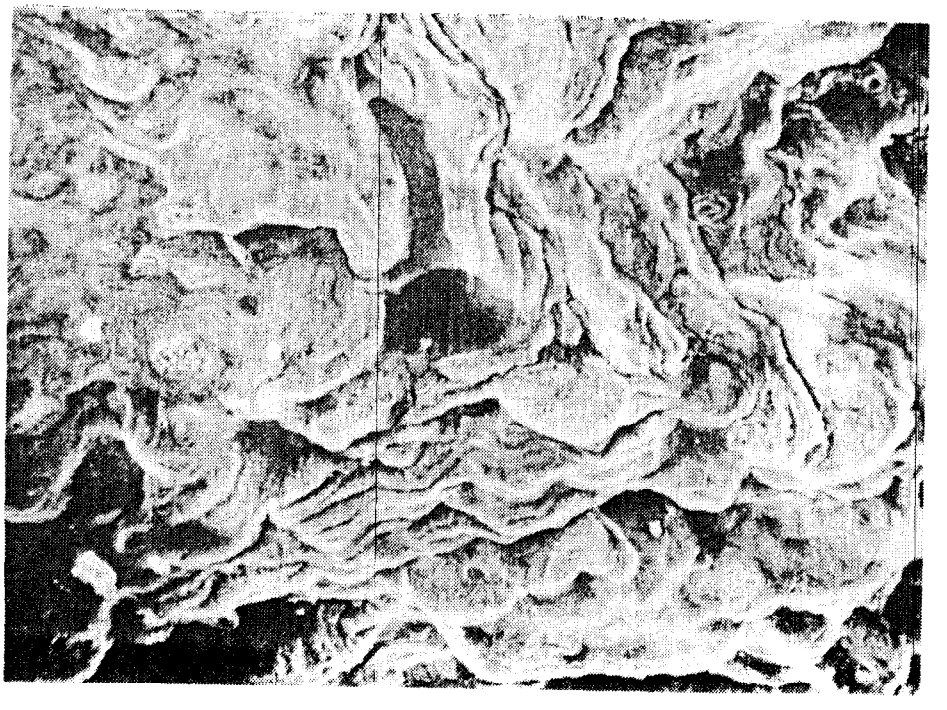

y

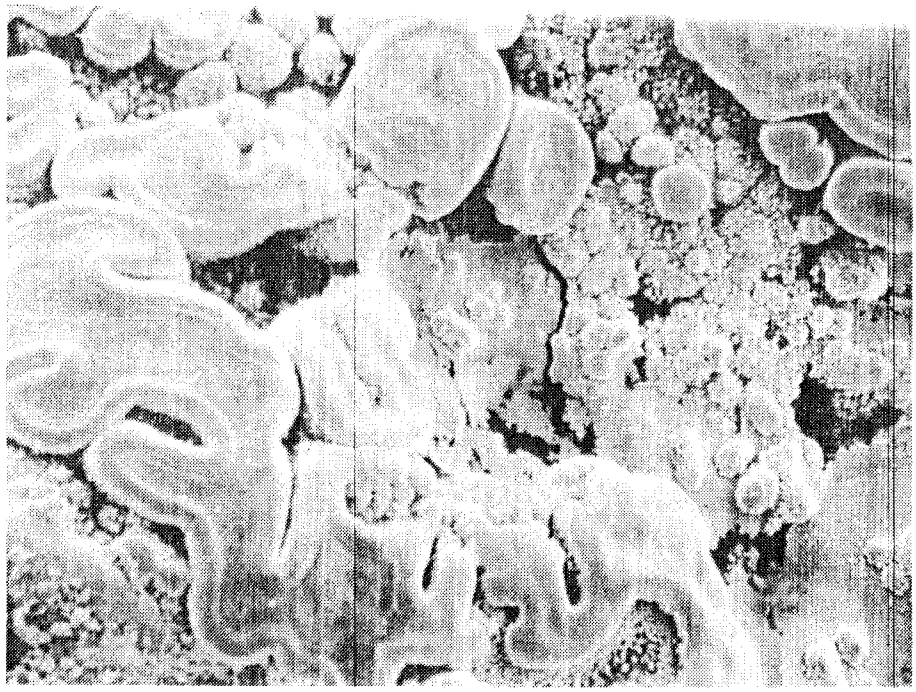

z 1

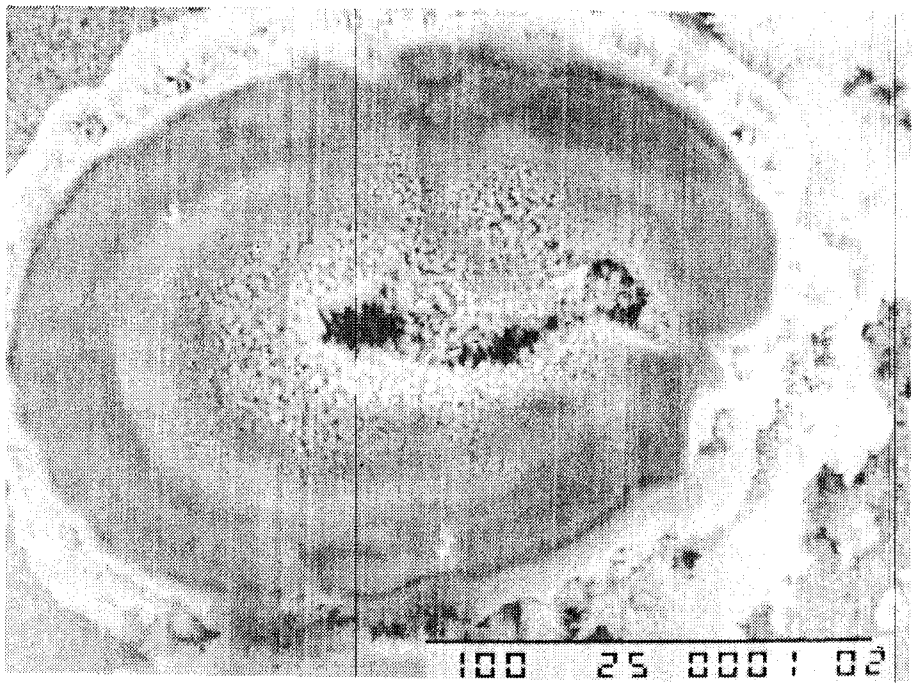

z 2

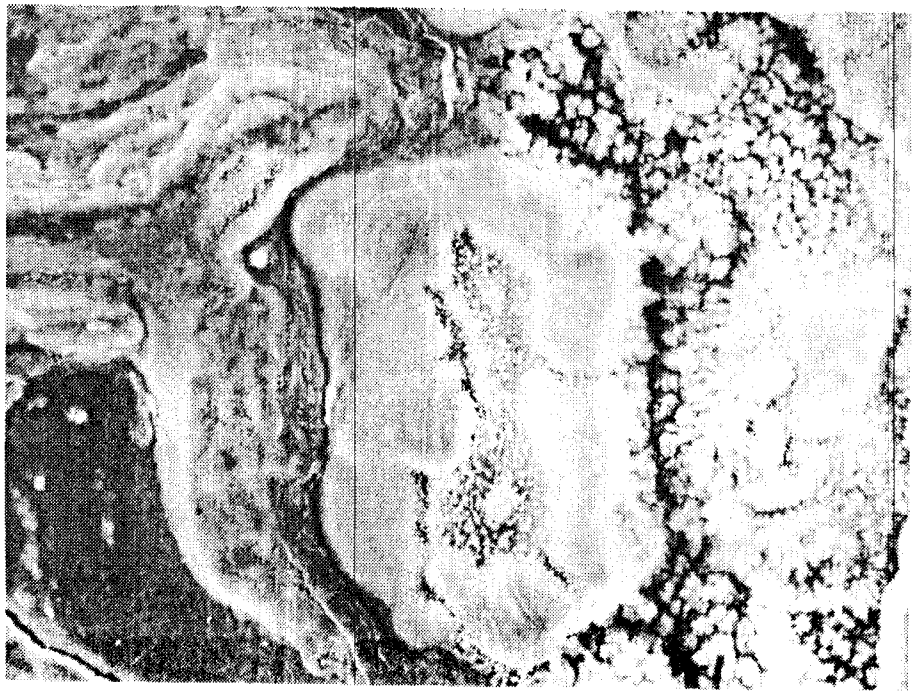

z 3

APPENDIX

Appendix:

Photographs taken in the field at bridge sites which illustrate the conditions observed and the techniques used.

Photograph:

(1) View of the Gibbstown bridge with the Weathering Steel A588 - grade A span.

(2) View of the Leesville railroad bridge with the Weathering Steel A588 - grade B span.

(3) Coarse rust seen on the Weathering Steel at High Island bridge.

(3a) Another view of the coarse rust at Doullut Canal bridge.

(4) Another photograph of the coarse rust at the Gibbstown bridge.

(5) Coarse rust seen at Larose bridge.

(6) Even the weld areas are affected as seen at Gibbstown bridge.

(7) Sheet-type of rust removed from the Kawasaki A588 - grade A steel at the Luling bridge.

(8) Sheet-type of rust from the LU-bridge; another view.

(9) This photograph shows fine to coarse type of rust samples collected from various bridges.

(10) The mill scale remains usually for the first few years only. This photograph shows the mill scale sticking to the steel in the approach span (U.S. Steel grade A) at LU.

(11) Partially enclosed and boxed areas at the entrance to the piers accumulate rust debris and bird wastes. This photograph is from the Larose bridge.

(12) Wildlife, usually owls, take shelter in such boxed locations and lay eggs. This photograph shows the owl eggs at the GT bridge.

(13) This photograph shows the owl chicks after hatching of the eggs. Note the debris. This is at the GT bridge.

(14) The rust debris collected in such partially boxed areas above the gusset plates can be seen here. The rust forms in sheets in such areas. Note the rust sheet also on the bolt-head. This is at the DC bridge.

(15) The sheet-type of rust can be seen after removing the debris. This photograph shows the appearance after partial sand blast cleaning in the boxed area. Note the sheet-type rust on the facing edge also. This is at DC.

(16) Pits can be seen after sand blast cleaning. This photograph shows the pits observed in the blast cleaned portion at the GT bridge.

(17) Pits seen on the steel at the DC bridge.

(18) Pits seen on the steel at the HI bridge.

(19) Pits seen on the top side of the horizontal span at HI.

(20) Pits seen on the horizontal span at GT.

(21) Severe pitting with pits as deep as 40-50 mils has been seen at Luling underneath the sheet-type of rust removed. A piece of the rust is laid back to illustrate the condition seen.

(22) After sand blast cleaning depths of pits were measured using a digital, linear electronic gauge. The gauge is attached to a magnetic chuck to hold the gauge in place and a translator was also used as shown attached to the magnetic chuck. This photograph shows the gauge located in place for taking the readings on the vertical side web plate at GT.

(23) The gauge in use to measure the pit depth on an inclined face at Luling.

(24) Readings are taken using the gauge and manipulating it suitably. Here the readings are being taken on the vertical face of the beam at LU.

(25) Section thickness losses were ascertained by measuring the thicknesses of the beams and plates at several locations annually. Here the initial readings are being taken in the first year after cleaning the steel at the Boeuf River bridge. Mr. Kirt A. Clement is taking and dictating the readings.

(26) Here Mr. Clement is taking the readings and dictating them to Mr. Ron Allen. The readings are taken at the HI bridge location on top of a pier.

(27) Specimens of Weathering Steel were located in racks installed at five different bridge sites and exposed. Here the racks are located in sheltered areas on the pier under the bridge and tied to the horizontal beam. Nine racks were located at each bridge site. This one is at GT.

(28) One of the interior, sheltered location racks in place at High Island. Racks are suitably identified. The number 21 identifies it as the rack at High Island bridge, removed after 1 month exposure (I set) and after cleaning and reinstalling the specimens in the same rack, re-exposed for 1.5 years at the same site (II set).

(29) One of the exterior racks at the bridge site located on the rim at the exterior at Gibbstown.

(30) Some of the areas were cleaned and treated with various rust-modifier-type (inhibitor) chemicals. This photograph shows the exterior vertical face of the steel in the tower at the Luling bridge after getting the treatment the first time. The numbers stand for respective treatments and III identifies the location on the bridge.

(31) Lower half of the treated areas were retreated with similar chemicals after 6 months. This photograph shows the color changes resulting after such a retreatment at LU.

(32) The vertical half of the treated and exposed areas were retreated after 1 year from the initial treatment. This photo shows steel in Location I on the LU bridge after getting such a retreatment. Loc. I is analogous to Loc. III.

(33) The investigators are taking the thickness readings. This shows the readings being taken at LU after 1 year from the first time readings were taken. An ultrasonic thickness gauge was used.

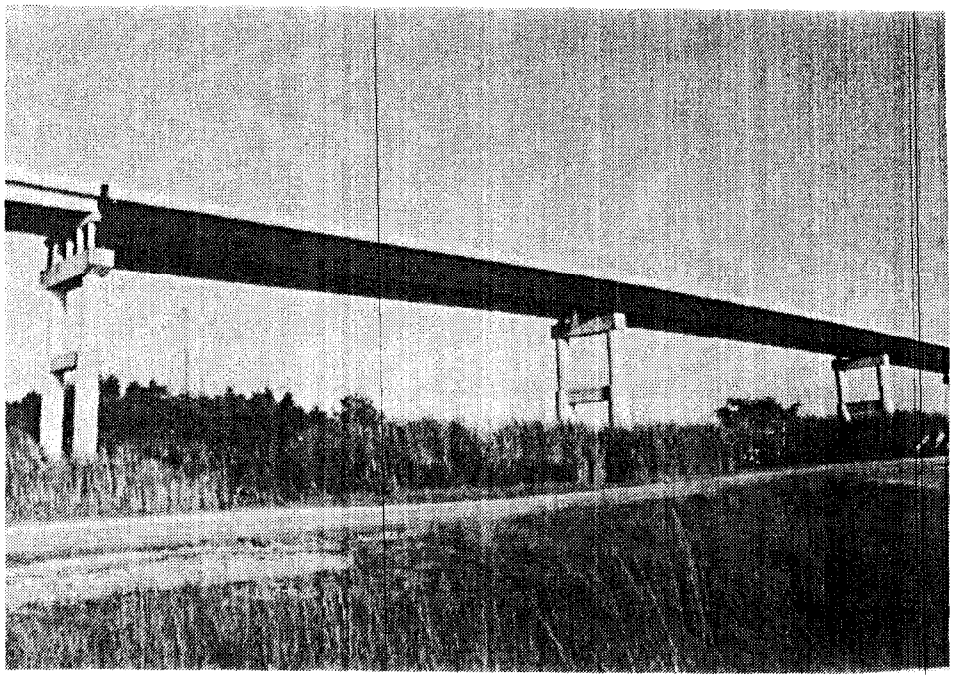

1

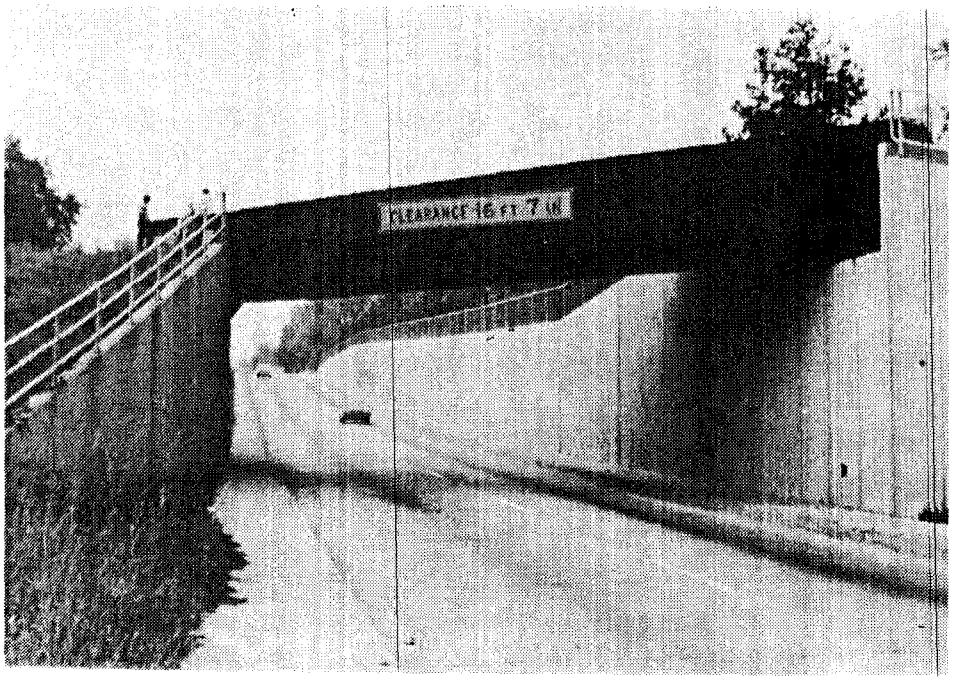

2

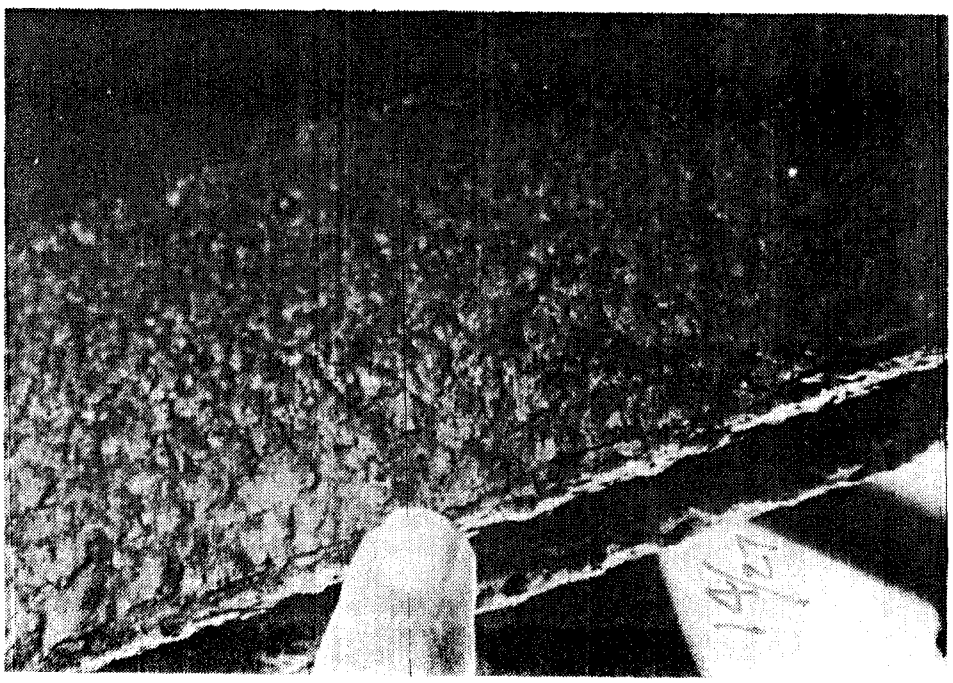

3

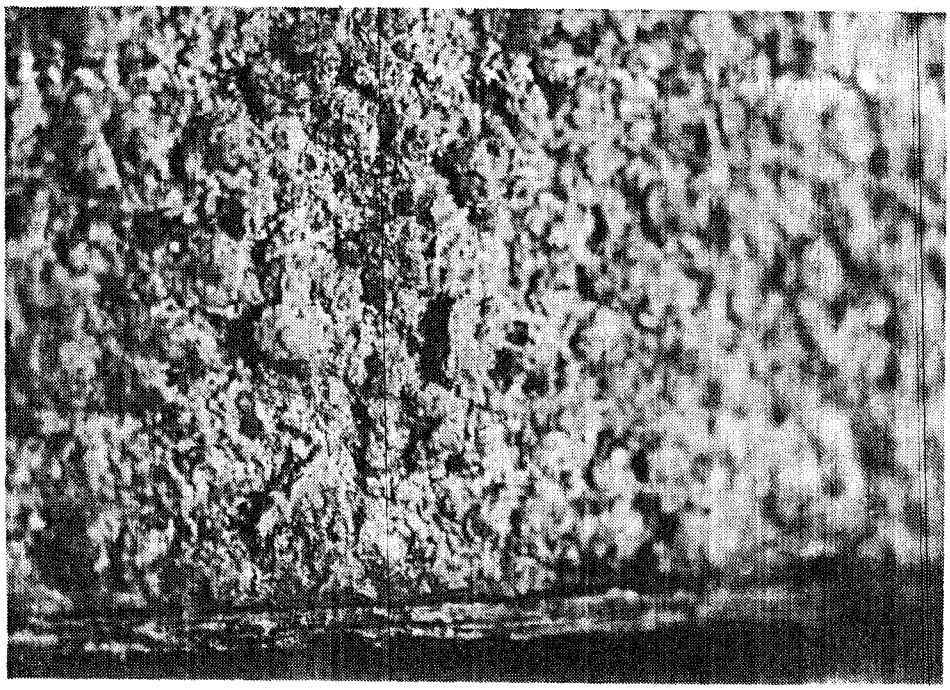

3A

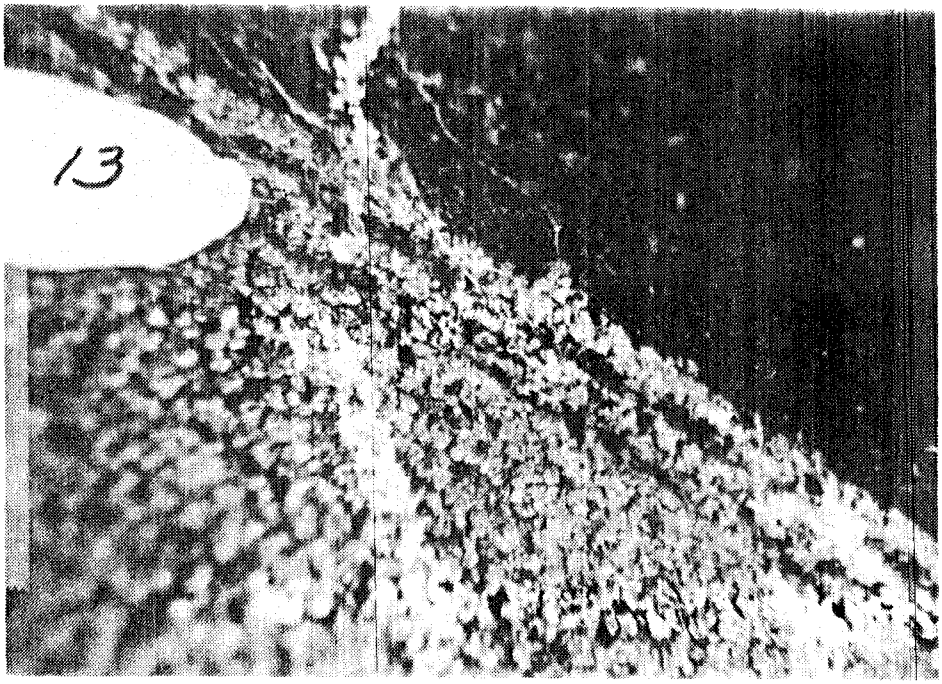

4

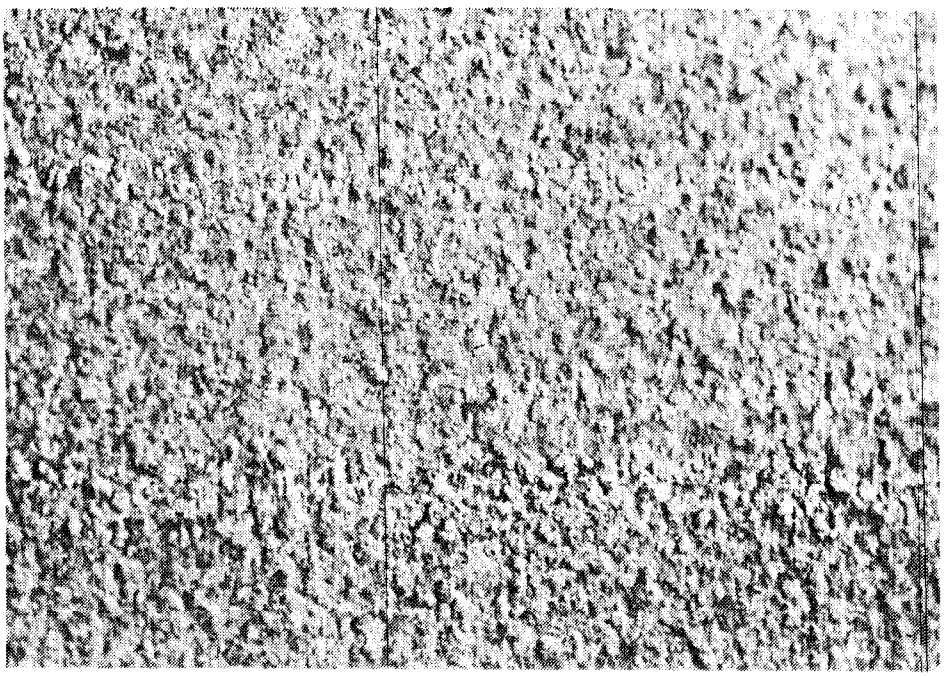

5

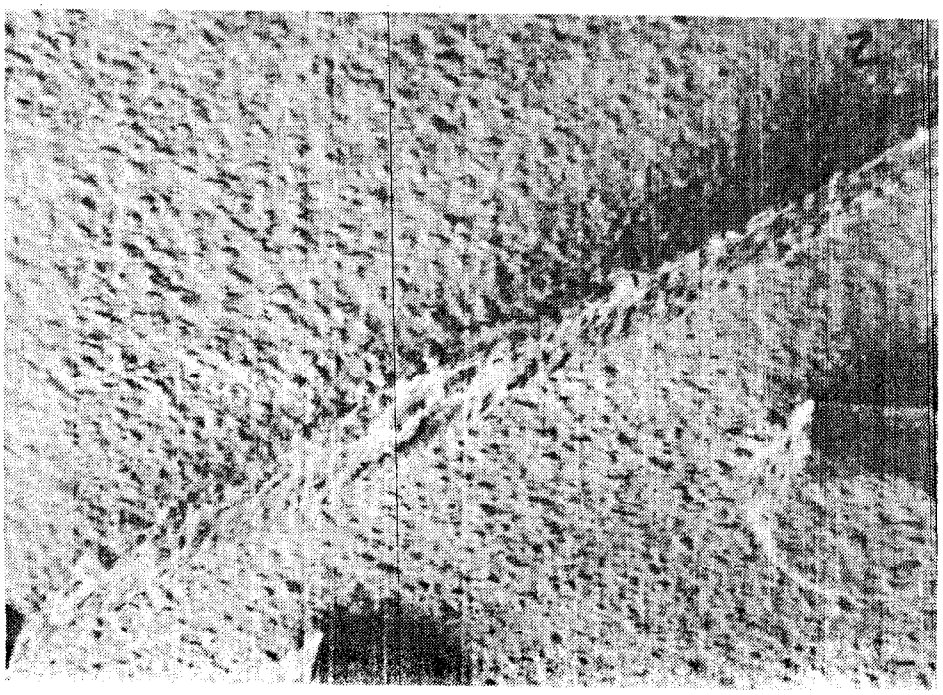

6

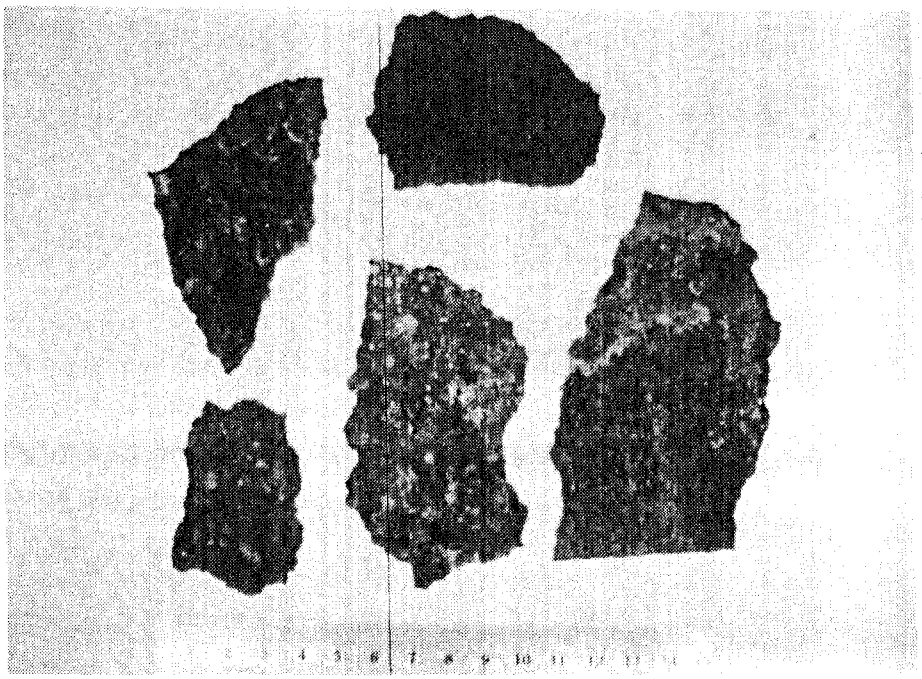

7

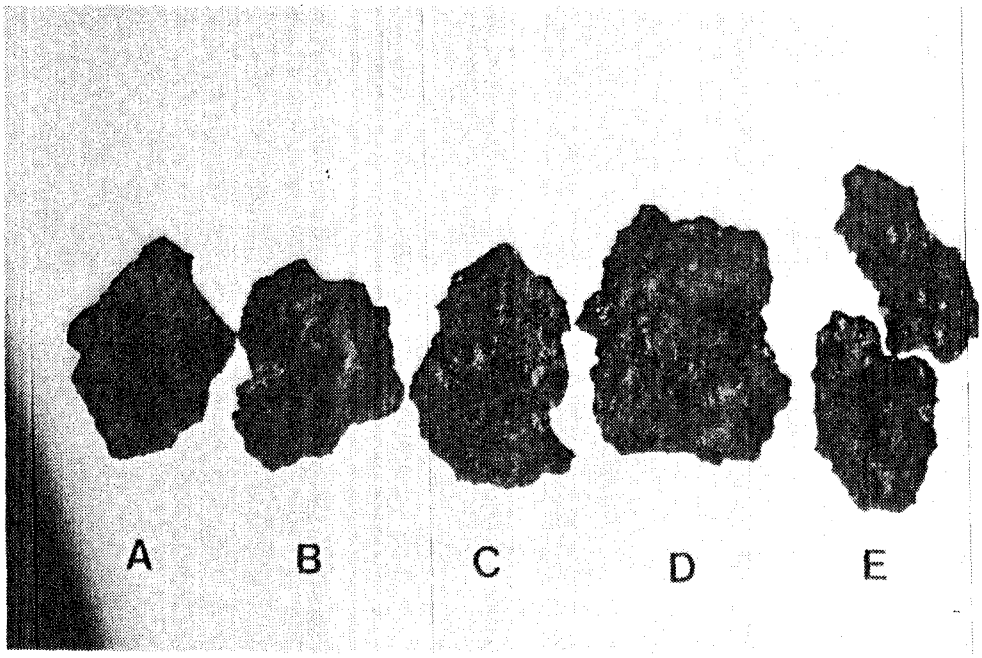

8

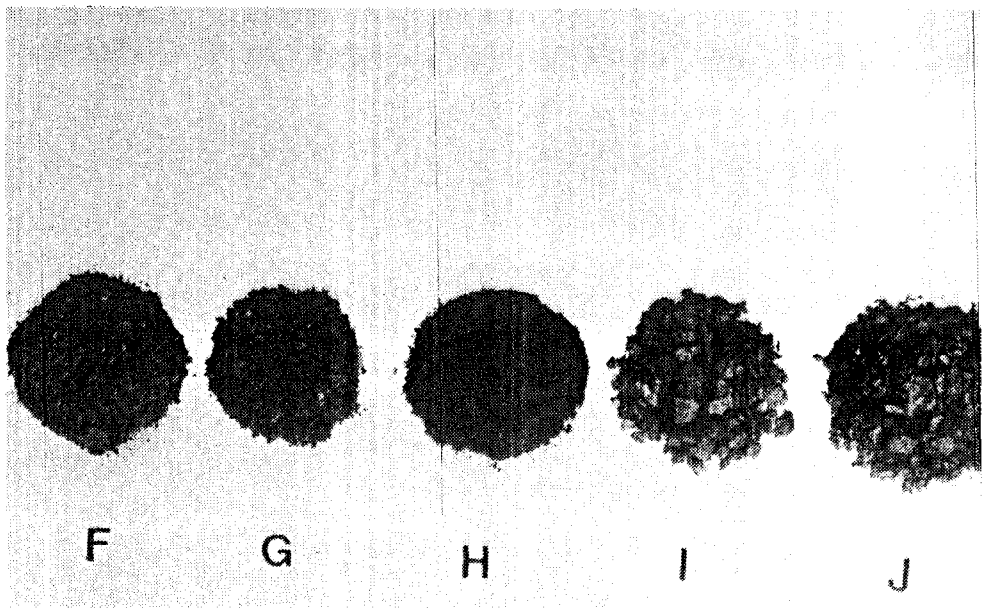

9

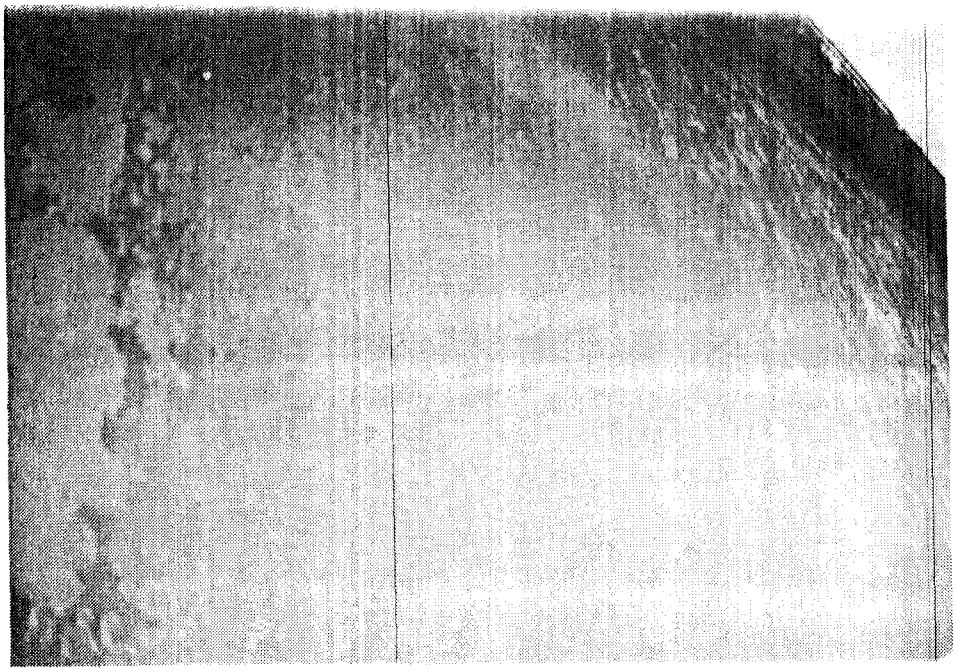

10

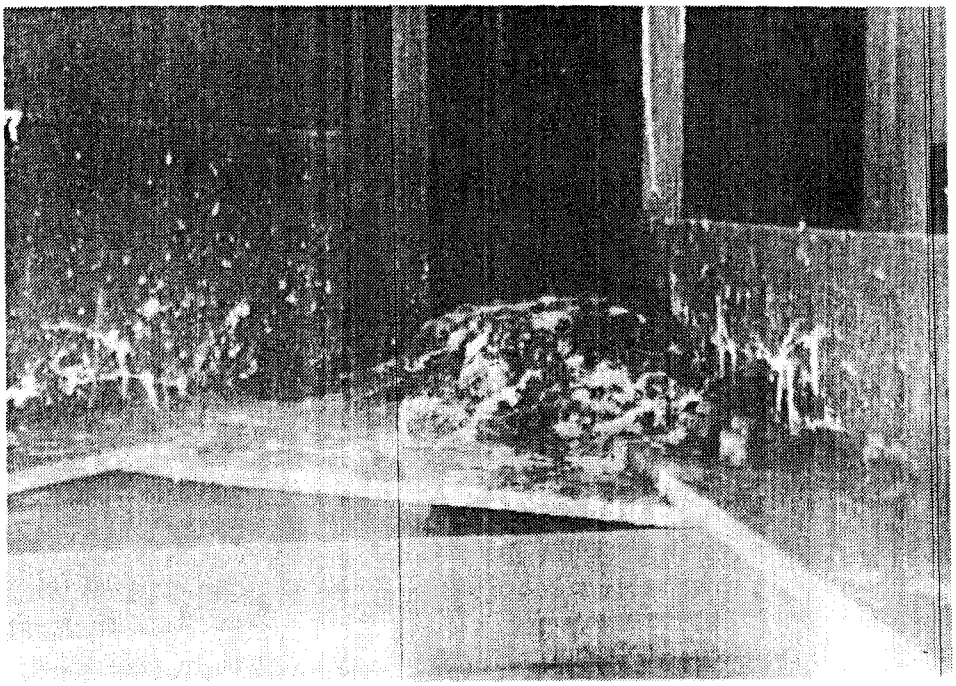

11

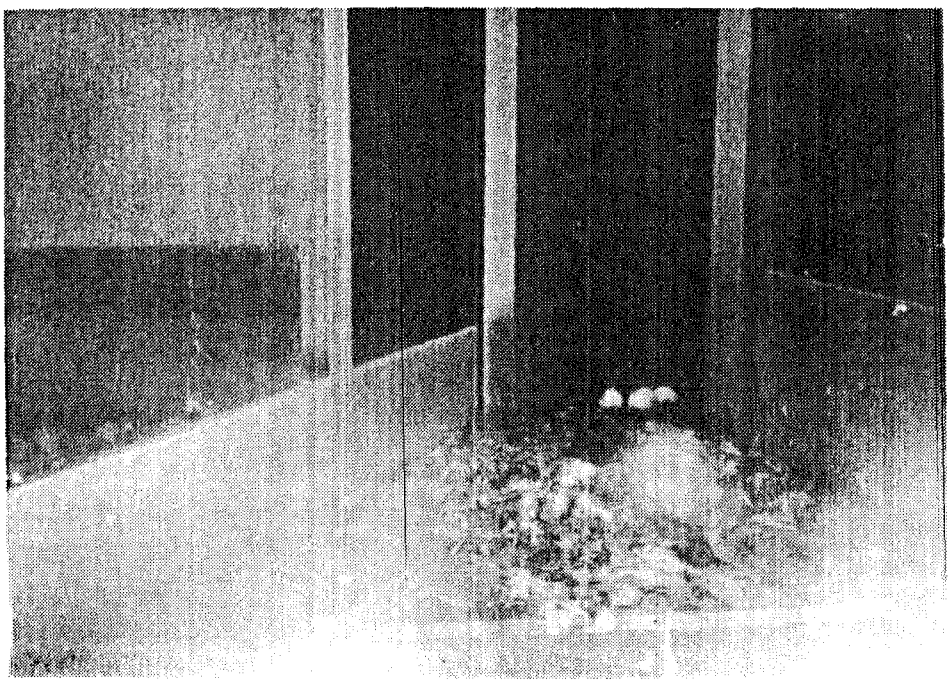

12

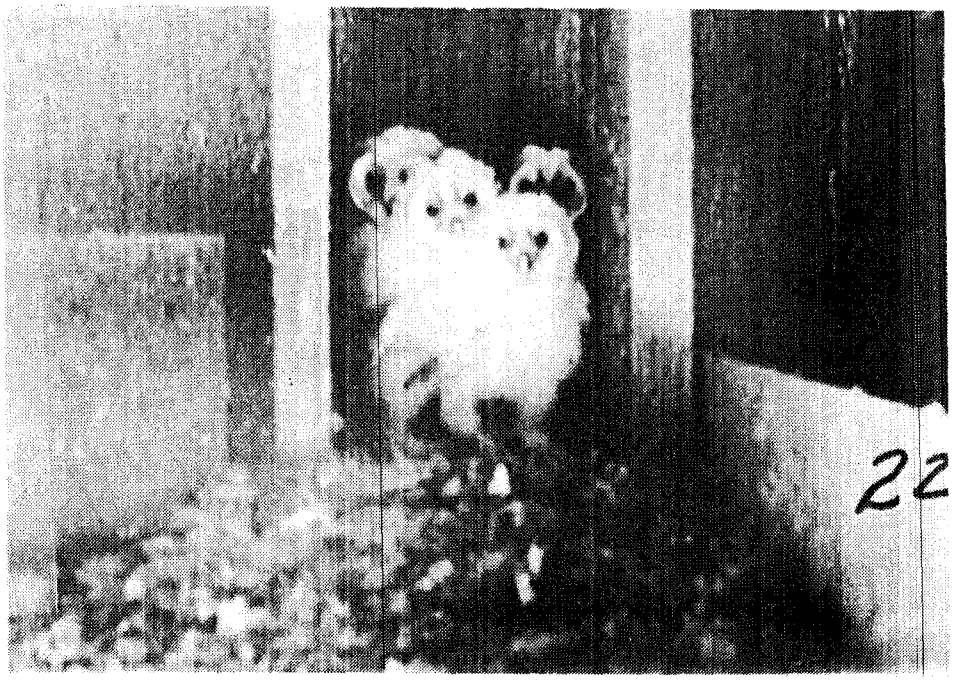

13

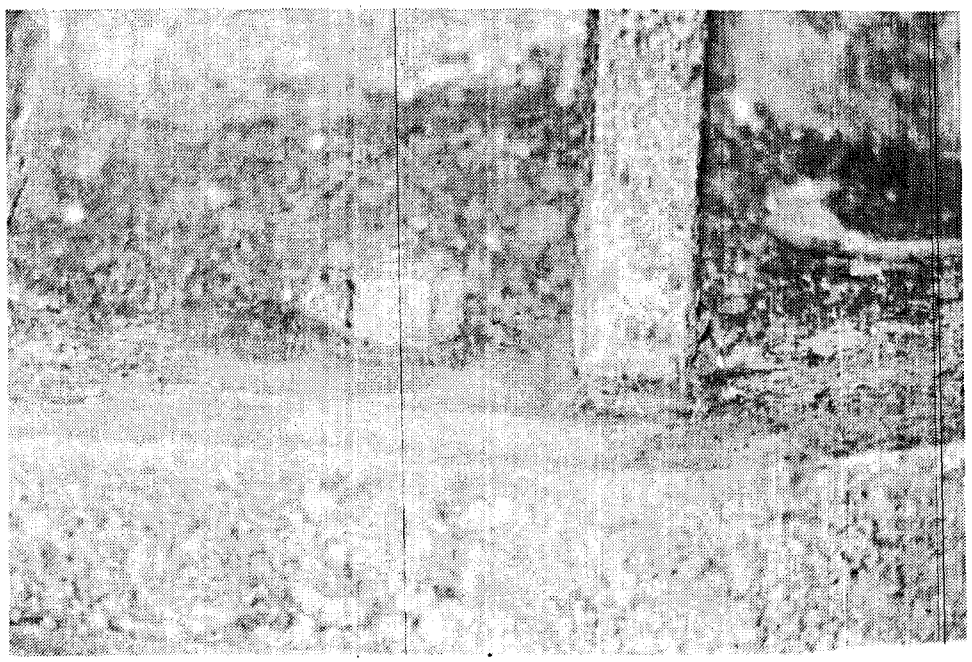

14

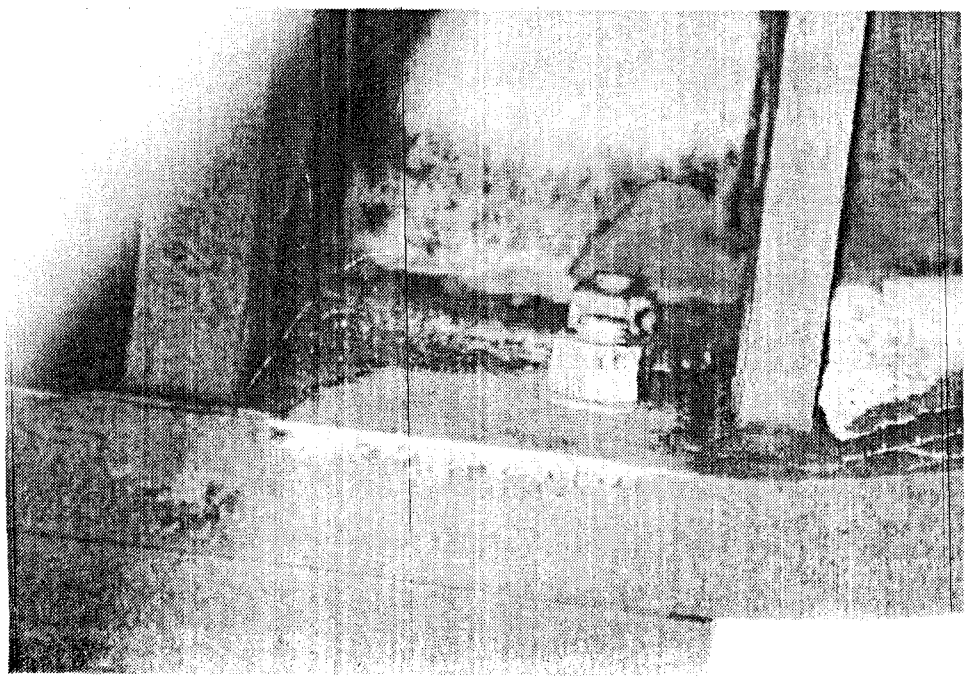

15

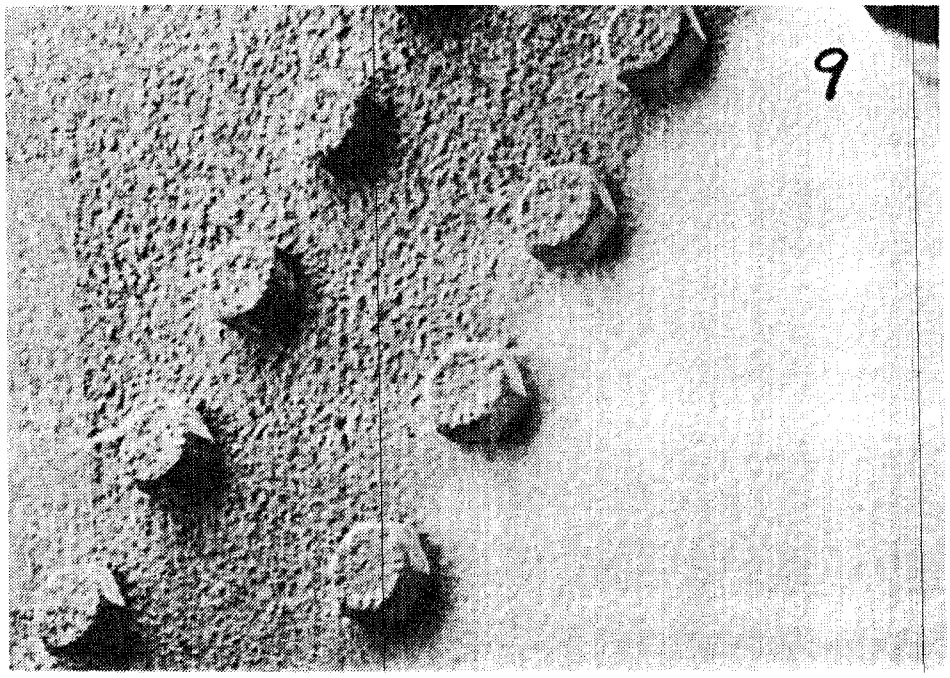

16

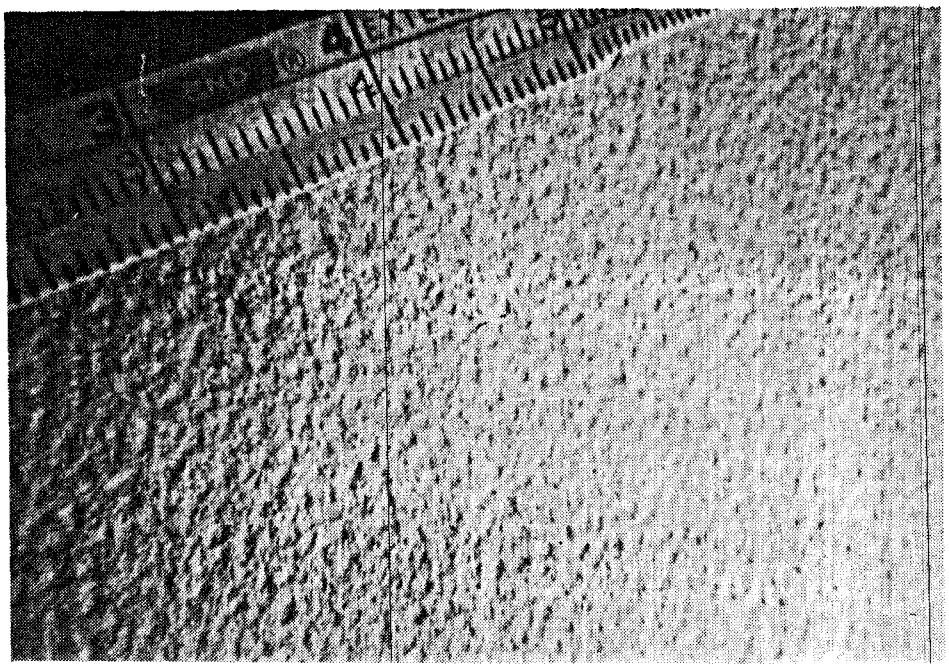

17

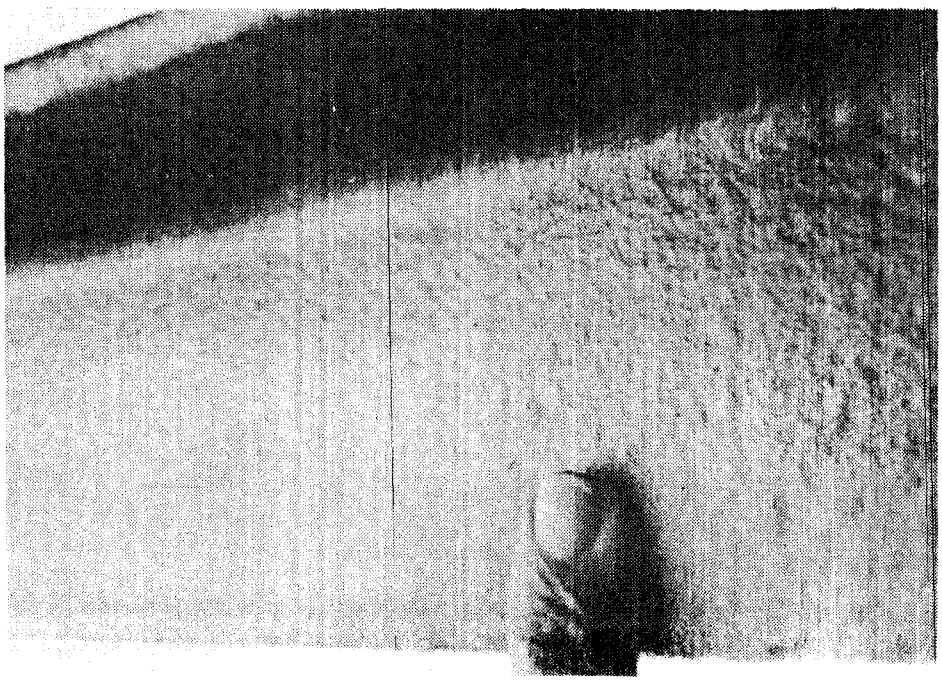

18

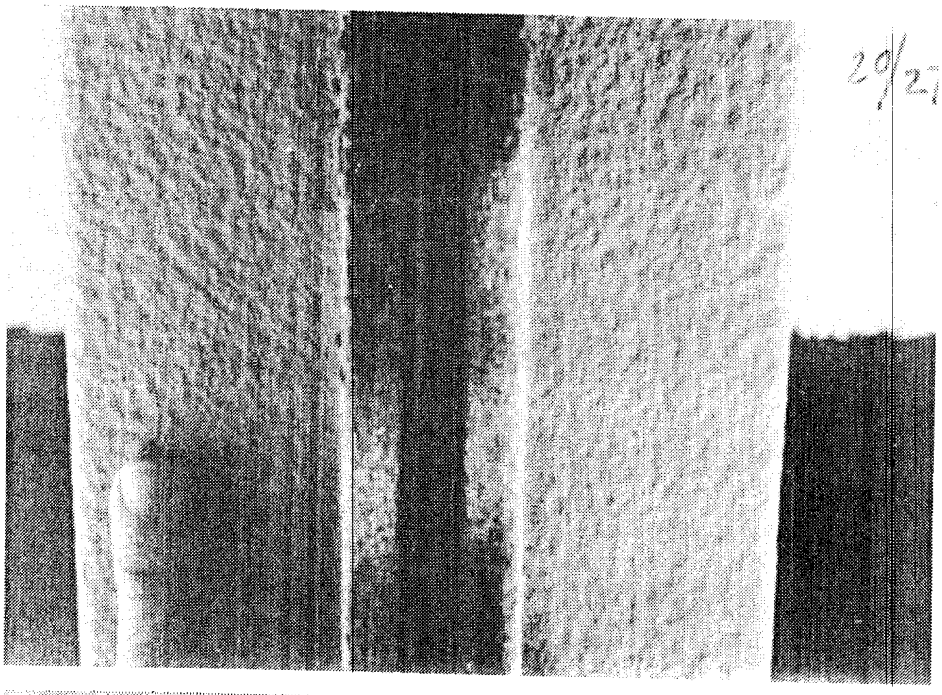

19

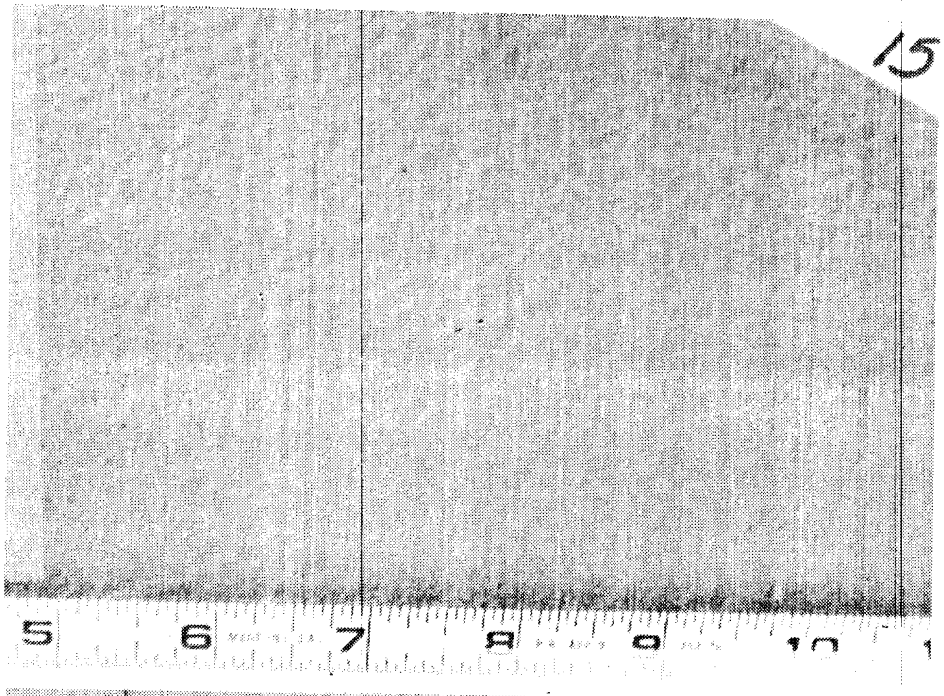

20

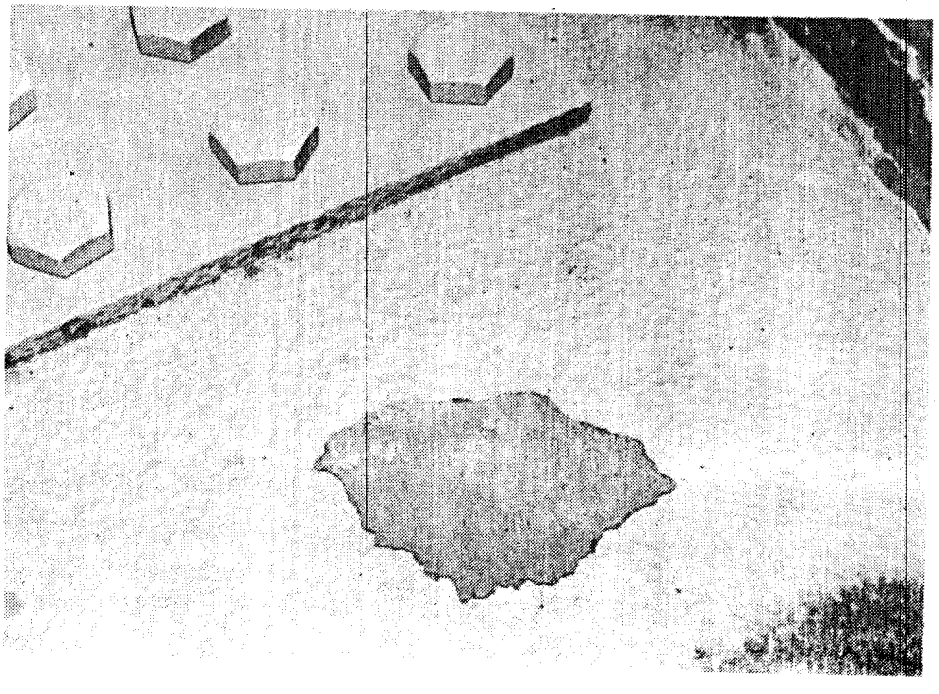

21

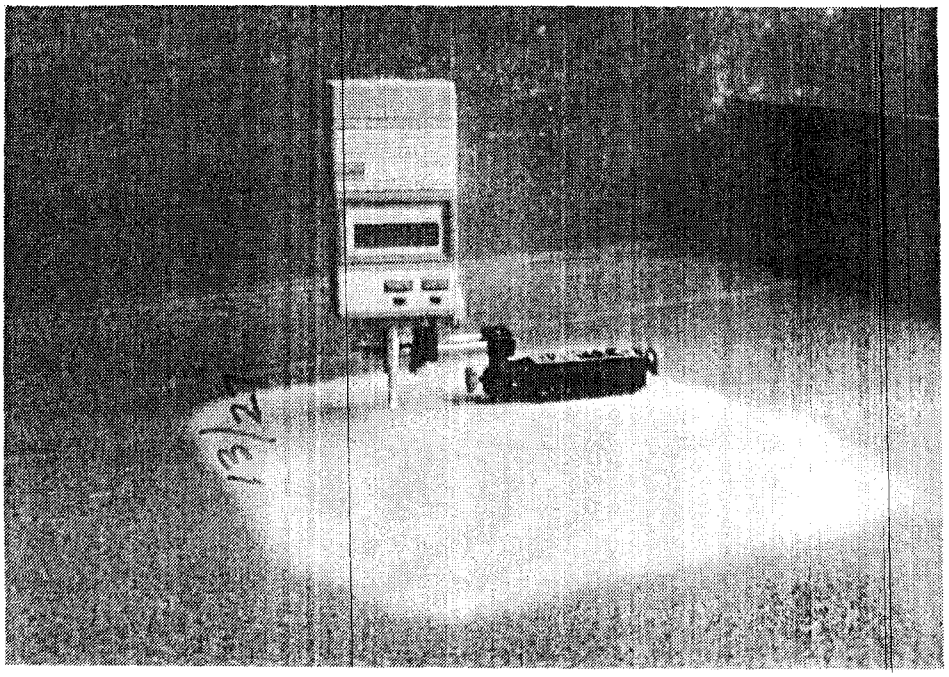

22

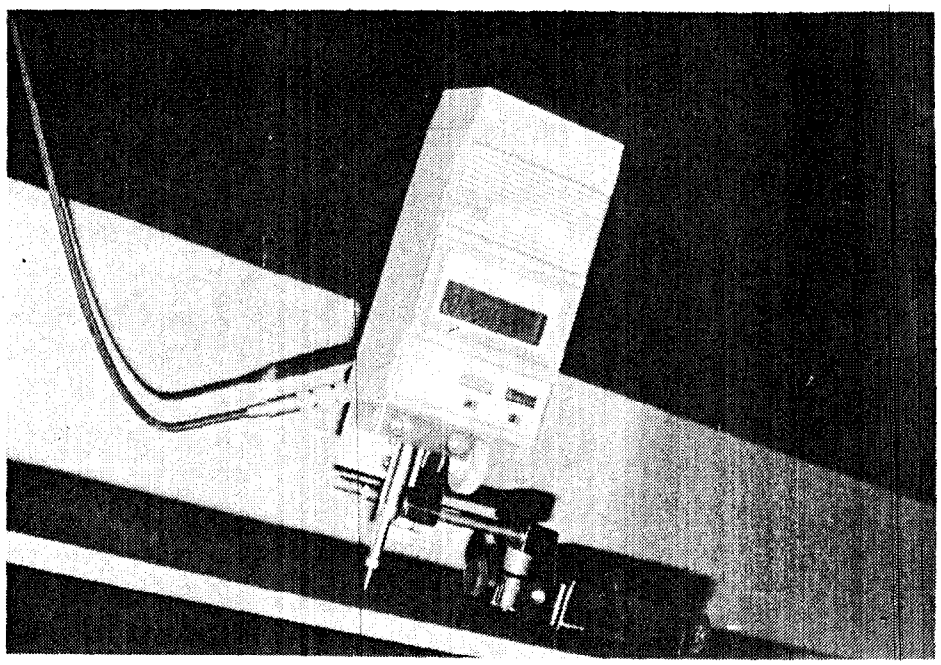

23

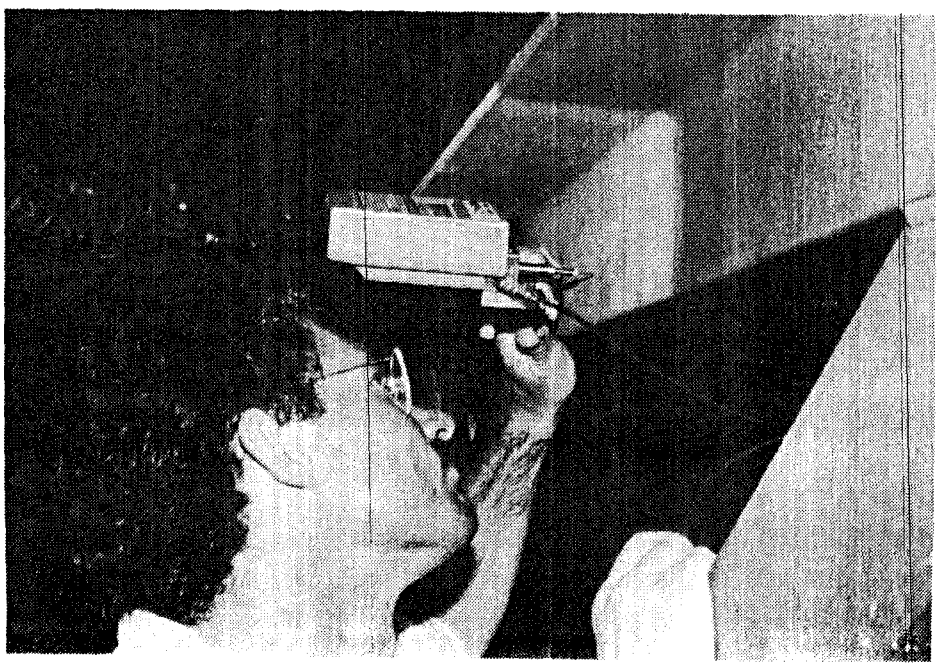

24

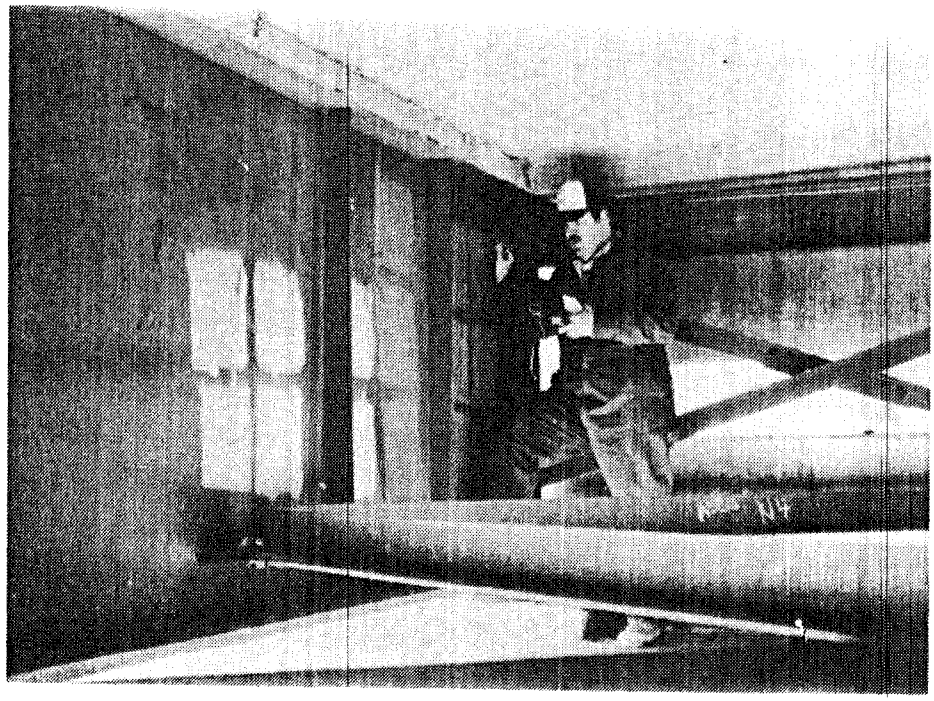

25

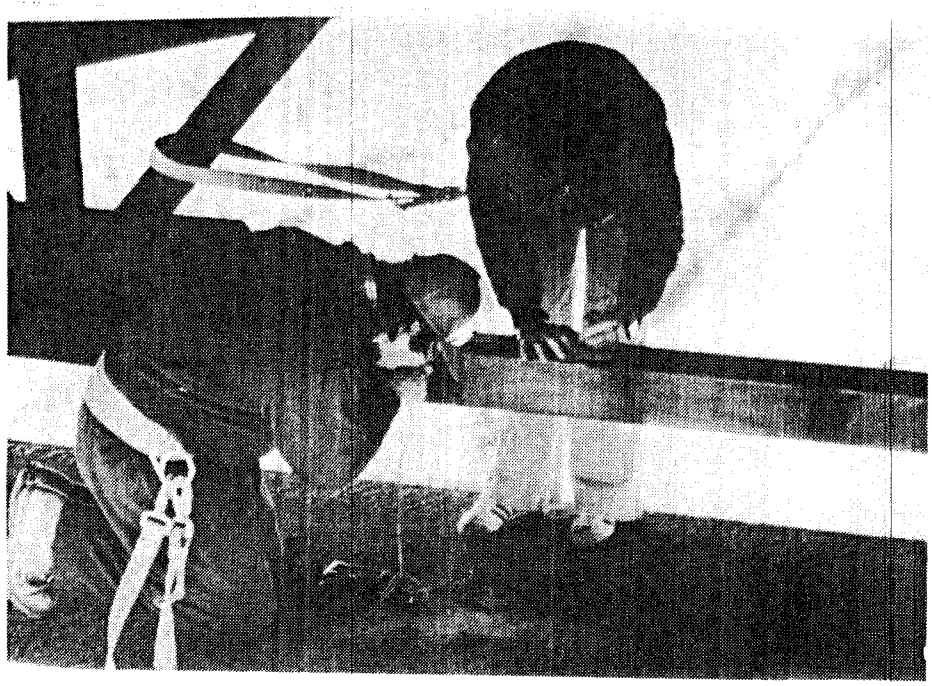

26

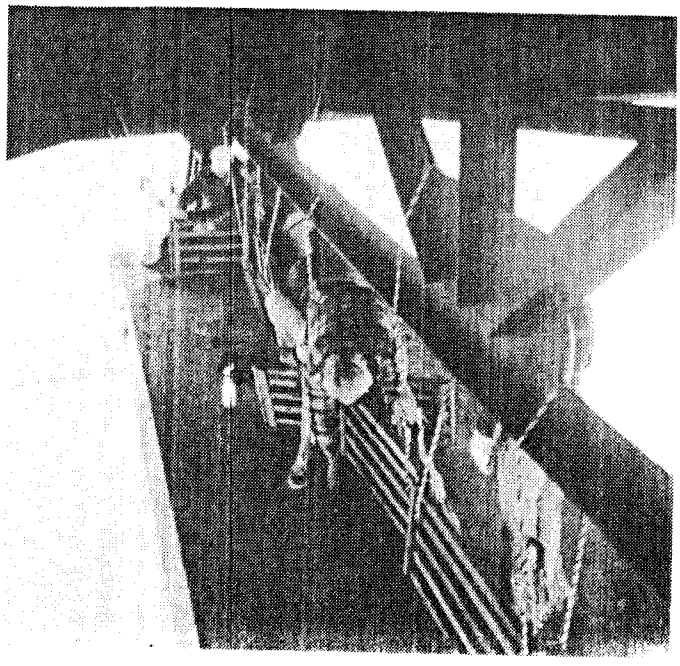

27

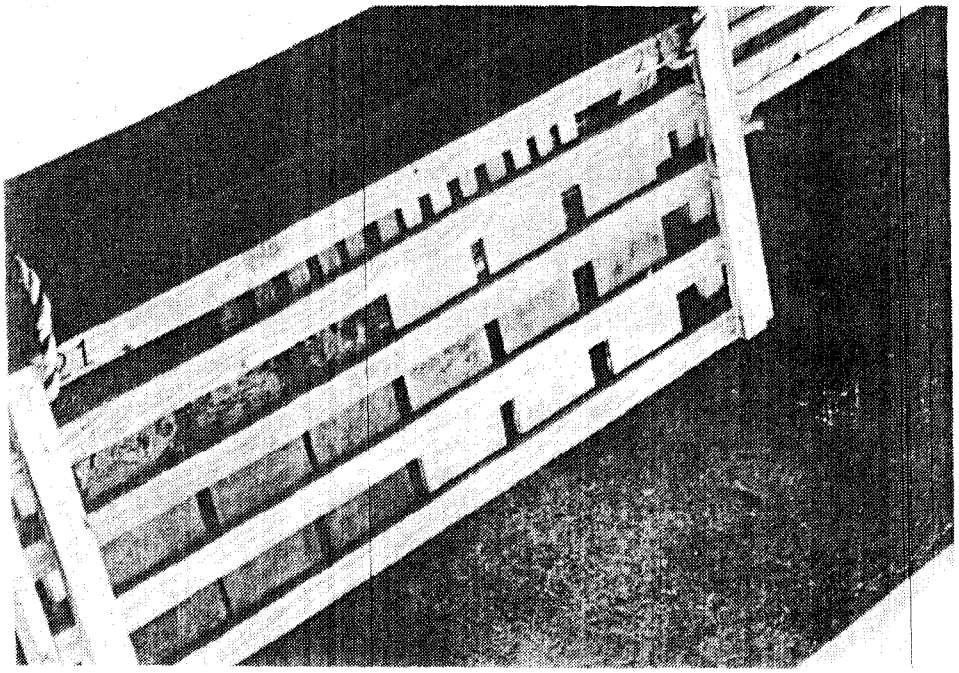

28

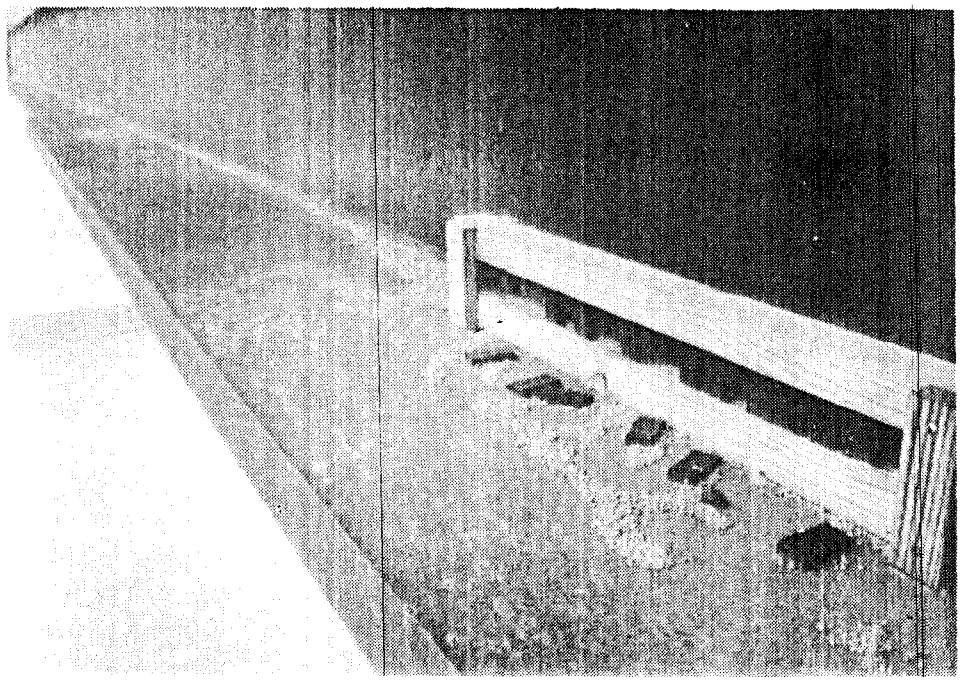

29

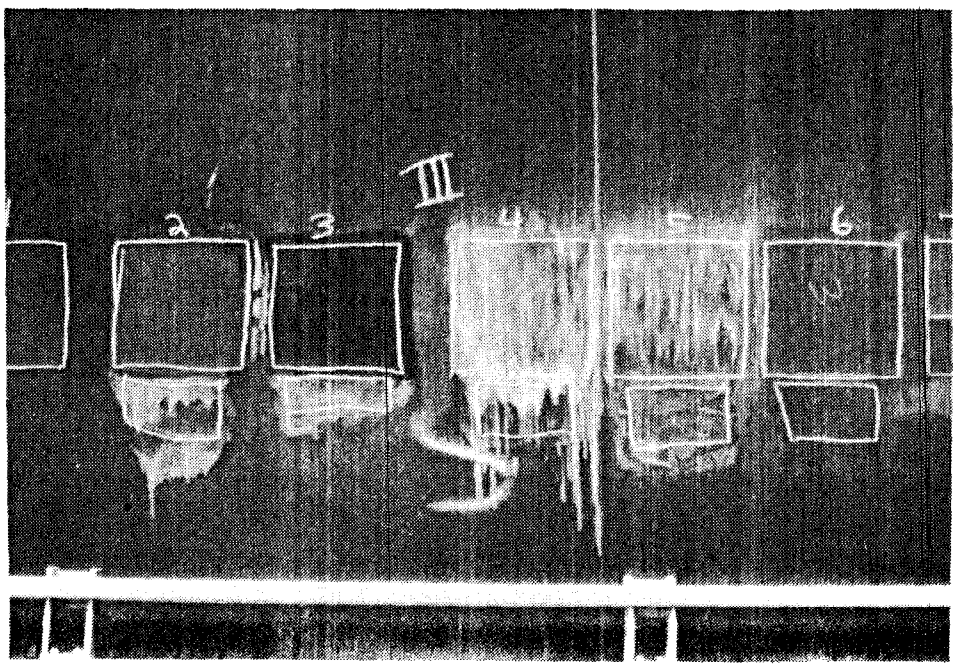

30

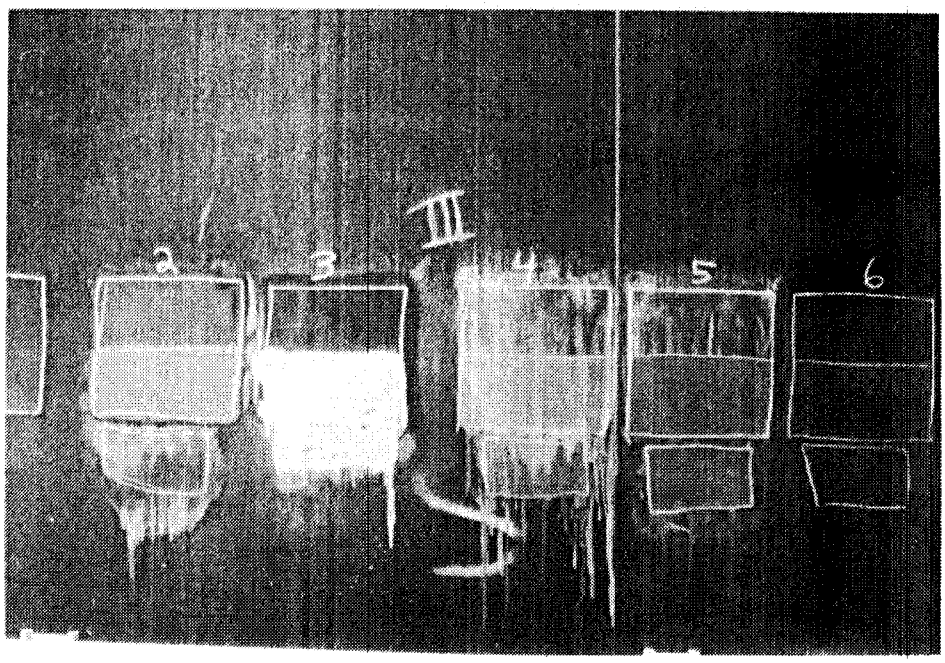

31

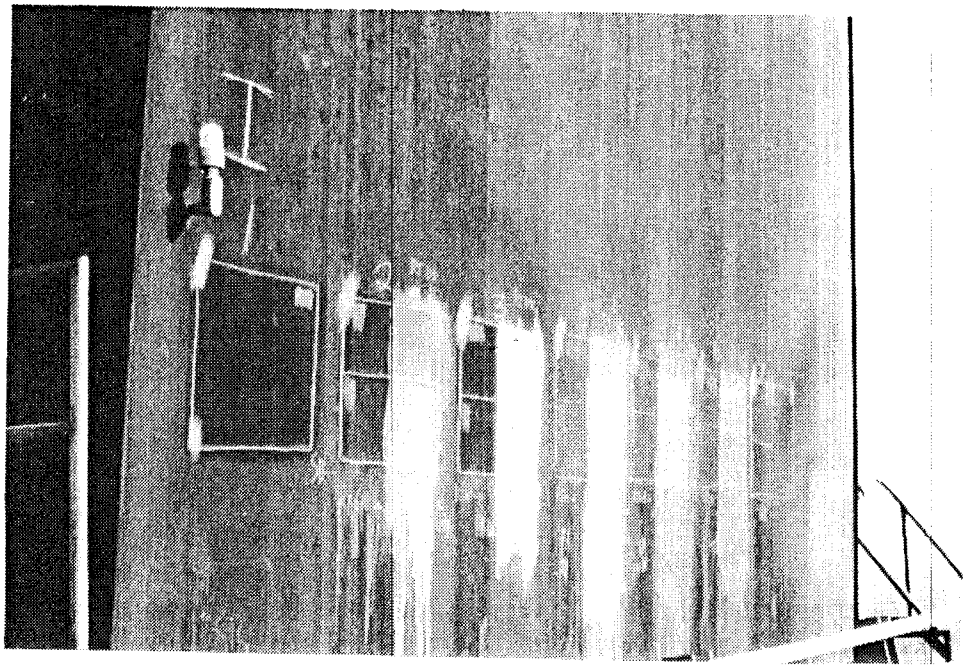

32

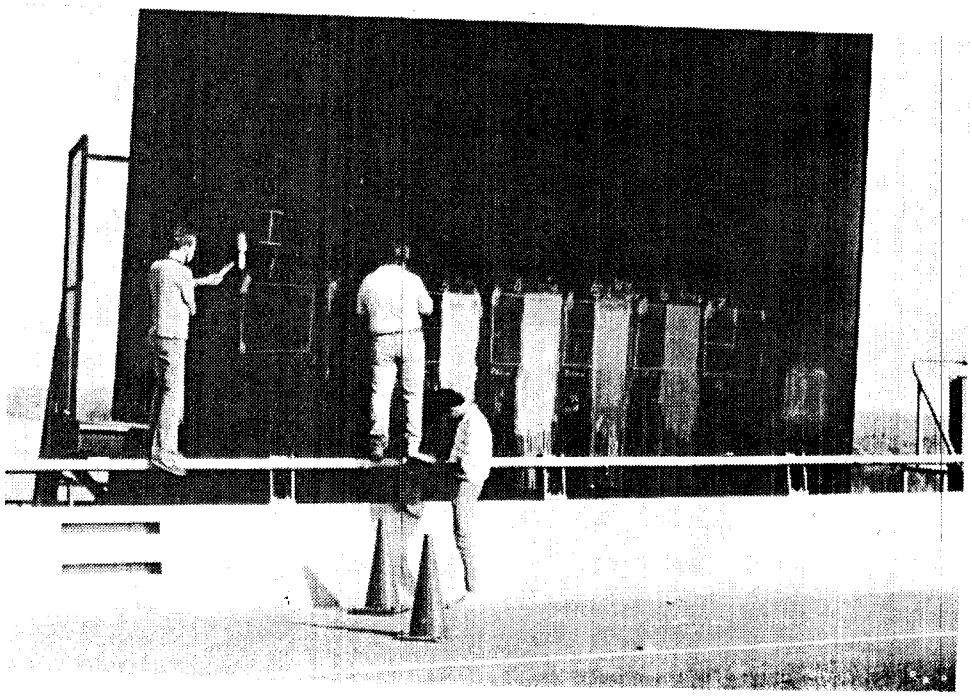

33